Factors affecting the kinetics of froth flotation

By

Jian-Guo Zhang

Department of Mining and Mineral Engineering
University of Leeds

June 1989

To my grandmother

ABSTRACT

In this research work, three types of flotation models (discrete, mean rate and the gamma function models) are modified based on the relationship between mass recovery and recovery. The modified models can be used to calculate both the recovery and grade of concentrate.

Experimental work was carried out by using three different samples, which are chalcopyrite, coal and complex sulphide. In the chalcopyrite and coal flotation, air flow rate (**AFR**) was varied and different size fractions were considered in coal flotation. In complex sulphide flotation, the impeller speed (**IPS**) and air flow rate were varied, different size fractions were also considered individually.

From the experimental results, the effect of air flow rate, impeller speed and particle size on the recovery and grade of concentrate are obtained, it is shown that an increase in air flow rate does not significantly increase recovery but reduce the grade of concentrate. High impeller speed can increase the recovery of fine and medium size, but it has very little effect on the coarse size. The effect of particle is that the medium size has the highest recovery in Fe minerals but the fine has the highest recovery in Zn and Cu minerals.

The air flow rate, impeller speed and particle size affect on the kinetics of flotation is discussed from the model results. Where the modified models are used, the results show that an increase in air flow rate will increase the flotation rate of all size fraction, but an increase in impeller speed can only increase the flotation rate of the fine and medium size. The medium size has the highest flotation rate in most of the case.

ACKNOWLEDGEMENTS

ABBREVIATION

CDM is Combined Discrete Model.

MCM is Modified Chen's Model.

GFM is Gamma Function Model (new).

AFR is Air Flow Rate.

IPS is ImPeller Speed.

Table of Contents

Chapter One

Introduction

With the increasing application of computers in the mineral industry, physical and mathematical models of each operational circuit in the mineral processing plant become urgently needed. Flotation, as an important process of mineral processing has attracted much attention from researchers, and flotation models have been used as early as the 1930's (Zuniga G. H. 1935, Morris T. M. 1952, Arbiter N. and Harris C. C. 1962, King R.P 1974). However due to the complexity of the flotation process and the limitations of the technology required to obtain the necessary information, most of the existing flotation models are still far from perfect.

Although the fundamentals of flotation models, i.e. the first order kinetics, have been developed, detailed information about the factors which affect flotation kinetics has still not been obtained. Remaining problems not only include the effect of factors, such as reagent type and concentration, air flow rate and impeller speed etc., on the parameters of flotation models, but also the flotation model itself, since most of the models are not well constructed in representing true flotation behaviour. In general, the models should follows the rules that the parameters in the model should have physical significance and the values of the parameters for one set of flotation conditions should be consistent.

Flotation can be affected by many factors. Because of limited time, this research work is only devoted to a small area of flotation kinetics. In order to obtain an applicable flotation model, two major fields are selected in this research work.

1. In order to overcome the problems of the inconsistency of the model parameters and to enable the calculation of both the concentrate grade and recovery, existing models are thoroughly analysed and three representative models, namely discrete, mean rate, and gamma function models are modified and used in this thesis. The modified models are developed based on the relationship between mass recovery and recovery.

2. In order to explore the factors which affect model parameters, the factors are separated into two major groups, which are the mineral properties and the operating factors. The first group is further divided into two subgroups, one of which is concerned with the chemical factors and the other with physical factors. The chemical factors are the natural floatability and the floatability of the feed after reacting with chemical reagents. As this subgroup is dependent on the individual minerals, and sometimes even on the site where the minerals were formed, these factors are beyond the scope of this research. The physical factors of minerals are the specific gravity and the grain size of the valuable mineral in the surrounding gaugue. This subgroup is considered here by floating coal and chalcopyrite. The operating factors include the flotation solids concentration, the air flow rate, impeller speed (or power input to a unit pulp volume), the feed size (mechanically possible to float), and the froth stability. Since the froth stability is closely related to the frother type and frother dosage, it is not included in this research work. Therefore this research work is devoted to find the effects of air flow rate (AFR), impeller speed (IPS) and particle sizes on flotation kinetics as shown in the chart below.
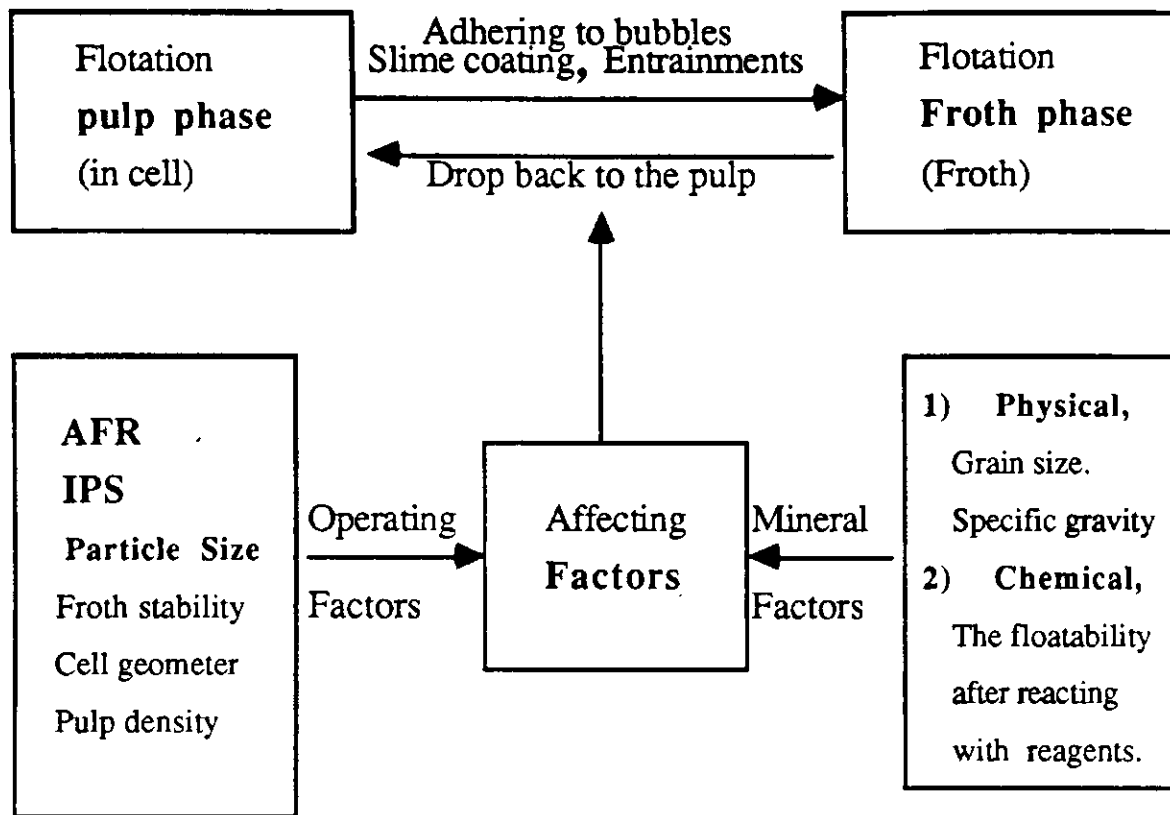
Affecting factors of flotation

Chapter Two

Literature Review

2.1 Introduction

This chapter will survey the literature related to different models and the effect of air flow rate (AFR), impeller speed (IPS) and the particle size on flotation. In this survey, attentions is concentrated on first order kinetic models, which include the discrete models, Gamma function models and mean rate model.

In the effecting factors, AFR and IPS are more emphasized. Although the IPS is not changed in most flotation operations and even AFR is not always taken as a variable in flotation operations, these two factors have a close relationship to flotation kinetics, and are dominant factors in the determination of the flotation rate. On the effect of AFR, since AFR has great effect on water recovery, researches have been carried out on AFR are related to bubble overloading and gangue entrainment by water recovery. On the effect of IPS, researches have been carried out mainly on the attachment of particles and bubbles.

Finally, the effect of particle size on flotation are also reviewed.

2.2 Review of flotation models

From the 1930's to late 1987, various mathematical models have appeared in order to describe the operation of mineral processing (Zuniga G.H. 1935, Arbiter and Harris 1962, Ball B. 1971, Kelsall 1961, Smith H. 1969, Woodburn E. 1970, Zaidenberg I. et al 1964, Mika T. 1969, Chen Z.M and Mular L. 1982, Lynch et al 1974). These mathematical models range through comminution, classification to

separation, each single process of mineral processing plant is covered by a mathematical model. Because of the different points of view of the authors and also because of the different purposes of modeling, there are a number of different models ranging from theoretical to empirical. In flotation, many models have been assumed, unfortunately each individual model is limited to certain conditions. Because of the different degree of complexity in existing models, the accuracy and precision of the model results are different from each other even when derived from the same experiment data (Ersayin, S. 1986). The results obtained by Ersayin show that the more parameters employed in the model, the more accurate it is for a group of experimental data, and the less the significance of each parameter in the model.

2.2.1 Different flotation models

Concerning flotation models, because of the complexity of flotation, it is very difficult to include the details of the variables in a model. Among the variables which affect flotation, some of them are manipulated variables and others are disturbance variables (Lynch A. J. 1981). Due to the existence of the disturbance variables, it is not possible to build a model from a completely theoretical analysis, even this is achieved, the model may become complicated to be impractical. Therefore to date, no purely theoretical flotation model has been achieved. Only models which are based on experimental results and analysis are used.

In the modelling of flotation, there are different starting points in building a model. There are probability models which are based on the relation of recovery rate to the probability of particles colliding with bubbles and probability of adhesion of particles to the bubbles after collision (Schuhmann 1942, Tomlinson et al 1965). By taking the particle size and cell volume and froth stability into consideration the final probability flotation model is shown below (Schuhmann).

$$P_x = P_c \cdot P_a \cdot F \cdot [x] \cdot V \qquad (2.1)$$

Where:

P_x -- the probability of successful recovery.

P_c -- the probability of particle-bubble collision.

P_a -- the probability of particle-bubble adhesion.

F -- froth stability factor.

$[x]$ -- average particle size.

V -- the volume of the flotation cell.

Since the various probability and independent factors are unknown in the whole process and there is no effective method to measure the individual probability and the effect of the factors, this model is not very practical. After Schuhmann's probability model, Kelsall (1961, 1971) reasoned that the probability model can be approached in an alternative way to make measurement much easier. This model is:-

$$W = W_0 \cdot (1 - p)^n \qquad (2.2)$$

Where:

W -- weight in tailing after flotation.

W_0 -- the weight in cell before flotation start.

p -- the probability of particles recovery.

n -- the factor which show the effect on processing.

In this model, time was not considered. The flotation process was taken as the whole procedure which finishes after a certain time period. This model is easy to use and the measurements are easy to take. However, the limitation of this model is that all flotation must be carried out in a certain time, there is no relation between

the independent factors and flotation time. This means that the optimum flotation time cannot be obtained from this model, and flotation as a process cannot be investigated in isolated states. As a basic flotation model, this model gives us inspiration which can lead to an improved form,

$$\frac{W}{W_0} = (1-p)^n \tag{2.3}$$

$$\frac{dW}{dp} = -W_0 \cdot n \cdot (1-p)^{(n-1)} \tag{2.4}$$

At the start of flotation, more fast floatable particles in the flotation cell are available to be recovered. The probability value of 'p' is high, with flotation proceeding the value of 'p' drops continuously. Therefore it is reasonable to make an assumption that 'p' is a function of time with the general form $p = P(t)$. Substituting p by $P(t)$ in equation (2.4), the following equation can be obtained:-

$$\frac{dW}{dP(t)} = -W_0 \cdot n \cdot (1-P(t))^{(n-1)} \tag{2.5}$$

Since $dP(t) = P'(t) \cdot dt$

$$\frac{dW}{dt} = -W_0 \cdot n \cdot P'(t) \cdot (1-P(t))^{(n-1)} \tag{2.6}$$

Since $W = W_0 \cdot (1-p)^n$ (2.2), let $K(t) = n \cdot \frac{P'(t)}{1-P(t)}$, the equation (2.6) becomes

$$\frac{dW}{dt} = -K(t) \cdot W \tag{2.7}$$

The equation (2.7) is the first order kinetic model which is widely accepted in flotation by researchers.

2.2.2 First order kinetic models

Among flotation models, the most acceptable model is the kinetic model which uses the first order reaction equation as the starting point. It is based on rules of mass trans-port from one phase to another. The simple equation is;

$$\frac{dC}{dt} = -K \cdot C \qquad\qquad (2.8)$$

Where:

C-- the concentration of mass at time t.

K-- the transport rate or reaction rate.

t-- the processing time.

For all particles with identical properties, the rate K is constant, therefore K becomes a rate constant. In flotation, when the clock is turned on, the mass concentration $C=C_0$. After a period of time, the mass concentration will reduce with time according to the equation (2.8).

Since particles in the flotation cell do not have identical properties, the rate in eq. (2.8) is not constant. For the purposes of flotation modelling, modified models with distributions of flotation rate constants have been proposed. These models are in three groups, the first includes discrete multiple rate constant models, the second continuous rate constant distribution models, and the final group includes mean rate constant models.

2.2.3 Kinetic Models with discrete rate constants

There are several discrete rate constant distribution models, the difference between them are simply the number of fractions assumed (Morris 1952, Kelsall 1961, 1971, Cuttris 1977, Jowett 1974, Imaizumi 1965). The two fraction kinetic

model with only two rate constants, the behaviour of each fraction is described with a corresponding rate constant. The two fractions are named as fast floating and slow floating fractions, this kinetic model is shown below (Kelsall 1961) :-

$$C = C_0 \cdot (a \cdot \exp(-k_s \cdot t) + (1 - a) \cdot \exp(-k_f \cdot t)) \tag{2.9}$$

Where:

C_0 -- the total concentration in the cell before flotation.

C -- the total concentration in the cell at time t.

a -- the slow floating fraction.

k_s -- the flotation rate of slow floating fraction.

k_f -- the flotation rate of fast floating fraction.

In the three fraction flotation model, one fraction with a medium flotation rate constant was assumed (Jowett, 1974). The model is shown below;

$$C = C_0 \cdot (a_1 \cdot \exp(-k_s \cdot t) + a_2 \cdot \exp(-k_m \cdot t) + a_3 \cdot \exp(-k_f \cdot t))$$

$$\dots (2.10)$$

Where

a_1 -- the slow floatable fraction.

a_2 -- the medium floatable fraction.

a_3 -- the fast floatable fraction.

And

$$a_1 + a_2 + a_3 = 1$$

the other parameters are as same as in the equation (2.9).

In the application of the discrete models, an unfloatable fraction is added due to the fact that not all of the potentially floatable material is actually recovered.

2.2.4 Kinetic Models with a continuous rate constant distribution

In the continuous rate constant distribution models, the fraction was treated as a function of the flotation rate constants. These models assumed that the rate constants are distributed as a continuous distribution between zero and Km, represented by a mathematical function (Harris 1970, Woodburn 1965, Loveday 1966, Kappur 1974, Ball et al 1971).

Assuming the distribution as a Gamma function. Harris proposed the model:-

$$\frac{df(t)}{dt} = \int \frac{1}{K_m \Gamma(n)} \cdot \left(\frac{k}{K_m}\right)^{(n-1)} \cdot \exp\left(-\frac{k}{K_m}(1 + K_m \cdot t)\right) dk \qquad (2.11)$$

Where:

f(t) -- the element recovery in the cell.

$\Gamma(n)$ -- the Gamma function.

k -- the flotation rate.

K_m -- the correction factor.

t -- the flotation time.

The above model, uses a single Gamma function distribution. If two Gamma functions are used, the rate distribution becomes bimodel (Harris 1970). This model shows;

$$\frac{df(t)}{dt} = \int \frac{a}{\Gamma(n)} \cdot k^{(n-1)} \cdot \exp(-k(1+t))dk + \int \frac{1-a}{\Gamma(m)} \cdot k^{(m-1)} \cdot \exp(-k(1+t))dk$$

$$...(2.12)$$

Where:

a, n, m, are parameters.

k is the flotation rate

Using the Laplace transform equation, on integration of k from zero to infinity, the equation (2.12) becomes (Kapur 1974),

$$f(t) = \left(\frac{1}{1+k_m \cdot t}\right)^{(n+1)} \qquad (2.13)$$

and for the bimodel distribution,

$$f(t) = \left(\frac{a}{1+t}\right)^n + \left(\frac{1-a}{1+t}\right)^m \qquad (2.14)$$

Loveday (1966) obtained a similar model by using the Gamma function,

$$R(k,0) = \frac{b^{(a+1)}}{\Gamma(a+1)} \cdot k^a \cdot \exp(-b \cdot k) \qquad (2.15)$$

Where R(k,0) is element recovery of feed and a, b, are parameters.

In all the flotation models, the parameters are strongly affected by operational conditions which includes AFR, IPS, particle size as well as the factors which depend on the properties of minerals and reagents.

2.2.5 The mean rate flotation model

The mean rate flotation model (Chen's model) was proposed by Chen (Chen Z.M. 1978, 1982), the model is shown below,

$$\frac{dC}{dt} = -\overline{K(t)} \cdot C \qquad (2.16)$$

and

$$\overline{K(t)} = K_0 \cdot \exp(-g \cdot t)$$

Where:

C -- the concentration of floatable material in the cell.

t -- the flotation time.

$\overline{K(t)}$ -- the mean rate function.

Ko -- the mean rate value at the beginning of flotation.

g -- parameter.

The mean rate model is generally based on the assumption that the rate of reduction in flotation mean rate is proportional to flotation mean rate, i.e.

$$\frac{dK}{dt} = -g \cdot K \tag{2.17}$$

This alternative approach in fitting experiment data has also been proved (Chen Z.M. 1978, 1982, Yi T. 1986, Xu C.L. 1984).

2.3 Factors affecting flotation kinetics

In this section, the effect of **AFR**, **IPS** and some other factors which affect flotation performance are reviewed. Although details of the effect of these factors on the parameters of flotation models is not widely available in the published papers, their general effect on the flotation recovery and grade can well offer scope for further research.

2.3.1 AFR affects on flotation

The fact that **AFR** has a significant effect on flotation kinetics, has been proved by a number of experimental results (Bennett et al 1958, Sutherland 1948,

Engelbrecht 1975). Generally speaking, air has two effects on flotation. When the AFR is very low, an increase in the AFR has a positive effect on flotation. It is shown by experiment that an increase in AFR can speed up flotation (Woodburn et al 1984, Laplant et al 1983a). Another effect of AFR is that air can also reduce the density of the flotation slurry, this causes a loss in the power input to the slurry and reduces the attachment, which is a negative effect. The experimental results also proved that excessive air flow will result in a lower recovery in the concentrate (Laplant).

It is worth noting that as early as when flotation was introduced, the effect of AFR on flotation has been investigated. The very early experiments on AFR were designed to increase the effectiveness of flotation (Gaudin A.M. 1957). When the flotation models were used, AFR was used to explain why the order of a flotation model did not exactly follow the first order kinetics (Bull,1965). The first equation which uses AFR to explain flotation kinetics is,

$$R = K \cdot C_s^m \cdot C_a^n \qquad (2.18)$$

Where:

R-- flotation rate, (mass per unit time per unit volume of pulp).

Cs--concentration of floatable solids in the cell (mass/unit volume of pulp).

Ca--concentration of air in the pulp, (volume air/unit volume of pulp).

K-- the flotation rate constant, (1/t)

m-- the order of the flotation reaction.

n-- power factor for air rate.

After Bull's model, most research has been directed to an investigation of 'm' values, and the variation of K with different reagent conditions and particle size. The results from the more reliable "steady-state" testing procedure in free flotation (Brown and Smith,1954a, 1952b; Jowett, and Safvi, 1960; Harris, et al. 1963)

generally proved that the value 'm' is 1 under conditions of constant air flow rate. In Bull's further experiments, he found that flotation results did not show exactly first order when he plotted flotation rate vs. the solid concentration in the cell. He explained that the AFR was not high enough to enable all the floatable particles to float during the short period at the start of flotation. In order to investigate whether this was because of lack of air bubbles or for any other reasons, he carried out a series of experiments by changing AFR from 104 to 565 ℓ/min per litre of cell pulp. His experimental results generally explained that over a wide range of conditions, there appears to be a linear relationship between R and Ca, i.e. n equal to 1, a first order relationship with respect to air concentration. The higher the AFR, the shorter is the residence time of air in the shearing zone of the impeller, so that a cell operating under excess air flow, contains, in effect, a higher concentration of larger air bubbles, having little effect upon K.

The effect of AFR on the flotation rate constant was also investigated by Szatkowski and Freyberger (1985), Dell and Farrar (1983). By using fine quartz sample Szatkowski (1985) employed the first order equation below.

$$dM = -FAF \cdot M \cdot dV_a \qquad (2.19)$$

Where:

M-- mass of floatable solid in the pulp.

Va-- volume of air introduced into the pulp.

FAF--function of air flow rate.

$$FAF = \frac{FAF_1}{V_s} \qquad (2.20)$$

Where:

FAF_1 -- air factor.

Vs -- the volume of pulp in cell.

The term FAF_1 is a function of diameters of bubbles and floatable particles.

$$FAF_1 = A \cdot dp \cdot \frac{0.806C_a^{-0.33} - 0.5}{(V_s \cdot db)^2} \qquad (2.21)$$

with, dVa=AFR*dt;

$$\frac{dM}{dt} = -A \cdot dp \cdot (0.806C_a^{-0.33} - 0.5) \cdot AFR \cdot \frac{M}{(V_s \cdot db)^2} \qquad (2.22)$$

Where:

A -- parameter.

dp-- medium diameter of floatable particles.

db-- medium diameter of air bubbles.

Ca-- volume of air entrained in unit volume of pulp.

$$C_a = AFR \cdot \frac{t}{V_s} \qquad (2.23)$$

Comparing with the first order kinetic model, it can be seen that the flotation rate constant can be expressed as;

$$K = A \cdot \frac{dp \cdot (0.806C_a^{-0.33} - 0.5) \cdot AFR}{(V_s \cdot db)^2} \qquad (2.24)$$

This equation shows that if an increase in AFR has very little effect on the bubble size, the flotation rate constant will increase, otherwise the change in flotation rate constant will depend on both the AFR and the bubble size. This equation explains the decrease in flotation rate constant with excessive air flow.

Dell and Farrar (1983) investigated AFR from another point of view. By proposing a bubble loading model, they found that if flotation was terminated at the same percentage solid yield, the flotation time is a function of AFR. They also found that in the middle range of air flow rate, 1/t shows a linear relationship with the bubble loading function. Where the bubble loading function is expressed as the weight yield from per volume of pulp per volume of air in flotation time t (when the flotation is terminated). They reported that both at very low AFR and very high AFR conditions, the relationship between 1/t vs bubble loading were nonlinear. The equation is shown as (for the medium air flow rate),

$$\frac{1}{V_a} = B - \frac{A}{t} \qquad (2.25)$$

Where:

A,B-- parameters

Va -- Total air introduced in t time

t -- flotation time to reach specified percentage weight yield.

Since $V_a = AFR \cdot t$

The equation (2.25) can be rewritten;

$$\frac{1}{AFR} = B \cdot t - A \qquad (2.26)$$

By assuming first order kinetics, i.e.

$$C = C_0 \cdot \exp(-k \cdot t) \tag{2.27}$$

Supposing AFR_1 is the **AFR** at one value with t_1 and K_1 being the flotation time and the flotation rate constant respectively, AFR_2 is the **AFR** at another value with t_2 and K_2. When the weight yield is same, it is apparent that the following equation exists;

$$-K_1 \cdot t_1 = -K_2 \cdot t_2 \tag{2.28}$$

From equation (2.26) $t = \left(\frac{1}{AFR} + A \right)/B$

$$\frac{t_1}{t_2} = \frac{\frac{1}{AFR_1} + A}{\frac{1}{AFR_2} + A} \tag{2.29}$$

Combining equations (2.28) and (2.29) and letting $K_1 = K_c$, $AFR_1 = AFR_c$, will result in,

$$K_2 = K_c \cdot \frac{\frac{1}{AFR_c} + A}{\frac{1}{AFR_2} + A} \tag{2.30}$$

Since K_c, AFR_c, and A are constants, by substituting $K_c \cdot \left(\frac{1}{AFR_c} + A \right)$ with A_0, the following result will be obtained,

$$K_2 = \frac{A_0}{\frac{1}{AFR_2} + A}$$

or

$$K_2 = A_0 \cdot \frac{AFR_2}{1 + A \cdot AFR_2}$$ (2.31)

From equation (2.31), it can be seen that the flotation rate constant is not simply proportional to the **AFR**. When the value of A is very small, $A \cdot AFR_2$ may become negligible, only under these conditions will the flotation rate constant be proportional to **AFR**.

On further investigation of the effect of **AFR** on the flotation rate constant, Woodburn and Wallin (1984) obtained a relationship between the **AFR** and the flotation rate constant. By employing the Gamma function distribution model, Woodburn obtained the equation,

$$\frac{C_i(t)}{C_i(0)} = \frac{1}{(1 + B \cdot K \cdot t)^\upsilon}$$ (2.32)

Where:

$C_i(t)$-- the concentration of solid in the flotation cell at t time.

$C_i(0)$-- the concentration before flotation.

υ -- parameter.

B -- multiplier, =a*Qa.

a -- froth stability parameter, =Qf/Qa.

Qa -- specific aeration rate, air volume per unit volume of pulp per minute.

Qf -- air flow over concentrate weir per unit volume pulp per minute.

Comparing equation (2.32) with the first order equation;

$$K_{av} = \upsilon \cdot B \cdot \frac{K}{1 + B \cdot K \cdot t}$$ (2.33)

Where Kav -- average rate constant.

In equation (2.33), B is substituted by Qa,Qf and a:-

$$K_{av} = \upsilon \cdot Q_f \cdot \frac{K}{1 + a \cdot Q_a \cdot K \cdot t} \qquad (2.34)$$

When the AFR is increased, both Qf and Qa are increased. Therefore Kav and the AFR will have a similar relationship as that derived from Dell's results. However in the equation above, a further investigation is needed to find the relationship between Qf and Qa.

From the review of the AFR effect, it is almost certain that the flotation rate constant is a function of AFR. It is also apparent that the flotation rate constant is not simply proportional to the AFR. The flotation rate constant not only depends on the value of total air flow, but also depends on the bubble size and the disturbance to the froth layer. As the AFR not only affects the particles of the floatable mineral, but also the unfloatable particles by hydraulic entrainment, this means that an increase in the AFR cannot be certain to improve flotation results. The effect of AFR on water recovery was also investigated by a few researchers (Laplante et al.(1984), Wu Yirui.(1986), Leonard (1985)). Wu's results show that water recovery could be described by first order kinetics. Leonard reported that the water recovery is proportional to the recovery of the unfloatable fraction. Combining Wu's results and Leonard's, It can be concluded that the flotation rate of unfloatable minerals will be proportional to $\left(\frac{AFR}{D}\right)^{0.51}$ (D is froth thickness).

2.3.2 IPS affects on flotation

Impeller speed has a significant effect on flotation mainly by:-

1) IPS will change the turbulence in the pulp which results in the change of the frequency of collision between particles and bubbles.

2) IPS will change the approach speed of particles which results in a greater impact

between particles and bubbles, therefore the probability of attachment is also changed.

3) IPS will affect the projection of unattached particles into the froth where they might be retained.

4) IPS will affect the stability of the froth layer.

5) IPS will affect the particles suspension in the flotation cell.

The effects of IPS are related to the turbulence in the pulp. Since the turbulence of the pulp is highly dependent on the shape of the impeller, very little work has been done directly on the relation IPS to flotation. However, in order to find the effect of IPS on flotation kinetics irrespective of the shape of impellers, power input can be measured. Once the general relationship between the power input and the flotation rate is obtained, in different flotation cells, by using a multiplier, a new relation can be used.

Generally speaking, from a low power input an increase in power input will improve flotation. However at high power input, flotation becomes unstable due to excessive turbulence (Bennett and Dell 1958, Harris et al 1970, Nonaka M. et al 1977, Schulze, H.J. 1984). Bull (1965, 1966) also proved that the increase in IPS results in two effects, first an increase in power input leads to an increase in flotation rate, but after 1300 rpm further increase in IPS results in a decrease in flotation rate.

In an approach to flotation modelling including power input, Schubert (1981) used a simplified turbulence theory in which free-turbulence (distant from a wall) was assumed. From a consideration of fluid dynamics, if the fluid turbulence is equal in all directions, the degree of turbulence is given by:-

$$T_u = (U_x^2)^{\frac{0.5}{\overline{v}}} \qquad (2.35)$$

Where:

Tu-- the turbulence of free-turbulent flow.

Ux-- the superimposed velocity fluctuation in one direction.

U -- the mean flow velocity.

In the flotation cell, it is explained (Schubert 1981) that the power input is firstly changed to the energy of macroturbulence and then the macroturbulence is changed to microturbulence, the microturbulence being small eddies. A lot of eddies carry the energy to create dispersion of the bubbles and keep the particles in suspension.

The effect of power input on the size of the bubble has also been obtained from the same principle:-

$$Db_{max} = W_e^{0.6} \cdot \left(\frac{\sigma}{\rho}\right)^{0.6} \cdot \eta^{-0.4} \tag{2.36}$$

Where:

Db_{max}--the maximum bubble size.

We -- the Weber number.

η -- dissipation in the dispersion zone.

σ -- interfacial tension.

ρ -- fluid density.

The relation between the impeller speed and the one second criterion power input (the power for which particles can be suspended for more than one second) has the equation below:-

$$\frac{P}{V_s} = K_3 \cdot Cl^p$$

Where:

P -- the net power input.

Vs-- the volume of pulp.

K_3-- coefficient of physical properties of pulp.

p -- parameter of impeller rotator system.

Cl-- the fluid number which has the following equation;

$$Cl = \frac{Vl}{n \cdot d_2^3}$$
(2.37)

Where:

Vl-- the air volume per minute.

n -- the impeller speed. (rpm)

d_2-- the diameter of the blade.

Experiments were carried out by Schubert at different IPSs and power inputs. The results show that at high IPS, the high power inputs resulted in a lower recovery in the +0.5 mm size range for Kaolin flotation. On the other hand, the concentrate quality improved with power input. The highest Kaolin recovery was reported at the power for the 1s-criterion.

Another approach to the IPS effect was carried out by Inoue and Imaizumi (1980). On the basis of first order flotation model the relation between the flotation rate constant and the power input was reported as:-

$$K_i = A \cdot Na_f^{0.5} \cdot i^{0.75} + B$$
(2.38)

Where:

Ki-- is the flotation rate constant.

A,B--coefficients.

Na_f-air flow number which is;

$$Na_f = \frac{Q_a}{N_i \cdot D_i^3}$$ (2.39)

Where:

Qa-- air flow rate. (AFR)

Ni-- rotating velocity of the impeller.

Di-- impeller diameter.

i-- the specific agitation energy which is;

$$i = \frac{P}{p \cdot V}$$ (2.40)

Where :

P-- agitation power.

p-- apparent density of the stirred pulp.

V-- the pulp volume.

The experiment carried out by Inoue was over a small range of power inputs, therefore the results only show a small part of the relationship between the flotation rate constant and the power input. In practice, this might be enough to find out the optimum operation conditions.

2.3.3 Particle size effect on flotation

Research on the effect of particle size on flotation can be separated into two groups, one of which is to explore the relationship between particle size and flotation

recovery, the other is to interpret the function of particles in flotation models. The earliest works on the relationship between particle size and flotation recovery was carried out by Gaudin et al (Gaudin et al 1931, Bishop et al 1976, Inoue et al 1968, Jowett et al 1980, Morris T. M. 1962, Ready D. et al 1975). In the experiments, different sizes of lead, zinc and copper sulphide samples were used. The results show that the highest flotation recovery was found at particle sizes between 10 and 50 microns. A sharp decrease in the recovery occurred when the particle size was above this limit, and gradual decrease for particle size below 10 microns.

In flotation models, the relationship between flotation rate constant and particle size was frequently studied by researchers. However, the use of different type of flotation models complicated comparison of the relationships obtained by different researchers. The difficulties are further increased by the use of different flotation methods (batch or continuous). In some cases, individual particle size fractions were floated separately. Therefore there is little agreement between the different results. However, an experimental result suggests that, for fine and medium sized particles:

$$K = A \cdot d^n \qquad (2.41)$$

Where:

K-- the flotation rate constant.

A-- proportional coefficient.

d-- particle diameter.

n-- parameter.

For individual particle fractions, the equation above was proved by Tomlinsion and Fleming (1965). The results showed that for apatite, hematite and galena, n=2.0, and for quartz n=1.0. 'A' was proved constant. The effect of particle size of a coal sample on flotation recovery was also studied by Bennett et al (1958). Their results

showed similar relationships to other samples. The results of coal flotation further proved that the decrease in flotation recovery for the excessively large particles is not only due to insufficient liberation, but also because of detachment of large particles in the flotation. From the mechanism of flotation it is clear that the IPS will have greater effect on the coarser particle flotation than the finer.

2.3.4 The effect of other factors on flotation

Along with **AFR, IPS** (power input) and particle size, there are still some other factors which affect flotation. These factors can be the pulp density, the reagent dosage, flotation temperature, pH etc. The reagent dosage, temperature and pH are closely related to the mineral properties, the effect of these factors are mineral specific. The pulp density, as factor in flotation, can be investigated and its relationship to flotation parameters can be used in the flotation of other minerals. The effect of pulp density on flotation can be expressed as follows. High pulp density will cause bubble overloading (Lynch A. 1981), and even make flotation impossible. A high density of pulp may also create very fine bubbles which are too heavy to float when mineralised (Schubert H. 1979).

Chapter Three

Development of Flotation Models

3.1 Introduction

In chapter two, flotation models have been reviewed. Amongst the various models, the first order kinetic models, i.e. discrete rate distribution, gamma function rate distribution and Chen's model, have been widely accepted and proved valid in experimental data fitting. In the models mentioned above, the recovery of element in the concentrate was calculated as a function of flotation time, however, the concentrate grade is not predicted.

In this chapter, flotation as a kinetic process will be examined and a method of calculating the concentrate grade will be developed by the combination of mass recovery and element recovery.

3.2 Development of a Combined Discrete Model (CDM)

By using a simple mathematical method, a function which links mass recovery and element recovery has been formulated as shown in the following sections.

3.2.1 The mass and element recovery models

That weight changes in a flotation cell as a first order kinetic process has been recognized as early as the 1930's (Zuniga, G.H. 1935). In fact, the theory of mass transfer from one phase to another without the involvement of chemical changes had already been established in chemical engineering even before flotation was introduced in mineral processing. In this regard the flotation model is only one of

several examples which uses the same theory as various engineering processes. However it should be noted that flotation feed has a distinctive characteristic of being extremely heterogeneous compared to the reactants in chemical engineering.

In earlier flotation models, either the relative weight or mass remaining in the cell was frequently expressed as a function of flotation time (Bull W.R. 1956,1966). Later the use of solids mass was repaced by the relative weight of valuable element without explanation. Although the new models could evaluate flotation directly in relation to the values recovered, the significance of mass recovery was underplayed in the new models. The replacement of mass recovery by element recovery was presumably due to the fact that for modelling purposes most of the laboratory tests in the past had been carried out by using pure minerals. In this case, the mass recovery and element recovery have the same value. But under actual flotation conditions, the feed material is heterogeneous, the content of a certain element in different particles varies greatly, the mass recovery is no longer the same as element recovery. Therefore mass recovery should be considered again and the relationship between the mass recovery and element recovery should be sought.

3.2.2 Factors determining particle floatability

In order to obtain a relationship between mass and element recovery models, the factors determining particle floatability are reviewed in the following text.

It is well known that mineral hydrophobicity depends on the nature of the mineral-water interface, where two factors are important (Gaudin 1957):-

1) The interaetion of water molecules with the mineral surface, both in liquid and gaseous environments.

2) The eleetrieal double layer at solid water interface.

These are two chemical factors which are both mineral and collector dependent, once the collector is chosen, the hydrophobicity will depend on the mineral properties.

Apart from the chemical factors, there are still two physical factors namely liberation and particle size:-

1) Since the liberation is affected by random breakage, the presence of composites in the flotation feed is inevitable. Two types of possible composites are either two gangue minerals or valuable and gangue minerals. The former docs not create problems in the flotation process, the latter causes problems since the surface of the particle is partially made up by gangue minerals which would reduce the floatability of the particle (Lynch A. J. 1981). The consequence of this would be that a fraction of valuable mineral will show low flotation rate or no flotation rate at all.

2) The effect of particle size on flotation has been demonstrated by many researchers (Gaudin 1931, Dell 1958). The experimental results show that both coarser and finer particles have lower recovery than the medium size particles. The explanation of this fact is that coarse particles have a higher detachment probability and are more difficult to maintain in suspension, while the fine particles have a lower collision probability.

To sum up, the factors determining particle floatability are the surface hydrophobicity of valuable mineral, the liberation ratio of valuable mineral from the gangue and the particle size of both the liberated minerals and the composites.

3.2.3 General assumptions

As discussed in the previous section, besides the mineral hydrophobicity, both particle size and composition play very important roles in flotation. In this section, some general assumptions will be made based on size and the composition properties. These assumptions are:-

1)   In the flotation feed, only the valuable mineral possesses surface hydrophobicity, i.e, the free gangue particles are hydrophilic and will never be recovered by adhering to bubbles.

2) Composite particles can be recovered by adhering to bubbles. Although the hydrophobicity of a composite is not as strong as that of free mineral particles of equal size, the composite particles still possess floatability due to the presence of valuable mineral, and the floatability of a composite lies between that of free valuable particles and free gangue. The floatability of a composite varies according to the proportional content of valuable mineral in the same size group, with free valuable and free gangue particles as two extreme cases.

3) Flotation feed can be divided firstly into size groups and then further divided into species by grade of valuable mineral.

4) In the same size group, each species of given grade has a corresponding rate constant. None of the species of different grade has the same flotation rate.

5) Each species in the cell will be recovered in accordance with first order kinetics. Here, the weight of each species is considered, i.e, the weight of a single species in the cell will vary with time so that;

$$\frac{dW_i(t)}{dt} = -K_i \cdot W_i(t)$$ (3.1)

Where:

$W_i(t)$ is the weight of the ith species at t.

K_i is the rate constant of the ith species.

t   is flotation time.

6) The entrainment of gangue particles can also be described as a first order reaction (Y. R. Wu 1986).

7) Finally, due to insufficient coverage of collector and the instability, there is still an unfloatable fraction in each size fraction.

3.2.4 Theoretical approach to Combined Discrete Model (CDM)

Based on these general assumptions, a relationship between mass and valuable element recovery models is obtained by an analytical method. Since each species has a corresponding grade in a size fraction, it is not difficult to obtain a relationship between the weight of species and the weight of valuable element of the same species at any time during flotation, that is:

$$M_i(t) = G_i \cdot W_i(t) \tag{3.2}$$

Where:

$M_i(t)$ is the weight of valuable element of the ith species at t.

G_i is the grade of the ith species.

$W_i(t)$ is the weight of the ith species in the cell at t.

t   is flotation time.

In the discrete rate constant distribution model, it follows that the total weight of all species in the flotation cell during flotation will be given by:

$$W(t) = \sum_{i=1}^{n} W_{i0} \cdot \exp(-K_i \cdot t) \tag{3.3}$$

Where:

$W(t)$ is the total weight of all species at t.

W_{i0} is the initial weight of the ith species.

n is the total number of species.

For the valuable element in a flotation cell, the total weight contained in all species is also the sum of valuable element contained in individual species. Therefore, the total weight of valuable element in the flotation cell at t will have a similar equation as the weight equation by combining eq. (3.2) and (3.3):

$$M(t) = \sum_{i=1}^{n} G_i \cdot W_{i0} \cdot \exp(-K_i \cdot t) \tag{3.4}$$

When $G_i \cdot W_{i0}$ is substituted by Mio, eq. (3.4) becomes:

$$M(t) = \sum_{n=1}^{n} M_{i0} \cdot \exp(-K_i \cdot t) \tag{3.5}$$

Where:

$M(t)$ is total weight of valuable element in the flotation cell at t.

M_{i0} is the initial weight of valuable element in the ith species.

n,Ki,t are same as before.

In flotation terms, mass recovery and recovery are frequently used. For clarity, the terms mass recovery and recovery are respectively defined as the relative weight of solid and valuable element during or after flotation. Hence the recovery in tailing stream is the relative weight of valuable element in the tailing, and mass recovery in tailing stream means the relative weight of tailing to the original feed weight.

In the eq. (3.3) and (3.5), when each side is divided by the total weight of all species in (3.3), and by the total weight of valuable element in eq. (3.5), the corresponding equations will be mass recovery and recovery models. The two equations are:

$$C(t) = \sum_{i=1}^{n} C_{i0} \cdot \exp(-K_i \cdot t) \qquad (3.6)$$

$$R(t) = \sum_{i=1}^{n} R_{i0} \cdot \exp(-K_i \cdot t) \qquad (3.7)$$

Where:

C(t) is mass recovery in the cell (tailing stream) at t.

R(t) is recovery in the cell at t.

Cio is the initial mass of the ith species in the cell.

Rio is the initial recovery of the ith species in the cell.

Comparing the two equations above, it can be seen that both mass recovery and recovery models have exactly the same form. However, the concepts of the terms included are different from each other except for the flotation rates, which are the same in both mass recovery and recovery models.

Since C_{i0} and R_{i0}, in eq. (3.6) and (3.7) respectively, are the initial mass and recovery of the same species, from general flotation concepts, the following relationship exists:

$$R_{i0} = \frac{C_{i0} \cdot G_i}{C_0 G_0} \qquad (3.8)$$

Where:

G_0 is the feed grade.

G_i is the grade of the ith species.

From the equation above it can be seen that the grade of each species can be obtained when the mass and valuable recovery are known through the fitting of experimental data with the models.

In practice, since the most beneficial flotation conditions are these resulting in a suitable combination of concentrate grade and recovery, i.e, in which the valuable is recovered as much as possible whilst the dilution of the concentrate by gangue should not be so much as to cause a decrease of monetary yield, there is a requirement therefore for the prediction of grade, and a model capable of achieving this should be built.

Under semi-batch flotation conditions, feed is neither introduced nor tailing removed during flotation, therefore the mass recovery and recovery to concentrate are simply equal to the original values minus the corresponding values in the cell at any time during the flotation (Ersayin, S. 1986);

$$R_c(t) = 1 - R(t)$$

or

$$R_c(t) = 1 - \sum_{i=1}^{n} R_{i0} \cdot \exp(-K_i \cdot t) \qquad (3.9)$$

$$C_c(t) = 1 - C(t)$$

or

$$C_c(t) = 1 - \sum_{i=1}^{n} C_{i0} \cdot \exp(-K_i \cdot t)$$

(3.10)

Where:

$R_c(t)$ is recovery of concentrate at time t.

$C_c(t)$ is mass recovery at time t.

By combining the eqs. (3.9) and (3.10), the cumulative concentrate grate can be obtained:

$$G_c(t) = \frac{1-R(t)}{1-C(t)} \cdot G_0$$

or

$$G_c(t) = \frac{1 - \sum R_{i0} \cdot \exp(-K_i \cdot t)}{1 - \sum C_{i0} \cdot \exp(-K_i \cdot t)} \cdot G_0$$

(3.11)

The eqs. (3.9) and (3.11) are recovery and grade models for concentrate at t respectively, both of the equations are discrete rate constant distribution models.

This concludes the attainment of a discrete rate constant distribution model which is termed the Combined Discrete Model (CDM). When the CDM is employed, both flotation recovery and grade of concentrate at any time during flotation can be calculated. The flotation efficiency, which is a curve of recovery against grade, as a function of flotation time can be optimised.

3.2.5 Analysis

When the CDM is used in the calculation of the grade and recovery of concentrate, some conditions must be met in order to enable effective use of the CDM in dealing with practical problems.

3.2.5.1 General conditions

Since the CDM is developed based on a series of assumptions, it is important that actual flotation conditions are close to those assumed for CDM. There are a few important points:-

1) One floatable mineral in the feed is the ideal case for using the CDM. If there are any other floatable minerals in the feed, competitive flotation may occur (Chen Z.M. 1985), in this case, the mass recovery may not have the same flotation rates as the recovery. However the models may still be applicable if each floatable mineral is treated separately.

2) Since the entrainment of free gangue was taken as a first order kinetic process and included in the model of mass recovery, overgrinding of feed will increase the mass recovery.

3) Water recovery is not included in the CDM, this by no means implies that water recovery is unimportant in flotation. Water as a media has two functions in flotation. Water will determine the solids concentration which is vital for both a single flotation cell and flotation circuit. Water recovery can entrain the free gangue particles to the concentrate launder which will cause a reduction of concentrate grade. Much research has been devoted to the investigation of the relationship between water recovery and free gangue recovery in recent years (Thorne et al 1976, Engelbrecht 1975, Lynch A. J. 1981, Ersayin S. 1986). From the entrainment theory, the recovery of free gangue can be predicted by water recovery, but this would make the model very complicated and inaccurate. First of all, apart from the entrainment of free gangue, composite and liberated valuable particles may also be entrained by water recovery to some degree, which can hardly be predicted. Secondly, the relationship between water recovery and free gangue recovery must be obtained from

experiments. Finally, It may be argued that it is not appropriate to take water recovery as an independent variable in the model since water recovery itself is affected by many variables, such as dosage of frother and AFR. However since water recovery is important for a plant model, its model is formulated by referring to the literature (Laplante et Al 1984, Wu Y. 1986, Leonard 1985), that is;

$$\frac{dC_w}{dt} = -K_w \cdot C_w \tag{3.12}$$

Where:

Cw is equivalent water concentration.

Kw is water recovery rate.

The equivalent water concentration in the model depends on the frother concentration and solid concentration in the cell. For further information about water recovery, researches should be conducted to find a relationship between water recovery and dosages of frother and collector and the concentration of solids in the cell. In this research work water recovery is not dealt with further.

3.2.5.2 The features of the CDM

From the CDM, some flotation phenomena can be explained. First of all, from eq. (3.11), it can be seen that the final concentrate grade is proportional to the feed grade. Therefore the cleaner product will have higher grade than the rougher product. However since a large fraction is fast floating in the cleaner section, the concentration ratio will be less than that of the rougher section. Secondly, under free flotation conditions, the CDM offers a means of analyzing the relationship between the flotation rate constant and the grade of any species. By suitable testwork it is possible to obtain flotation rate constants as a function of the grade. Finally, the CDM has four advantages over the old model:-

1) The CDM can not only predict the flotation recovery but also the grade of concentrate.

2) The water recovery is not included in the calculation of the concentrate grade, which avoids the direct difficulties in predicting water recovery.

3) Since the CDM is the combination of mass recovery and recovery models, the number of parameters in the model is reduced, the consistency of the parameters is increased.

4) Finally, although the models do not distinguish between true flotation and entrainment, it can better explain the flotation of composites.

Generally speaking, the CDM has wider utility than the old models due to its many advantages.

3.3 Development of Modified Chen's Model (MCM)

In this section, Chen's model (a mean rate model) will be studied and modifications to the model made. The Modified Chen's Model (MCM) will, as the CDM, be able to predict both the recovery and the grade of concentrate. The advantages of the MCM over CDM are also discussed at the end of this section.

3.3.1 Chen's model

As reviewed in chapter 2, Chen's model is an alternative approach to flotation modelling, in which, the weighted mean of flotation rate constants is used and the change of the mean rate with flotation time is studied. On the assumption that the rate of reduction of mean rate is also a first order kinetic process, the Chen's model is (Chen Z.M. 1978, 1982):-

$$\frac{dR(t)}{dt} = -\overline{K(t)} \cdot R(t) \tag{3.13}$$

Where:

$$\overline{K(t)} = K_0 \cdot \exp(-g \cdot t) \tag{3.14}$$

Where:

R(t) is the recovery in the tailing at t.

$\overline{K(t)}$ is the weighted mean rate at t.

g is the reduction rate of weighted mean rate.

Ko is the original weighted mean rate.

In the model, the weighted mean rate was used instead of the individual rate constants in the discrete model. If a feed containing a distribution of material of different flotation rates, $\Phi(k,0)$, is assumed. It is clear that the mean rate is:-

$$\overline{K(t)} = \frac{\int_0^{K_m} k \cdot \Phi(k,0) \cdot \exp(-k \cdot t) \cdot dk}{\int_0^{K_m} \Phi(k,0) \cdot \exp(-k \cdot t) \cdot dk} \tag{3.15}$$

Where:

$\Phi(k,0)$ is the original rate constant distribution.

By using the weighted mean value theorem of integration (Burden R. L. 1985), μ and λ will exist between zero and km and satisfy the equation below:

$$\overline{K(t)} = \frac{\exp(-\mu \cdot t) \cdot \int_0^{K_m} k \cdot \Phi(k,0) \cdot dk}{\exp(-\lambda \cdot t) \cdot \int_0^{K_m} \Phi(k,0) \cdot dk} \tag{3.16}$$

Where:

μ and λ are constants.

Since

$$K_0 = \frac{\int_0^{K_m} k \cdot \Phi(k,0) \cdot dk}{\int_0^{K_m} \Phi(k,0) \cdot dk}$$

therefore

$$\overline{K(t)} = K_0 \cdot \exp(-(\mu - \lambda) \cdot t) \tag{3.17}$$

In the existing mean rate model, $(\mu - \lambda)$ is taken as a constant, which then gives eq. (3.14).

3.3.2 The analysis of Chen's model

It is doubtful that the assumption of constant value for $(\mu - \lambda)$ in eq. (3.15) is valid. It can hardly be true that $(\mu - \lambda)$ would be a constant while both μ and λ are functions of flotation time.

In the following text, μ and λ as functions of flotation time will be examined by a numerical method when discrete and Gamma function rate constants distributions are assumed.

a) In the case of discrete rate constants distribution, when Kf and Ks are assumed the flotation rate constants of the fast and slow floatable species, with the fraction of fast floatable equal to 'a', $\mu(t)$ and $\lambda(t)$ are defined by the following equations:

$$\mu(t) = \frac{-1}{t} \ln \frac{K_f \cdot a \cdot \exp(-K_f \cdot t) + K_s \cdot (1-a) \cdot \exp(-K_s \cdot t)}{K_f \cdot a + K_s \cdot (1-a)} \qquad (3.18)$$

and

$$\lambda(t) = \frac{-1}{t} \ln(a \cdot \exp(-K_f \cdot t) + (1-a) \cdot \exp(-K_s \cdot t)) \qquad (3.19)$$

The values of $\mu(t)$ and $\lambda(t)$ are presented in Fig 3-1 with respect to flotation time. From Fig 3-1 it can be seen that $\mu(t)$ and $\lambda(t)$ are functions of flotation time as well as $\mu(t) - \lambda(t)$. Although $\mu(t) - \lambda(t)$ varies less than $\mu(t)$ and $\lambda(t)$ with the change of flotation time, it is sufficient to disprove the assumption of a constant value of $\mu(t) - \lambda(t)$.

b) Similarly, when the gamma function is assumed, the numerical results of $\mu(t)$ and $\lambda(t)$ are obtained and presented in Fig 3-2. Again, the constant assumption of $\mu(t) - \lambda(t)$ is disproved.

In conclusion, the existing Chen's model is inadequate in predicting flotation recovery if either the discrete or gamma function model is valid. As an alternative approach, a Modified Chen's Model (MCM) is developed.

3.3.3 Modified Chen's Model (MCM)

In this section, the Modified Chen's Model (MCM) is developed based on a theoretical and empirical method. The procedures of the development are shown in the following four steps:-

The flotation time (min)

K1=0.25, K2=1.95, a=0.27

Fig 3-1. μ and λ in CDM

The flotation time (min)

Km=2.35, n=1.25 in (n)
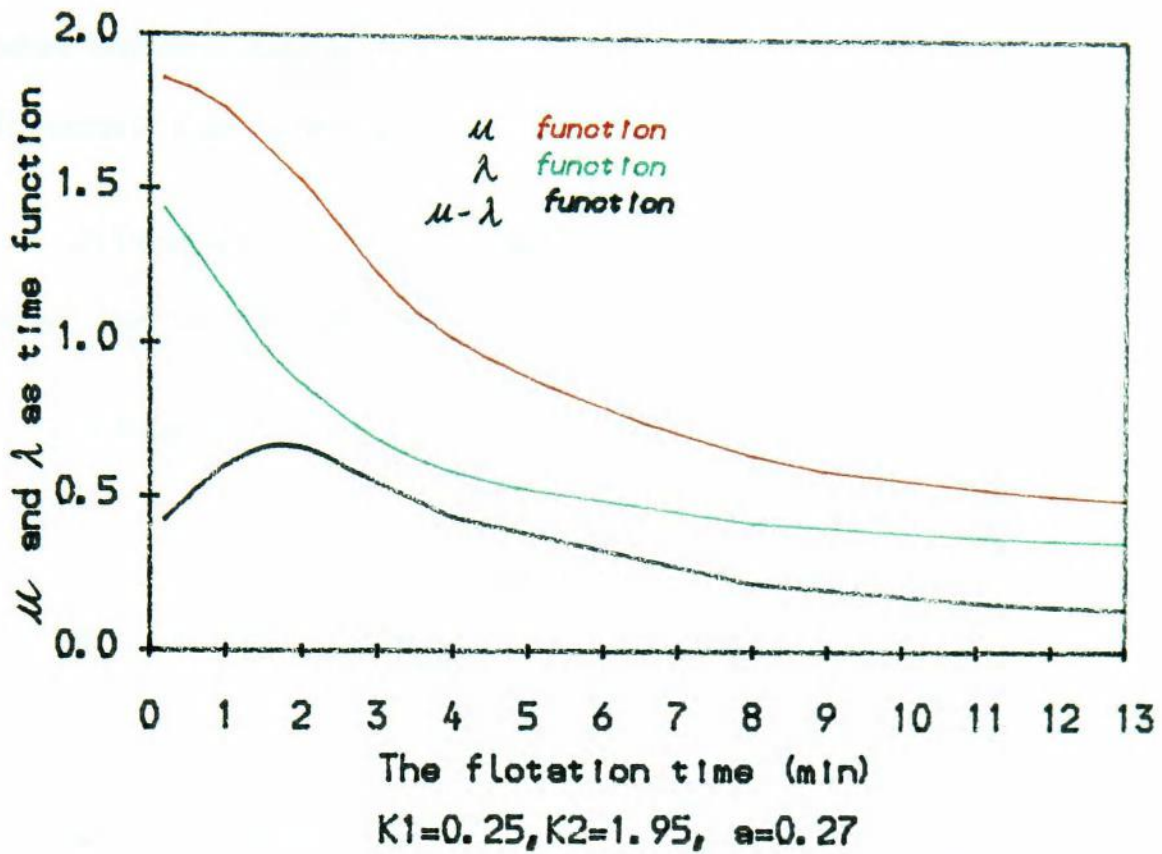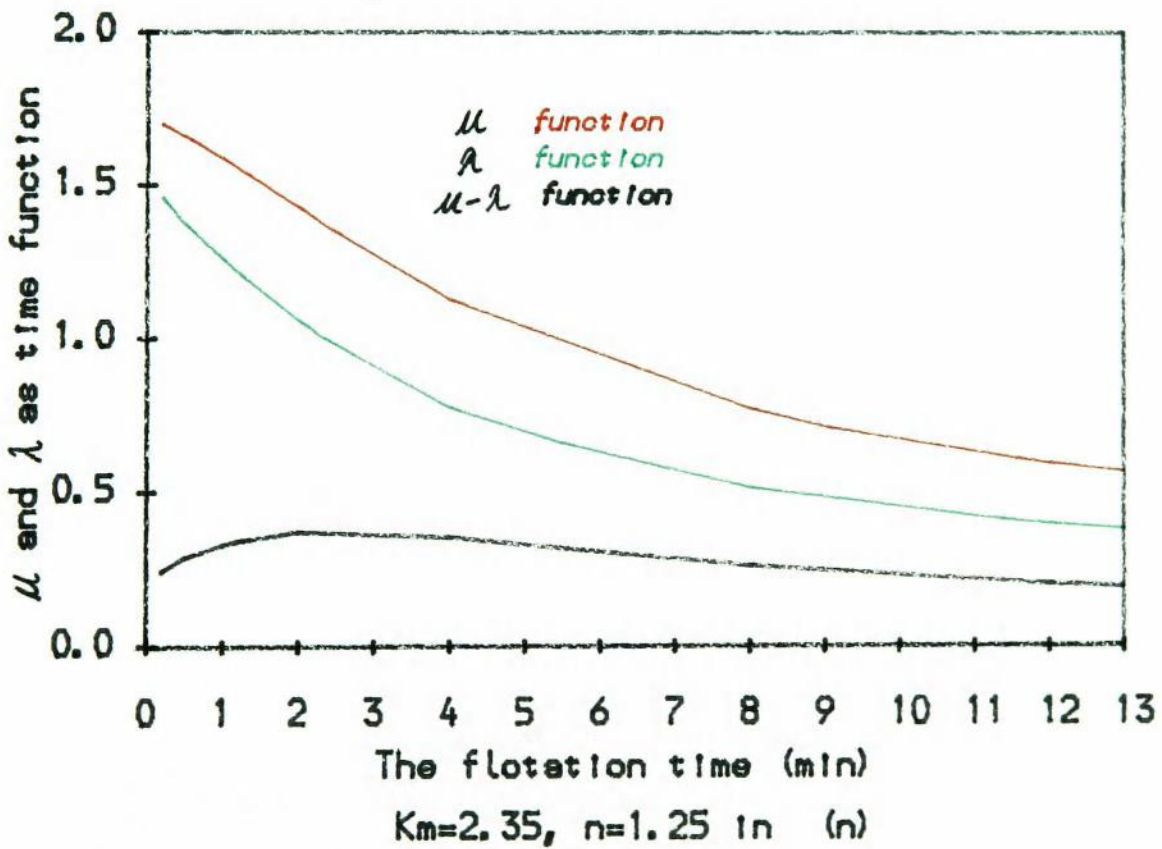
Fig 3-2. μ and λ in GFM

1) If the flotation feed is a combination of different species, each of which possess a different flotation rate constant and obeys the first order kinetic process, when $\Phi(k,0)$ is used as the distribution of flotation rate constants, the mean rate of flotation at a given flotation time would be given by eq.(3.15).

2) From the theorem of weighted mean of an integral, there exists two values of $\mu(t)$ and $\lambda(t)$ between zero and Km which satisfies eq.(3.16).

3) From eq. (3.16) the following equations can be obtained:-

$$\mu(t) - \lambda(t) = -\frac{1}{t} \cdot \ln \frac{\int_0^{K_m} k \cdot \Phi(k,0) \cdot \exp(-k \cdot t) \cdot dk}{\int_0^{K_m} \Phi(k,0) \cdot \exp(-k \cdot t) \cdot dk} \tag{3.19}$$

and when t tends to zero:

$$\lim_{t \to 0} \ln \frac{\int_0^{K_m} k \cdot \Phi(k,0) \cdot \exp(-k \cdot t) \cdot dk}{K_0 \cdot \int_0^{K_m} \Phi(k,0) \cdot \exp(-k \cdot t) \cdot dk} = \lim_{t \to 0} \ln 1 \tag{3.20}$$

when t tends to a very large value M:

$$\lim_{t \to M} \ln \frac{\int_0^{K_m} k \cdot \Phi(k,0) \cdot \exp(-k \cdot t) \cdot dk}{K_0 \cdot \int_0^{K_m} \Phi(k,0) \cdot \exp(-k \cdot t) \cdot dk} = \lim_{t \to M} \ln 0 \tag{3.21}$$

4) If the two case in 3) must be satisfied, suitable simple equations are possibly:-

$$\ln \frac{\int_0^{K_m} k \cdot \Phi(k,0) \cdot \exp(-k \cdot t) \cdot dk}{K_0 \cdot \int_0^{K_m} \Phi(k,0) \cdot \exp(-k \cdot t) \cdot dk} = \ln \frac{1}{1 + g \cdot t} \tag{3.22}$$

or

$$\ln \frac{\int_0^{K_m} k \cdot \Phi(k,0) \cdot \exp(-k \cdot t) \cdot dk}{K_0 \cdot \int_0^{K_m} \Phi(k,0) \cdot \exp(-k \cdot t) \cdot dk} = \ln(\exp(-g \cdot t)) = -g \cdot t$$

Where the second assumption will result in the existing Chen's model and the first will result in:-

$$\mu(t) - \lambda(t) = -\frac{1}{t} \cdot \ln\left(\frac{1}{1+g \cdot t}\right) \tag{3.23}$$

By combining the eq. (3.17) and (3.23), the MCM will be obtained:-

$$\overline{K(t)} = K_0 \cdot \left(\frac{1}{1+g \cdot t}\right) \tag{3.24}$$

Since both mass recovery and recovery are first order kinetic processes, therefore mass recovery model will be given by:-

$$C(t) = C_0 \cdot (1 + g \cdot t)^{(-K_0/g)} \tag{3.25}$$

and for recovery:

$$R(t) = R_0 \cdot (1 + g' \cdot t)^{(-K_0'/g')} \tag{3.26}$$

Where:

g', g are parameters.

K'_0, K_0 are weighted mean flotation rate constants for valuable and mass.

From the mass recovery and recovery models, the grade change in the pulp phase can be calculated by the model:-

$$G(t) = \frac{R(t) \cdot G_0}{C(t)} = \frac{(1 + g \cdot t)^{(K_g/g)}}{(1 + g' \cdot t)^{(K_0'/g')}} \cdot G_0 \qquad (3.27)$$

and the concentrate grade would be:

$$G_c(t) = \frac{1 - (1 + g' \cdot t)^{-(K'_g/g')}}{1 - (1 + g \cdot t)^{-(K_g/g)}} \cdot G_0 \qquad (3.28)$$

Where:

G_0 is the grade of feed.

$G_c(t)$ is the grade of concentrate at t.

In the equations above, it can be seen that both the grades of tailing and concentrate are related to the feed grade.

3.3.4 Analysis of MCM

This section is composed of two subsections, one of which is devoted to a comparison between the MCM and the gamma function model with respect to the parameters in the models, whilst the other is an analyses of the advantages of the MCM.

3.3.4.1 MCM and gamma function model

In chapter 2, the continuous distribution model using the gamma function was reviewed, the final result after integration from zero to infinity is obtained in the literature as:-

$$R(t) = \left(\frac{1}{1 + K_m \cdot t} \right)^{n+1}$$

from the equation above the mean rate could be obtained:

$$K(t) = \frac{n \cdot K_m}{1 + K_m \cdot t} \tag{3.29}$$

Where:

n is a power exponent.

Comparing the eq. (3.29) with the eq. (3.26) in the previous section, the relationship between parameters could be obtained, so that:

$$K'_0 = n \cdot K_m$$

and

$$g' = K_m \tag{3.30}$$

Since g' is the parameter which represents the rate of reduction of the mean flotation rate, Km in the gamma function model will be same as g'. In the gamma function model 'n' represents the ratio of Ko' to g'.

3.3.4.2 The features of MCM

The MCM has two advantages in general, which are:-

1) The modified models can be used to predict not only the recovery but also the grade of concentrate.

2) The MCM employs fewer parameters than the CDM, the parameters are also consistent in data fitting.

In fact the development of flotation models primarily involves seeking equations which fit experimental data and satisfy the two points above.

3.4 Development of the Gamma Function Model (GFM)

In the continuous distribution models, either the gamma function or the bimodal gamma function distribution is frequently used. However neither is capable of calculating concentrate grade. In the following text, the GFM is developed. From the developed GFM, both recovery and grade of concentrate can be calculated.

3.4.1 Gamma function model

There is an improvement in going from a discrete model to a continuous distribution model due to the fact that the flotation feed is obviously a heterogeneous material which can hardly be divided into finite species. However, from the existing information about the relationship between floatability and the physical properties of the particles, such as particle size and the proportional surface coverage by value in the composite, a continuous distribution is very difficult to achieve. Among the continuous distribution models, the gamma function model is widely accepted because of its simplicity and robustness in fitting the experiment results. The distributions using the gamma function proposed by Harris (Harris and Chakravarti 1970) is shown below:-

$$\Phi(k,0) = \frac{1}{K_m \cdot \Gamma(n)} \cdot \left(\frac{k}{K_m}\right)^{(n-1)} \cdot \exp\left(-\frac{k}{K_m}\right) \tag{3.31}$$

Where:

Km   the maximum flotation rate.

$\Gamma(n)$ gamma function.

$\Phi(k,0)$ the distribution of fraction with flotation rate constant k.

n   the power exponent of gamma function

When the upper limit of the integral is finite, the integration of gamma function becomes difficult. Therefore most of the researchers in treating this problem have extended the upper limit of the integral to infinity. In this case, the gamma function model becomes:-

$$R(t) = \left(\frac{1}{1+K_m \cdot t}\right)^{n+1} \qquad (3.32)$$

There is some disagreement in treating the upper limit of the integral, the people in favour of infinity thought that it is unlikely that the distribution of $\Phi(k,0)$ terminates abruptly, the people who disagree with infinity thought there will be no particles which can possess the flotation rate constant greater than that of pure mineral, and the flotation rate constant of pure mineral particles is limited dependent on the properties of the mineral. The finite upper limit was reported to have a better fit to the experiment results. (Loveday 1966).

3.4.2 Modified GFM

Instead of using the gamma function only for recovery model, mass recovery is also assumed to be described using a gamma function distribution. When the mass recovery is assumed to use a gamma function model, the upper limit of the integral of the gamma function cannot be assumed to be infinity since this does not support the relationship of flotation rate constants and the fractional grade. The modification of GFM is carried out in the following three steps.

1) The general assumptions are:-

a) The grade of a fraction which is in a small interval of flotation rate constants k to k+dk can be taken as constant when the interval is sufficiently small.

b) The grade changes continuously from one fraction to the next, that is, when one fraction is in a small interval from k to k+dk and the next interval from k+dk to k+2dk, their grade is very close.

c) The grade of a small interval of k to k+dk has a unique value.

Therefore, on these three assumptions, the grade becomes a function of flotation rate which satisfies continuity and singularity. The relationship between mass and element recovery can also be expressed:-

$$G(k) = \frac{G_0 \cdot R(k,0)}{C(k,0)} \qquad (3.33)$$

Where:

$G(k)$ is grade function.

$R(k,0)$ is recovery distribution.

$C(k,0)$ is mass distribution.

2) From the CDM, it is proven that the mass recovery has a similar behaviour to recovery. Therefore the gamma function (as Woodburn and Loveday's model, 1965) can fit both recovery and mass recovery:-

$$C(k,0) = N \cdot \exp(-k) \cdot k^{(n-1)} \qquad (3.34)$$

$$R(k,0) = M \cdot \exp(-k) \cdot k^{(m-1)} \qquad (3.35)$$

Where n and m are parameters of the gamma function and N and M are coefficients of the gamma function.

$$N = \frac{1}{\int_0^{K_m} \exp(-k) \cdot k^{(n-1)} dk}$$

$$M = \frac{1}{\int_0^{K_m} \exp(-k) \cdot k^{(m-1)} dk}$$

c) By combining eq. (3.33) and (3.34) (3.35), a function related to G(k) (grade distribution) will be obtained as below:-

$$G(k) = G_0 \cdot \frac{M}{N} \cdot k^{(m-n)} \qquad (3.36)$$

From the equation above, it can be seen that the relationship between grade and flotation rate constant is a power function. In pure mineral flotation, m is equal to n and G(k) will be a constant which equals the feed grade.

By analyzing the grade function, we can find that while flotation rate extends to infinity, the grade of the corresponding fraction will also extends to infinity, which is obviously not possible. Therefore in conclusion, the flotation rate constants cannot extend to infinity.

So far, the modified GFM of mass recovery and recovery has been obtained, which are:-

$$\frac{R(t)}{R_\infty} = \int_0^{K_m} M \cdot \exp(-k + k \cdot t) \cdot k^{(m-1)} \cdot dk \qquad (3.37)$$

$$\frac{C(t)}{C_\infty} = \int_0^{K_m} N \cdot \exp(-k + k \cdot t) \cdot k^{(n-1)} \cdot dk \qquad (3.38)$$

3.4.3 Analysis of modified GFM

The modified GFM will be proven by experimental results in the following chapter.

In the modifled GFM, when pure mineral is not used, a graph of recovery and mass recovery will show that the recovery curve is above the mass recovery curve. Therefore the value of m is greater than n. It follows that as can be seen in eq. (3.36) for $G(k)$, the species with the higher flotation rate constant will have the higher fractional grades. In R(k,0) and C(k,0) the distribution will also show that more fractions lie in the higher flotation rate constants in the eq. (3.35) for R(k,0) than in that (eq. 3.34) for C(k,0).

Generally, the modified GFM is better than the discrete model because the GFM employs fewer parameters. Although the modified GFM involves a more complicated calculation, it is solvable by means of a computer.

3.4 Summary

By adding the mass recovery into flotation models, the prediction of both the recovery and grade of concentrate becomes possible. This improvement is achieved with the three types of existing kinetic model, namely, discrete, mean rate and the gamma function models. From the features of the modified models, it can be concluded that:-

1) All the new models are capable of the calculation of not only the recovery to but also the grade of concentrate.

2) The parameters in the models are clearly defined.

3) The number of parameters in the new models are minimised without losing accuracy in prediction of the recovery and grade.

The developed models are:-

1) CDM for concentrate grade and recovery:-

$$G_c(t) = \frac{1 - \sum R_{i0} \cdot \exp(-K_i \cdot t)}{1 - \sum C_{i0} \cdot \exp(-k_i \cdot t)} \cdot G_0$$

$$R_c = 1 - \sum_{i=1}^{n} R_{i0} \cdot \exp(-K_i \cdot t)$$

2) MCM for concentrate grade and recovery:-

$$G_c(t) = \frac{1 - (1 + g' \cdot t)^{(-K'_0/g')}}{1 - (1 + g \cdot t)^{(-K_0/g)}} \cdot G_0$$

$$R_c(t) = R_0(1 - (1 + g' \cdot t)^{(-K_0'/g')})$$

3) GFM for concentrate grade and recovery:-

$$G_c(t) = \frac{1 - \int M \cdot \exp(-k + k \cdot t)k^{(m-1)} \cdot dk}{1 - \int N \exp(-k + k \cdot t)k^{(n-1)} \cdot dk} \cdot G_0$$

$$R_c(t) = 1 - \int_0^{k_m} M \cdot \exp(-k + k \cdot t)k^{(m-1)} \cdot dk$$

Chapter Four

Evaluation of Parameters by Computational Methods

4.1 Introduction

Although there are many methods of evaluating the parameters in flotation models, computer curve fitting has proved to be the must efficient one (Ersayin S. 1986, Ball B. et al 1974, Black, K. G. et al 1972, Carpenter B. H. et al 1965, Lewis C. L. 1971). In this chapter, their use is discussed in the fitting of experimental data.

Since errors are inevitable during the evaluation of parameters, attention is also paid to the analysis of errors which are associated either with the calculation methods or with the performance of the experiments.

4.2 Starting Time and unfloatable fraction

In batch flotation, the start of flotation is neither the time at which air is turned on nor the time from which the first sample is collected. The start of flotation is actually at some indeterminate time between these two events. Both times are likely to be different to the starting time calculated as that which gives the best fit to the flotation model. However for convenience, the starting time from the model fitting is used as the real flotation start and the difference between this starting time and the moment the clock is started is called the starting time error.

In the flotation feed, the unfloatable fraction is a fraction which is actually unrecoverable under certain flotation conditions. The error associated with the unfloatable fraction is usually due to the limit of flotation time and the effect of inadequate operational conditions.

4.2.1 The effect of starting time error

Starting time error is inevitable due to two factors:-

1) In batch testing, there is a short period between the moment when air is turned on and the time at which collection of the concentrate starts. This period is usually called the froth building time (King R.P et al 1974, Laplant A. R. et al 1983b). Flotation starts at some point during this time.

2) The concentration of hydrophobic particles is highest at the beginning of a test. As soon as air is turned on, most of the hydrophobic particles tend to float in a few seconds, during this period flotation might be hindered and the first order rate equation may no longer be able to fit the data (Bull W.R 1966, Laplant, A.R et al 1983a, Jameson, G.J. et al 1977, Harris C.C. et al 1966).

The effect of starting time error on flotation is great because of the exponential nature of the flotation rate. The effect can be analyzed as follows:

If flotation started at t, and the clock was turned on dt before t, i.e, time error dt, for a single species, the recovery would have a error given by:-

$$dR_i = R_{i0} \cdot \exp(-K_i \cdot t) \cdot (1 - \exp(-K_i \cdot dt)) \tag{4.1}$$

In the equation above, the recovery error caused by dt is largely dependent on the flotation rate and the flotation time.

In practice, starting time error is normally less than two seconds, and the value of flotation rate less than six. Therefore the approximation of $\exp(-k \cdot dt)$ may be represented by eq.(4.2) with a level of error less than 2.5%.

$$\exp(-K_1 \cdot dt) = 1 - K_i \cdot dt \tag{4.2}$$

Substituting eq. (4.2) to eq. (4.1), a simple relationship between dR and dt can be obtained:

$$dR_i = R_{i0} \cdot \exp(-K_i \cdot t) \cdot K_i \cdot dt \qquad (4.3)$$

When the flotation time is zero, the equation (4.3) will have the maximum error:-

$$dR_{im} = R_{i0} \cdot K_i \cdot dt \qquad (4.4)$$

Where:

dR_{im} is the maximum error in the recovery.

It can be seen that the error of recovery dRi caused by dt could be several times bigger than dt during the first few seconds of flotation since Ki actually amplifies the error. Therefore the effect of starting time error will be mostly shown on the first two concentrates during the test, and a positive dt will lead a positive dRi.

4.2.2 The effect of unfloatable fraction

The unfloatable fraction is composed of three fractions:-

1) In the flotation feed, free liberated gangue will most likely be unfloatable, which is most of the unfloatable fraction in mass terms.

2) The composite particles with a high gangue surface coverage will be unrecoverable when their size is large, which is most of the unfloatable fraction in value terms (Johnson, N.M. 1972, Lynch, A.J. et al 1981).

3) Finally a small portion of liberated valuable particles may also become unfloatable due to slime coating or lack of collector, etc. This fraction is also a unfloatable fraction in value term (Gaudin, A.M. 1931, 1957, Bushell, C.H. 1962).

Beside these three categories, some other species might also contribute to the unfloatable fraction. However, compared to these three listed, the other species, such as the presence of extra coarse or extra fine particles of liberated valuable mineral, are marginal.

The effect of the unfloatable fraction on flotation recovery is also large which can be demonstrated as follows.

If R_{io} is an error introduced by the unfloatable fraction, the recovery error associated with Ro can be represented by:-

$$dR_i = \exp(-K_i \cdot t) \cdot dR_{io} \qquad (4.5)$$

When t equal zero, the maximum error in dR_i occurs:-

$$dR_{im} = dR_{io} \qquad (4.6)$$

Comparing eqs. (4.4) and (4.6), the effect of unfloatable fraction error seems less important than the starting time error. However since the level of error in the unfloatable fraction is far higher than that of starting time, the effect of the unfloatable fraction error is not negligible and largely presented in the first two concentrates.

4.2.3 The method of correcting errors

Methods for the correction of the errors associated with starting time and unfloatable fraction vary greatly in the literature (Carpenter, B.H. 1965, Wu, Y.R. 1986, Kapur, P. C. et al 1974). However two methods are typical.

1) A simple method for eliminating the effect of starting time error and unfloatable fraction error is to discard the first flotation product of each test (Laplante

A.R. 1982). This method is only effective when a graphical method is used for calculating the flotation rate constants with sufficient flotation products. In this method, the effect of the first product is ignored.

2) The method of computer aided parameter evaluation using curve fitting techniques is widely accepted when the number of products is limited. This method usually employs a Simplex search (Ersayin S. 1986, Carpenter, B.H. 1965). In order to obtain an accurate solution of starting time and unfloatable fraction, this method is very time consuming, because the starting time and unfloatable fraction must be added to the Simplex and grid search of flotation rates.

In the following text, an alternative approach is developed to solve the problems.

a) From eq. (4.3), it is shown that in a multi-species system the error in recovery associated with error of flotation time is:

$$dR = \sum_{i=1}^{n} R_{i0} \cdot \exp(-K_i \cdot t) \cdot K_i \cdot dt \qquad (4.7)$$

when t equal to t_j, dR_j can be written as:

$$dR = R_j - \sum_{i=1}^{n} R_{i0} \cdot \exp(-K_i \cdot t_j) \qquad (4.8)$$

When dR in the eq. (4.7) is substituted by dR above, dt may be represented such that:-

$$dt_j = \frac{R_j - \sum R_{i0} \cdot \exp(-K_i \cdot t_j)}{\sum R_{i0} \cdot K_i \cdot \exp(-K_i \cdot t_j)} \qquad (4.9)$$

In a continuous distribution model:-

$$dt_j = \frac{R_j - \int_0^{K_m} \Phi(k,0) \cdot \exp(-k \cdot t_j) \cdot dk}{\int_0^{K_m} \Phi(k,0) \cdot \exp(-k \cdot t_j) \cdot dk} \qquad (4.10)$$

If several products exist, the mean value of dt_j may be written as the following equation:-

$$dt = \frac{1}{m} \cdot \sum_{j=1}^{m} dt_j \qquad (4.11)$$

Where:

m is the number of products

t_j is the time measured for the jth product

R_j is the recovery in the tailing stream at t_j

K_i is the flotation rate of ith species.

R_{i0} is the fraction of valuable in ith species.

b) By using eq. (3.5) and a similar procedure, the unfloatable fraction will have the equation below:

$$dR_\infty = \frac{1}{m} \cdot \sum_{j=1}^{m} \frac{R_j - \sum R_{i0} \cdot \exp(-K_i \cdot t_j)}{\sum R_{i0} \cdot \exp(-K_i \cdot t_j)} \qquad (4.12)$$

In continuous distribution models:

$$dR_\infty = \frac{1}{m} \cdot \sum_{j=1}^{m} \frac{R_j - \int_0^{K_m} \Phi(k,0) \cdot \exp(-k \cdot t_j) \cdot dk}{\int_0^{K_m} \Phi(k,0) \cdot \exp(-k \cdot t_j) \cdot dk} \qquad (4.13)$$

When Rio and ki are calculated by a grid search, eq.(4.12) and (4.13) can be used to calculate dt and dR_ω. Then t and dR_ω can be corrected, new values of Rio and ki can be again obtained by a Simplex search until the model fits the experimental data within a predetermined tolerance level.

4.3 Computational method for CDM

A Simplex search for the parameters, Ki and a multi-linear regression technique for Rio, Cio are used in the computer program for CDM. In the program, when the cumulative mass recovery and recovery are input, the grade and mass fraction of each species are calculated.

4.3.1 Mathematical procedures

In eqs. (3.9), (3.10) in chapter three, when m products are obtained during flotation, the mass recovery $C_c(t_j)$ and recovery $R_c(t_j)$ can be represented by the following equations:

$$R_c(t_j) = 1 - \sum_{j=1}^{n} R_{i0} \cdot \exp(-K_i \cdot t_j)$$

$$C_c(t_j) = 1 - \sum_{j=1}^{n} C_{i0} \cdot \exp(-K_i \cdot t_j) \tag{4.14}$$

Where:

n is number of species in the same size group.

When a matrix is employed, the equations above become:-

$$|R(t)|_{m \times 1} = |A|_{m \times n} \times |R_0|_{n \times 1} \tag{4.15}$$

$$|C(t)|_{m \times 1} = |A|_{m \times n} \times |C_0|_{n \times 1} \tag{4.16}$$

Where:

$$|A| = \begin{bmatrix} e^{-k_1 t_1} & e^{-k_2 t_1} & \cdots & e^{-k_m t_1} \\ e^{-k_1 t_2} & e^{-k_2 t_2} & \cdots & e^{-k_m t_2} \\ \cdots & & & \\ e^{-k_1 t_n} & e^{-k_2 t_n} & \cdots & e^{-k_m t_n} \end{bmatrix}$$

$$|R(t)| = \begin{bmatrix} 1 - R_c(t_1) \\ 1 - R_c(t_2) \\ \cdots \\ 1 - R_c(t_m) \end{bmatrix} \tag{4.17}$$

$$|C(t)| = \begin{bmatrix} 1 - C_c(t_1) \\ 1 - C_c(t_2) \\ \cdots \\ 1 - C_c(t_m) \end{bmatrix} \tag{4.18}$$

$$|R_0| = \begin{bmatrix} R_{10} \\ R_{20} \\ R_{30} \\ \cdots \\ R_{n0} \end{bmatrix} \qquad |C_0| = \begin{bmatrix} C_{10} \\ C_{20} \\ C_{30} \\ \cdots \\ C_{n0} \end{bmatrix}$$

The combination of the eq. (4.15), (4.16) will result in:-

$$\begin{bmatrix} A & 0 \\ 0 & A \end{bmatrix} \times \begin{bmatrix} \alpha \cdot C_0 \\ R_0 \end{bmatrix} = \begin{bmatrix} \alpha \cdot C(t) \\ R(t) \end{bmatrix} \tag{4.19}$$

Where:

α is a multiplier.

The value α is the ratio of the maximum value of Rc to Cc, which enables the levels of errors to be the same for both mass recovery and recovery.

From eq. (4.17) it can been seen that $|C_0|$ and $|R_0|$ can be obtained by a multi-linear regression while Ki is obtained by a Simplex search.

4.3.2 Computer program

A diagram of the computer program for CDM is shown in Fig 4-1. In the program, when cumulative Rc(t) and Cc(t) and corresponding flotation times are input, a grid search will start to find the optimum start point for a Simplex search. From the Simplex search Ki will be obtained, meanwhile, a multi-linear regression will also obtain the value of $|C_0|$ and $|R_0|$. On completion of the program, the grade of each species will be calculated from $|C_0|$ and $|R_0|$. Finally the result of the fit will be output.

During the search for the optimum Ki, the standard deviation of measured and calculated Cc and Rc is minimized, represented by:-

$$STD = \sum_{j=1}^{m} [R_c(t_j) - R_{cc}(t_j)]^2 + \{\alpha \cdot [C_c(t_j) - C_{cc}(t_j)]\}^2 \tag{4.20}$$

The Simplex search of Nelder and Mead is employed in the program (Nelder J.A. And Mead R.1965). The presence of the grid search in the program is to avoid a local minimum point of standard deviation in the n dimensional space of Ki.

The multi-linear regression is a combination of Least-square method and the Gaussian Elimination with Backward Substitution for linear system (Burden R.L. And Faires J.D. 1985).
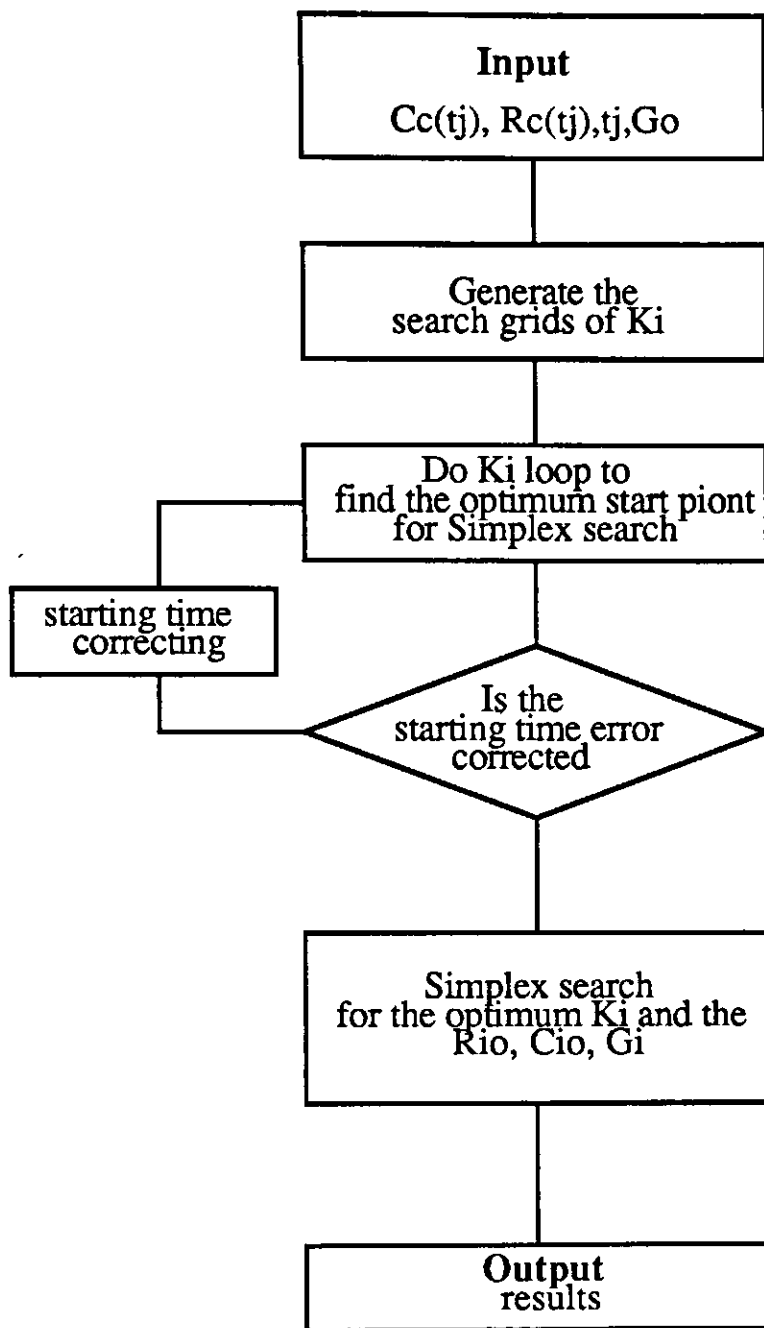
Fig 4-1   Diagram of CDM program

4.4 Computer programs for MCM

Based on the same procedures as the **CDM**, a program of **MCM** has been developed. Since fewer parameters are included, the program for **MCM** is simpler than that for **CDM**. The details of the program will be discussed in the following text.

In the **MCM**, the models of mass recovery and recovery become:- (refer to eqs. 3.25, 3.26 in Chapter 3)

$$\frac{C(t)}{C_0} = (1 + g \cdot t)^{\left(-\frac{K_0}{t}\right)} \tag{4.21}$$

$$\frac{R(t)}{R_0} = (1 + g' \cdot t)^{\left(-\frac{K_0'}{t'}\right)} \tag{4.22}$$

When a natural logarithm scale is applied to both sides of the equations (4.21), (4.22) and a substitution is conducted such that:

$$Y_1 = \ln C(t) = \ln(1 - C_c(t))$$

and

$$X = 1 + g \cdot t$$

$$A_1 = -\frac{K_0}{g}$$

$$B_1 = \ln C_0$$

and

$$A_2 = -\frac{K_0'}{g'}$$

$$Y_2 = \ln R(t) = \ln(1 - R_c(t))$$

$$B_2 = \ln R_0$$

the corresponding equations of (4.21) and (4.22) may be written as:

$$Y_1 = A_1 \cdot X + B_1 \tag{4.23}$$

$$Y_2 = A_2 \cdot X + B_2 \tag{4.24}$$

As a linear system, the parameters in the eqs. (4.23) and (4.24) can be calculated by Linear regression, the g and g' can be optimised by Golden Section Search (Bunday B.D. 1984). The diagram of computer program is shown in Fig 4-2.

4.5 Computational method for GFM

Due to the nature of GFM, numerical integration is used. In the computer program, two functions are included. The first function calculates an approximate value for the parameters by using an infinite upper limit. Then the second function uses the approximated parameters and a numerical integration with a finite upper limit to obtain the final solution of parameters.

4.5.1 Estimation of parameters

Since the GFM with a finite upper limit cannot be transferred into either a linear or a multi-linear system, the parameters in the model cannot be obtained by similar methods as these for CDM. In solving this problem, many methods can be used for obtaining a solution (Harris C.C. et al 1963, Woodburn E.T. 1970, Inoue, T. et al 1980). The following is one such method.
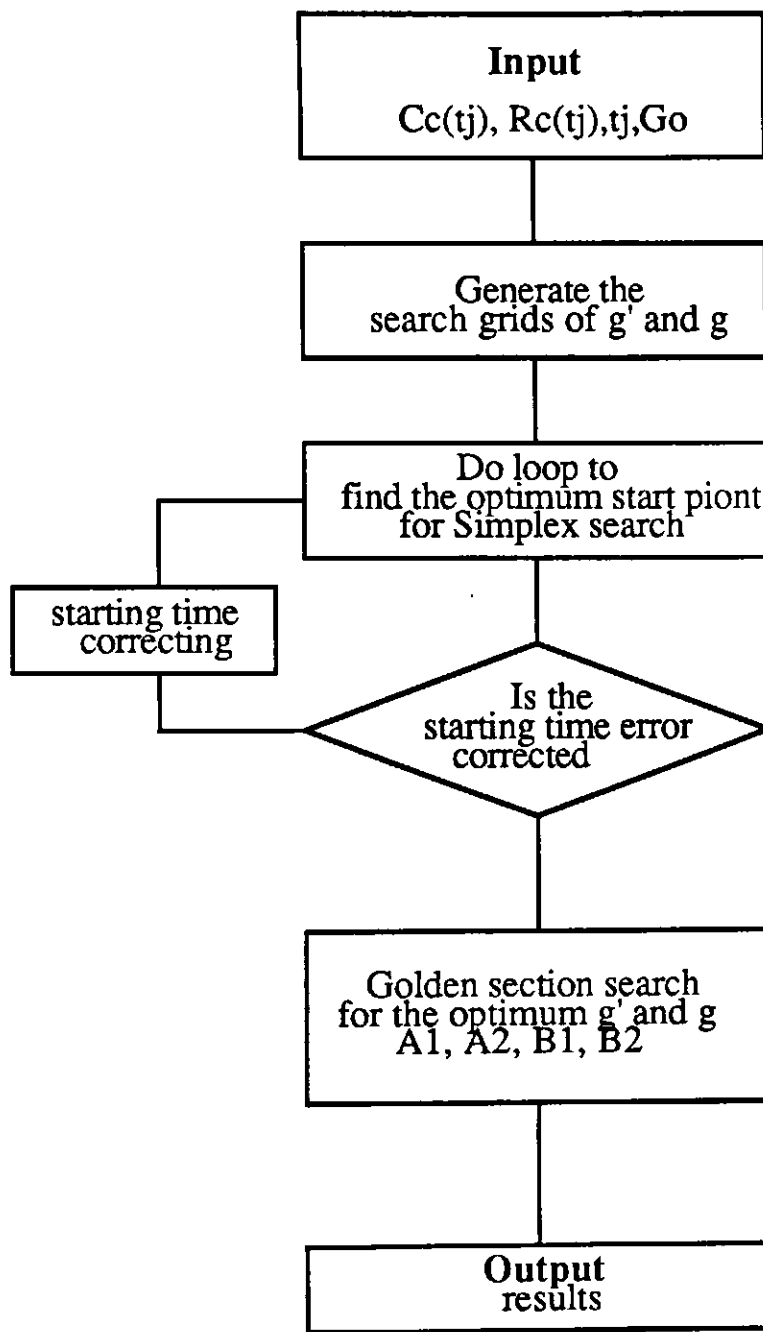
Fig 4-2 Diagram of MCM program

a) In the gamma function, since most of the fractions are distributed in the lower rate constants, the finite upper limit therefore can be replaced by infinity to obtain an approximation to the model parameters (refer to eqs. 3.37, 3.38 in Chapter three).

$$\frac{R(t)}{R_0} = \int_0^\infty \exp(-k(1+t)) \cdot M \cdot k^{m-1} \cdot dk \tag{4.25}$$

$$\frac{C(t)}{C_0} = \int_0^\infty \exp(-k(1+t)) \cdot N \cdot k^{n-1} \cdot dk \tag{4.26}$$

Where:

M, N are the coefficients as defined in Chapter three.

After integration, the corresponding eqs. (4.25) and (4.26) become:-

$$C(t) = C_0 \cdot \left(\frac{1}{1+t}\right)^n \tag{4.27}$$

$$R(t) = R_0 \cdot \left(\frac{1}{1+t}\right)^m \tag{4.28}$$

By taking the natural logarithm of both sides, eq.(4.27) becomes:-

$$\ln C(t) = \ln C_0 + n \cdot \ln\left(\frac{1}{1+t}\right) \tag{4.29}$$

If a substitution of variables is made such that:-

$$Y = \ln C(t) \text{ and } X = \ln\left(\frac{1}{1+t}\right)$$

and $A = \ln C_0$

Eq.(4.29) can be re-written as:-

$$Y = n \cdot x + A \tag{4.30}$$

Similarly eq. (4.28) can be converted to a linear equation:-

$$Y' = m \cdot X' + B \tag{4.31}$$

Once the values of n, m, Ro and Co are obtained, they can be used as an initial point of a Simplex search in the following procedure when the upper limit of the integral is substituted by Km.

4.5.1 Computer program

In the program, if the upper limit of the integral is a variable, a numerical integration will be difficult insofar as the selection of the intervals of the steps. Therefore a substitution of the upper limit is carried out to avoid this problem. The substitution is carried out such that:-

$$X = \frac{k}{K_m}$$

The integrals of mass recovery and recovery models (3-40) and (3-41) in Chapter 3 are re-written as.

$$\frac{R(t)}{R_0} = \int_0^1 M' \cdot \exp(-x \cdot K_m(1+t)) \cdot x^{m-1} \cdot dx \tag{4.32}$$

$$\frac{C(t)}{C_0} = \int_0^1 N' \cdot \exp(-x \cdot K_m(1+t)) \cdot x^{n-1} \cdot dx \tag{4.33}$$

Where:

$$M' = \frac{1}{\int_0^1 \exp(-x \cdot K_m) \cdot x^{m-1} dx}$$

$$N' = \frac{1}{\int_0^1 \exp(-x \cdot K_m) \cdot x^{n-1} dx}$$

When the approximated values of parameters n, m, Ro, Co are obtained in the eq. (4.27),(4.28), they can be used as initial values of Simplex search. The program diagram of GFM is shown in Fig 4-3.

4.6 Summary

When a computer method is used in the evaluation of the model parameters, errors associated with the method will also occur due to several reasons:-

1) In the programs, standard deviations of measured and calculated values are used as an indication of the fit quality. Although a predetermined tolerance is achieved, the final results from the Simplex search may not necessarily be the universal minimum point.

2) Since in the conversion of the function, logarithms are frequently used, errors can also be introduced by this treatment.

3) In the GFM, numerical integration will also increase the errors in fitting the results.

However, in conclusion, even though many possible errors exist, the computer programs for the purpose of parameter evaluation are proved good at fitting experimental data since the standard deviations of measured and calculated values are fully minimised.

```
┌─────────────────────────────┐
│            Input            │
│     Cc(tj), Rc(tj),tj,Go    │
└─────────────────────────────┘
               │
┌─────────────────────────────┐
│       Estimate the n,m      │
│    by using infinity Km     │
└─────────────────────────────┘
               │
┌─────────────────────────────┐
│        Generate the         │
│      search grids of Ki     │
└─────────────────────────────┘
               │
┌─────────────────────────────┐
│         Do Km loop to       │
│  find the optimum start piont│
│      for Simplex search     │
└─────────────────────────────┘
               │
┌──────────────┐
│ starting time│
│  correcting  │
└──────────────┘
               ◇
            Is the
      starting time error
           corrected
               │
┌─────────────────────────────┐
│       Simplex search        │
│     for the optimum Km      │
│         m,n,Ro,Co           │
└─────────────────────────────┘
               │
┌─────────────────────────────┐
│           Output            │
│           results           │
└─────────────────────────────┘
```
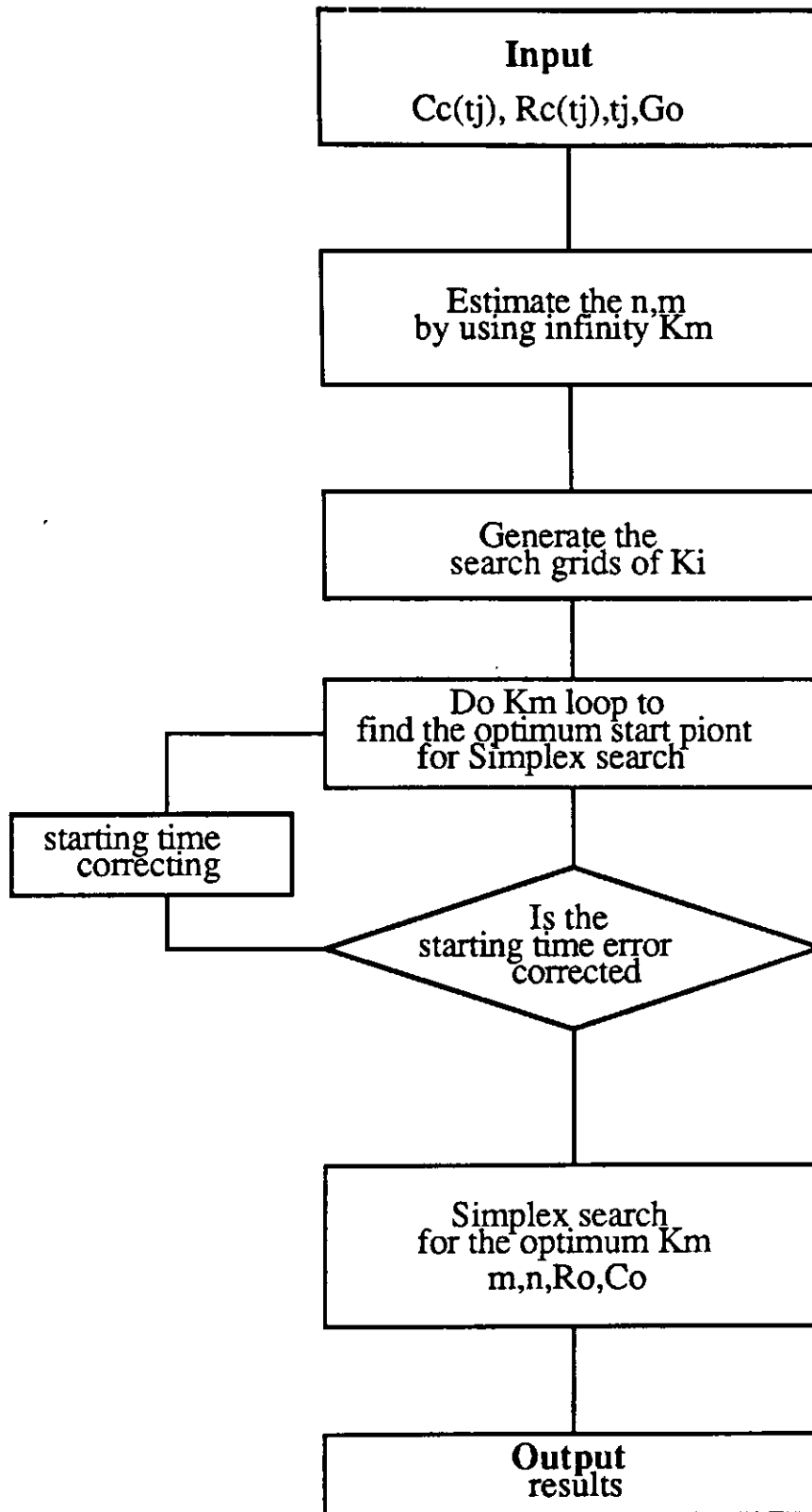
Fig 4-3 Diagram of GFM program

Chapter Five

Experimentation One

--Preliminary test

5.1 Introduction

As has been expressed in Chapter 1, this work is devoted to observe the effect of IPS and AFR on the flotation kinetics of different size fractions. Because the IPS and AFR can affect the bubble surface area and power input into the pulp, which subsequently affects the flotation kinetics, experiments were also carried out to establish the relationships between the AFR, IPS, bubble sizes and power input. In the standardization of flotation procedures, a chalcopyrite ore sample from Santiago, N.W. Spain, was used since considerable work had been previously carried out by Ersayin (Ersayin S. 1986) and Osborn (Osborn G. 1984).

5.2 Bubble surface area measurement

The purpose of the measurement of bubble surface is to obtain a general relationship between the AFR, IPS and bubble surface, which will enable the interpretation of the effects of AFR and IPS on flotation rate constants. As it has been noted by Grainger-Allen (1970) that the presence of solids does not affect the generation of air bubbles in the cell, bubble size measurement in this research were carried out in an air-water system.

5.2.1 Bubble size measurement

A photographic method was used in the measurement of bubble size. A camera mounted on a tripod was fixed beside the cell. With the empty cell, a scale was stuck on its inside wall and one photograph was taken for scaling purposes. Then the scale

was removed from the cell. By keeping the camera position unchanged, the cell was filled with three litres of tap water. Then the impeller was turned on and the IPS was adjusted to the required value, 5 ml 1% frother was added, the air was turned on after three minutes.

At different AFR and IPS, photographs were taken using an electronic flash. The successful printing out of the photographs enabled the measurement of bubble size as shown in Fig 5-1.

To minimize errors in the measurement of bubble size, five parallel pencil lines were drawn on each photo. The bubbles crossed by the lines were measured by using a transparent ruler. In cases where the bubble was fast moving, the size was measured along the width. The bubbles adhering to the cell wall were ignored in the measurements. Approximately 30 bubbles were measured in each photograph. The results of the measurement can be referred in Appendix 1.

5.2.2 The calculation of hubble surface area

In the calculation, the bubbles present in the flotation cell were assumed spherical. The mean volume of the bubbles was calculated such that,

$$\overline{Vb} = \frac{\pi}{6} \cdot \frac{1}{n} \cdot \sum_{i=1}^{n} d_i^3 \qquad (5.1)$$

where:

d_i is the diameter of the ith bubble measured.

n is the number of bubbles measured.

$\overline{Vb}$ is the mean of the bubble volume.

By using the mean volume of bubbles, the number of bubbles in the flotation cell can be calculated by the equation below:-
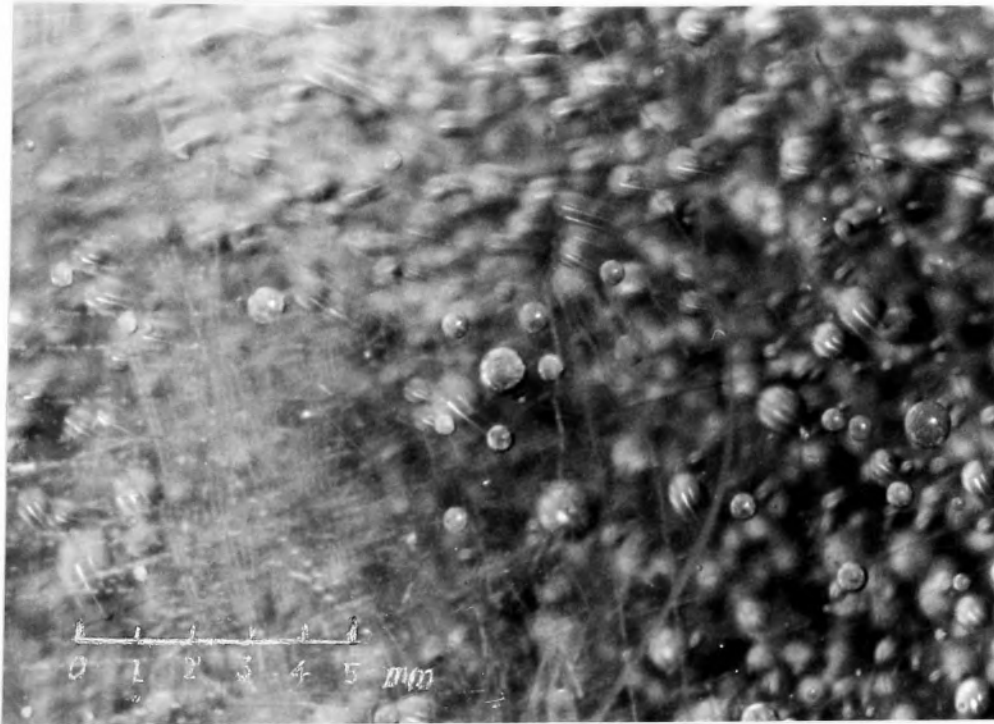
AFR = 1.0   1/min, IPS = 1200 rpm
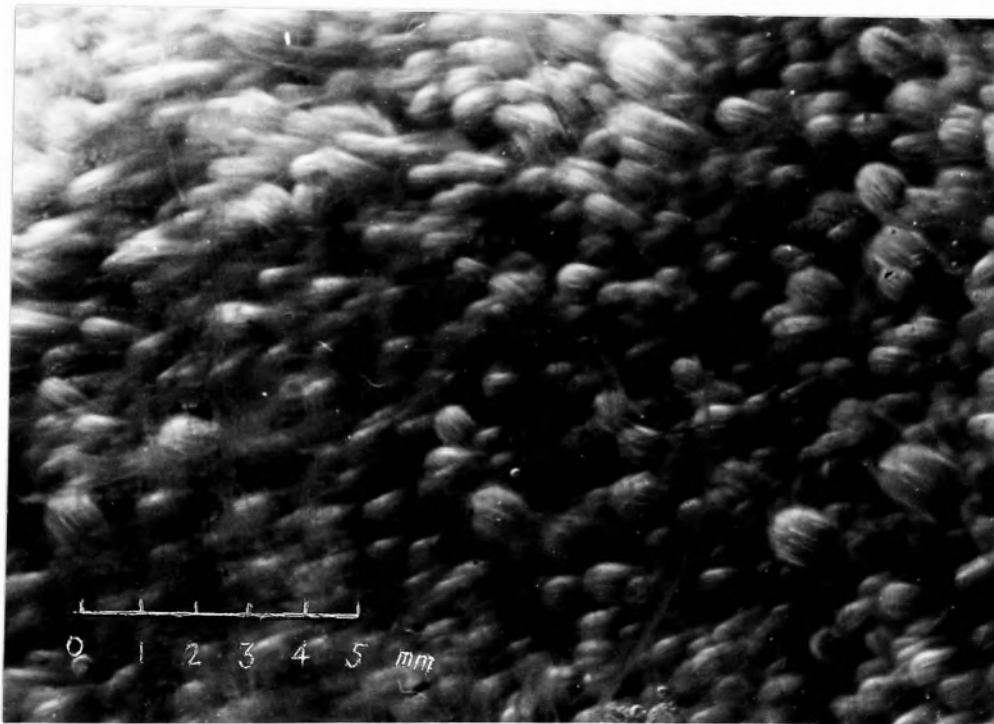
AFR = 7.0   1/min, IPS = 1450 rpm

Fig 5-1   Photographs of bubble size

$$N = \frac{V_a}{\overline{Vb}}$$ (5.2)

Where Va is the volume of water replaced by the air, The value of Va was measured when the AFR and IPS were varied as shown in Appendix 2.

When the total number of bubbles in the flotation cell was obtained, the total surface area of bubbles can be calculated by the equation:-

$$S_t = N \cdot S_m$$ (5.3)

and

$$S_m = \pi^{1/3} \cdot (6 \cdot V_t)^{(2/3)}$$ (5.4)

where:

S_m is the mean surface area of a single bubble.

S_t is the total bubble surface area.

By using the method above, the value of AFR and IPS can be interpreted in terms of bubble surface area.

5.2.3 AFR and bubble surface area

From the experimental results, it is observed that a linear relationship exists between the AFR and the bubble size as it is shown in Fig 5-2. Although a higher AFR would generate slightly bigger bubbles, the change of bubble size has very little effect on their total surface area, as it is shown in Fig 5-3. The effect of AFR on the bubble size and bubble surface area is also dependent on the IPS as can be seen in the same graph.
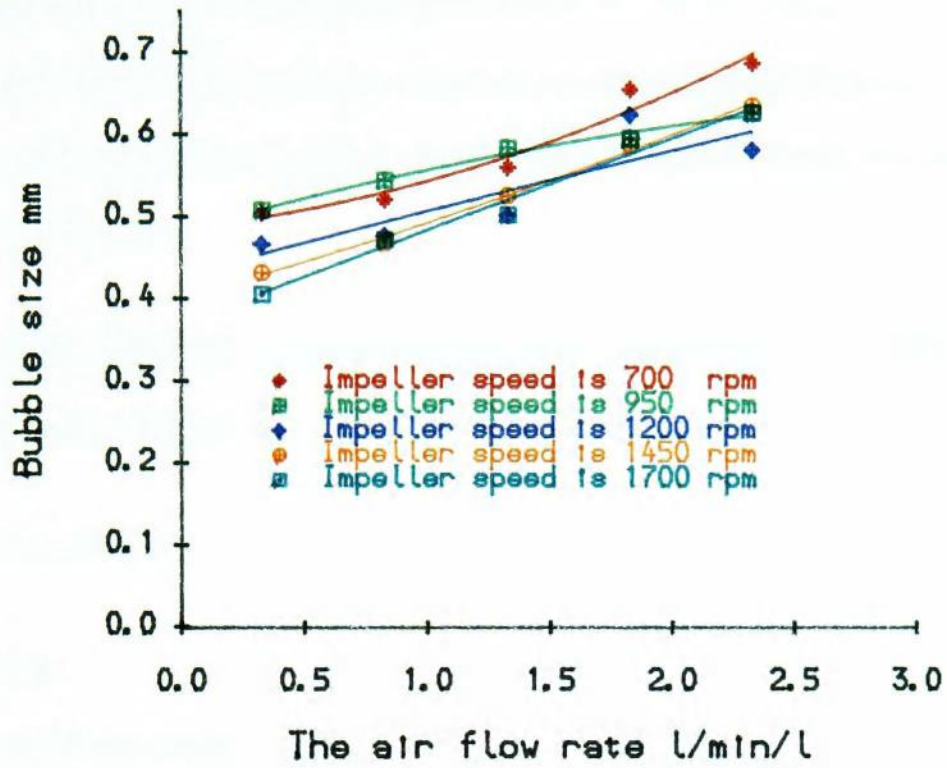
Fig 5-2. AFR and bubble size
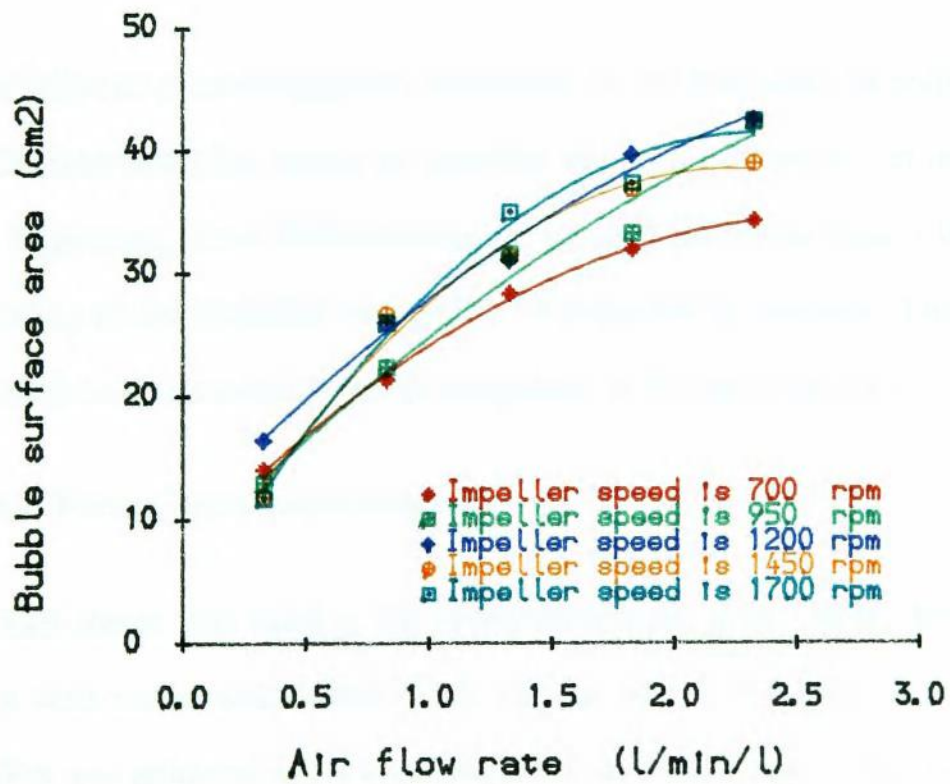
Fig 5-3. AFR and Bubble surface

5.2.4 IPS and bubble surface area

Generally, at a constant AFR, an increase in IPS will result in an improvement in the dispersion of air, the bubble size is therefore reduced. However when AFR is also changed, the relationship between the IPS and bubble size becomes complicated as shown in Fig 5-4.

From Fig 5-4, it is suggested that the relationship between the IPS and the mean of bubble size is linear. It is proposed as shown below:-

$$D = \alpha \cdot IPS + \beta \tag{5.5}$$

Where:

α and β are parameters.

D is the mean of bubble size.

5.3 Power measurement

The flotation process is greatly dependent on the frequency of collision between air bubbles and particles, where an impeller plays an important part in the collision process. In general, when IPS is increased, power input to the pulp is increased, and the frequency of the collision would also be expected to increase. Therefore power input should be measured for the investigation of flotation kinetics.

5.3.1 Power input measurement

A watt meter was used in the measurement of power input. Before flotation started, a watt meter was linked to the control box of flotation cell. With the cell empty, IPS was adjusted to the required value and the power output from the power meter was recorded. This reading was taken as the power consumed by the equipment.
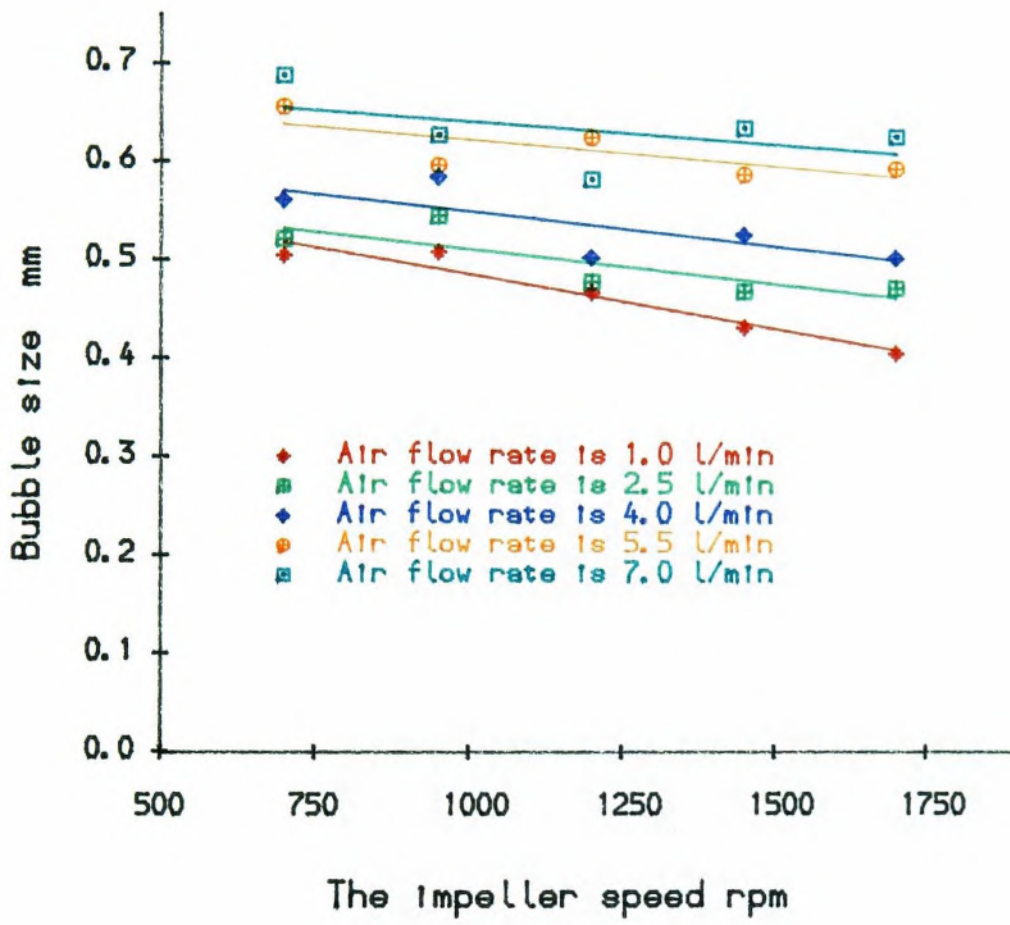
Fig 5-4. IPS and bubble size

Then flotation was performed as normal at the same **IPS**, the power output was again recorded, twice, once at the beginning and then at the end of flotation. The net power for the mixture of flotation pulp is calculated by subtracting the power consumed by the equipment from that of the mean value in normal flotation. The whole procedures were repeated at different **IPS** and **AFR**. The details of the measurement can be referred to in Appendix 3.

5.3.2 Power input and AFR

Since the **AFR** will affect the density and viscosity of the pulp, the power input for the mixture of pulp therefore is also affected by **AFR**. In the test it was noted that the effect of **AFR** on the power input was significant when the **AFR** was changed from 1.0 l/min to 7.0 l/min (that is 0.33 to 2.33 l/min/l). Although the reduction of power input was proportional to the increase of **AFR** in the lower range of **AFR**, over the whole range of **AFR**, the relationship between the power reduction and **AFR** was not linear. This can be seen in Fig 5-5.

5.3.3 IPS and power input

The **IPS** is a major factor which affects the power input to the pulp. As an increase in **IPS** will result in an increase of turbulence in the pulp, the power input to a unit pulp therefore will increase. The relationship between the power input and the **IPS** can been seen in Fig 5-6 as shown below,

Where the unit of **IPS** was rpm and the power input was w/l. At a constant **AFR**, a simple relationship between the **IPS** and power input was observed. An empirical equation was assumed such that,

$$P = A \cdot IPS^b \tag{5.6}$$
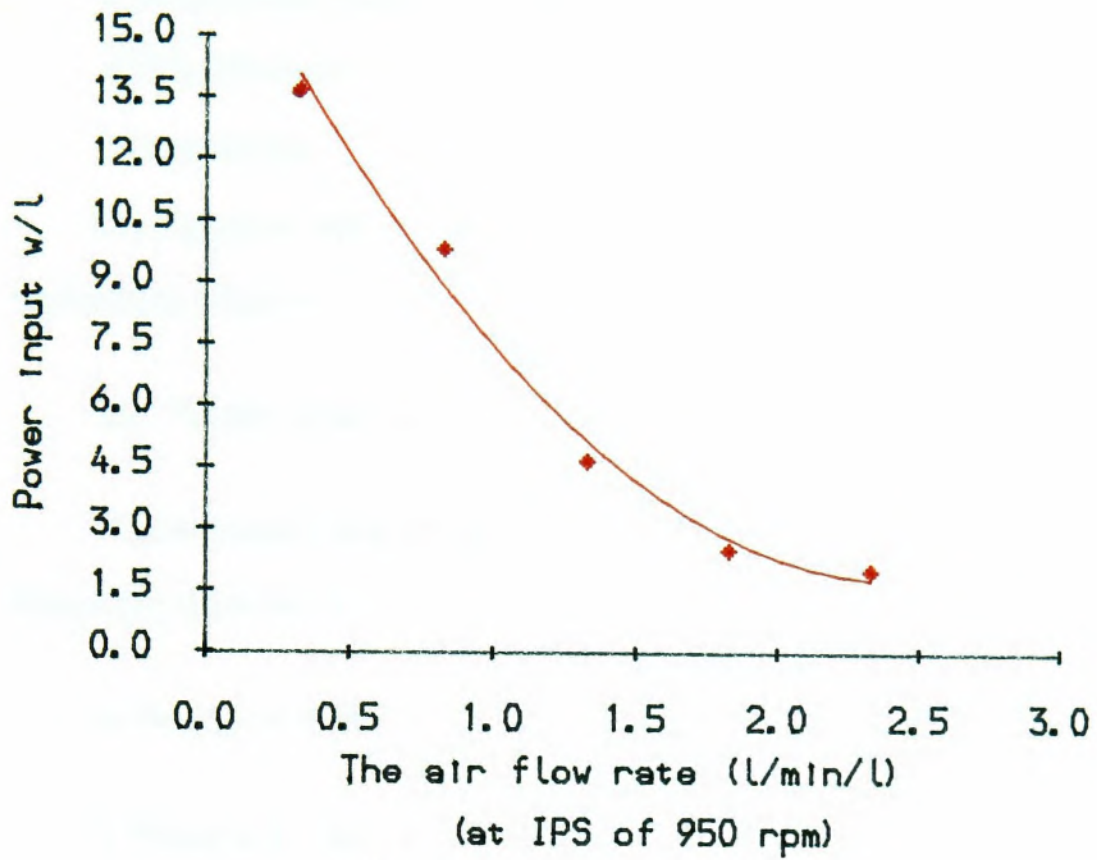
Fig 5-5 AFR and Power Inpu

(at IPS of 950 rpm)
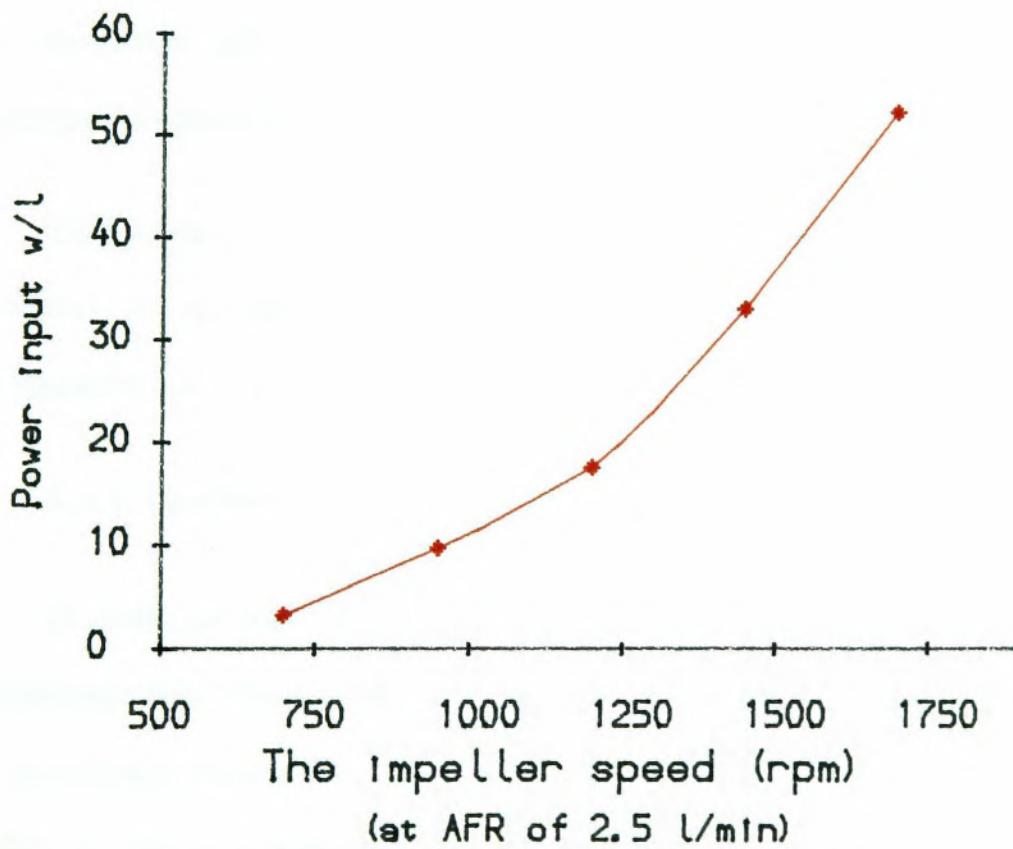
Fig 5-6 IPS and Power Input

(at AFR of 2.5 l/min)

Where:

P is the power input for the mixture. (Watt/l)

A is a parameter.

b is parameter.

The equation will be used for the subsequent interpretation of the IPS effect on flotation kinetics.

5.4 Water recovery measurement

Water recovery is an important factor in the modelling of flotation performance. Water can enter the concentrate launder by different methods as shown:-

1) Water could be trapped in the middle of an aggregation of bubbles.

2) Water is a important part in the bubble film.

3) Water can be absorbed on the particle surface even, without exception, for a hydrophobic particles. Although water is not present on the intimate surface of hydrophobic particles, it could cover the collector layer on the surface of the particle.

Due to the complexity of water recovery, research into the factors affecting is complex. An accurate prediction of water recovery can be as difficult as prediction of flotation recovery. Nevertheless, water recovery has been studied as follows.

5.4.1 Method of water recovery measurement

In water recovery measurement, the procedures carried out were similar to that of flotation test. When a sample was floated, six concentrate products were collected in previously weighed bowls. During flotation, no concentrate washing water was added. As the weight of solid was not significant in the test, a small quantity of solid particles might not have been collected. When the test was finished, the six products

were wet weighed individually. Then, the products were filtered and dried in an oven. The dried products were weighed again. The test was repeated at different **AFR**. The water recovery corresponding to flotation time was calculated by the following equation:-

$$Water(t) = TWW(t) - Bowl - DrW(t) \qquad (5.7)$$

Where:

Water(t) is water recovery at time t.

TWW(t) is the wet weight of product and bowl at time t.

DrW(t) is the weight of dried product at time t.

The details of the results can be referred to in Appendix 4.

5.4.2 AFR and water recovery

Apart from the froth height and the frother dosage, **AFR** was believed to be the most important factor which affects the water recovery. Therefore in the following, the effect of **AFR** on water recovery is studied. When **AFR** was varied from 1.0 to 7.0 l/min, experimental results showed that water recovery was greatly increased. The relationship between the **AFR** and water recovery can be seen in Fig 5-7

The effect of **AFR** on water recovery may be dominated by two mechanism such that:-

1) When flotation starts, a higher **AFR** immediately replaces a larger volume of pulp in flotation cell and consequently more wet froth was obtained in the concentrate.
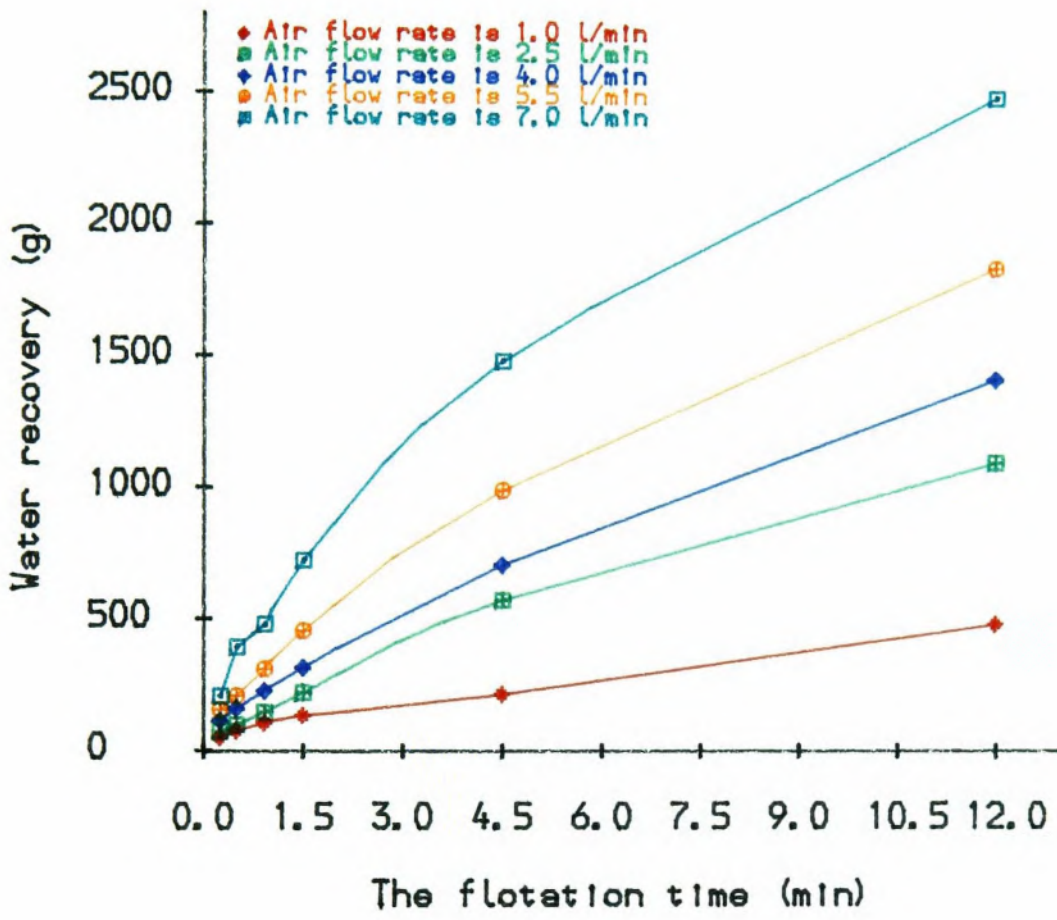
Fig 5-7. AFR and water recovery

2) A higher **AFR** results in a higher rate of bubble production. The higher rate of bubble production leads to a higher transfer rate of bubbles from the pulp to the concentrate launder. Water recovery therefore is increased.

5.5 Chalcopyrite flotation

By using a three litre Leeds Flotation Cell (Dell C.C. 1972, 1981), Chalcopyrite flotation was carried for the standardization of flotation conditions. After the standardisation of the flotation, tests were conducted at different **AFR**.

5.5.1 Sample preparation

An ore sample of 40 Kg with particle size below 30 mm was prepared for subsequent flotation. As oxidization of the ore sample had been noted, particles of size below 6.35 mm were removed by washing through a sieve to eliminate the effect of oxidization. Then the remaining sample was dried on the laboratory floor. After jaw crushing, roller crushing and sieving, 1.0 Kg batch samples with the particle size less than 3.18 mm were obtained by riffling. The batch samples were stored in polythelene bags for subsequent test work.

5.5.2 Grinding time test

Grinding time test was carried out in a Podmore mill which provides a grinding action by vibrating simultaneously two separate cylindrical sample containers (15 cm length by 12 cm diameter) placed on each side. In each sample container, five rods, each of 0.55 Kg, were charged as the grinding media. Both the container and the media were stainless steel. A volume of 150 ml water, followed by 500 g sample and another 150 ml water were put into each container, which made the solids concentration during grinding to be 62.5% in weight.

After grinding, the samples in the two containers were transferred into a 3 litre Leeds flotation cell. Then flotation was carried out up to 7.5 minutes. The grinding time was selected at which the highest copper recovery was obtained by flotation. The corresponding grinding time and the recovery of copper is shown in table 5.1.

Table 5.1 Grinding time test results

Grinding time (Min)	4.0	5.5	7.0	8.5
Flotation Recovery (%)	59.10	73.70	80.28	64.44

From the Table 5.1 it can be seen that when the grinding time was 7.0 minutes, the flotation recovery of copper was the highest with the value of 80.28%.

After the grinding time test, a sieve analysis test was also conducted. The sample was ground for 7.0 minutes, then a representative sample of approximately 100 g of the ground product was wet sieved through a series sieves of British standard. The size distribution was obtained as shown in Fig 5-8.

5.5.3 Standardization of flotation

Because accuracy of the experimental results was vitally important to the flotation models, primary test work was devoted to the standardization of flotation (Apling A.C. 1986). Apart from the flotation cell, the standardisation of operational procedure such as the time at which clock was switched on, pulp level, and the scraping of froth was also standardised.

The three litre Leeds flotation cell designed by Dell has the features of :-
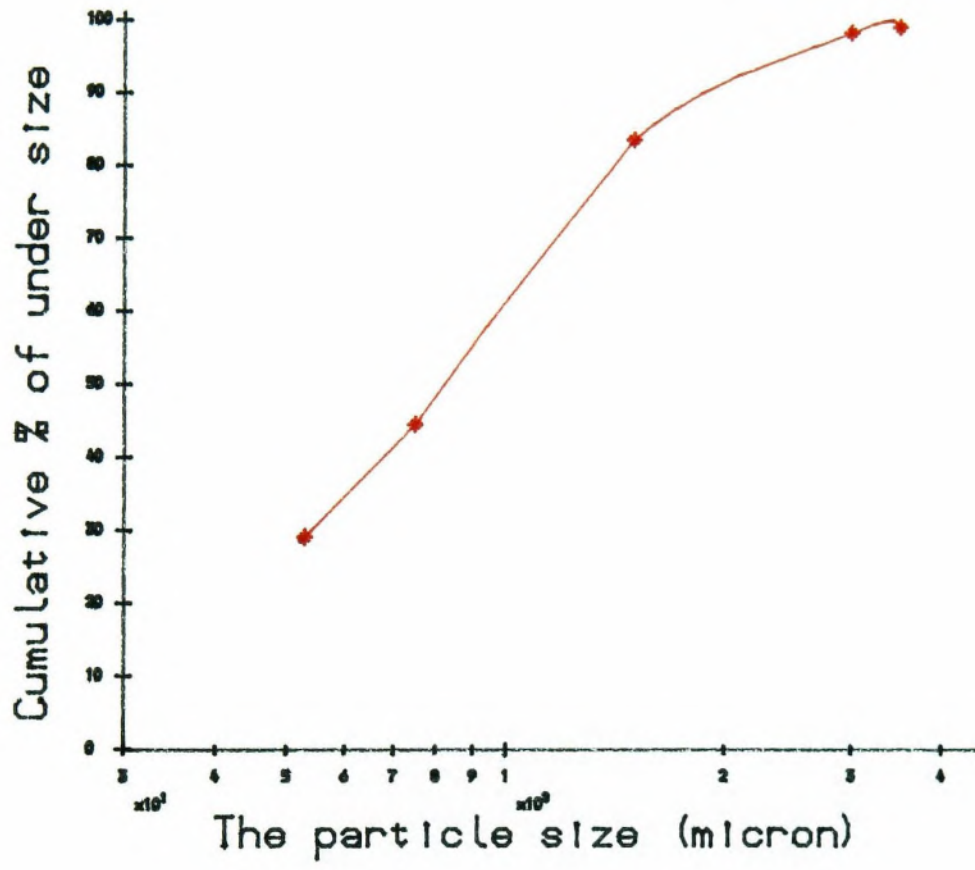
Fig 5-8 Particle size distribution

1) A three litres 'Perspex' cell body is mounted on the top of the base unit in which the impeller and its drive is installed. As the impeller is driven underneath the cell body, the cell can be perfectly accessed for froth scraping.

2) Switches and speed control equipment are housed in a separate box connected to the base unit by an umbilical cable. The impeller speed (rpm) is shown in a digital display window on the box. The speed is continuously adjustable from 1 to 1850 rpm.

3) **AFR** is controlled by a flostat controller, and measured by a Platon 'Gapmeter' which is mounted on a pole attached to the back of the base unit. The inlet of the compressed air to the cell can be adjusted from 0.0 to 10.0 l/min.

4) The pulp level is sensed by an electronic sensor with a controller which operates a solonoid valve admitting water to the cell whenever necessary. The sensitivity of the pulp control system is 1-2 mm for water and 2-4 mm for pulp (S. Ersayin 1986).

The standardization of the flotation procedures was carried out as follows:

1) The ground sample pulp was transferred into the flotation cell running with an impeller speed of 600 rpm. Before the speed was adjusted to 1200 rpm, tap water was added to the cell to make up the total pulp volume approximately 1.5 litres.

2) Keeping the speed at 1200 rpm, pH was adjusted to 10.5 by adding lime water and the clock was started. Lime water was continuously added to keep the pH at 10.5 for 2 minutes, then the collector was added. After 5 minutes frother was added. After another 5 minutes, the pulp level was brought to the marked position which was 15 mm below the cell top. Finally pH was again adjusted to 10.5 and left for 2 minutes.

3) After conditioning, air was turned on. Then, the pulp level controller was switched on before the froth wash water flow was started. Finally the clock was reset to zero just before scraping of froth from the top of cell started. The whole procedures took up to 4 seconds.

The froth wash water system consisted of a plastic pipe surrounding the cell. On the pipe, a line of pin pricked holes were directed against the outside of the cell wall. When the froth concentrate was scraped, the water washed it from the cell wall together with that in the concentrate launder to the concentrate bowl. The wash water was an assistance in making a clean cut between the products. This was very important for the first four products because of the high flotation rate at the beginning of flotation.

After the collection of the fourth product, the wash water was turned off because its continuous use would result in too much water in the concentrate to be collected in one bowl and giving a filtering problem. After the wash water was turned off, bottle washing was used whenever necessary.

The frequency of the froth scraping was kept at 65-68 per minute during flotation.

The reagent conditions used in the flotation is shown in table 5.2, which had been standardized by Ersayin (1986).

Table 5.2 The reagent condition of Chalcopyrite flotation

Type	Name	Dosage	Conditioning time
Collector	R348 (Steetley Chemicals)	0.04 Kg/T	12.0 mins
Frother	Frother SS	0.04 Kg/T	7.0 mins
pH controller	Lime water	pH = 10.5	14.0 mins

During flotation, tap water was added automatically to maintain the pulp level. It was noted however that after flotation the pH had dropped to 9.0-9.5, and the pulp level has increased by approximately 4 mm above the marked position due to the reduction of the pulp density.

5.5.4 AFR test

As the AFR would affect both bubble size and bubble surface area, the tests of AFR were carried out at the standard conditions. During the AFR test the impeller speed was kept at 1200 rpm for both conditioning and flotation. The details of the flotation conditions are shown in Table 5.3. When the AFR tests were finished the samples were dried and the Cu% analysed by AAS method which can be referred to in Appendix 5.

Table 5.3 AFR and collecting time of concentrate

Test No	Test1	Test2	Test3	Test4	Test5
AFR (l/min)	1.0	2.5	4.0	5.5	7.0
No.	C1	C2	C3	C4	C5	C6
Time (min)	0.5	1.5	2.5	4.5	7.5	12.0

The table of the tests results for **AFR** can be referred to in Appendix 6. Where the maximum recovery of copper occurred at **AFR** of 7.0 l/min.

Chapter Six

Experimentation Two

--Coal and complex sulphide flotation

6.1 Introduction

The effect of **AFR** and **IPS** on the flotation of different size are further studied in this chapter. In the flotation tests, a fast floating coal and a complex sulphide ore were used and the products from flotation were sieved. In coal flotation, only the **AFR** was varied, from 1.0 to 7.0 l/min, in the complex sulphide flotation, not only the **AFR**, but also **IPS** was varied. Ash and XRF analysis were carried out after the tests.

6.2 Coal flotation

As in the case of chalcopyrite flotation described in Chapter 5, coal flotation was also carried out in a three litre Leeds flotation cell. Previous to the **AFR** test, several tests were conducted in order to obtain a consistently good flotation performance. In the preliminary tests, the reagent dosages and solids concentration of flotation and flotation time was varied. In order to obtain sufficient weight of sample for size analysis, at least three parallel tests were performed, the corresponding products from each test were combined.

6.2.1 Sampling

The coal sample was collected from the CEGB generating station at Drax near Leeds, England. The total weight of the sample was approximately 50 Kg with the

particle size below 0.300 mm. From the experimental results, it was shown that the coal is fast floating. As the sample was already ground, no further treatment was required before flotation.

6.2.2 Preliminary tests of coal flotation

In the preliminary tests, the solid concentration for flotation was first tested at two levels, one at 9.1% and the other at 6.25% of solid by weight. From the experimental results, it was shown that at a solids concentration of 6.25% the yield of mass was greater than that at 9.1%. Therefore 6.25% solid concentration was used in further flotation.

Following the solids concentration tests, dosages of collector and frother were also tested over a small range which was covered by three experiments as shown in Table 6.1

Table 6.1 Reagent condition tests

Test No	1	2	3
Collector (ml)*	5.5	3.5	7.5
Frother (ml) **	3.0	2.0	2.0

*The collector was 5% paraffin in alcohol.

**The frother was 5% frother SS in distilled water.

From the experimental results, it was shown that the coal sample was not very sensitive to the change in reagent dosage over that range. However a slightly higher mass yield was obtained at Test No1 when 5.5 ml and 3.0 ml frother were added and that dosage was used subsequently.

Finally in these preliminary tests, the cut time between products was also varied with the aim of producing a reasonable weight distribution amongst the products without difficulties in timing. When parallel tests were carried out at the conditions indicated above, the recovery of mass was plotted against the flotation time, then the time and weight were carefully selected from the plot. The feasibility of the selected cut time was proven by an additional experiment. The final cut time obtained is shown in Table 6.2.

Table 6.2 Collecting time tests

Product No	1	2	3	4	5	6
Cutting Time	10"	25"	45"	1.5'	2.5'	6.0'

" Time, seconds.

' Time, minutes.

6.2.3 AFR test

When the IPS was kept at a constant value of 1200 rpm, the AFR was varied from 1.0 to 7.0 l/min in a series of tests. In order to keep a constant pulp level, make up water, which contains the same frother concentration as the pulp, was added. Although the cut time had been carefully selected, when the AFR was high, the mass distribution amongst the products was still unsatisfactory. The weight of the fifth and the final products was so small that it was impossible to carry out sieve test in each case. Therefore the fifth and the final products were combined. At each AFR, the test was repeated at least three times to obtain sufficient sample for sieve analysis. At AFR greater than 4.0 l/min, the test was repeated up to six times to the same ends. During the test, if any pulp overflow was observed, the result from that test was

abandoned. When the experiments at the same **AFR** were completed, the corresponding products were combined and filtered and dried in an oven at 70°C. The dried samples were stored in self-sealing plastic bags for size analysis. From the experimental results, it was observed that the **AFR** had an obvious effect on the weight of products as it can be seen in Fig 6-1.

In Fig 6-1, the total weight of products was plotted against the **AFR** to a unit cell volume. The cumulative weight against flotation time at different **AFR** was also plotted as shown in Fig 6-2 which shows the **AFR** effect on flotation as a process.

6.3 Analyses of eoal samples

The samples from flotation tests were firstly sieved then ash assayed by a combustion method.

6.3.1 Size analysis

Three British Standard sieves with the mesh size 125, 75, 53 microns were used in the size analysis. The dried samples were sieved in a vibrating sieve for 15 minutes, the oversize products were wet sieved until the wash water through the sieve was clear. The four different size fractions, of size +125 -125+75 -75+53 and -53 were filtered and dried at 70°C. The -53 fraction was sieved through a 10 micron sieve using an ultrasonic bath. However due presumably to the low specific gravity as well as the effect of remaining reagent on the particle surface, this ultrasonic sieving proved unsuccessful.

The size distribution of the feed was also determined by sieve analysis, the results are shown in Fig 6-3. The details of the results from the size analysis of all samples is tabulated in Appendix 7.
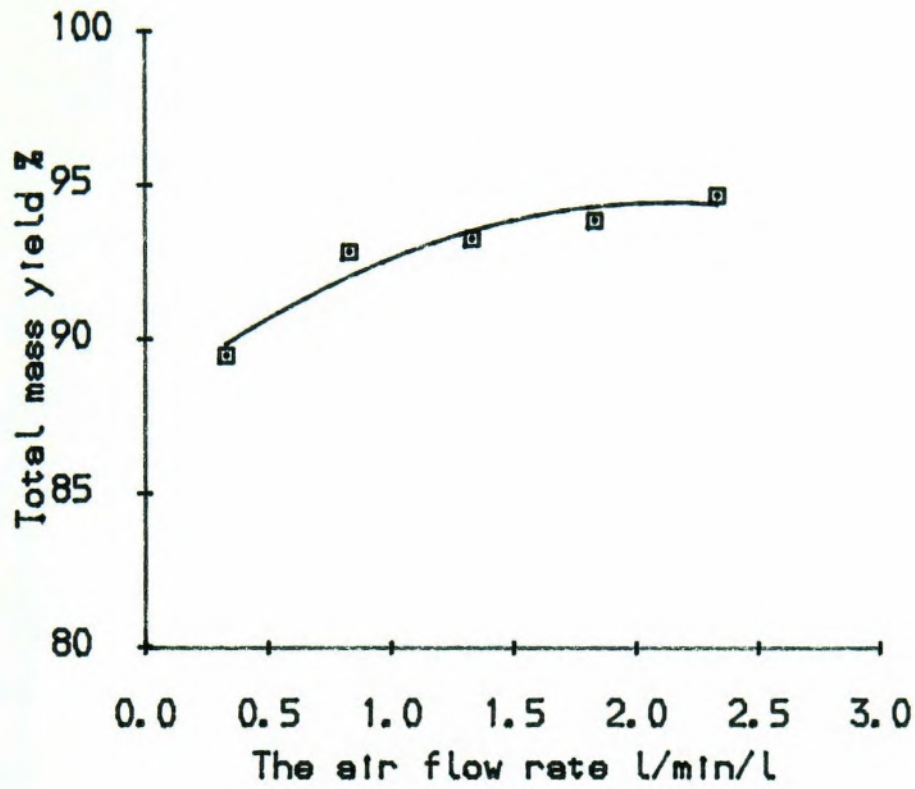
Fig 6-1. AFR and total product weigh
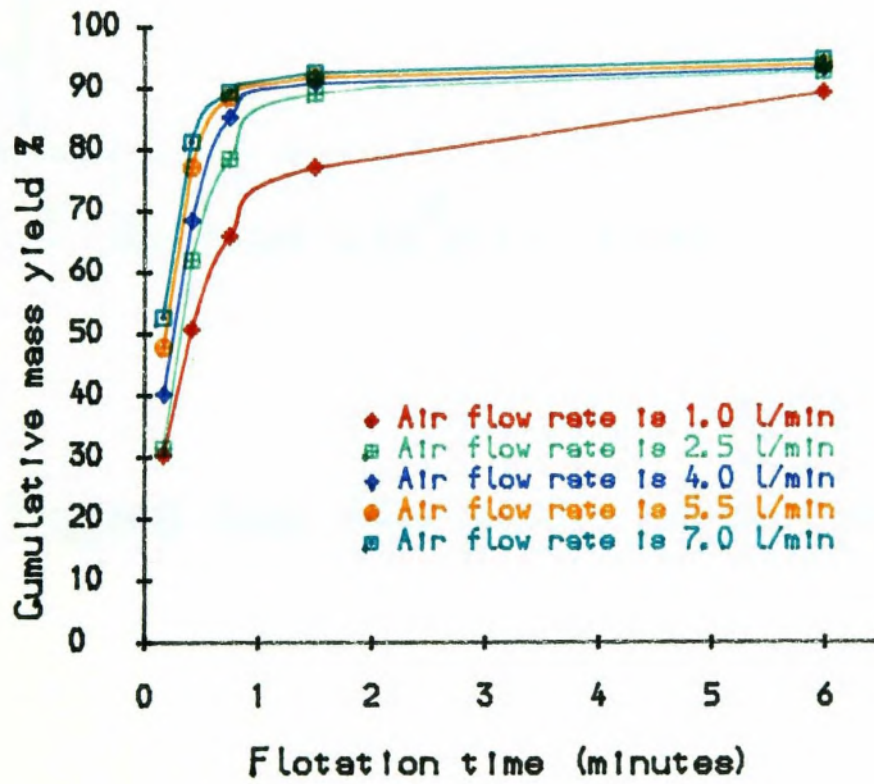
Fig 6-2. AFR and cumulative mass
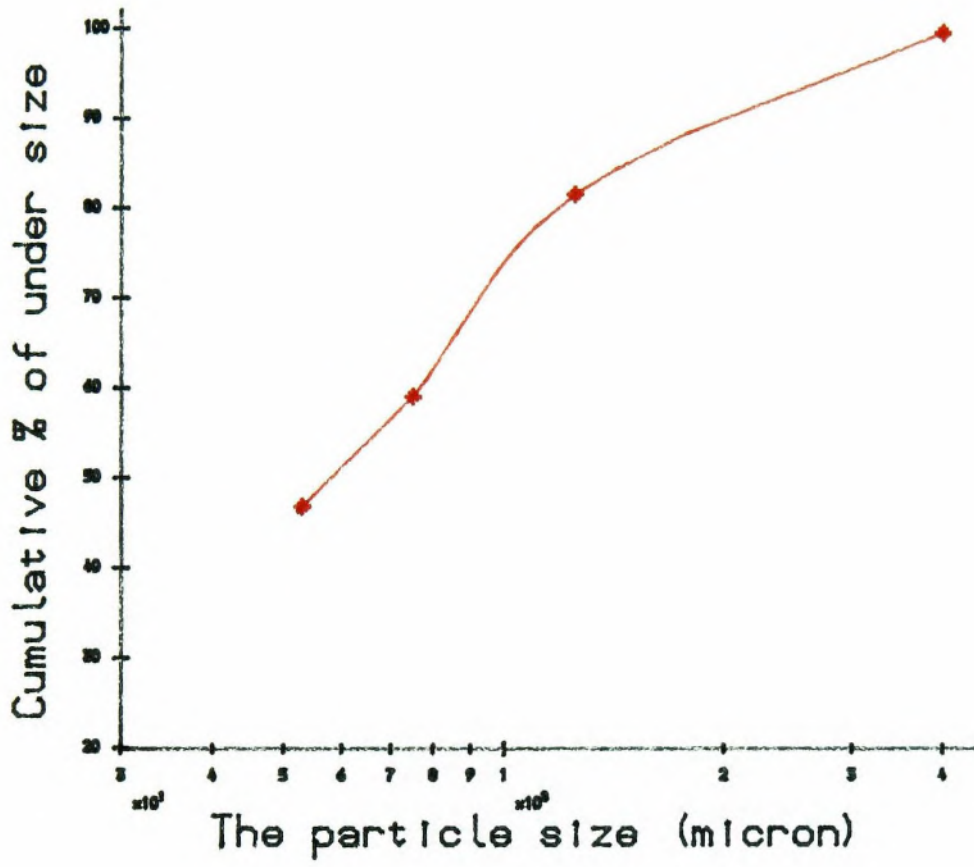
Fig 6-3 Coal feed size distribution

6.3.2 Ash analysis

In the ash analysis, a representative sample, approximately 4 grammes in weight, was taken from each sample and finely ground in a mortar. Then 2 g out of the 4 g was weighed to four decimal places and placed into a weighed silica crucible. At 1000°C the sample was ignited and burned for 30 minutes in a furnace. When the crucible was taken out from the furnace, it was cooled in a desiccater. The cooled crucible with the residue was weighed and the ash content in the sample was calculated from the equation as shown below:

$$Ash(\%) = \frac{The \quad weight \quad of \quad residue}{The \quad initial \quad weight} * 100$$

In the same way, all the samples were analyzed. The details of the results from the ash analysis can be referred to in Appendix 8. The plot of **AFR** effect on the ash content of products in the different size fractions can be seen in Fig 6-4 as shown below.

6.3.3 Error analysis

Although the flotation operation was standardized in chapter 5, the fast floating feature of coal could still cause many errors in the test. An error associated with the starting up of flotation was noted in most of the tests, which resulted in a difference of weight in the corresponding products at the same **AFR**. However the difference of weight in the corresponding products caused by the starting time error was less than 5%. Combining products at the same **AFR** may well reduce that error to even lower level.

Another error that might occur during the test was the cut time error. The error was much more likely to occur in the first two products as a slight hesitation in
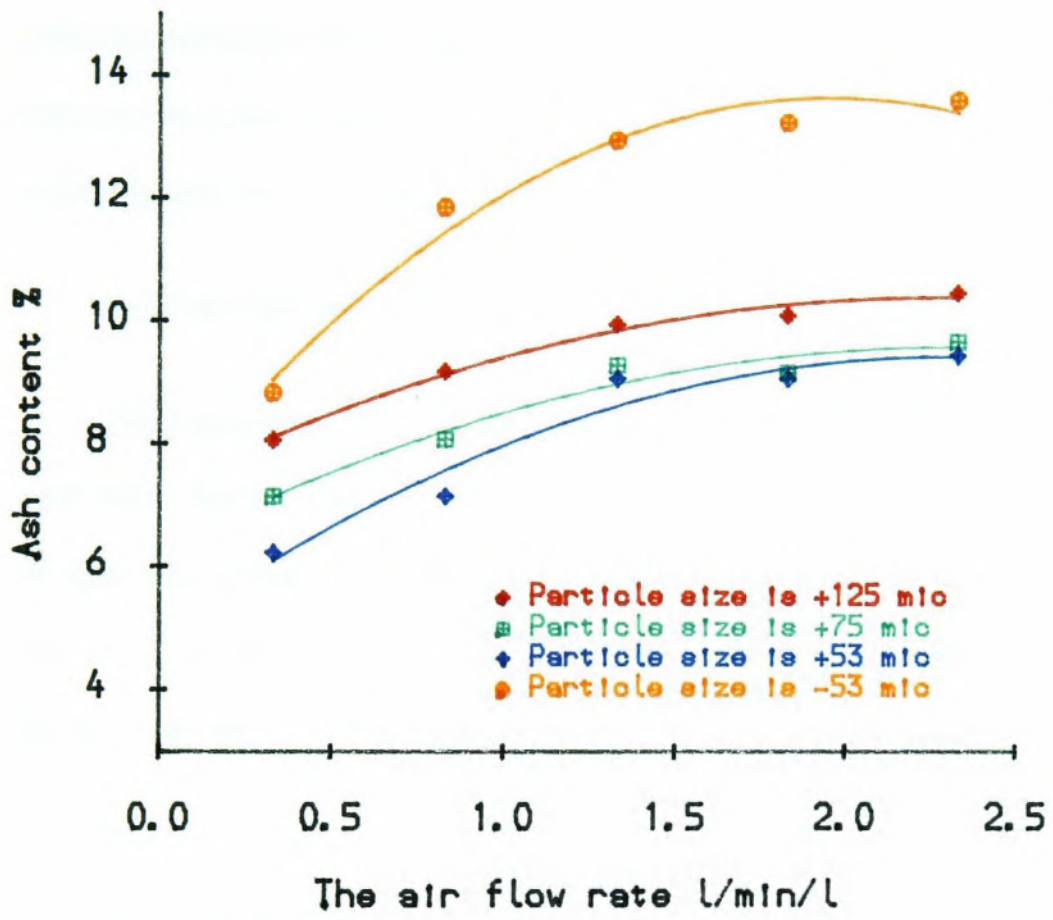
Fig 6-4. AFR effect on ash content

changing the product container would result in a significant error. When this error was observed, the data from that particular test was abandoned and the test was repeated.

6.4 Complex sulphide flotation

After coal flotation, complex sulphide flotation was carried out in order to find out the behaviour of complex sulphide at different **AFR** and **IPS**. In the tests, all sulphide minerals were floated. From the results of the tests, competitive flotation between minerals was observed. When the test was finished, the samples were sieved and analyzed for the content of Fe, Cu, and Zn.

6.4.1 Sampling

The experimental sample of complex sulphides was collected from Wheal Jane mill feed, Wheal Jane, Carnon Consolidated, Cornwall, England. A total of 45 Kg sample with particle size below 300 mm was collected from about 30 spots around a heap of the ore. The collected sample was stored in a plastic bag and transported by rail to its destination in 4 days.

The ore sample generally contained two groups of mineral. The first group consisted of sulphides namely chalcopyrite, pyrite, arsenopyrite and sphalerite. The second group consisted of oxides in which the valuable mineral is cassiterite and others are iron oxides and gangue minerals. The contents of valuable elements can be referred to in Table 6-3.

Table 6-3 The feed grade

Elements	Cu	Sn	Zn	Fe
Grade %	0.438	3.50	5.089	17.05

The values listed in the above table are higher than those of plant operation. The difference was expected as the inconsistency in the properties of the feed ore had been noted during sampling.

As a large proportion of slime was noted in the sample, desliming was performed by washing the whole sample in a container. After desliming, the sample was dried on the laboratory floor. The dried sample was crushed in a rolls crusher, the size of the crusher product was controlled by a 1/8 inch sieve. When crushing was finished, the product was separated into batch samples of approximately 1.6 Kg and the batch samples were stored in plastic bags for subsequent use.

6.4.2 Preliminary tests for flotation

The best condition for grinding time, solids concentration and reagent dosages for flotation were generally optimized in a preliminary series of tests with the complex sulphide.

From the experience of the previous chalcopyrite grinding test, three different length of grinding time of 6.0 9.0 and 12.0 minutes, were carried out at 66.7% solid concentration using four rods as grinding media. The ground products were wet sieved through three sieves at mesh size 125, 75 and 53 microns. The different sized products were filtered, dried and weighed. Instead of using flotation to find the best grinding time, simple liberation analysis was performed by counting the liberated particles of +125 fraction under a microscope. The result of counting showed that the degree of liberation for chalcopyrite was 89.2%, for sphalerite 93.1% and for pyrite 94.9 %. The details of the counting data can be found in Appendix 9. The evidence of the liberation counting clearly shows that the sulphide minerals are eoarsely disseminated. As long as the size meets the needs of flotation, liberation

was not a problem. The -53 fraction was analysed by using a Warmen cyclosizer which gives size fractions at 39.9, 27.8, 20.7, 14.5 and 11.0 microns. The size distribution of the products from 6.0, 9.0 and 12.0 grinding can be seen in Fig 6-5.

In the graph, 9.0 minutes grinding time was selected for the later tests, because with that grinding time the size effect on flotation could be analysed better.

Following the grinding time test, a reagent dosage test was carried out by varying the addition of collecter and activator over a small range close to the plant conditions. From the test results it was shown that when 4.0 ml 1% copper sulphate was used as an activator, sulphuric acid used as a pH controller, 6.5 ml of 1.0% Ethyl-Xanthate as collector and 5.0 ml of 0.5% MIBC as frother the flotation mass recovery was at a maximum with a value of 24.28%. Therefore the flotation reagent conditions above were used in subsequent tests. Details of the conditions for sulphide flotation can be seen in Table 6-4 below.

Table 6-4 Sulphide flotation reagent condition

Reagent Name	Type	Dosage	Condition time
Collector	Ethyl-Xanthate	81.3 g/T	8.0 mins
Frother	MIBC	31.3 g/T	3.0 mins
Activator	Copper Sulphate	56.3 g/T	16.0 mins
pH adjustor	H_2SO_4	pH=5.8	9.0 mins

As flotation was performed at low pH (5.8) no sulphide minerals was depressed. Flotation results from these test conditions can be seen in Fig 6-6 below.
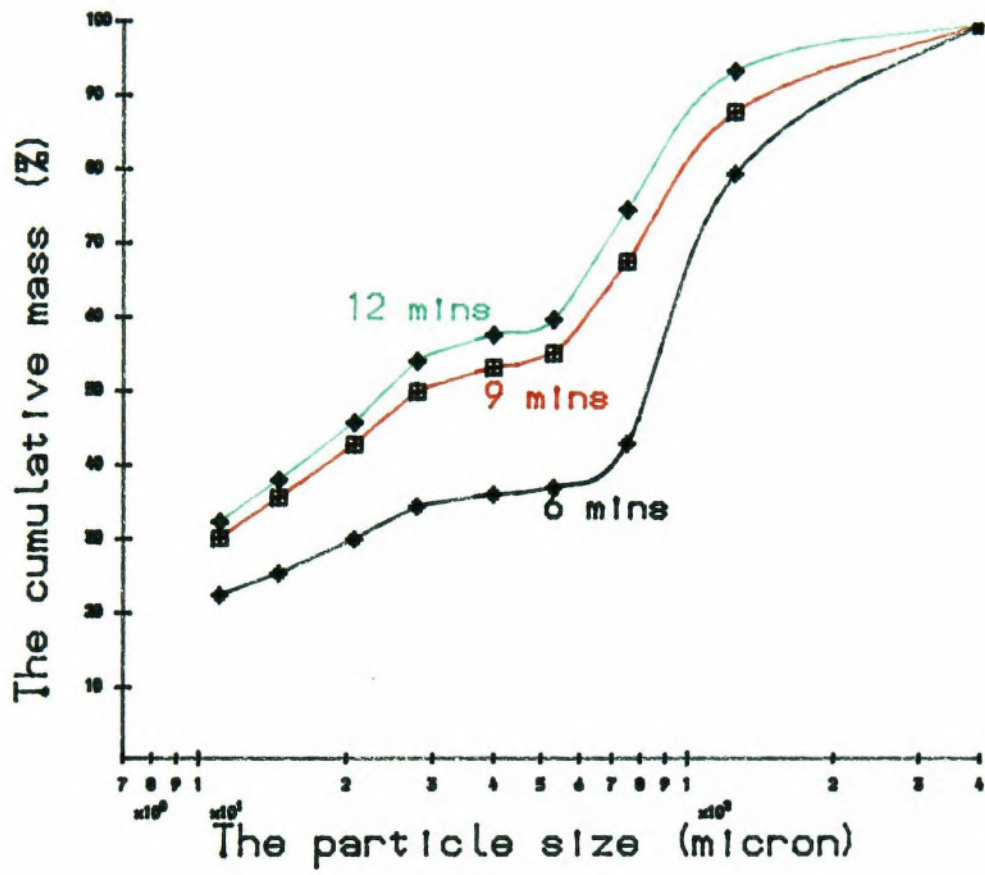
Fig 6-5 Grinding time test
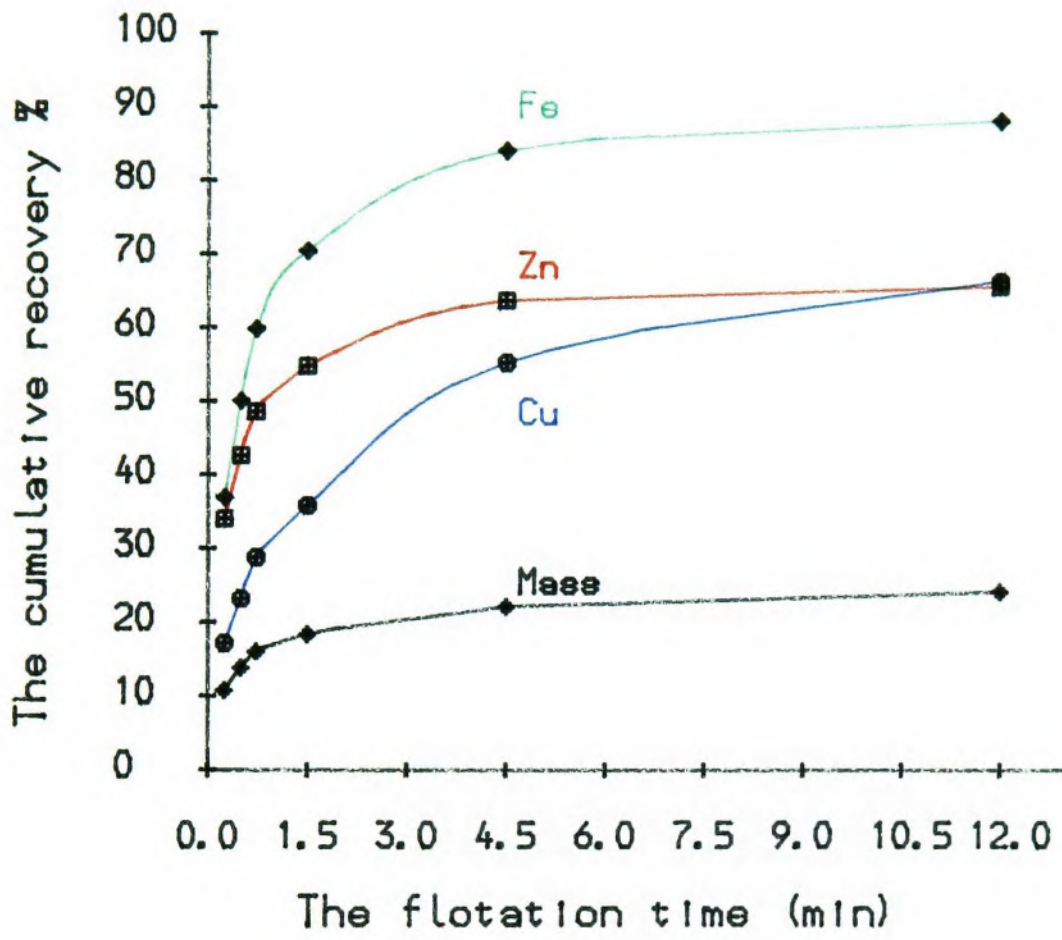
Fig 6-6 Conditional test result

After the flotation of sulphide minerals, tin flotation was attempted. Unfortunately, this was unsuccessful due to the inadequate liberation of SnO2 and tin flotation was abandoned subsequently.

6.4.3 AFR and IPS test

At the reagent conditions shown in table 6-4, the AFR and IPS tests were carried out in order to find out their effect on flotation kinetics. Although this test was a major part of the research project, because of limited sample quantity and also time limitation, the test was carried out only at selected points which are shown in Table 6-5.

Table 6-5 Experimental points

IPS AFR (l/min)	700	950	1200 (rpm)	1450	1700
1.0		T(1)			
2.5	T(6)	T(2,7)	T(8)	T(9)	T(10)
4.0		T(3)			
5.5		T(4)			
7.0		T(5)			T(11)

T(*): The test number

Each experiment under the conditions shown in the table was repeated three times and the corresponding products were combined. The time for collecting the products were carefully selected, based on the same technique as coal flotation. The times selected were 15", 30", 50", 1.5' 4.5' and 12.0'. As the characteristics of the

feed material was the same in all tests, flotation tailings were discarded. The concentrate samples were collected in the concentrate containers before they were sieved. The recoveries were calculated based on the same feed composition, which may introduce some error and will be discussed later.

The effect of AFR and IPS on the mass recovery of different size fractions can be seen in Fig 6-7 and 6-8 as shown in the following page. Full details of test results is reported in Appendix 10.

6.5 Analyses of complex sulphide samples

To determine the effect of AFR and IPS on the different size fractions, both size analysis and XRF tests for the contents of Fe, Cu and Zn were performed.

6.5.1 Size analysis

Size analysis was performed in two parts, the first part by wet sieving for the +53 microns fractions and the second part for the -53 microns fraction was achieved by using a 10 micron sieve in an ultrasonic bath.

1) In the +53 wet sieve, the flotation concentrate products were sieved through sieves with mesh sizes 125, 75 and 53 microns. The sieve test was carried out such that a brush is used to speed up the passage of undersize when a small stream of water was added. When the water passing the sieve did not contain any visible solid particles, sieve test was stopped and all the size fractions were then filtered and dried in an oven at 80° C. The dried samples were weighed. A representative sample of approximately 15 g was taken from the +53 microns fraction and stored in plastic bags for subsequent analysis for Fe, Cu, Zn.
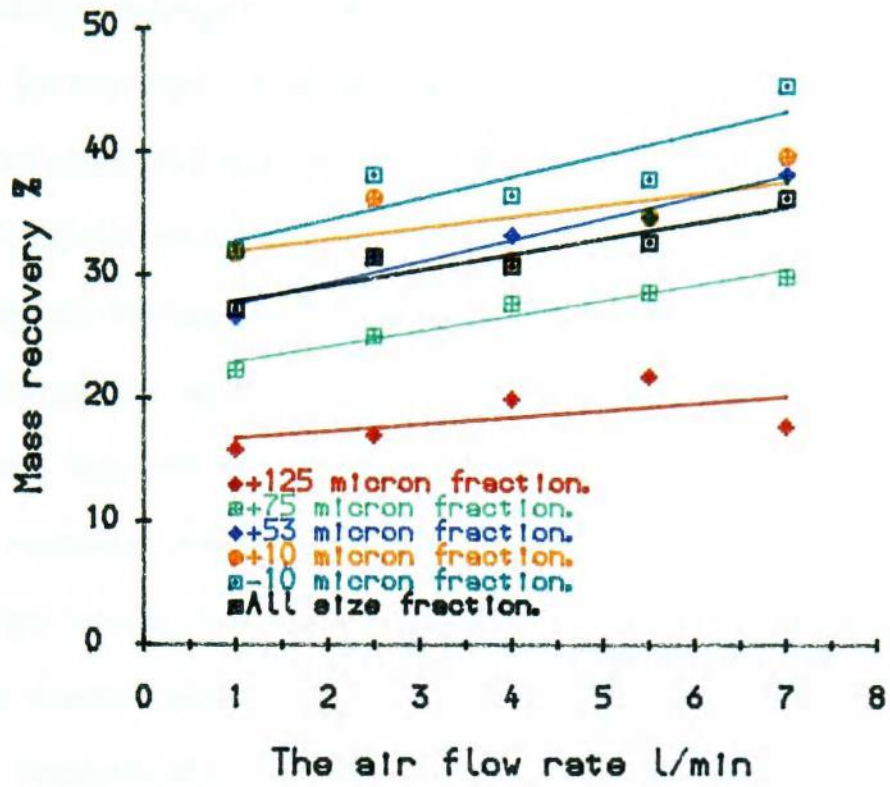
Fig 6-7. AFR vs mass recovery
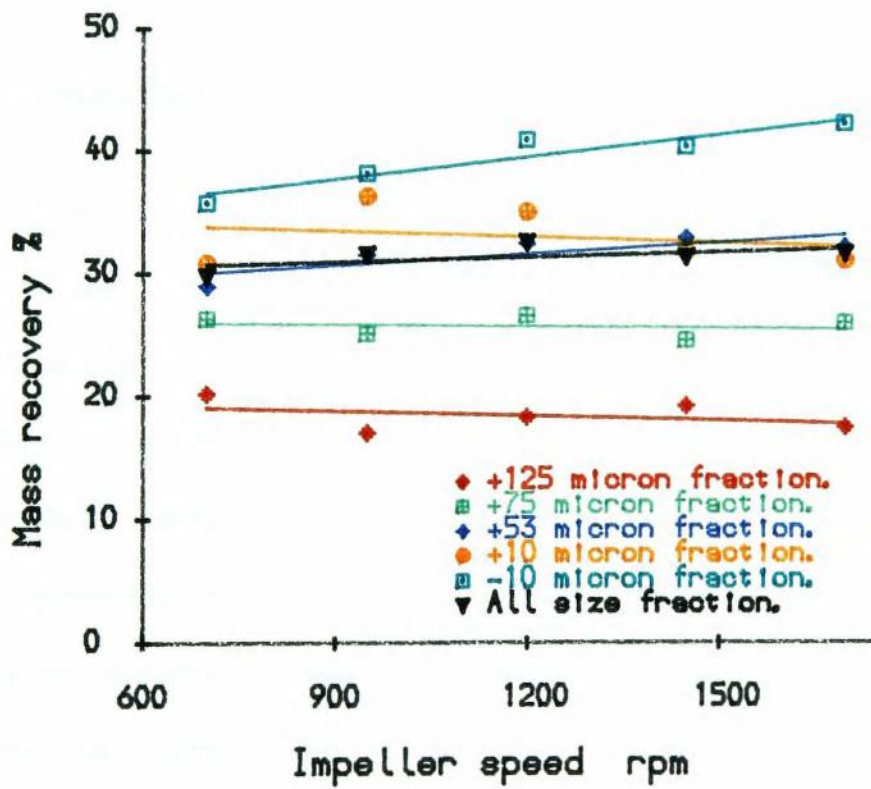
Fig 6-8. IPS vs mass recovery

2) For the -53 micron fraction, when the sample was dried and weighed, the lumps of sample were gently broken by using a rubber bar. 15 g of sample was taken for assay, the rest was sieved through a 53 micron sieve. 5 g from the under size fraction was taken and removed into a 400 ml beaker. Approximately 50 ml water was added to the breaker together with 2 ml 10% Calgon to de-aggregate the particles. With a magnetic bar stirring in it, the beaker was heated on a hot plate for 10 minutes to break the particle aggregations. The pulp was then sieved in a 10 micron sieve (Stork, Veco. bv) with the sieve about 5 mm submerged in circulating water in an ultrasonic container. When the water in the ultrasonic container contained no visible particles, the sieving was stopped and the over size filtered, dried and weighed. Finally the samples were stored in plastic bags for assay of Fe, Cu, Zn.

6.5.2 Analysis of Fe, Cn, Zn

An XRF (X-Ray Florescence) technique was used for the determination of Fe, Cu, Zn due to its convenience for multi-elements analysis.

6.5.2.1 Preparation of XRF dics

Discs need to be prepared for the presentation of samples for XRF analysis. Two types of disc either compressed or fused can be used. The former was easy to make and less time consuming (S. Ersayin 1986), but the disc is so weak that it is easily broken. As it was suspected that the dust from the compressed disc may be harming the XRF machine, a fused disc was suggested by Mr Hanusch (Mining and Mineral Engineering Dept, Leeds University). Due to the high concentration of sulphide in the samples, a mixture of sample with flux could not produce a disc without cracking. Therefore Eschka mixture (2:1 MnO_2 to Na_2CO_3) was added and the proportion of different constituents was tested. The procedures for making disc was as follows:

a) 0.500 g of sample mixed with 0.800 g of Eschka mixture was put into a silicon crucible and covered with 0.200 g of Eschka mixture. The crucible was then put into a furnace at 750 C. After one hour, the sulphides were oxidized, the crucible was removed from the furnace to a desiccater for cooling. When the crucible cooled to room temperature, the sample was cleaned off and ground in a mortar.

b) The oxidized sample was finely ground and transferred into a glass bottle, 8.500 g of Flux 200 was added. The bottle was then well shaken to achieve a good mixture. Using 3 Bunson burners, the mixture was fused in a gold platinum crucible for 20 minutes. During the fusion, the crucible was swirled around for further mixing. The hot fused liquid was cast in a pre-heated graphite mould (recommended by Mr Hanusch. A graphite mould is cheaper, more easily cleaned after casting the discs). After an hour, the disc was taken out from the mould. The successfully cast disc was 3 mm in thickness and 39 mm in diameter with two parallel smooth surfaces. The size of the disc can well fit the XRF machine. The discs were stored in labelled self-sealing plastic bags and ready for XRF scan.

6.5.2.2 XRF analysis

With the help of a technician, the XRF was started and the scanning time for each sample was set to 100 seconds. The scan readings from the XRF were printed out in a connected line printer. Twelve elements was detected in the XRF scan.

6.5.2.3 Calibration of XRF resnlts

Since the XRF reading of one element was proportional to the concentration of the element in the disc, when the concentration is low, a series of discs which contain the elements at known concentration can be used as XRF standards. Usually, the standard was made of pure chemicals. However, as the disc from actual sample contain very low percentage of the elements of interest, the XRF readings of samples

were out of the calibration range of standards made from pure chemicals. Instead of repeating to make standards by using pure ehemicals, a series of samples with different XRF readings were selected, Atomic Absorption Spectrometer (AAS) analyses were used to determine the contents of Fe, Cu, and Zn. The other samples were calibrated by linear regression by using AAS results. Detailed results from the XRF readings and the assay of Fe, Cu, Zn from the calibration can be found in Appendix 11.

6.5.3 Error analysis

Since the sulphides have lower flotation rates than the coal sample, the errors in its flotation were also expected to be less than that in coal flotation. Parallel test results had proven that the difference in mass recovery caused by the starting time error in sulphide flotation was less than 5% and there were no anomalous results. However since the tailings in the sulphide flotation were discarded, when the recovery was calculated from the same feed, error may be introduced, but this error may become less important when concentrates of flotation of same condition were combined.

The errors in the XRF test may occur when the Eschka mixture and sample was heated. It was noted that in making the XRF discs the weight of Eschka mixture and sample was increased after oxidization. However, the increase of the total weight was approximately 0.20 g which was 11.76% of the weight of Eschka mixture and sample. When Flux 200 was added, the total weight became 10.0 g, the 0.2 g was only 2% of the total weight. Therefore the possible error in the concentration of elements will be less than 2%, i.e. if the concentration of an element in the sample was 10.0%, the error caused by the increase of weight during oxidization was only 0.2%, which was acceptable in the test.

6.6 Summary of experimentation

The experimentation included the flotation of three types of minerals, namely chalcopyrite, coal and complex sulphide flotation. Each of the flotation tests were aimed at finding the effect of AFR on flotation kinetics. In the coal and sulphide flotation tests, different size fractions were also considered when AFR effect on the flotation kinetics was studied. The IPS effect on the flotation kinetics was only investigated for sulphide flotation.

Since the AFR and IPS affect flotation kinetics by changing the bubble surface area and the turbulence to the pulp phase, basic research was also carried out to find relationships between the bubble size, the power input and the AFR, the IPS. However, it needs to be declared that the bubble size was measured in clear water with the same frother dosage as complex sulphide flotation. As is well known, the difference in the frother type and dosage will affect the bubble size. The bubble measurements in Chapter Five may thus only be relevant to the complex sulphide flotation. However it is assumed that the pattern of the effects of AFR and IPS on bubble size will be same for other cases. The power input was also measured during complex sulphide flotation.

In addition to the AFR and IPS test, water recovery as a general aspect in flotation modelling was also tested.

Chapter Seven

Discussion of Experimental Results

7.1 Introduction

In this chapter, the effects of **AFR**, **IPS** and particle size on the flotation results of different minerals are analyzed. When flotation kinetics is considered, the relationships between the bubble size, power input, **AFR** and **IPS** are used in the explanation of the experimental results.

7.2 AFR effect on chalcopyrite flotation

Since a small fraction in the feed is floatable, in chalcopyrite flotation, only the effect of **AFR** on mass recovery was observed. These results can be seen in the plot of mass recovery vs flotation time (Fig7-1). At low **AFR**, when **AFR** is increased, mass recovery is increased, since the recovery is much less affected as can be seen in Fig 7-2, the grade of concentrate is therefore reduced.

The effect of **AFR** is explained from two stand points, one is when the **AFR** is increased, the number of bubbles generated is increased. The increase in the number of bubbles will subsequently increase the transfer rate from the pulp phase to the froth and from froth to concentrate launder. When the transfer rate is increased, the residence time of bubbles in the froth phase is reduced and more water is presented to the concentrate, which is proven in chapter five. Consequently, the water entrains more unfloatable and slow floating particles which results in an increase in mass recovery and a slightly increase in recovery. On the other hand, when the **AFR** is increased, the power input to the pulp is reduced, as shown in Fig5-5 (Chapter 5), in this case, bubble dispersion and the particle suspension is worse, collision between the bubbles and the floatable particles is reduced. Therefore the overall effect of
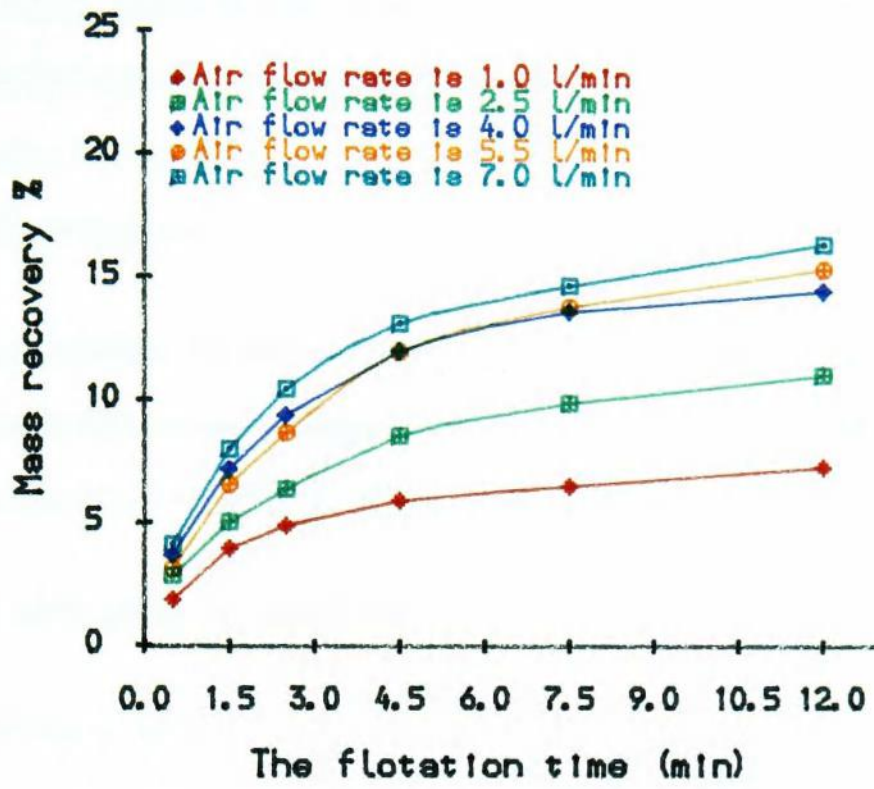
Fig 7-1. Mass recovery at different AFR
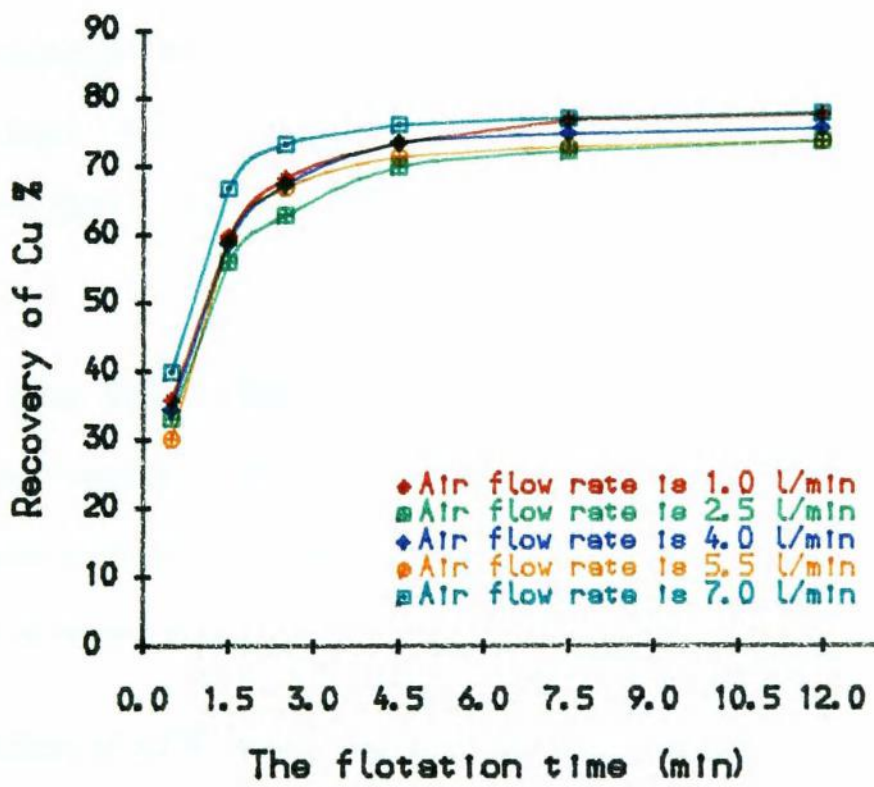
Fig 7-2. Cu recovery at different AFR

AFR on the final recovery show that both very low AFR and very high AFR have higher recovery, where at low AFR the true flotation contributed the increase in recovery and at high AFR, the entrainment contributed to the increase in the recovery as can be seen in Fig7-2.

7.3 Coal flotation

In coal flotation, not only the effect of AFR is investigated but also the particle size. However, because of the large fraction of floatable material and its fast floating behaviour, the effect of AFR is different from the effect on chalcopyrite flotation.

7.3.1 AFR effect on coal flotation

The effect of AFR on the flotation of coal is observed both on recovery and on the grade of combustible. With low AFR, the grade of concentrate is high and recovery is low, when the AFR was increased from 1.0 to 7.0 l/min, the recovery of combustible in +125 fraction was increased from 97.33% to 98.80% and mass recovery increased from 89.42% to 93.25%. In the -53 fraction, when the AFR increased from 1.0 to 7.0 l/min, the recovery of combustible was increased from 97.75% to 99.22%, and mass recovery increased from 90.28% to 95.09% as is shown in Fig7-3.

The effect of the AFR on the concentrate grade is determined by the mass recovery and recovery, since the increase in the AFR has more effect on the mass recovery than recovery, therefore the grade of concentrate is reduced by the increase in AFR as is shown in Fig7-4

The effect of AFR on coal can be explained as when the AFR is low, flotation is inhibited and becomes more selective. The higher selectivity results in a higher concentrate grade, but the inhibited flotation reduces the possibility of attachment
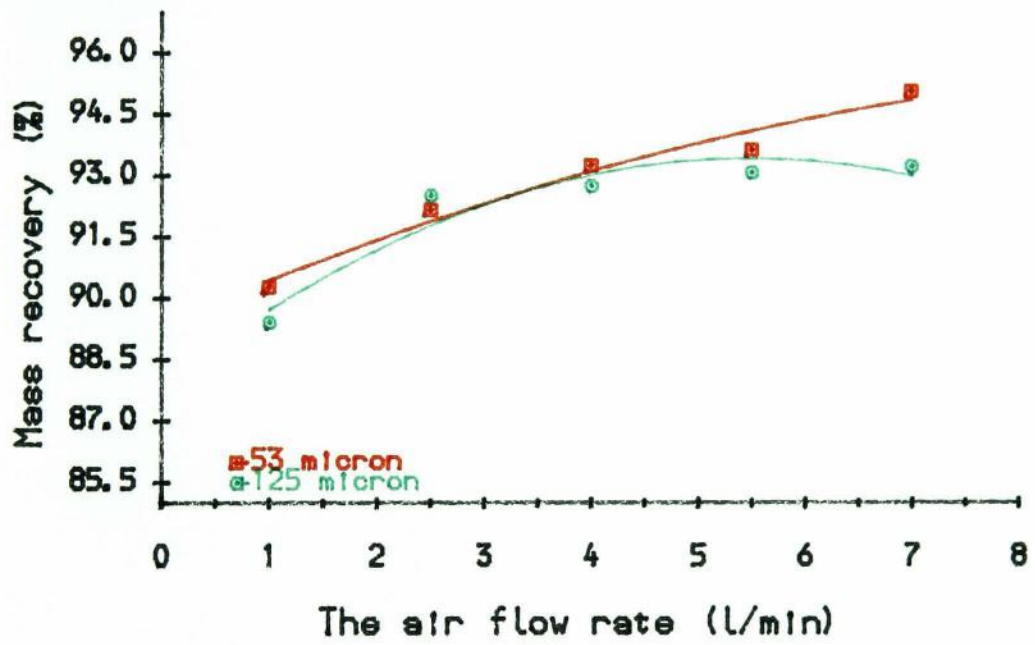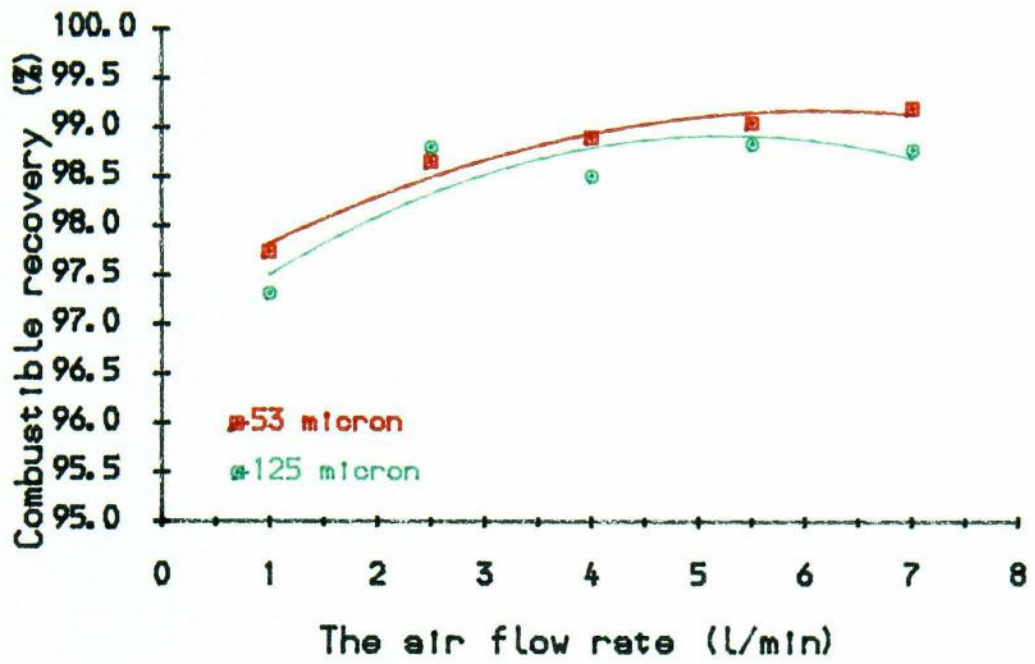
Fig7-3 The AFR effect on coal flotation
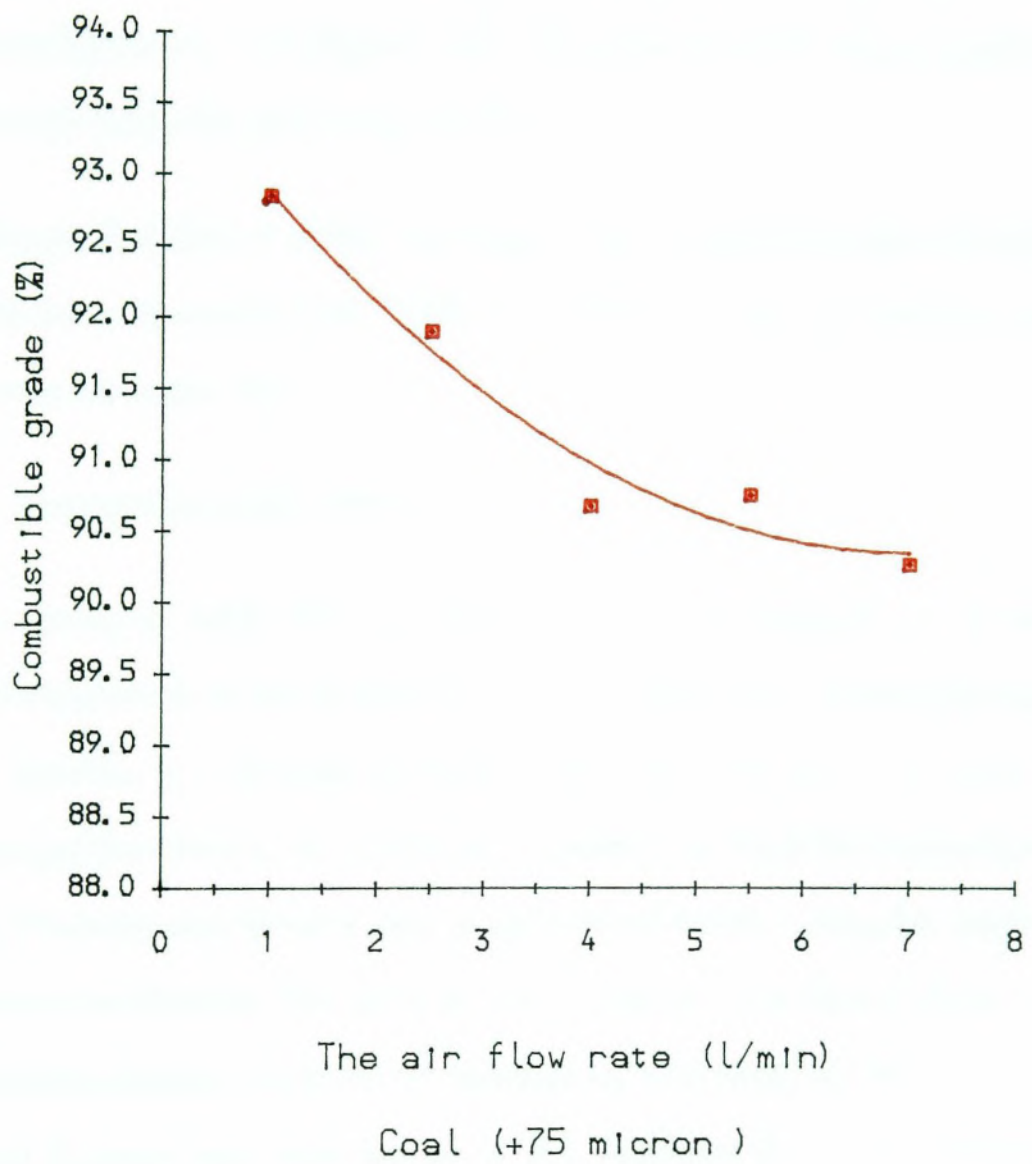
Fig7-4 AFR effect on the grade of concentrate

of slow floating particles and results in a lower recovery. Therefore, in coal flotation, if the concentrate grade is more important, low **AFR** should be used, otherwise a high **AFR** should be used.

7.3.2 The effect of particle size on coal flotation

The effect of particle size on coal flotation is observed from the experimental results. However since the low specific gravity of coal sample, the effect of particle size (from 0 to 200 micron) on recovery is not very significant. At AFR of 7.0 l/min, the difference between +125 fraction and -53 fraction is only 0.42% in recovery and 1.76% in mass recovery as is shown in Fig 7-5.

Although the effect is small, it still shows that the medium size fraction has the maximum recovery except at the **AFR** of 1.0 l/min in which the inhibited flotation may become the major effect.

7.4 Complex sulphide flotation

The effects of **AFR**, **IPS** and particle size on the flotation of the complex sulphide flotation will be discussed in the following sections. Since complex sulphide flotation involves a multi-mineral system, the recoveries of Fe, Cu and Zn are calculated and the effect of the operating parameters on the individual elements are analysed. From the experimental results, differences between complex sulphide and coal flotation are observed. The first difference is that because of the different features of the floatable minerals, the floatable minerals are selectively inhibited at low **AFR**, but in coal flotation since only one mineral is floatable, this is not observed. The second difference is that the effect of particle size is more obvious than in coal flotation.
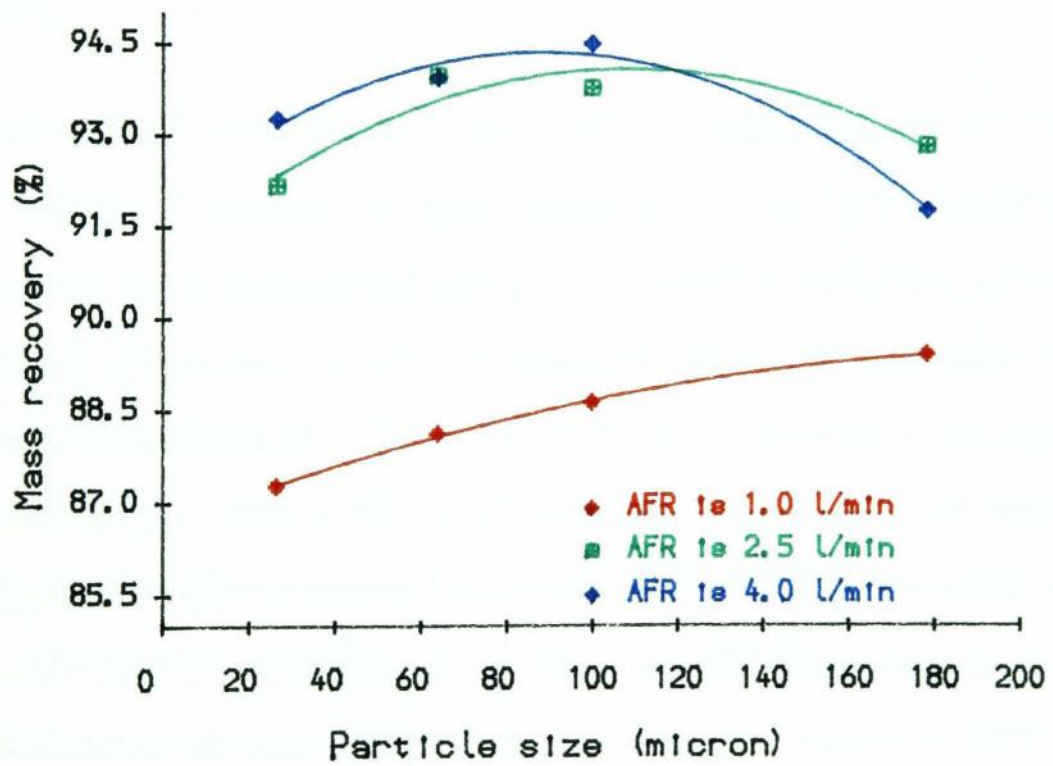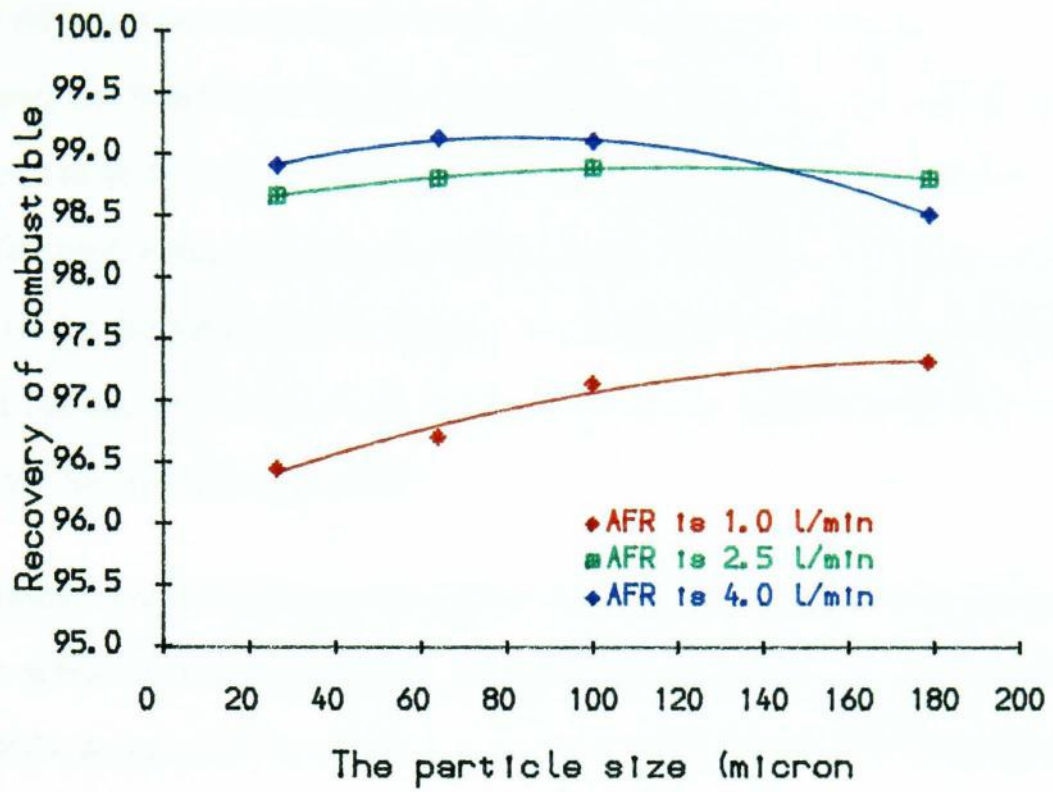
Fig7-5 Size effect on coal flotation

7.4.1 The effect of AFR on complex sulphide flotation

The AFR has two major effect on the complex sulphide flotation, firstly, when AFR is low, the flotation of complex sulphide is inhibited, the air bubbles become more selective in the successful attachment with mineral particles and resulting in Fe (fast floating) being less inhibited and Cu (slow floating) very much inhibited. Because of the difference in the relative flotabilities, Fe recovered preferentially. But from the experimental results, it can be seen, the recoveries of all floatable minerals are increased at high AFR.

Secondly, since AFR has a large effect on water recovery, the increase in AFR increases water recovery and more particles are entrained by water recovery. Therefore the consequent results show that when AFR is increased, the grade of the concentrate is reduced.

The AFR effect on mass recovery and Fe, Cu and Zn is shown in Fig7-6, 7-7, 7-8, and 7-9.

In Fig7-6, in the +125 fraction, when AFR is increased from 1.0 to 5.5 l/min, the mass recovery is increased, however further increase in AFR from 5.5 to 7.0 l/min, mass recovery is reduced. This can be explained from two points, firstly, high AFR results in a lower power input, the suspension of the coarse particles at high AFR may not be as good as at low AFR, therefore the recovery of the coarse is reduced. Secondly, at high AFR, air bubbles are not very well dispersed, excessively large bubbles are generated and these bubbles will disturb the froth phase, therefore mass recovery especialy for the coarse at high AFR is reduced. In other size fractions, mass recovery is generally increased with the increase of AFR which may reply the particle suspension is not significantly affected by the reduction of power input. In Fig7-7 and Fig7-9, the effect of AFR on the recovery of Fe and Zn
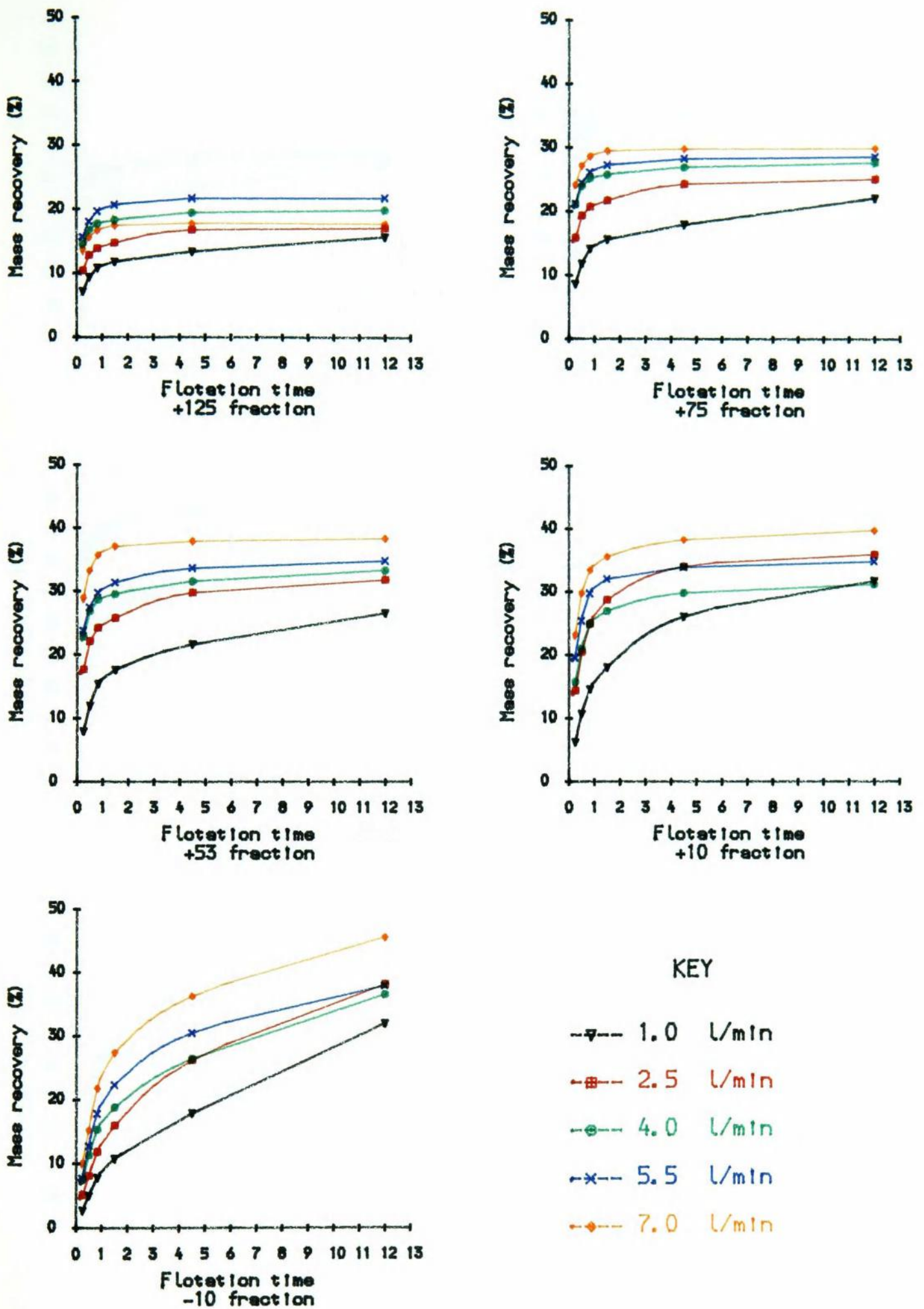
Fig 7-6 AFR effect on Mass recovery

of complex sulphide flotation
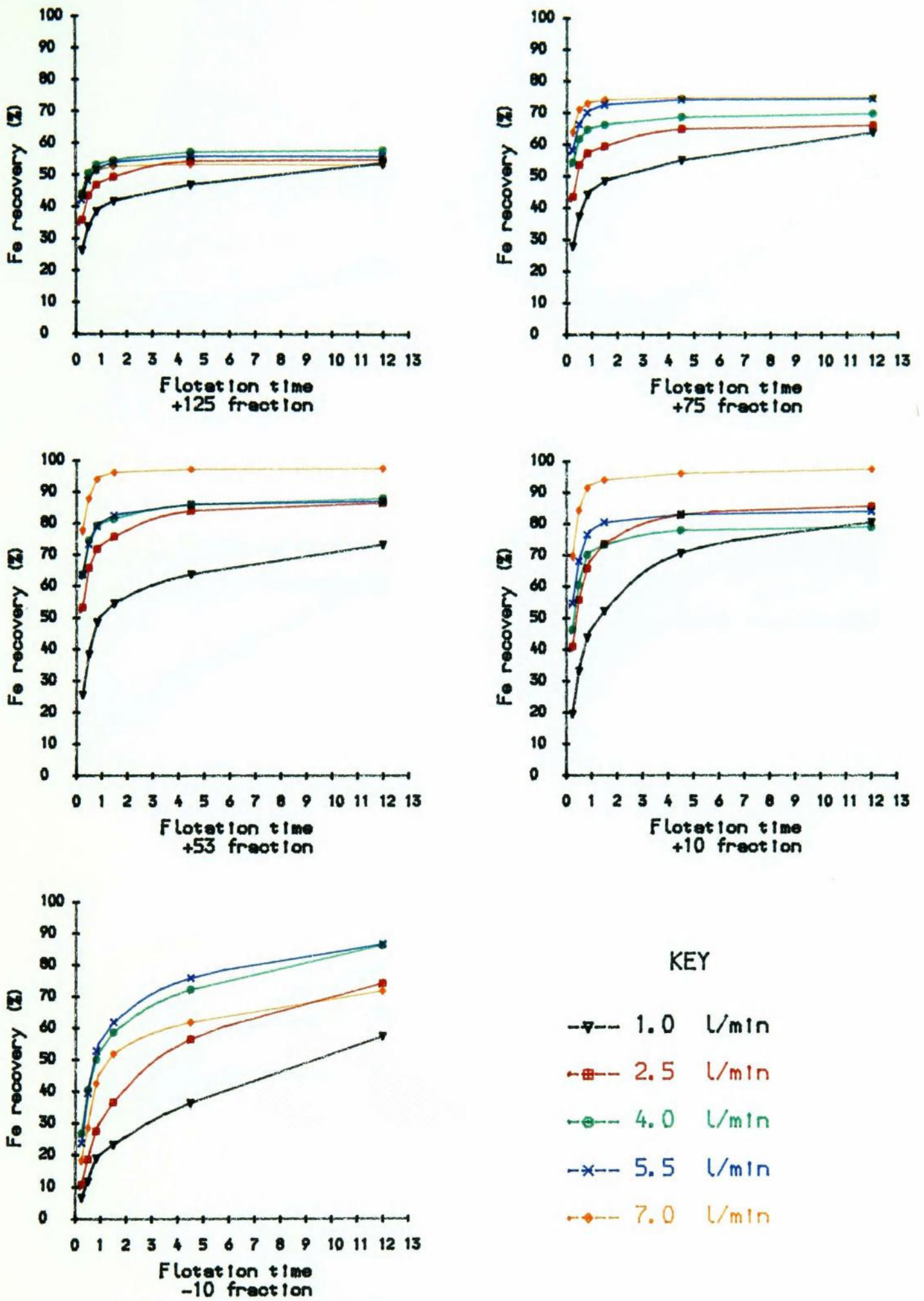
Fig 7-7   AFR effect on Fe recovery

of complex sulphide flotation
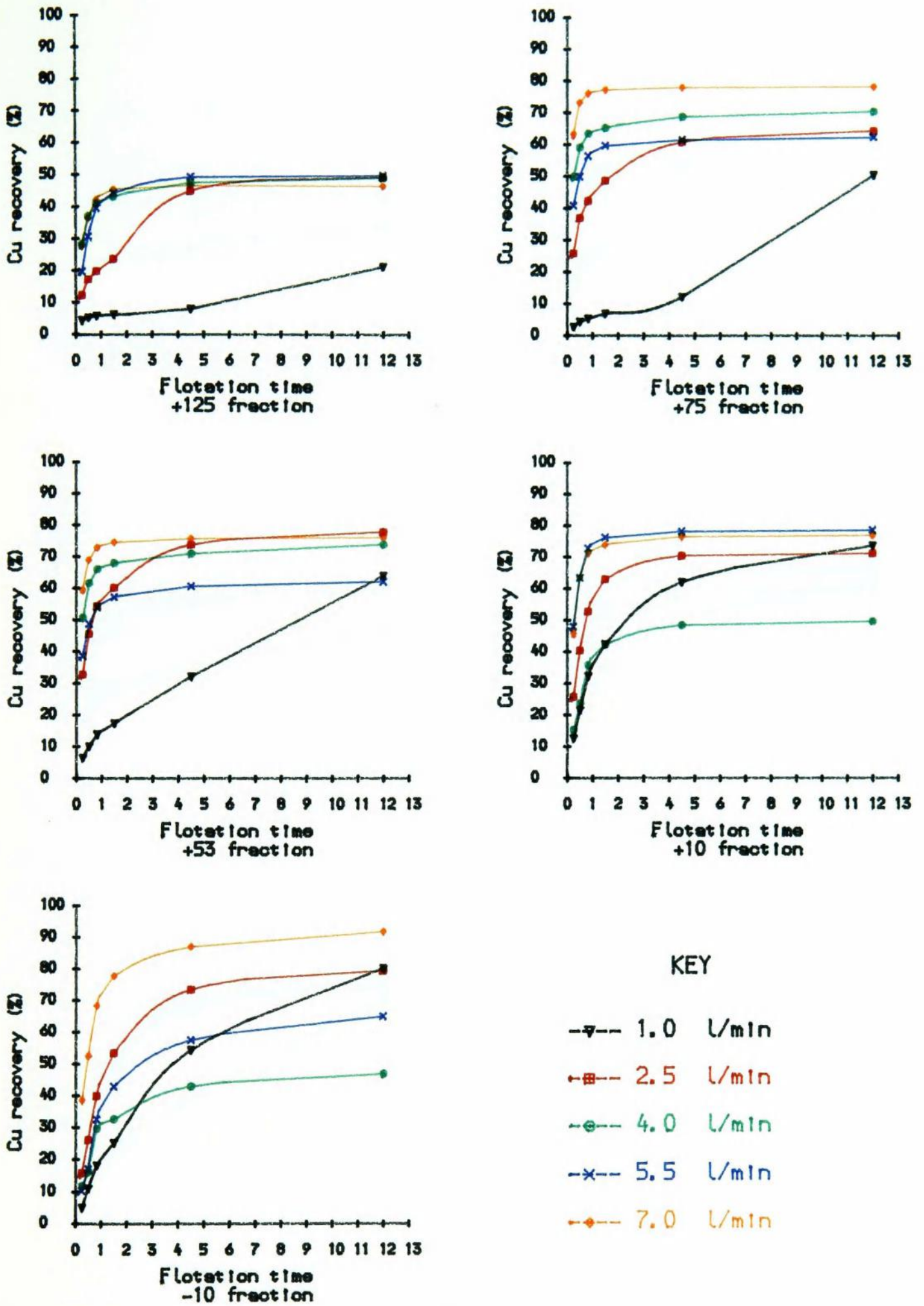
Fig 7-8 AFR effect on Cu recovery

of complex sulphide flotation
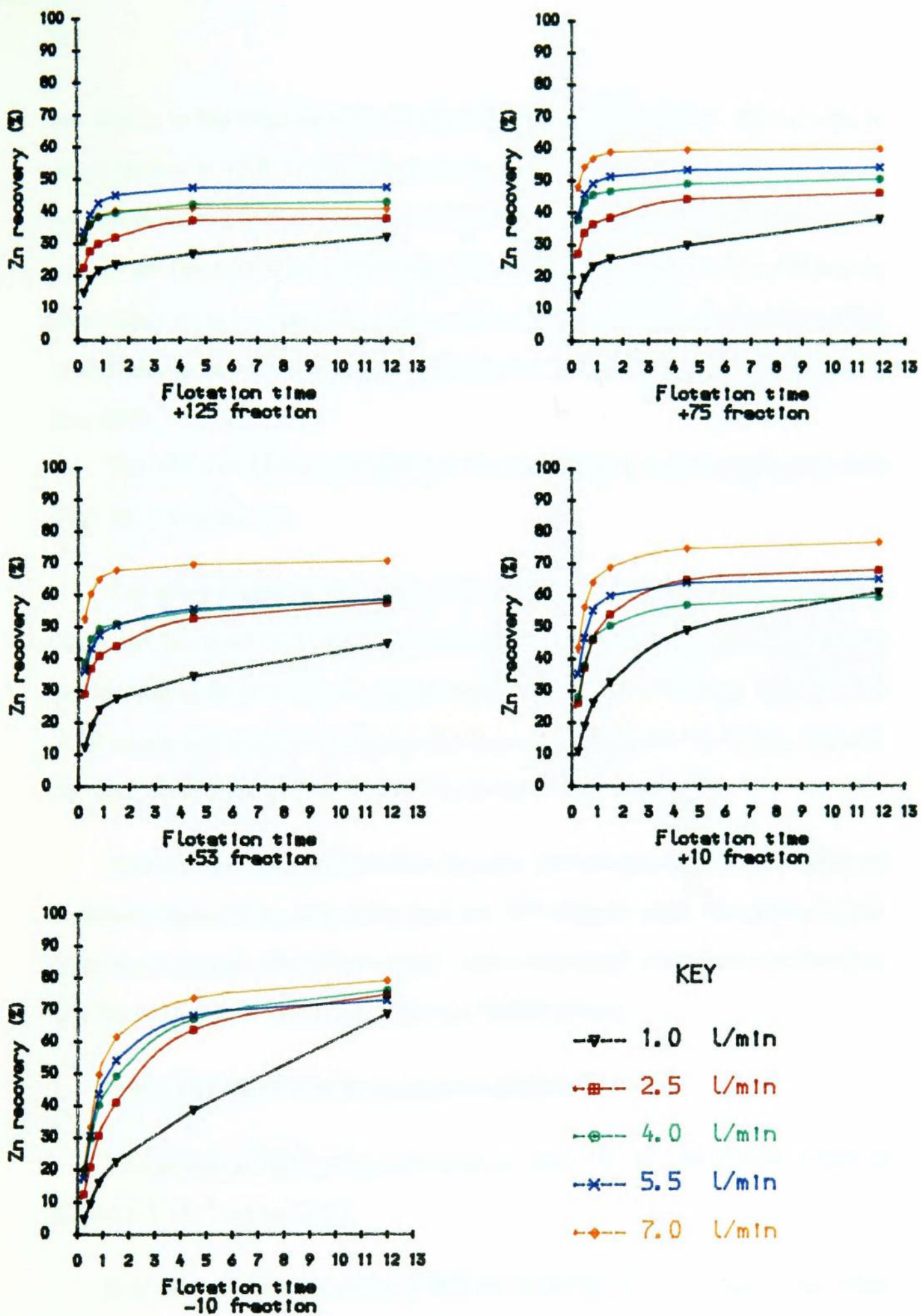
Fig 7-9 AFR effect on Z_n recovery

of complex sulphide flotation

are similar to the mass recovery. In Fig7-8, the effect of AFR on Cu recovery is observed that at **AFR** 1.0 l/min, the recovery of Cu is very much inhibited for all size fractions, at 2.5 l/min, only the +125 and +75 fractions are still slightly inhibited but not the fine size. This result indicate that at low **AFR**, the coarse particles are more likely to be inhibited. The pattern of the effect of **AFR** on the recovery of Cu is also similar to Fe and mass recovery except that the inhibitation is observed at low **AFR**.

The effect of **AFR** on the grade of Fe, Cu and Zn in concentrate is shown in Fig7-10, 7-11 and 7-12.

The effect of **AFR** on the grade of Fe, Cu and Zn are such that when **AFR** is increased, the grade of Fe is reduced, the grade of Cu is increased in the medium and the coarse fractions, but no regular pattern is observed in the fine. The effect of **AFR** on the grade of Zn is similar to the Cu and it is clear that in the fine size, the increase in AFR reduces the grade of Zn as can be seen in Fig7-12.

Another interesting result is that the grade of Fe decreases with the increase of flotation time and the grade of Cu increases with flotation time. The grade of Zn is almost not affected. From these result it can be predicted that during the flotation, the Fe are preferentially floated and Cu is finally floated.

7.4.2 The effect of IPS on complex sulphide flotation

The effects of **IPS** on the recoveries of mass, Fe, Cu and Zn are shown in Fig7-13, 7-14, 7-15 and 7-16.

It is observed that the effect of **IPS** on recoveries is not as large as the effect of AFR. On mass recovery, when **IPS** is changed from 700 rpm to 1700 rpm, mass recovery is varied by only 2.7% in +125 fraction. An increase in **IPS** will reduces
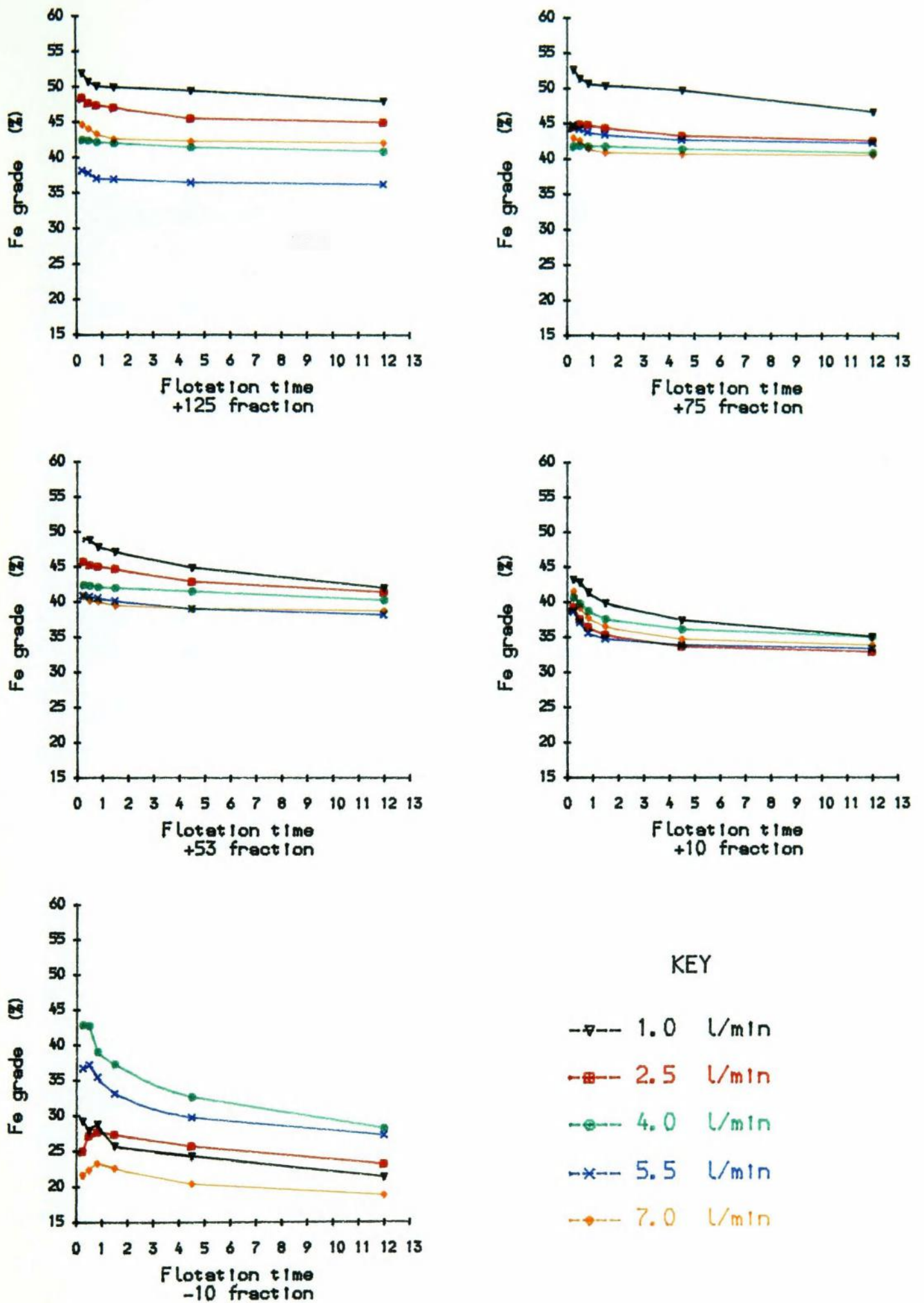
Fig 7-10 AFR effect on grade of *Fe*

in complex sulphide flotation
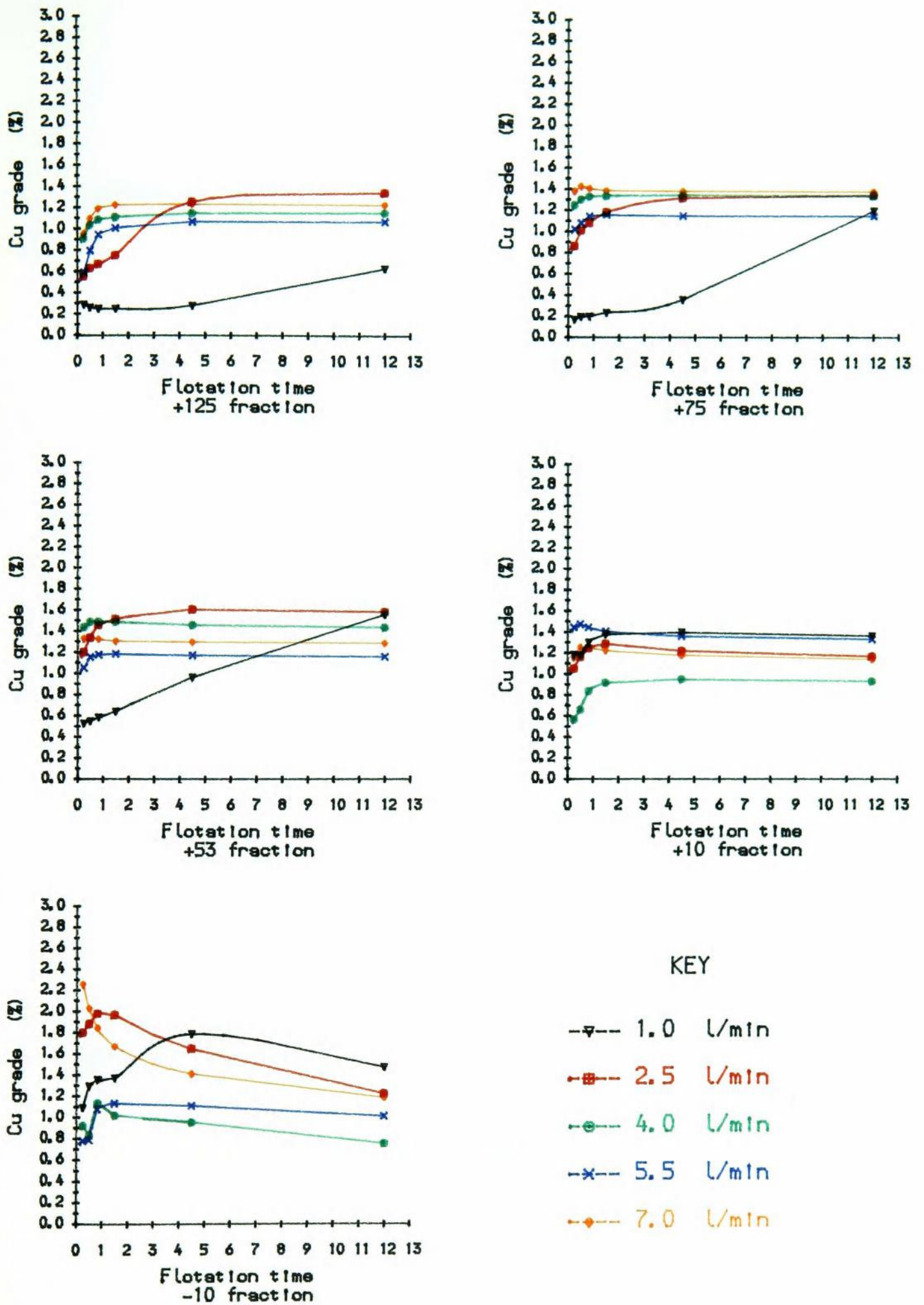
Fig 7-II AFR effect on grade of Cu

in complex sulphide flotation
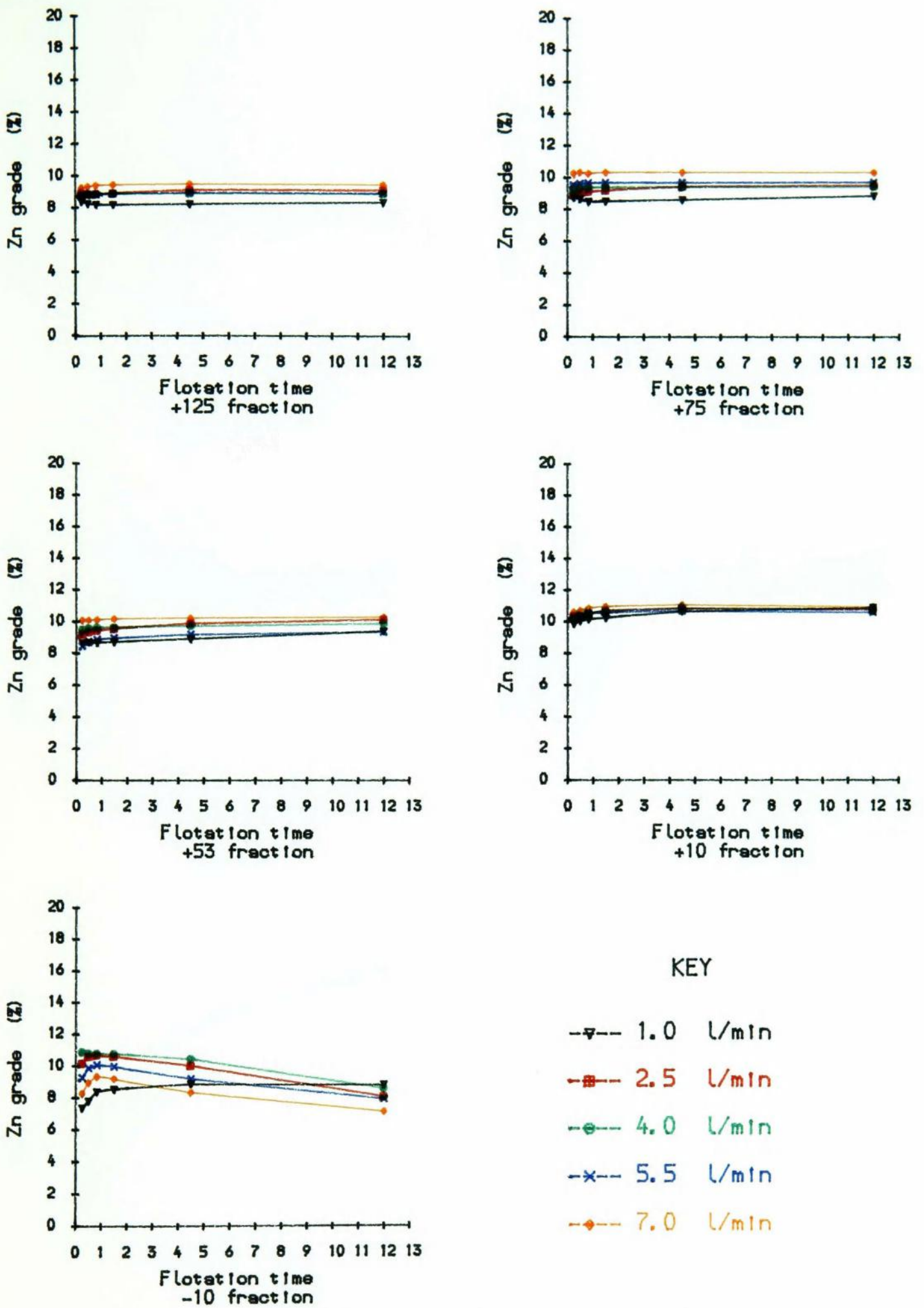
Fig 7-12 AFR effect on grade of Zn

in complex sulphide flotation
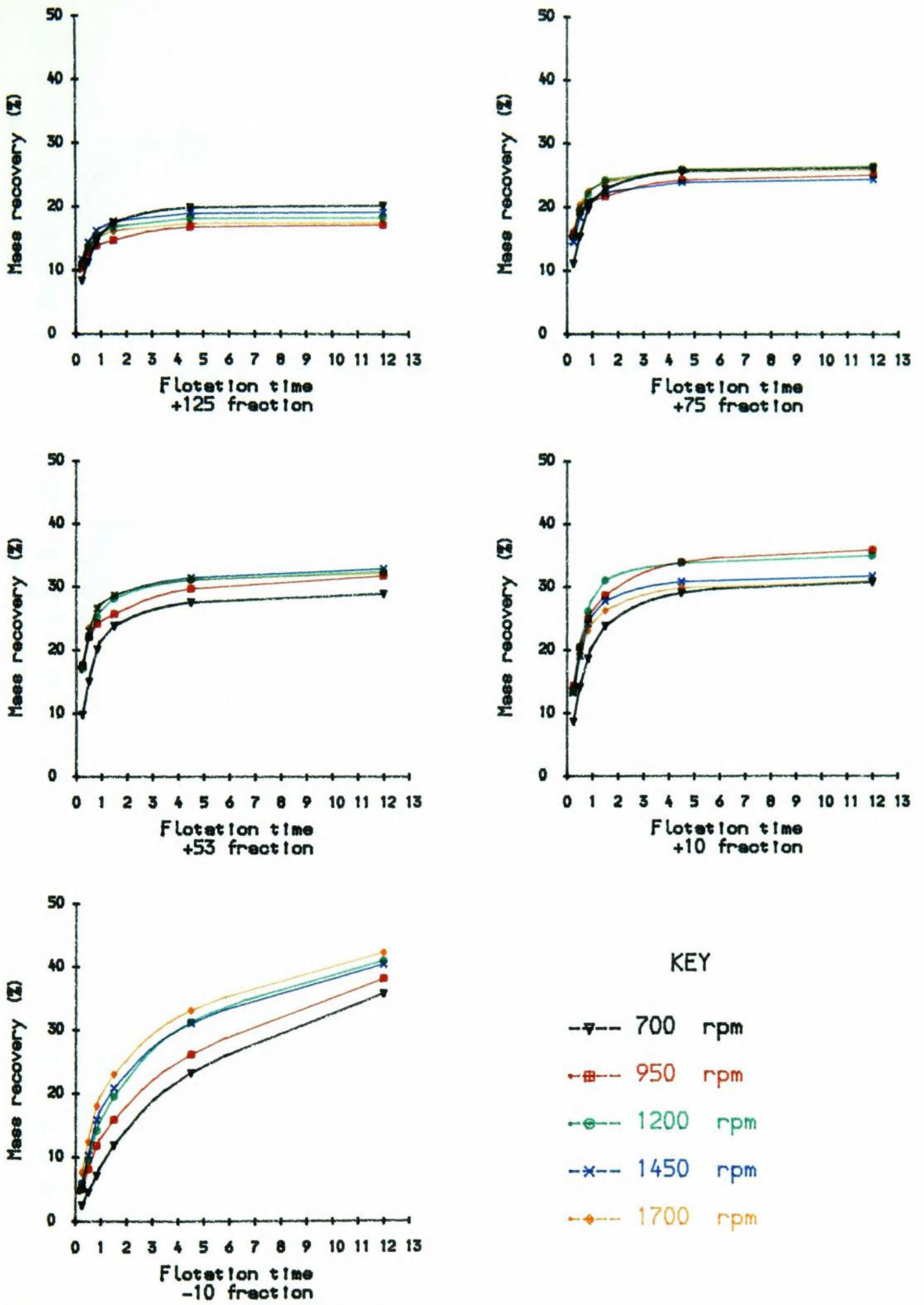
Fig 7-13 IPS effect on Mass recovery

of complex sulphide flotation
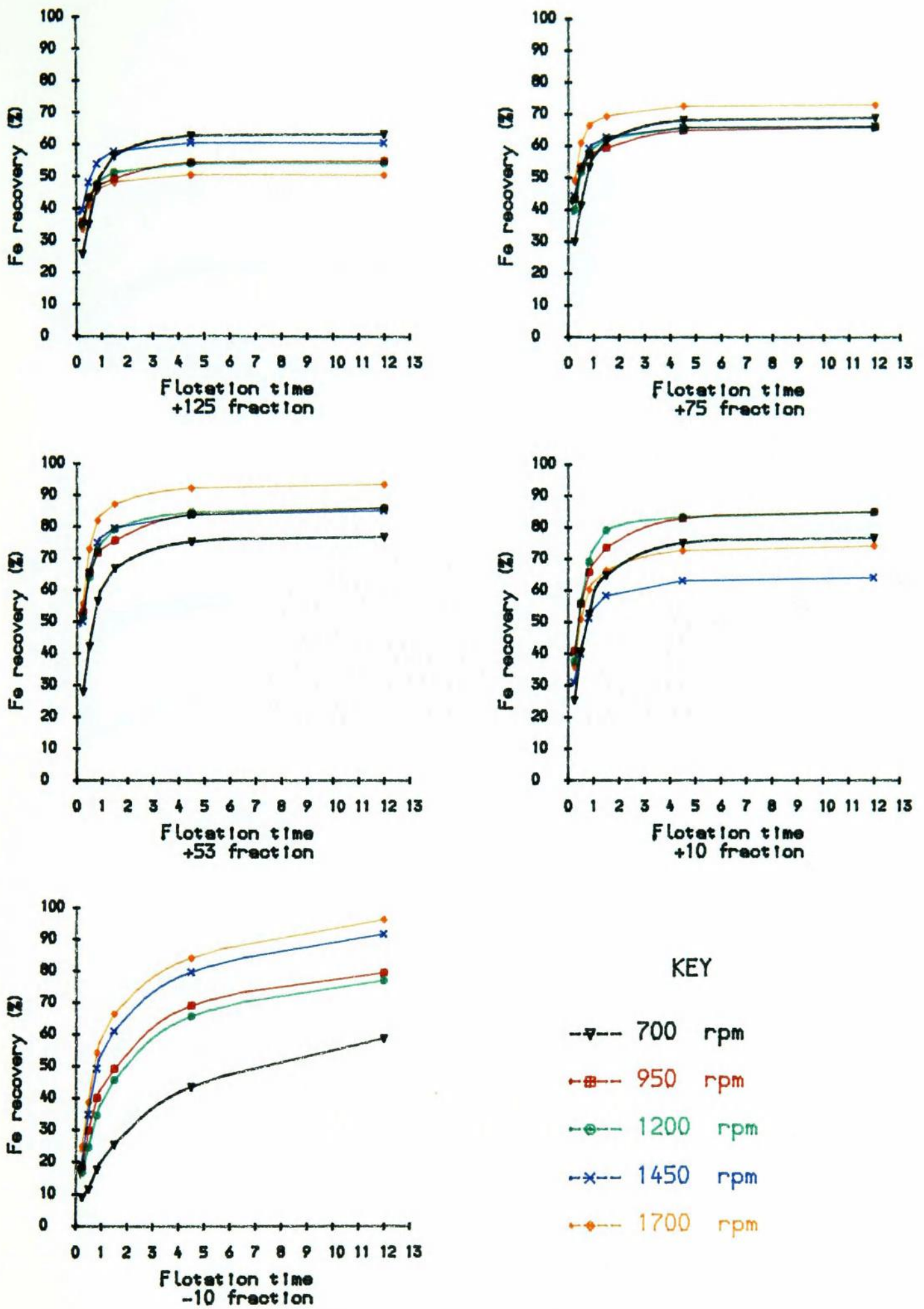
Fig 7-14   IPS effect on Fe recovery
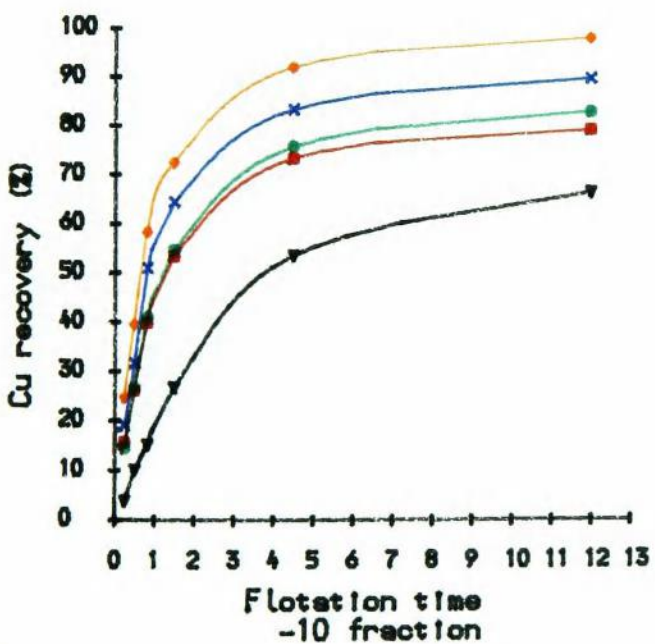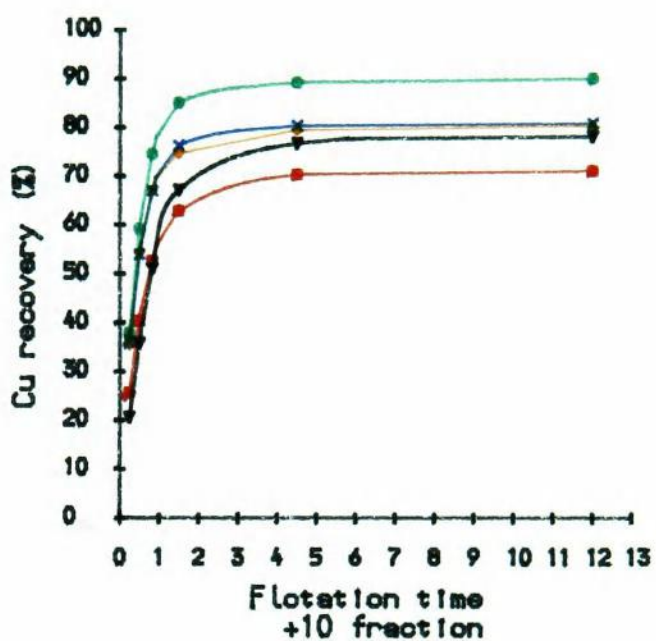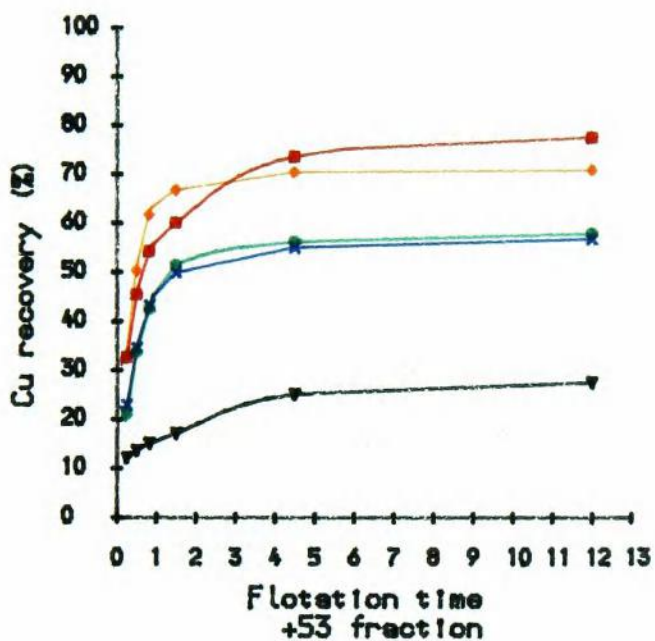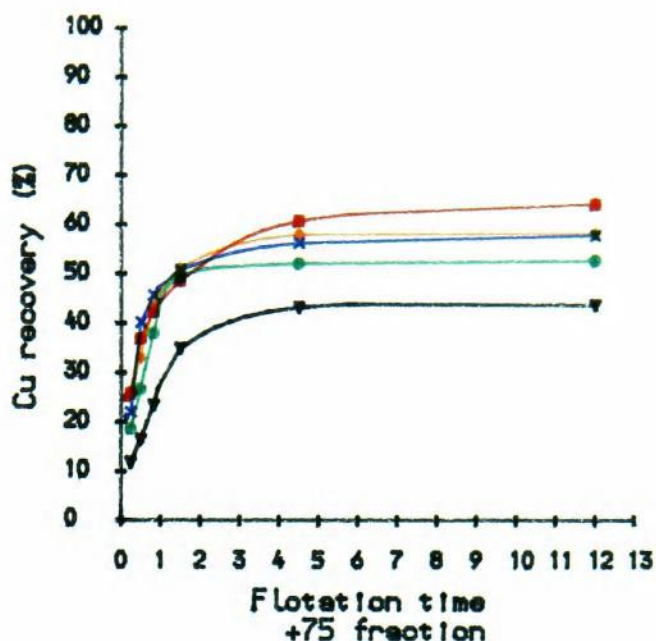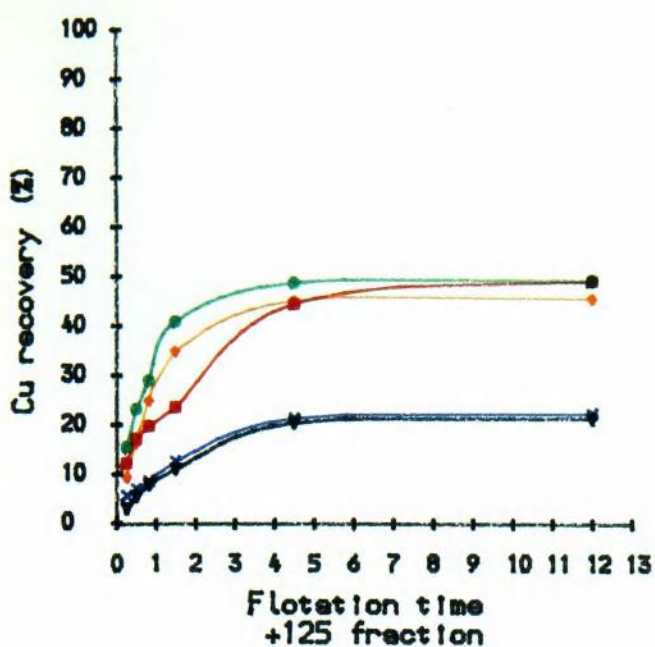
of complex sulphide flotation

Fig 7-15 IPS effect on Cu recovery

of complex sulphide flotation
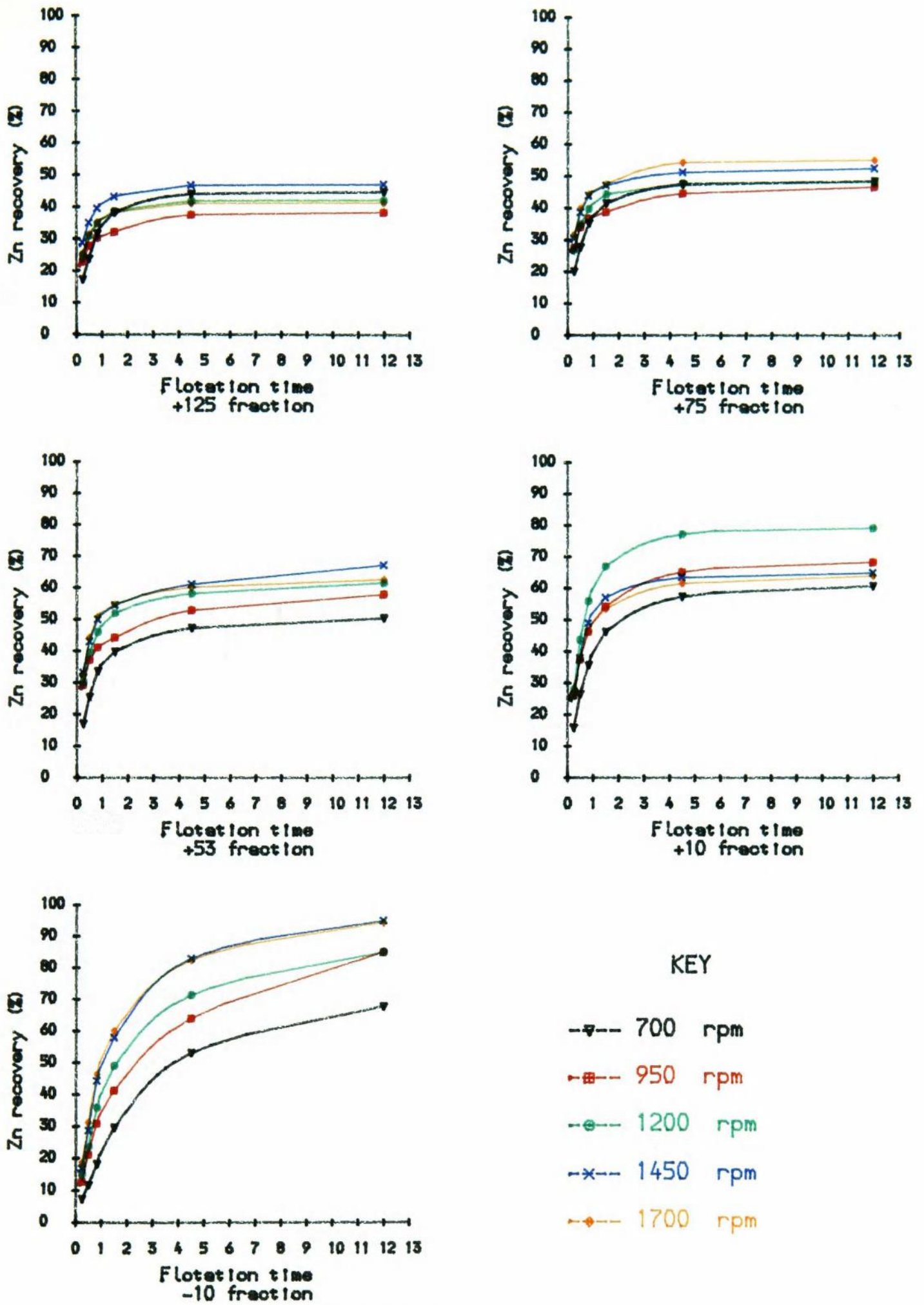
Fig 7-16 IPS effect on Zn recovery

of complex sulphide flotation

the recovery of all elements and mass, which may be due to the effect of excessive disturbance to pulp and cause some detachment of coarse particles. In -10 micron fraction, an increase in IPS increases the recoveries of mass and of all elements, this is different from the coarse and can be explained as an increase in IPS does not increase the detachment of fine particles, the increase in recovery of all elements may be due to the fact that high IPS results in generating small bubbles and creating more surface area, during the generating of the bubbles, fine particles, especially -10 micron, will be captured by frother and then attached to the bubble surface. But in the other size fractions, the effect of IPS does not have the similar pattern.

7.4.3 The effect of particle size ou complex sulphide flotation

The effect of particle size on recovery of different minerals has long been established, in this experiment, the same pattern between the particles size and the flotation recovery is observed in Fe. The effect of particle size on Cu and Zn are slightly different as shown in Fig7-19 and Fig7-20, it can be explained as the effect entrainment in the fine size and the inhibition in the coarse size, since the coarse fraction is more likely being inhibited as it can be seen in Fig7-8. Therefore the recovery of Cu and Zn is reduced when the size is increased. The effects of particle size on the recoveries of mass, Fe, Cu and Zn are shown in Fig7-17, 7-18, 7-19 and 7-20.

In Fig7-17, it should be noted that the IPS has very little effect on mass recoveries of all size fractions, the only effect of IPS on flotation recovery is the elements of Fe Cu and Zn, therefore from the results it is suggested that the increase in IPS can improved the selectivity of flotation, both the flotation recovery and grade are increased at high IPS. The effect of IPS may be due to the fact that the increase
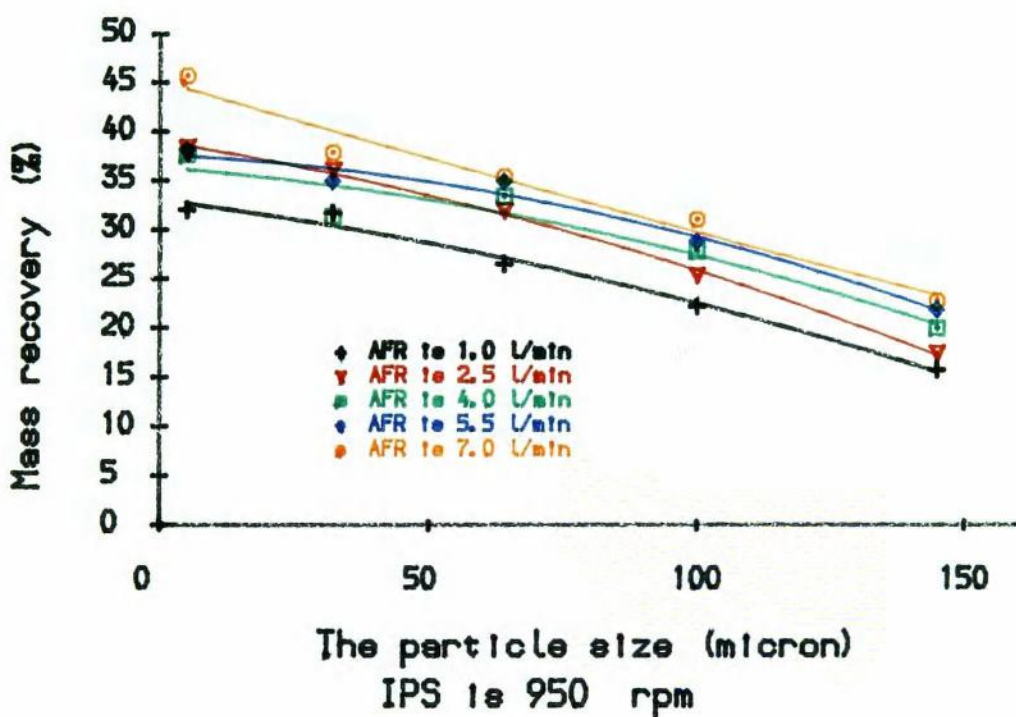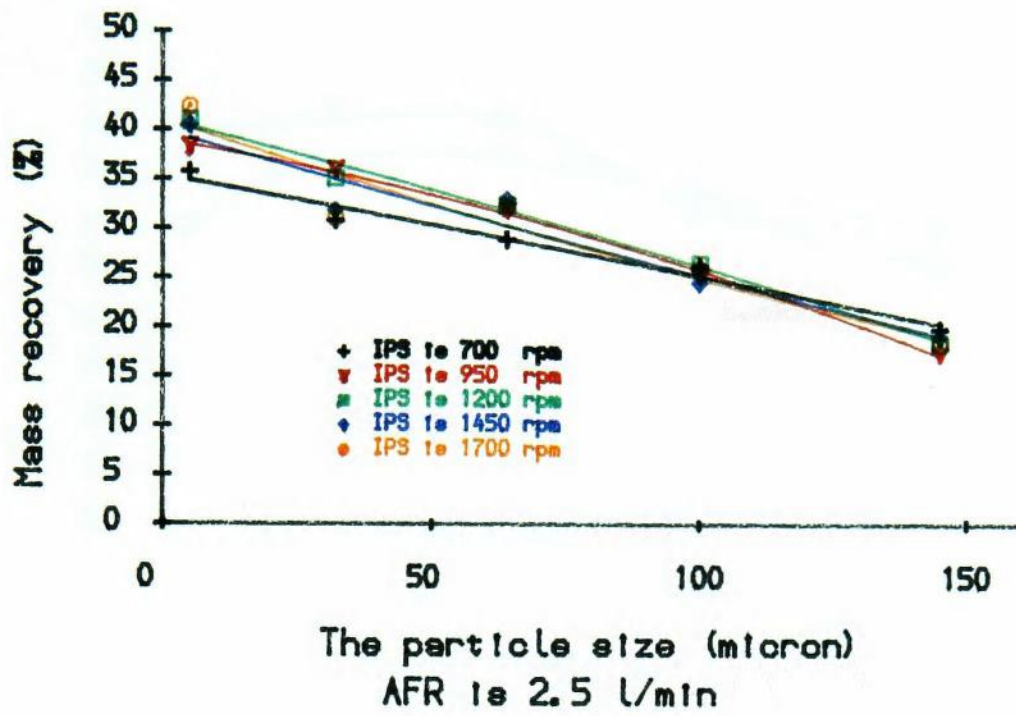
Fig7-17 The size effect on mass recovery
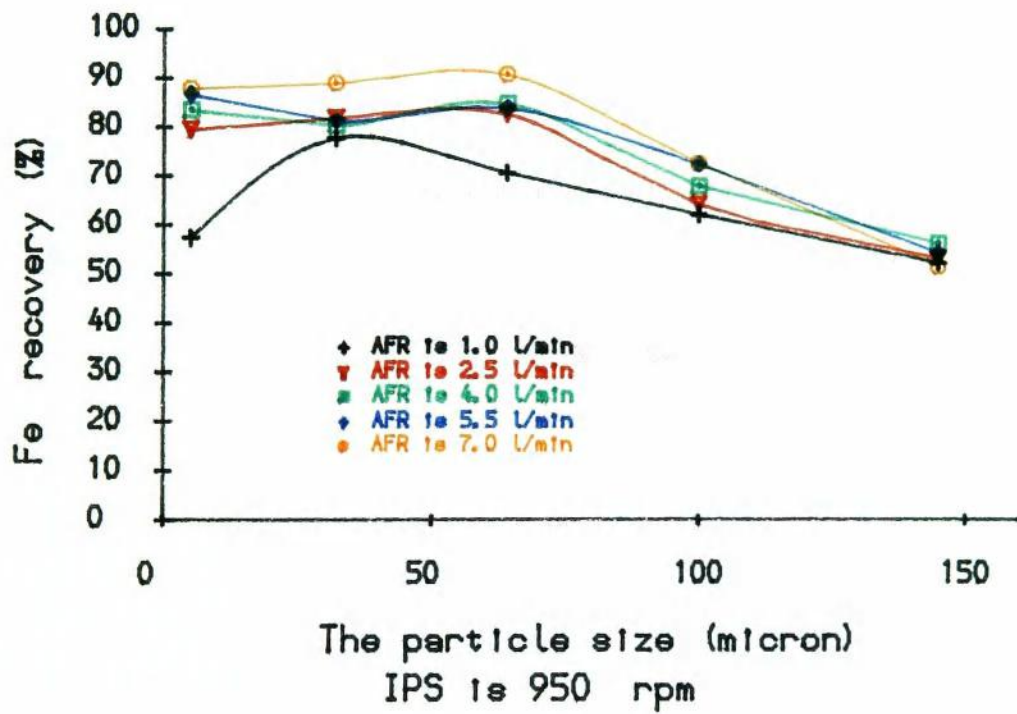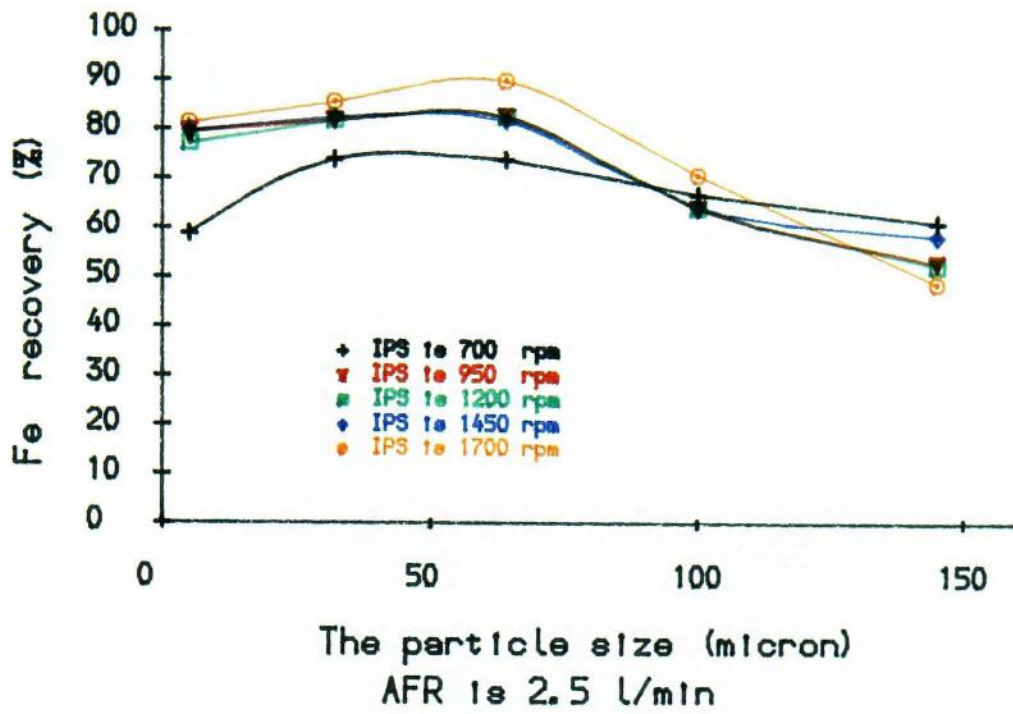
Fig7-18 The size effect on Fe recovery
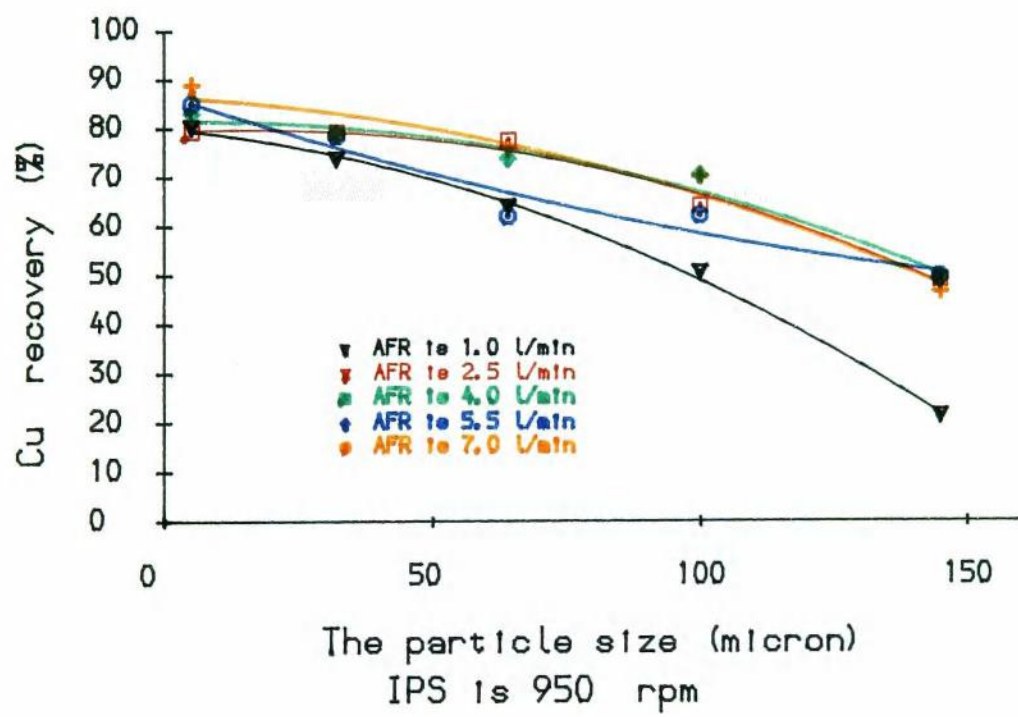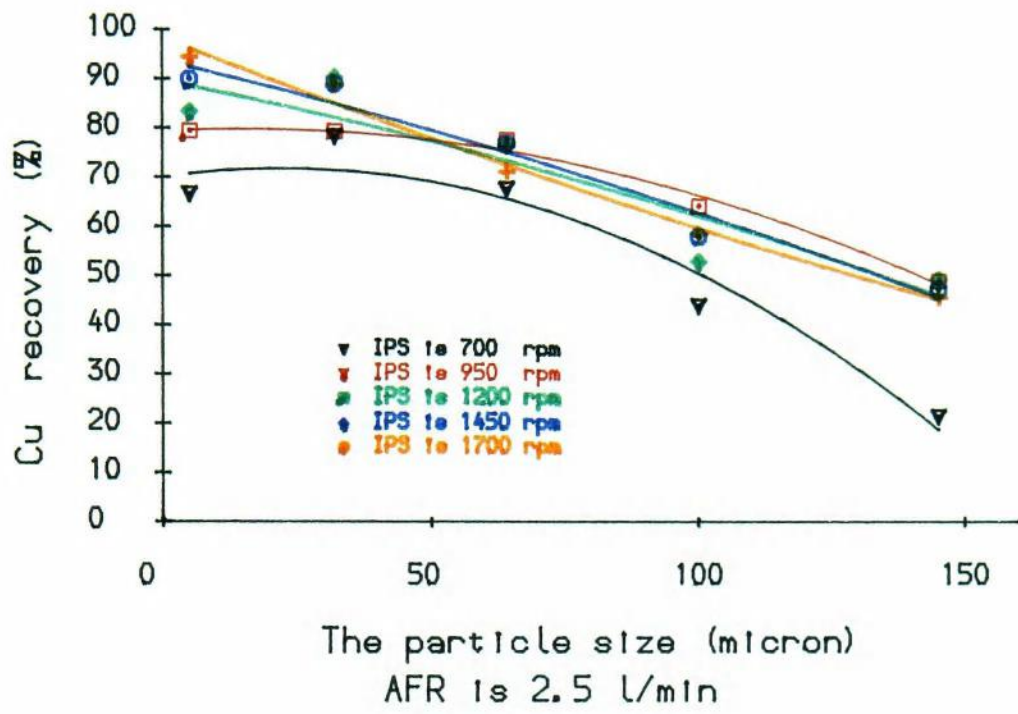
Fig7-19 The size effect on Cu recovery
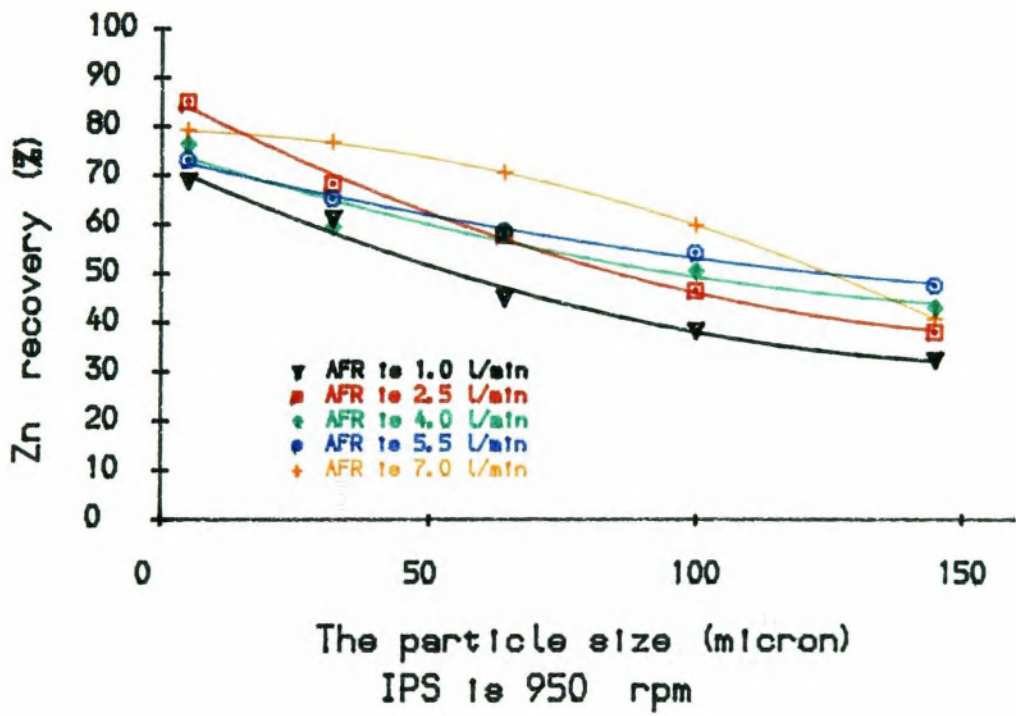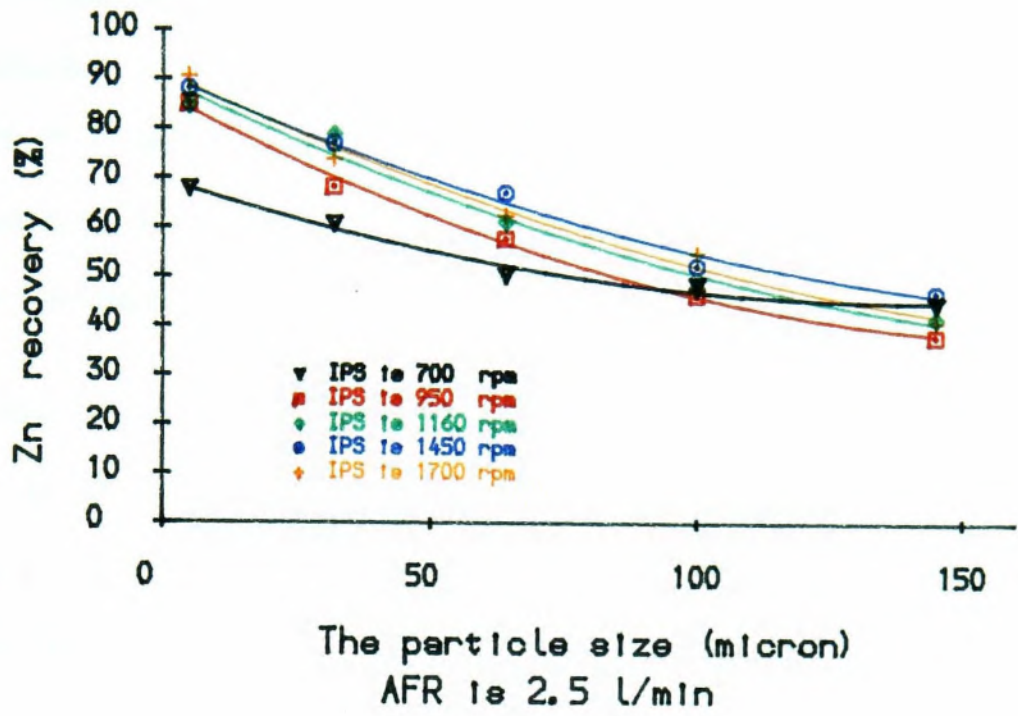
Fig7-20 The size effect on Zn recovery

in IPS offered more chance for the particles and bubbles collision, as the bubble surface are limited, therefore the highly floatable particles replace some of the less floatable particles.

In Fig7-17, 7-18, 7-19 and 7-20, it can be seen that the effect of AFR on mass recovery and element recovery is great. From the effect of AFR on the recoveries of mass and elements, it is suggested that AFR increased the entrainment.

From Fig7-18, the effect of particle size on the recovery of Fe show when the particle size is increased from -10 to 53-75 microns, Fe recovery is increased, for the particle size larger than 75 microns, Fe recovery is reduced. For Cu and Zn recovery, the pattern is similar to the Fe recovery for the size large than 53 microns, but the decrease of recovery in the -53 is not observed.

The effect of particle size can be explained as since the Cu and Zn are slower floating minerals and fine particles is less inhibited, therefore flotation recovery shows a continuous reduction from the fine to the coarse particles.

7.5 Summary

From the discussion of the experimental results, the effects of AFR, IPS and particle size on the flotation recovery and grade are obtained. AFR influences flotation in two ways. One is by its influence on the bubble surface area and water recovery, which subsequently affects the transfer rate of solid materials from froth over the cell lip and from the pulp to froth which leads to entrainment. The other is the effect on the power input which changes the suspension of particles and reduce collision. The overall effect of AFR on flotation results are shown at high AFR, the grade of concentrate is reduced and the recovery is increased due to entrainment. The results imply that the entrainment is the major effect of AFR in most of the experiments in this research work. IPS has also two effects, one is the effect on the

power input which can increase either collision between the particles and bubbles or the detachment of particles from bubbles. The other effect is on the dispersion of bubbles which may eventually affect the bubble surface area, the recovery of fine particles and water recovery. The outcome of the experiments shows that the effect of **IPS** on the recovery of coarse particles is negative and on the fine particles is positive. This conclusion is that for the coarse particles, the first effect is dominant and for the fine particles the second is dominant. The effect of particle size on flotation recovery is dependent on both the specific gravity and the floatability of the floatable minerals. For the coal flotation, since the specific gravity is low, the effect of size is small. In complex sulphide flotation, the highest recovery of the medium size is observed for the less inhibited Fe and which is expected.

Chapter Eight

Discussion of Models Results

8.1 Introduction

In this chapter, mass recovery and recovery results are fitted by the **CDM**, **MCM** and **GFM** models. The parameters from these models, as functions of the operating factors, **AFR**, **IPS** and particle size, are analyzed and the relationships between these model parameters and **AFR**, **IPS** and particle size are obtained. Finally a comparison between the different models is carried out.

8.2 Results from CDM

By using computer data fitting as discussed in chapter four, the parameters of the **CDM** are calculated. Since in the **CDM**, one mineral system is different from a multi-mineral system, the two cases are treated separately. The difference between a one mineral system and multi-mineral system is that in one mineral flotation mass recovery is dependent only on the floatable mineral, while in multi-mineral flotation, the flotation rate for mass recovery no longer depends on any particular mineral and therefore it can only be treated independently. In this research work, coal and chalcopyrite flotation are the one mineral systems. Complex sulphide flotation is an example of a multi-mineral system.

8.2.1 One mineral system

When the flotation results from chalcopyrite and coal flotation are used, the CDM parameters are obtained and are tabulated in Appendix 12.

In a one mineral system, since the process of flotation is not affected by any other minerals, flotation shows that the pure or liberated mineral particles have the highest flotation rates. Flotation is affected by factors such as **AFR, IPS**, particle size and the floatability of the floatable mineral.

From the **CDM** results in Appendix 12, it can been seen that the grade of the unfloatable fraction is not zero, this implies that 100% flotation recovery cannot be reached. In the results, it is also shown that the fast floatable fraction has a higher grade than the slow floatable and unfloatable fractions, which implies that the flotation rate of the high grade fraction is higher. The relationship between the fractional grade and the flotation rate constant is shown in Fig 8-1.

Although in a one mineral system, Fig 8-1 is typical for the relationship between the grade and the flotation rate constant, this relationship may also be changed if other factors come into effect, such as if fine particles or a small fraction of unexpected mineral which has high flotation rate constant is presented in the flotation feed. When this happens, the flotation process should be considered as a multi-mineral system.

In Fig 8-1, the non-zero grade of the unfloatable fraction can be explained as the consequence of inadequate liberation, insufficient reagents or the presence of extra large particles.

The model results of CDM for chalcopyrite and coal flotation are shown in Fig 8-2 and 8-3.
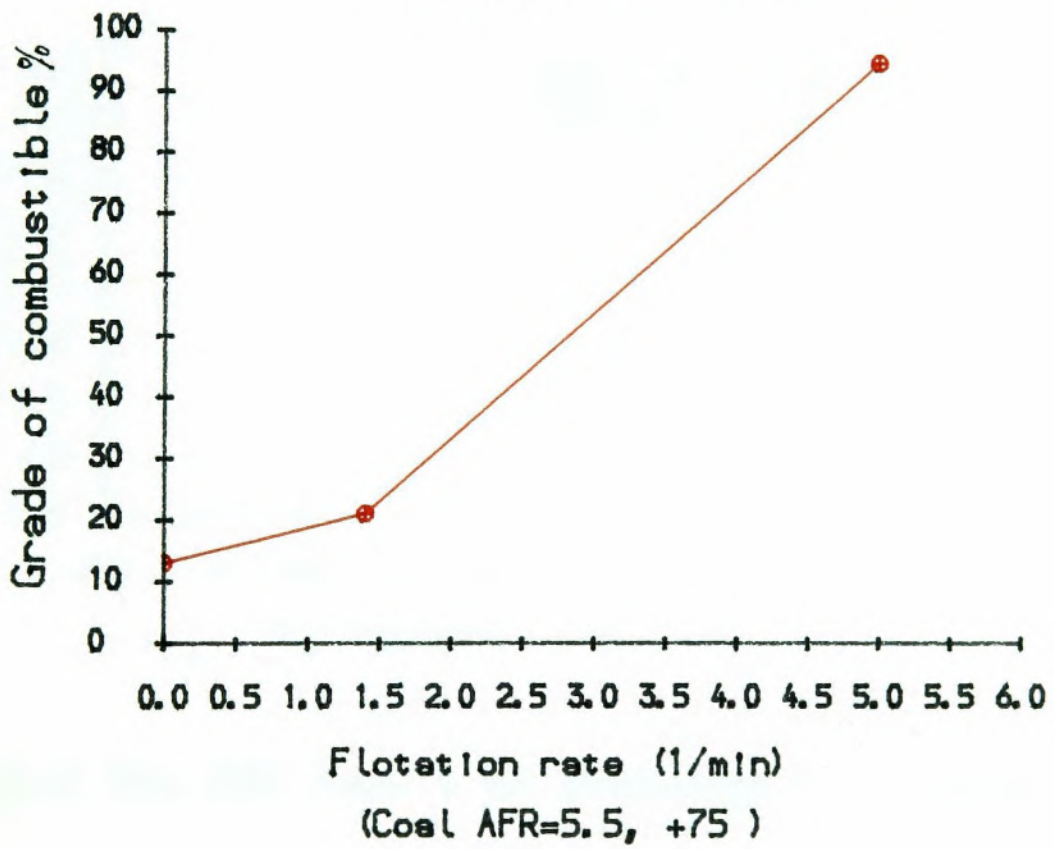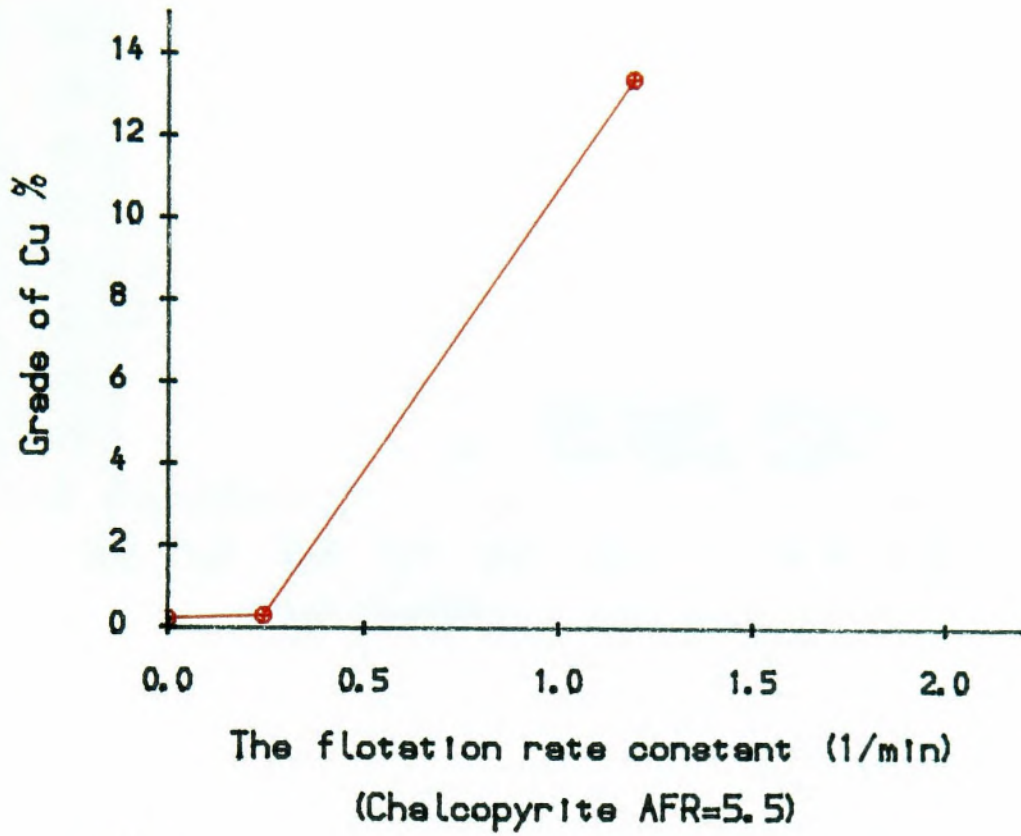
Fig 8-1. Fractional grade vs flotation rate
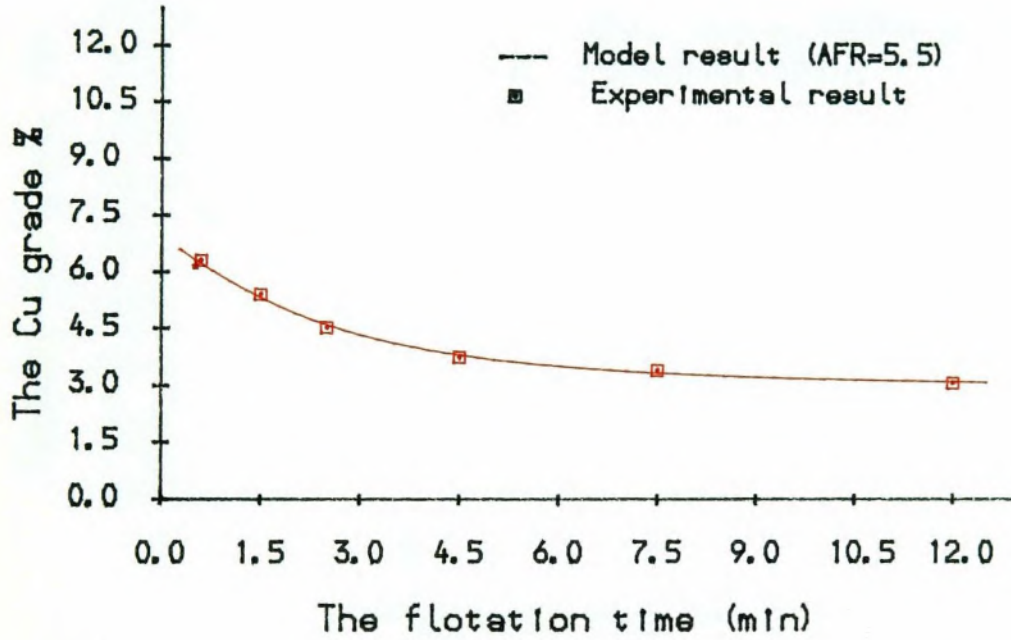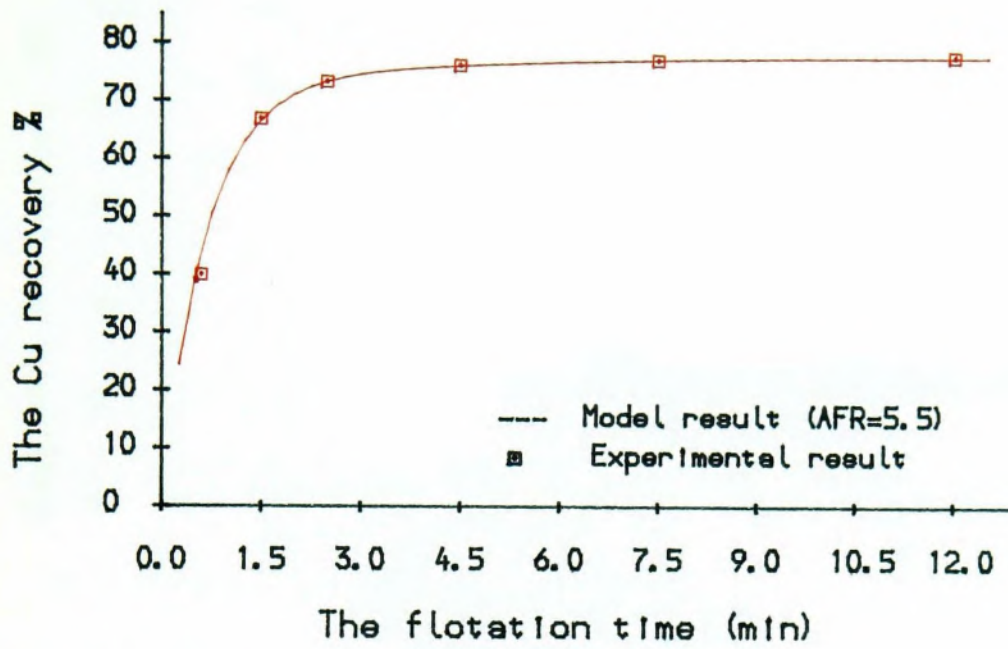
Fig8-2 The CDM result of chalcopyrite flotation
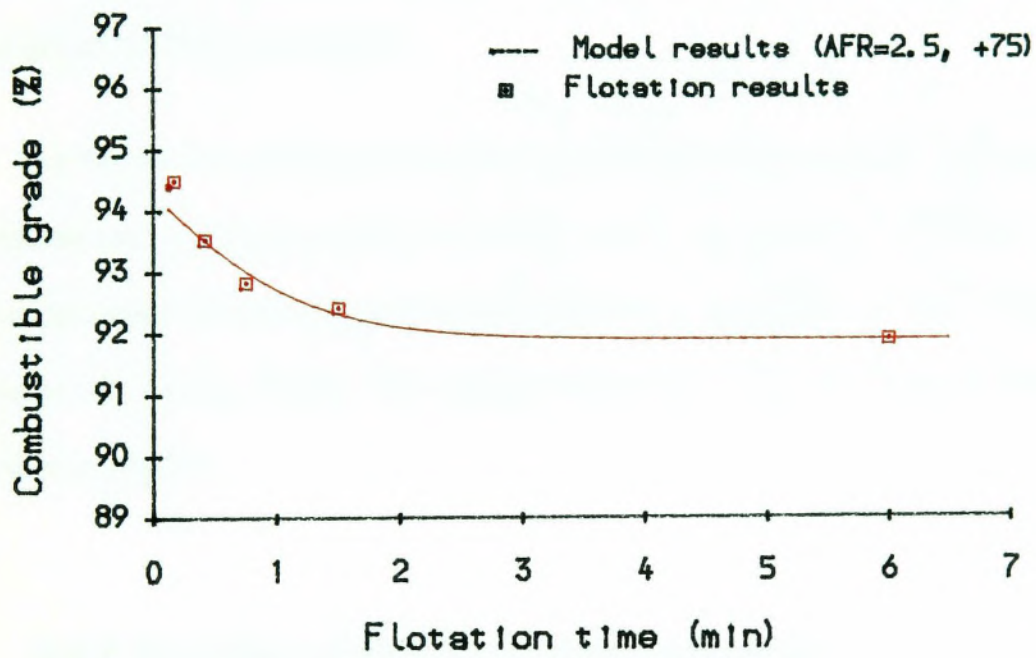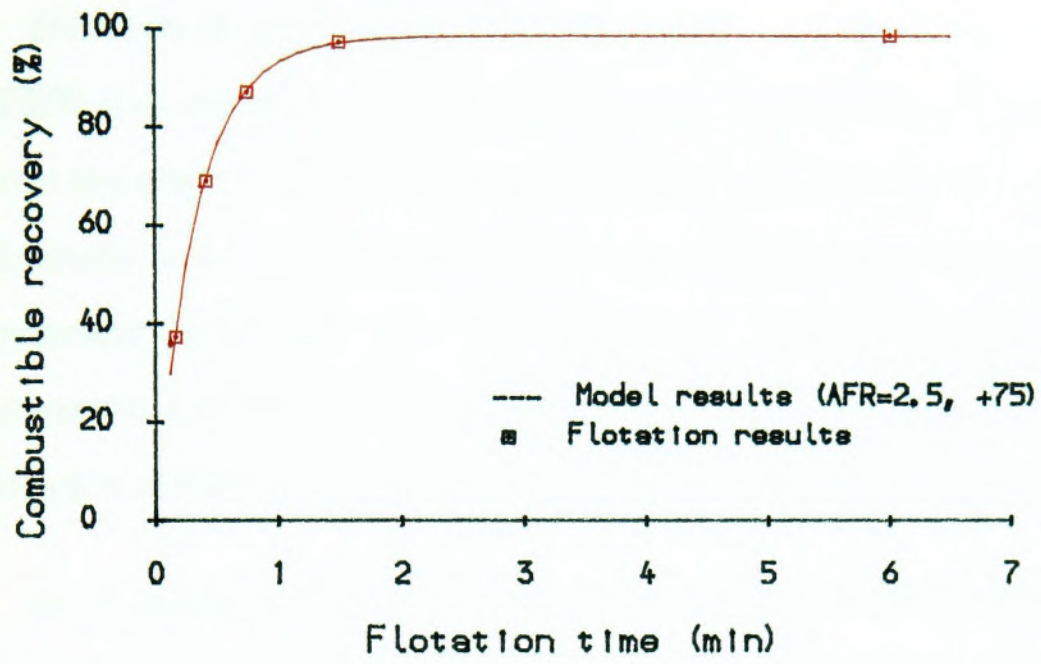
Fig8-3 The CDM result of coal flotation

8.2.2 Multi-mineral system

Due to the presence of many floatable minerals, fitting of the flotation results by **CDM** for a one mineral system cannot be used and the method for multi-mineral system described in chapter four is used. Each floatable mineral and mass is treated individually in the multi-mineral system, where the element in the mineral is used to represent the mineral, i.e, · Fe represents for arsenopyrite and pyrite (Fe in chalcopyrite is subtracted), Cu represents for chalcopyrite and Zn for sphalerite. The parameters of **CDM** for the complex sulphide are presented in the Appendix 13.

In the model results, the error of Cu fitting is observed to be greater than the others. The reason for this could be due to the lower grade of Cu in the samples which, with a small error in the assay value, can result in a significant error in the final recovery. Therefore Fe and Zn are mainly used in the discussion of the factors that affect **CDM** parameters.

In the multi-mineral system the relationship between the fractional grade and flotation rate constant cannot be obtained since the recovery of mass and elements have different flotation rate constants. However, the grade of the concentrate can be obtained by using **CDM**. The model results in -125+75 (micron) size fraction is shown in Fig8-4.

8.2.3 The effect of AFR on the parameters of CDM

The effect of **AFR** on the parameters of **CDM** is mainly shown on the floatable fraction of mass and the flotation rate constants. In chalcopyrite flotation, the effect of **AFR** is that when the **AFR** is increased from 1.0 to 5.5 l/min, the fraction of slow floating mass increases from 5% to 12.6%. With further increase in **AFR**, the fraction
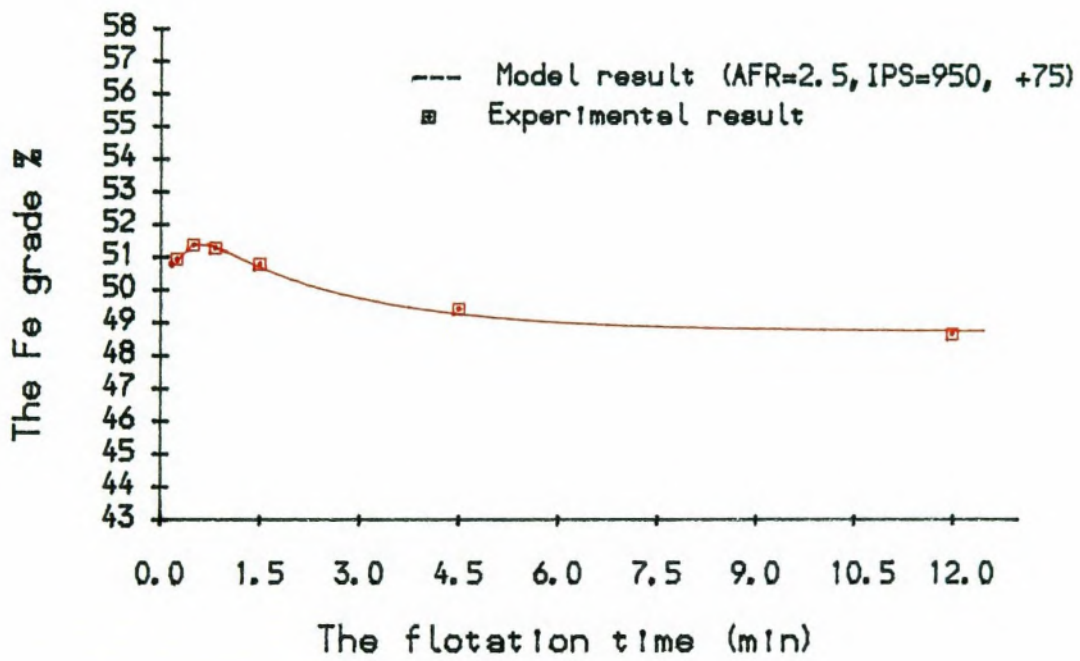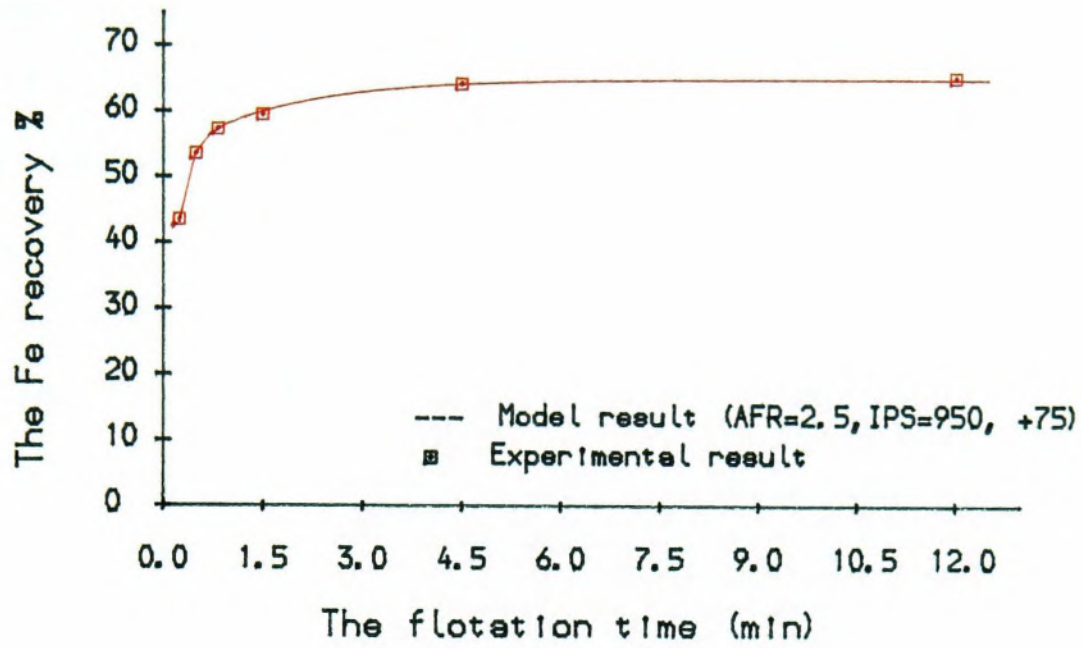
Fig8-4 The CDM result of complex sulphide flotation

of slow floating mass stays constant (Fig8-5). The effect on the fraction of fast floating component, when **AFR** is increased, the mass fraction shows a linear increase from 2.5% to 3.8%. However when **AFR** is increased, only a little effect on the flotation rate constants of slow and fast floating components has been observed as shown in Fig8-6.

The effect of **AFR** on the fraction and the flotation rate constants in coal flotation is that when the **AFR** is increased, the fraction of fast floating is increased and the slow floating is reduced, the flotation rate constants of both the fast floating and the slow floating are increased. The coal flotation result could in part be explained on the basis that when **AFR** is low, both fast and slow floating fractions are inhibited, when **AFR** increases, some slow floating component becomes fast floating, at the same time the flotation rate is increased by increasing the collision. The **AFR** affects on the parameters of the slow and fast floating components in coal flotation are also shown in Fig8-5 and Fig8-6.

From the discussion above, it is concluded that the effect of **AFR** on flotation results is that when the **AFR** is increased, entrainment is increased and therefore a lower concentrate grade and higher recovery are obtained in a certain flotation time. When the fraction of floatable material is small, the increase in the recovery is small when flotation time is longer enough, but when the fraction of floatable material is large, the increase in recovery may have a large increase but the concentrate grade is reduced. The balance of the two effects will determine the final results. From the one mineral flotation result, it is suggested that for coal flotation, high **AFR** is better then low **AFR**, and for chalcopyrite flotation, low **AFR** is better than high **AFR**.

The pattern of the effect of **AFR** on the unfloatable fraction of one mineral system, coal and chalcopyrite flotation, is shown in Fig8-7.

1. Chalcopyrite flotation
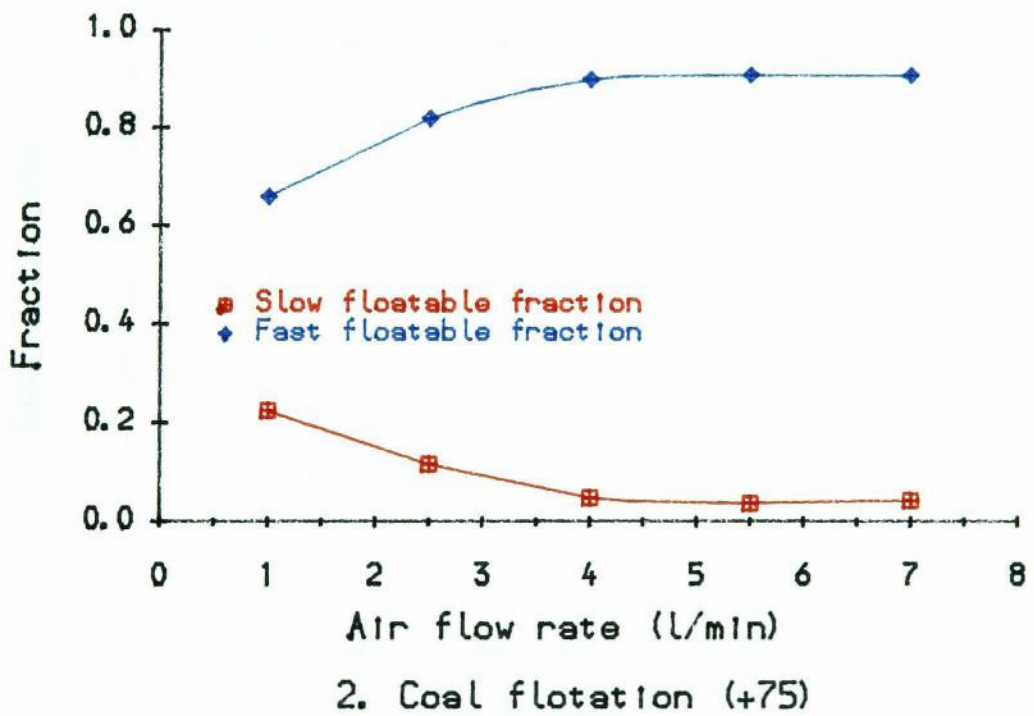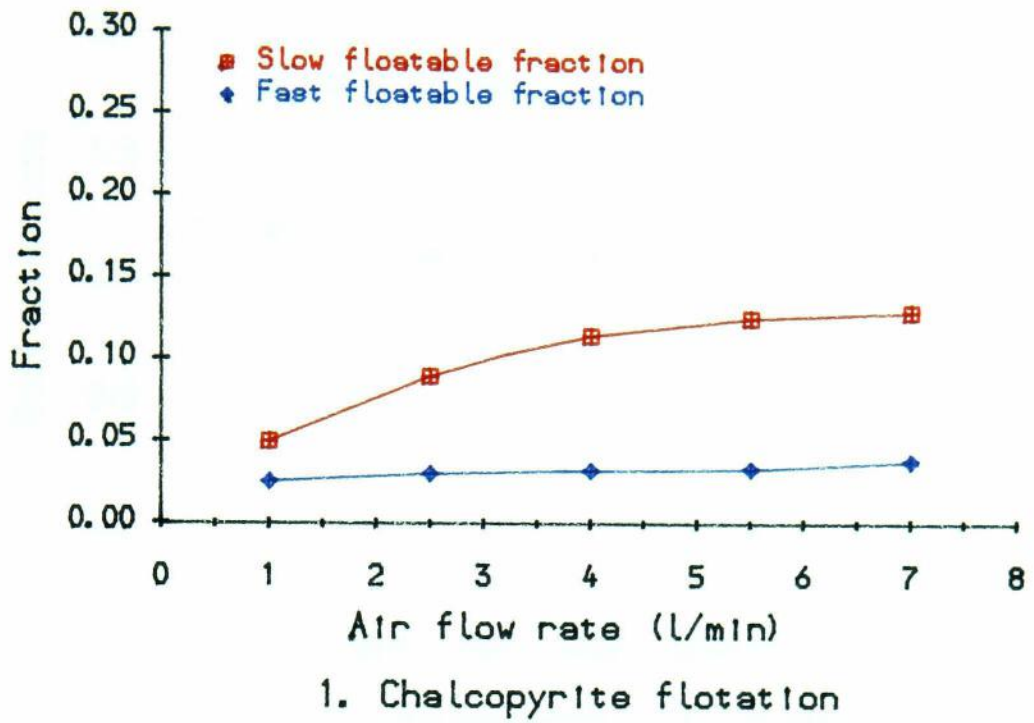
2. Coal flotation (+75)

Fig8-5 The effect of AFR on fractions
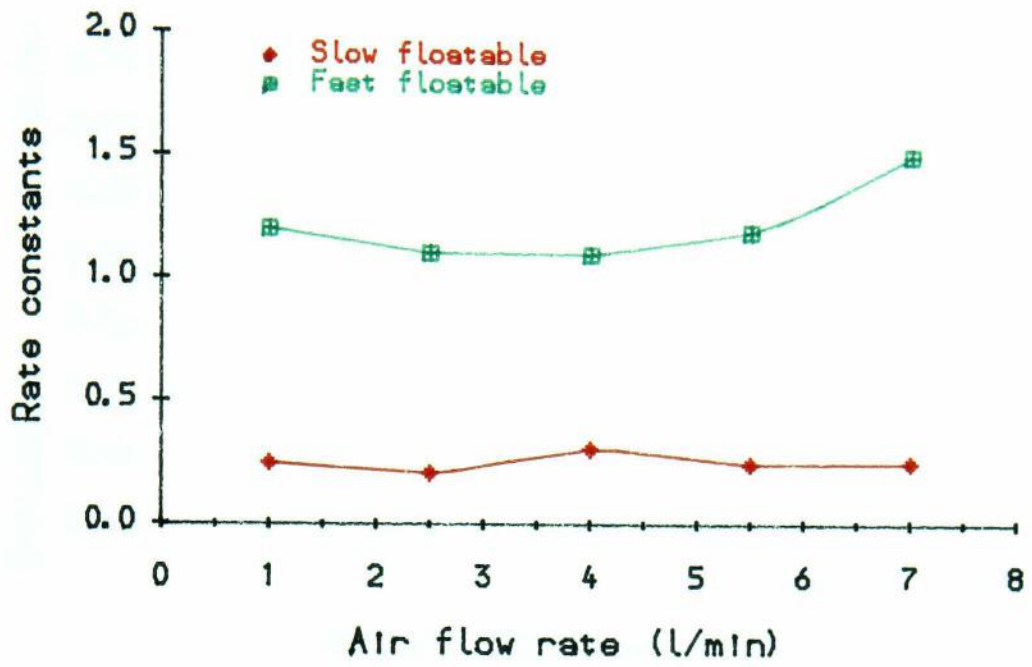
1) Chalcopyrite flotation
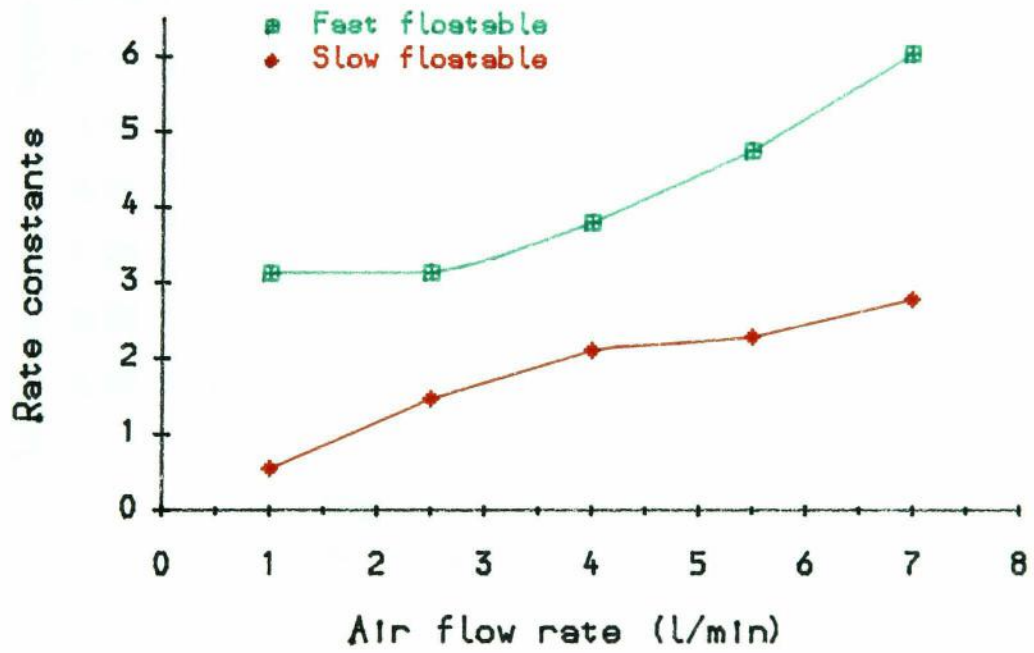
2. Coal flotation (+75)

Fig8-6 The effect of AFR on rate constants
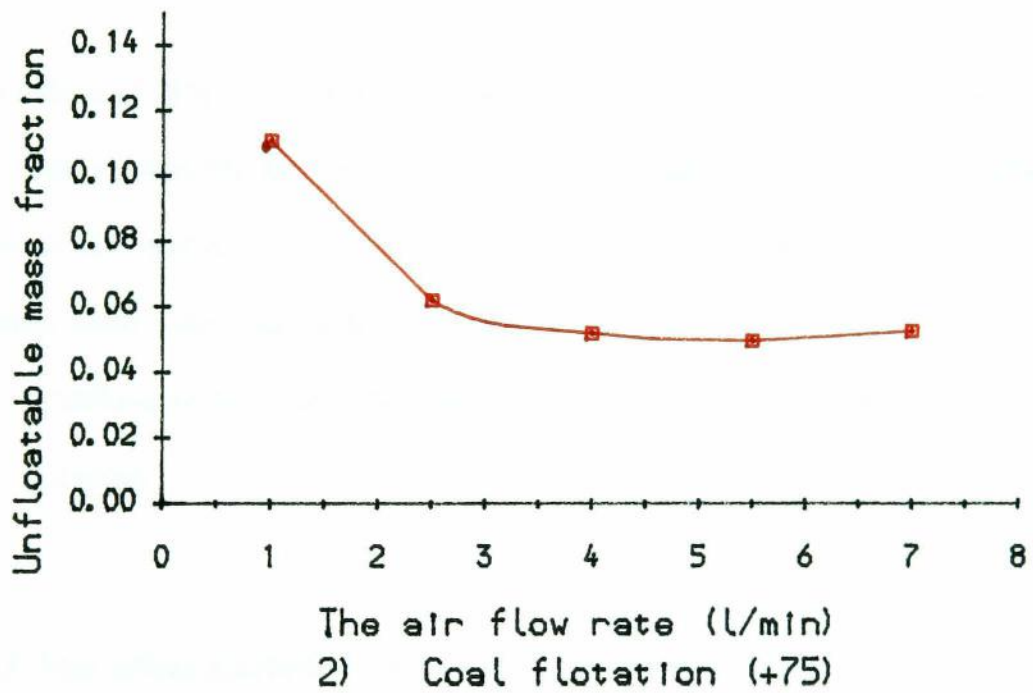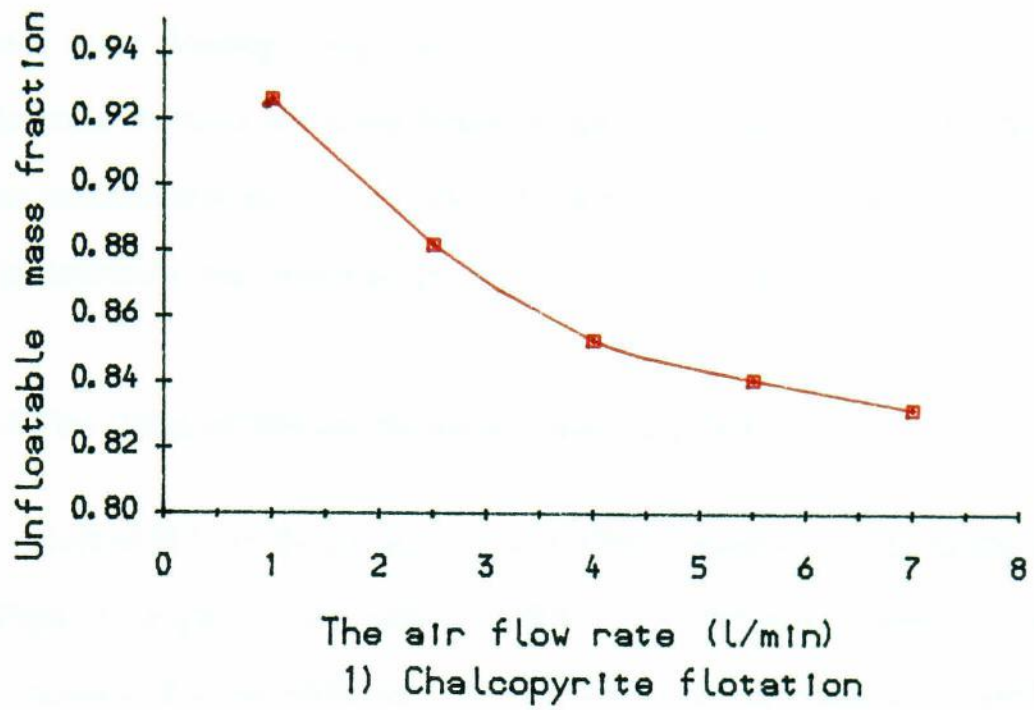
Fig8-7 The AFR effect on unfloatable fraction

In the multi-mineral system, the effect of **AFR** on the flotation rate constants of fast and slow floating components is complicated since mass and element recoveries does not have the same flotation rates. The parameters in **CDM** for Fe and Zn are inconsistent and are shown in Fig8-8 and Fig8-9. From the results it is difficult to determine the flotation rate as functions of **AFR**.

8.2.4 The effeet of IPS on the parameters of CDM

The effect of **IPS** on the parameters of **CDM** is observed in the multi-mineral system (Fig8-10, Fig8-11), the effect of **IPS** on the different minerals is similar. However, compared to the **AFR**, the effect of **IPS** on the parameters of **CDM** is less consistent. The effect of **IPS** on the flotation rates of multi-mineral system Fe and Zn (+75) is shown in Fig 8-10 and Fig8-11.

The effect of **IPS** on the flotation rate constants may be due to two factors, one of which is that when the **IPS** is increased,a better suspension of particles and better dispersion of air bubbles are achieved, therefore the flotation recovery is increased. On the other hand when the **IPS** is increased, excessive disturbance to the pulp can result in detachment between the particles and bubbles, which may reduce the recovery of coarse.

8.2.5 The effeet particle size on the parameters of CDM

In coal flotation, the effect of particle size on the flotation rate constants and the fractions of fast and slow floating components is shown in Fig8-12, when the size changed from the -53 to +125 microns, the flotation rate constants is reduced
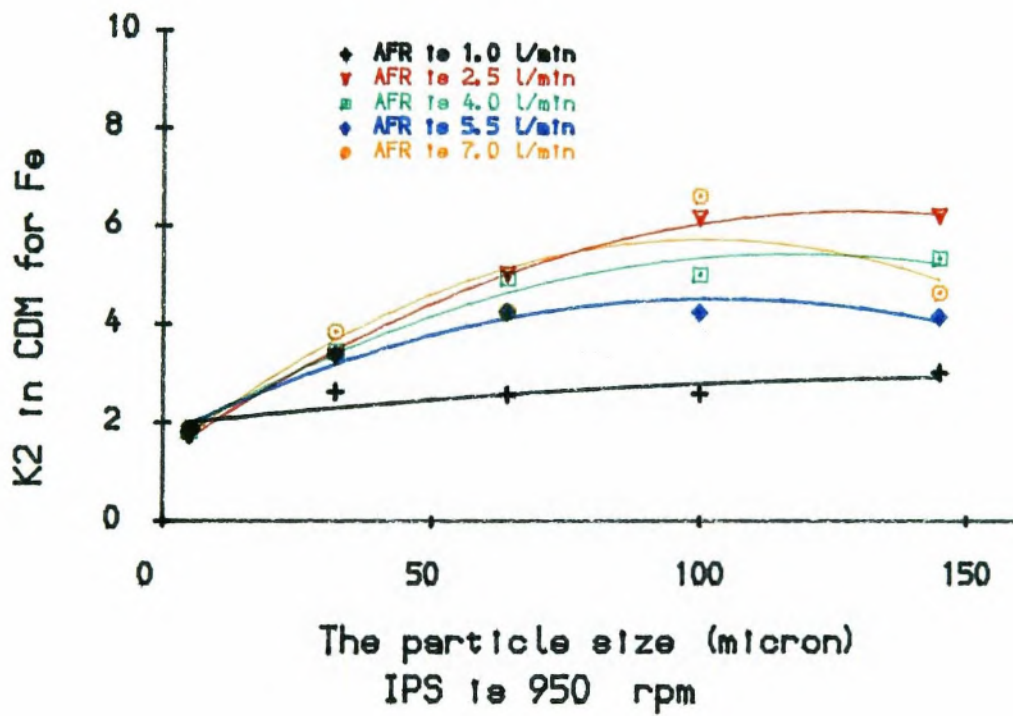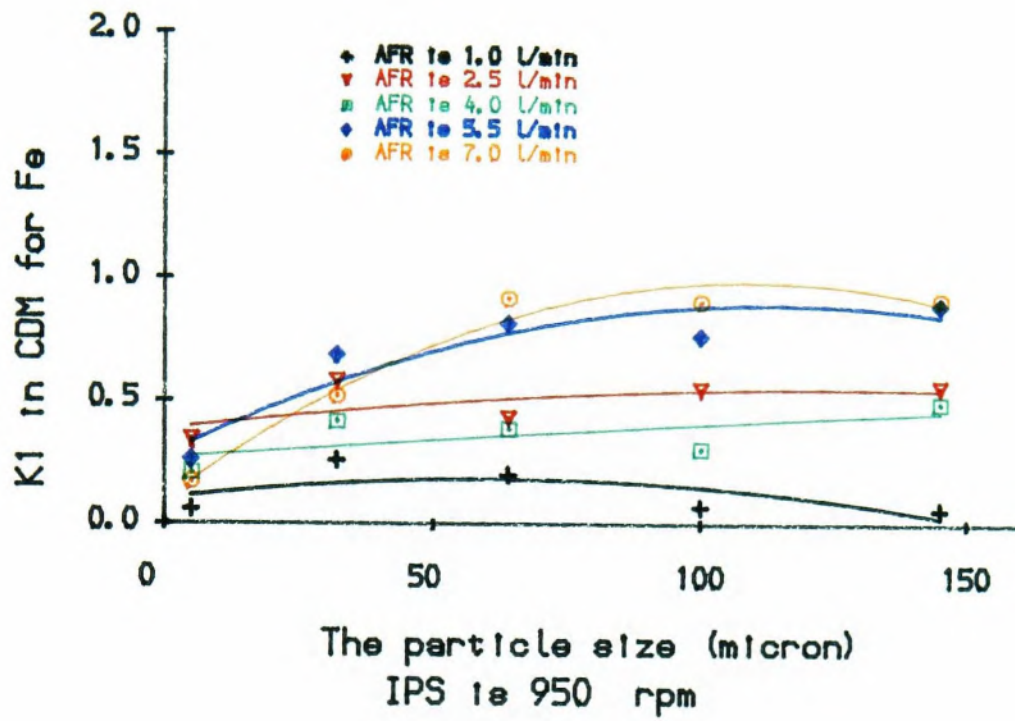
Fig8-8   AFR effect on the CDM parameters of Fe
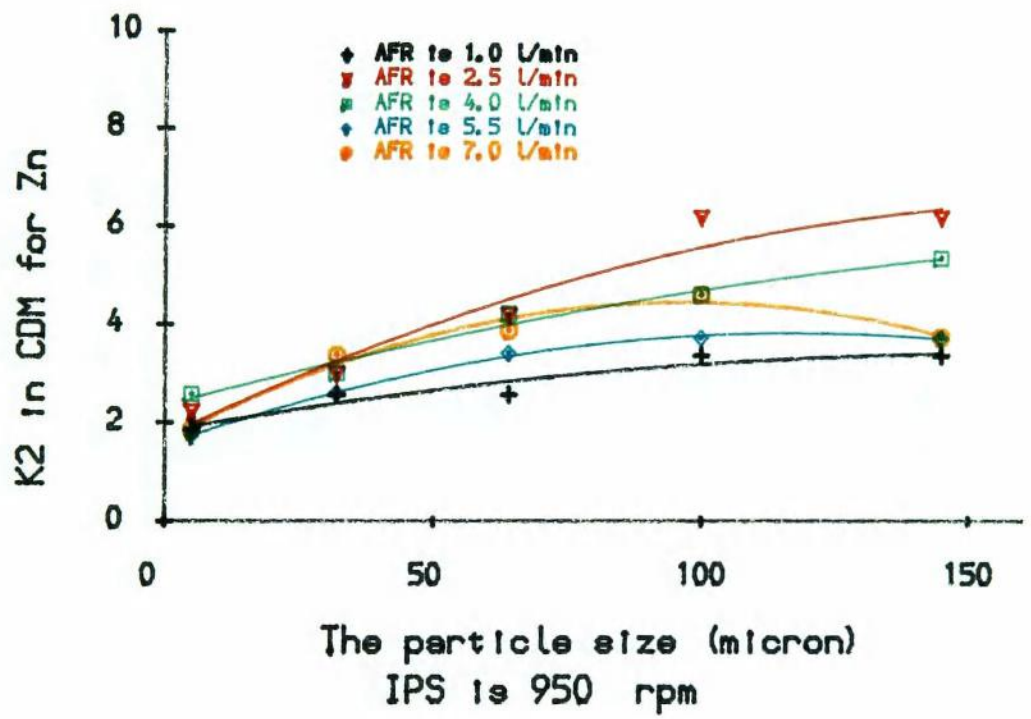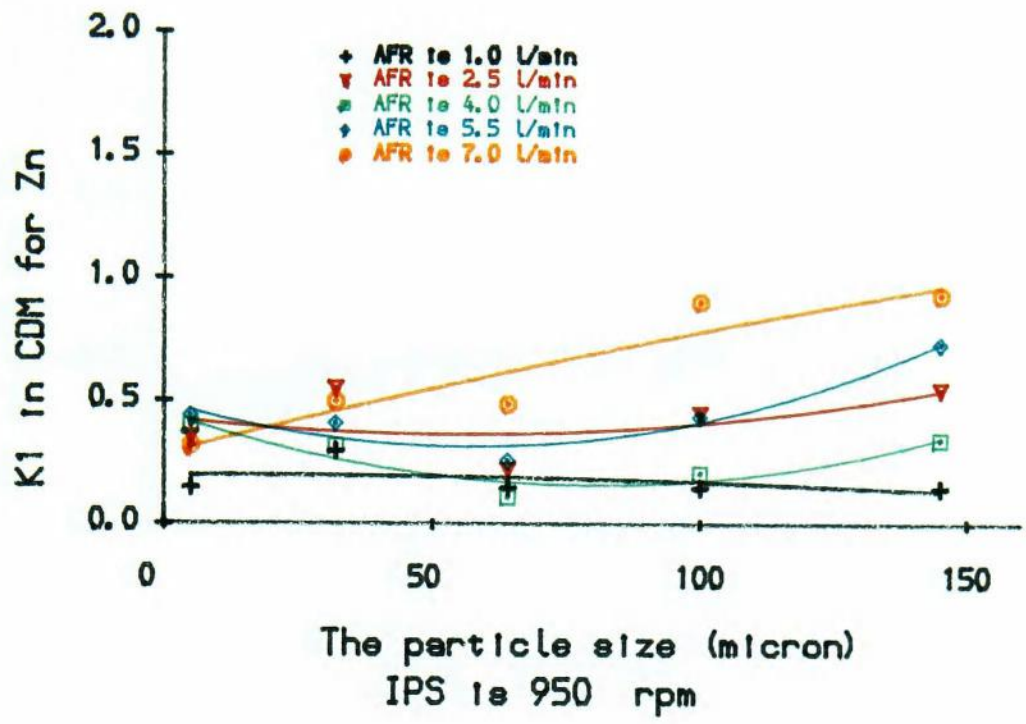
Fig8-9 AFR effect on the CDM parameters of Zn
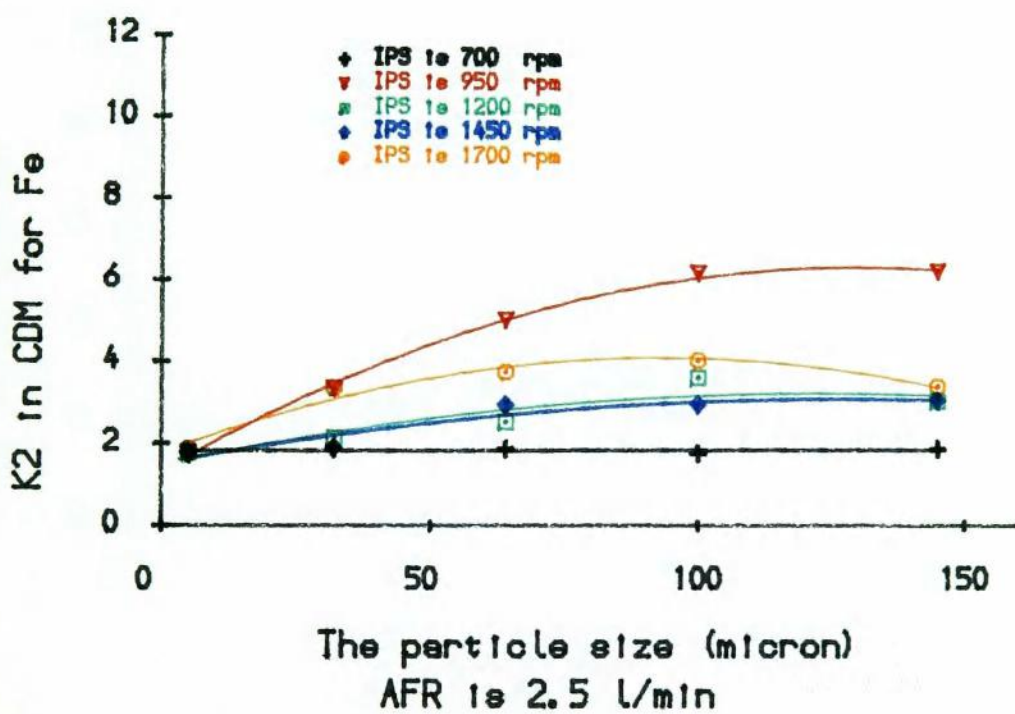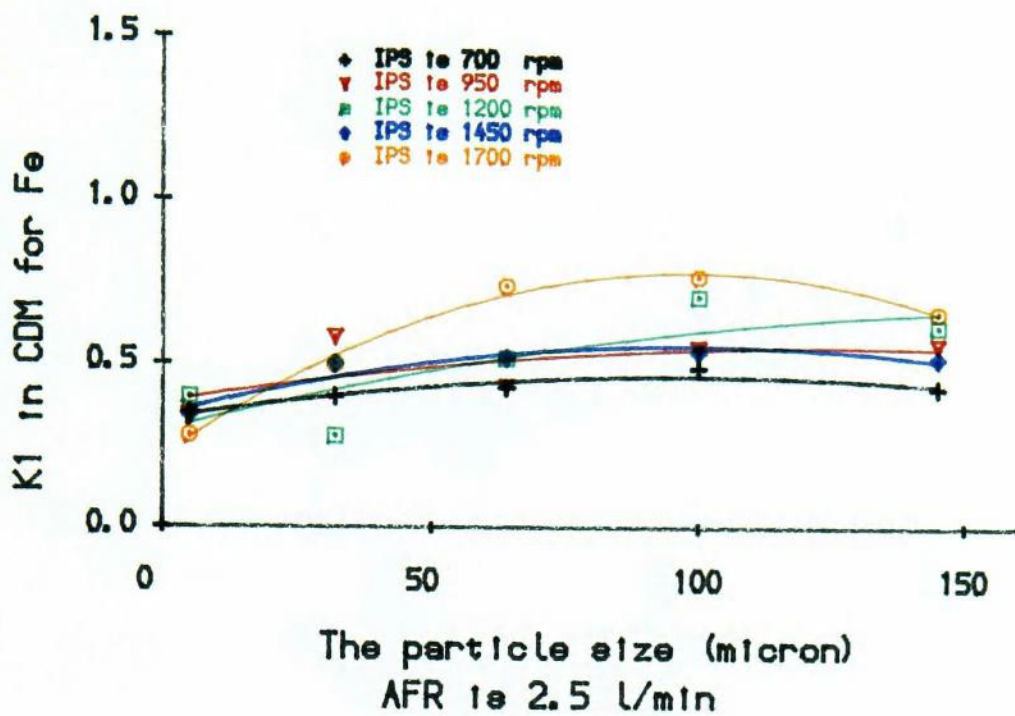
Fig8-10 IPS effect on the CDM parameters of Fe
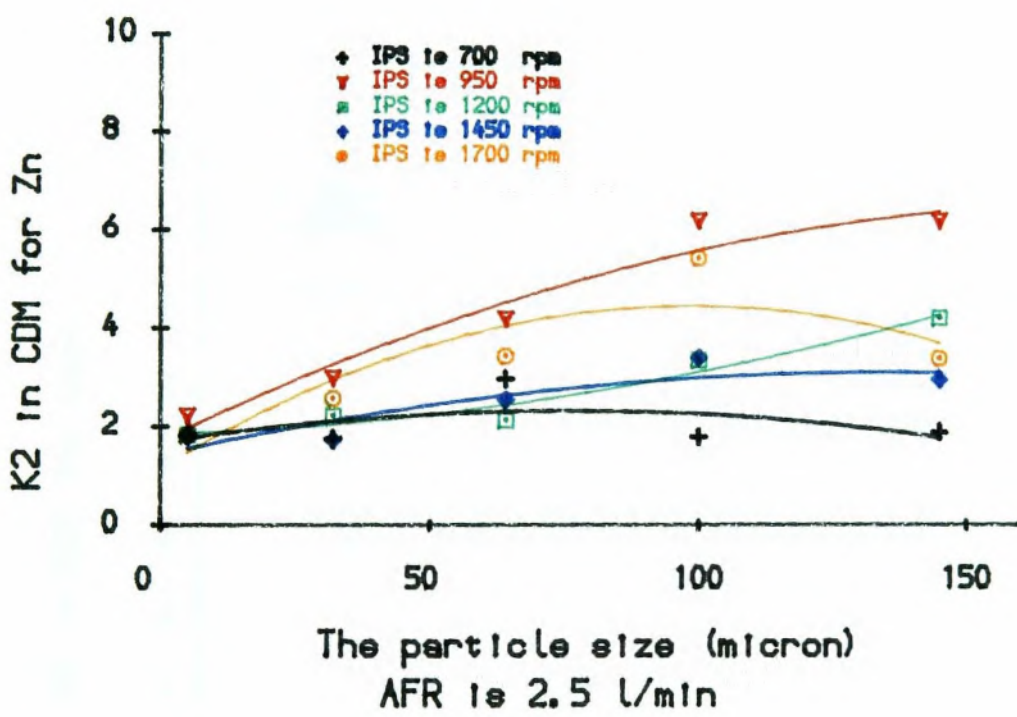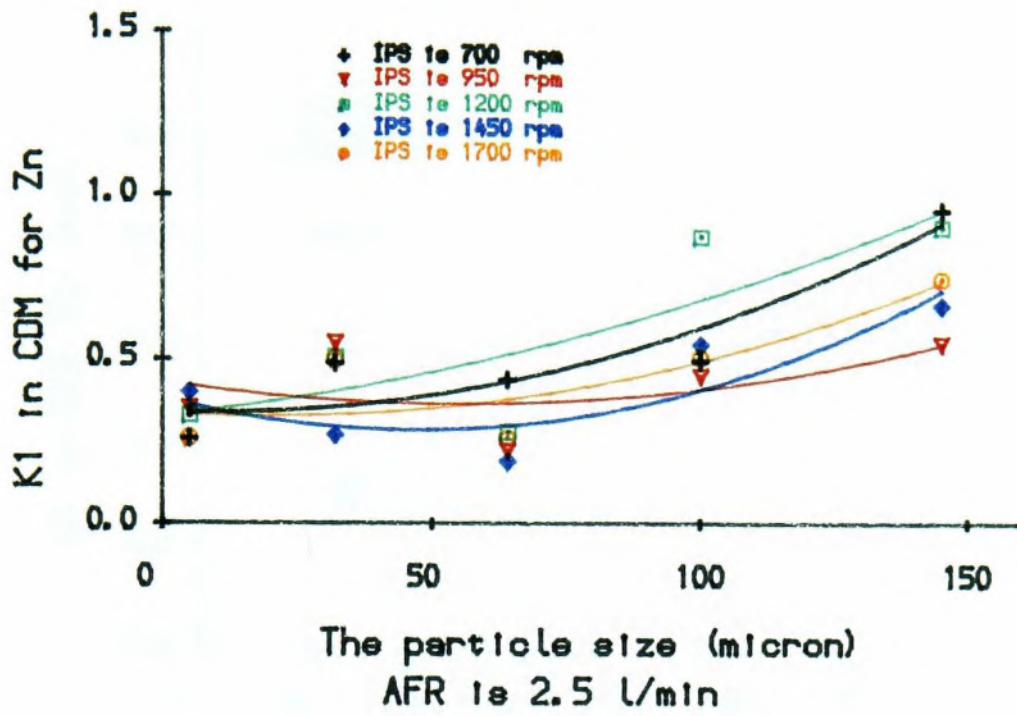
Fig8-11 IPS effect on the CDM parameters of Zn
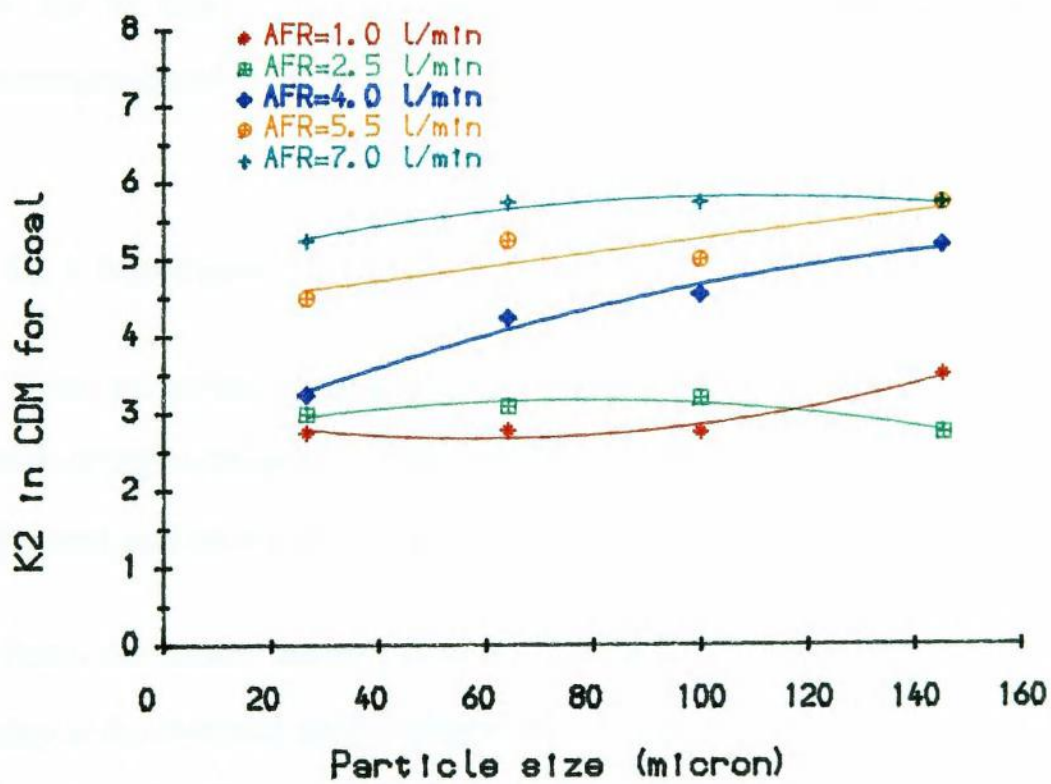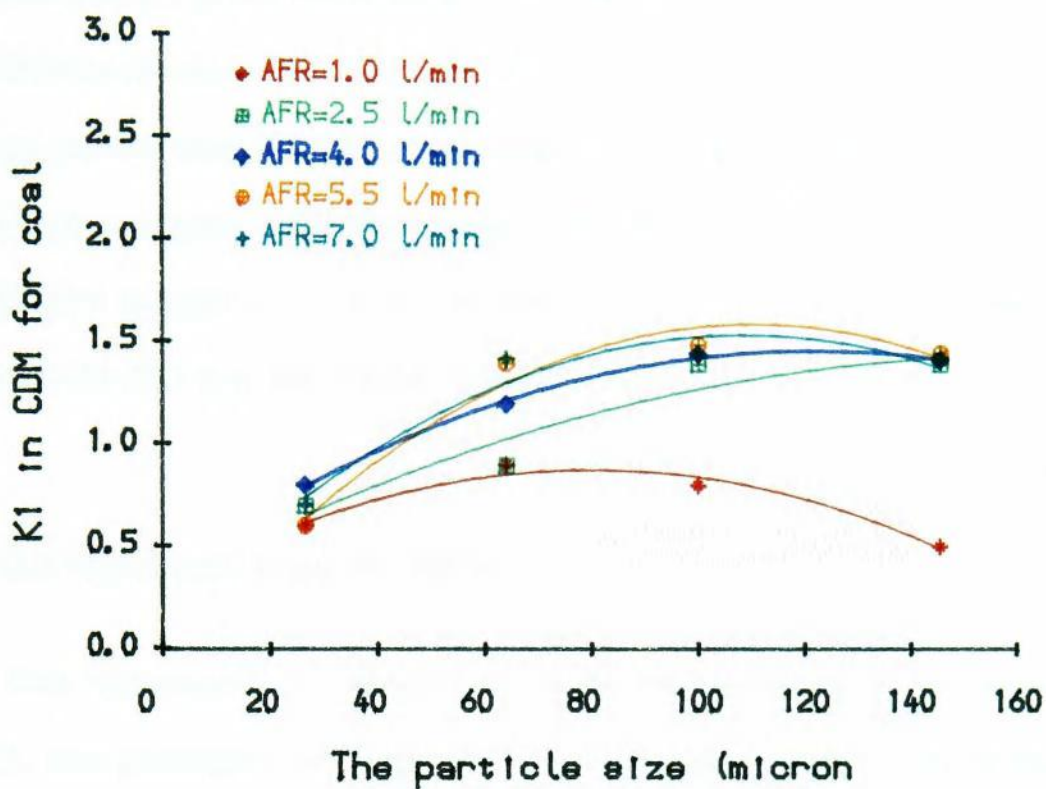
Fig8-12 The effect of size on CDM of coal lotation

from 5.08 to 3.7, at 4.0 l/min **AFR,** for fast floating component and reduced from 3.7 to 3.2 for the slow floating component, while **AFR** is at 1.0 (l/min), both the fast floating and the slow floating components are not significantly affected.

On the complex sulphide flotation, the effect of size on the flotation rates, from Fig8-8 to Fig8-11, is shown that the medium size has the highest flotation rates and the fine size has lowest flotation rates.

8.3 The results from the MCM

As it was described in Chapter 3, the **MCM** is a modified Chen's model. In the **MCM**, two parameters are employed for the mean flotation rates of element and mass recovery, two parameters for the reduction factors of the mean flotation rates, two for the unfloatable fractions of element and mass and one for the time correction. In the **MCM** there is no difference between the one mineral system and the multi-mineral system.

8.3.1 Parameters in the MCM

When the computer programs in chapter 4 are employed, the results from the flotation of different minerals are fitted by **MCM** and the parameters of the **MCM** are obtained and tabulated in Appendix 14 and 15.

From the model results, it is observed that the mean flotation rate of copper recovery at the flotation start is greater than that of mass recovery in the chalcopyrite flotation. This implies that a larger fraction of copper is distributed to the region of

high flotation rate than the fraction of mass. This shows in the flotation results such that the concentrate at the beginning of flotation has a higher grade than later in the process.

However in coal and complex sulphide flotation, some of the mean flotation rates for mass are greater than the mean rates of combustible or elements. This implies that the selectivity of the flotation for one mineral can be reduced by the effect of reduction in particle size or increase in **AFR** (coal).

Generally, the **MCM** is good in fitting the experimental results, the **MCM** results of chalcopyrite and coal flotation (+75 micron) are shown in Fig 8-13 and 8-14 and the **MCM** results of complex sulphide is shown in Fig8-15.

From the model results for complex sulphide, it is observed that the Fe (pyrite and arsenopyrite) is fastest floating amongst the three minerals and followed by sphalerite, and then chalcopyrite. The characteristics of the fast floating mineral is indicated by the mean flotation rate (Kmean) and the rate of reduction of the mean flotation rate (G). When Kmean and G is large, flotation of that mineral is fast. When the Kmean and G of mass recovery are not changed, an increase in Kmean and G for recovery of element means the flotation result is improved.

8.3.2 The effect of AFR on parameters of MCM

The **AFR** has a significant effect on the mean rate and the rate of reduction of the mean rate. The net result is either a positive or negative on grade, since the **AFR** not only affects the parameters in element recovery but also in mass recovery. When the **AFR** increases Kmean of mass more than that of element recovery, the flotation results will be worse. Therefore the best performance of flotation is at an **AFR** in
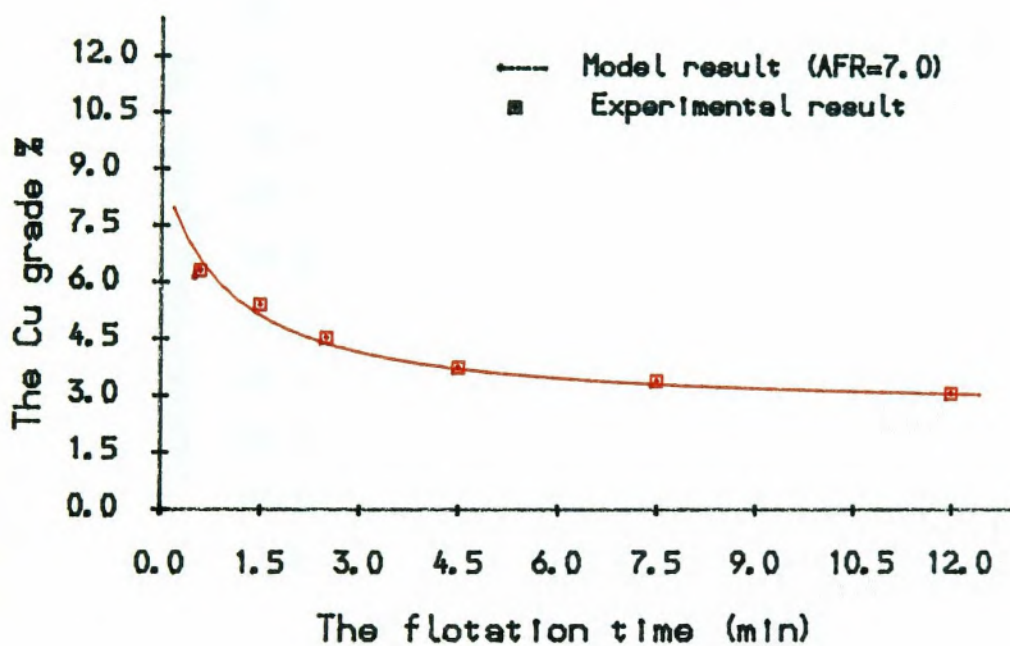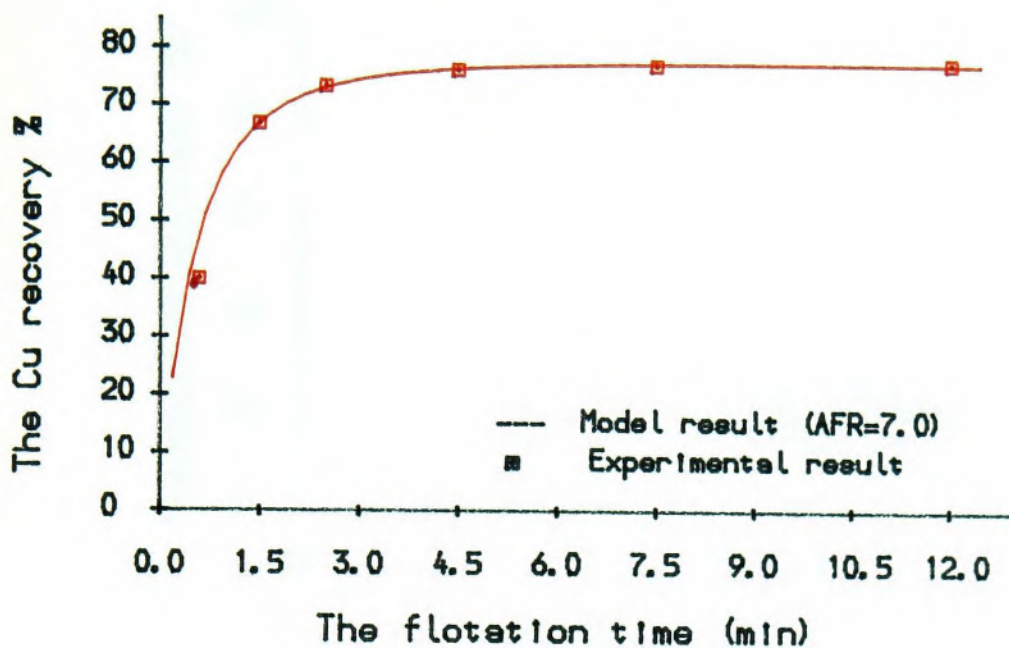
Fig8-13 The MCM result of chalcopyrite flotation
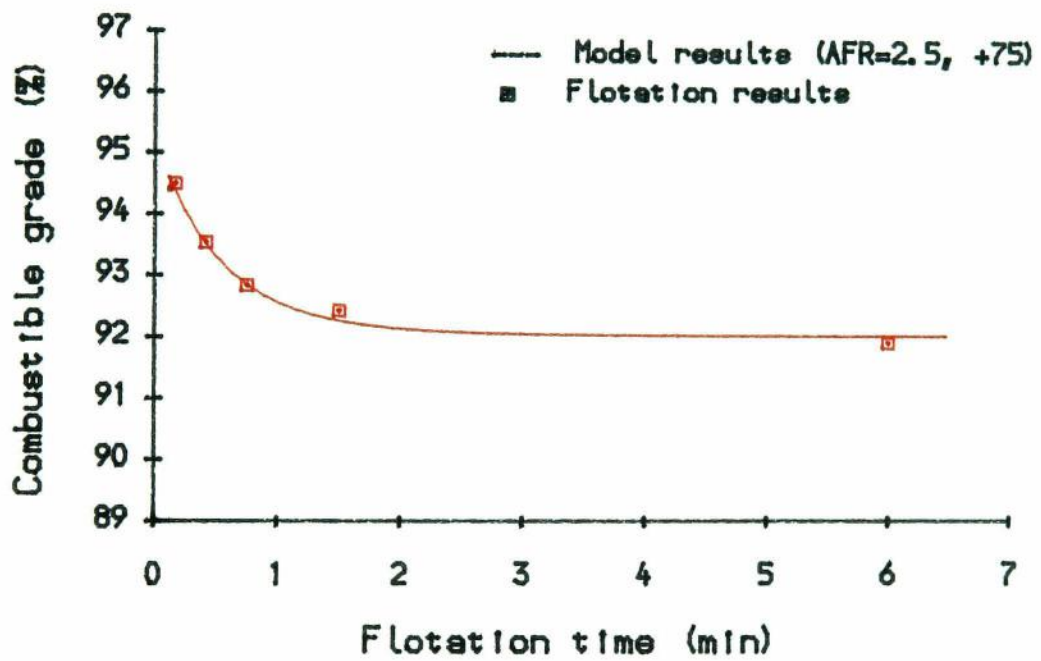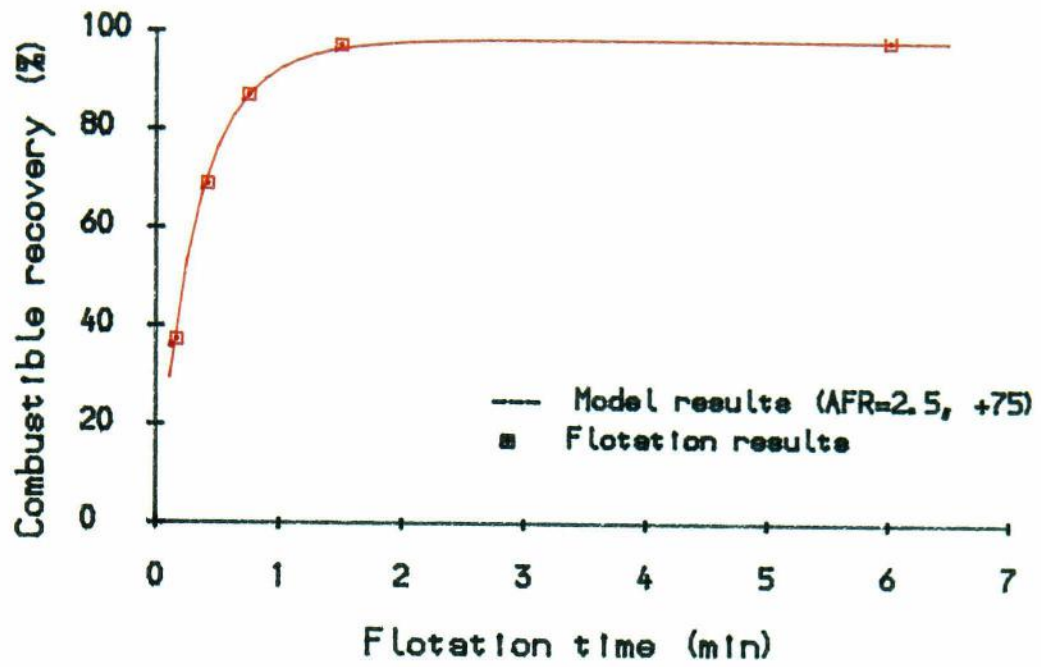
Fig8-14 The MCM result of coal flotation
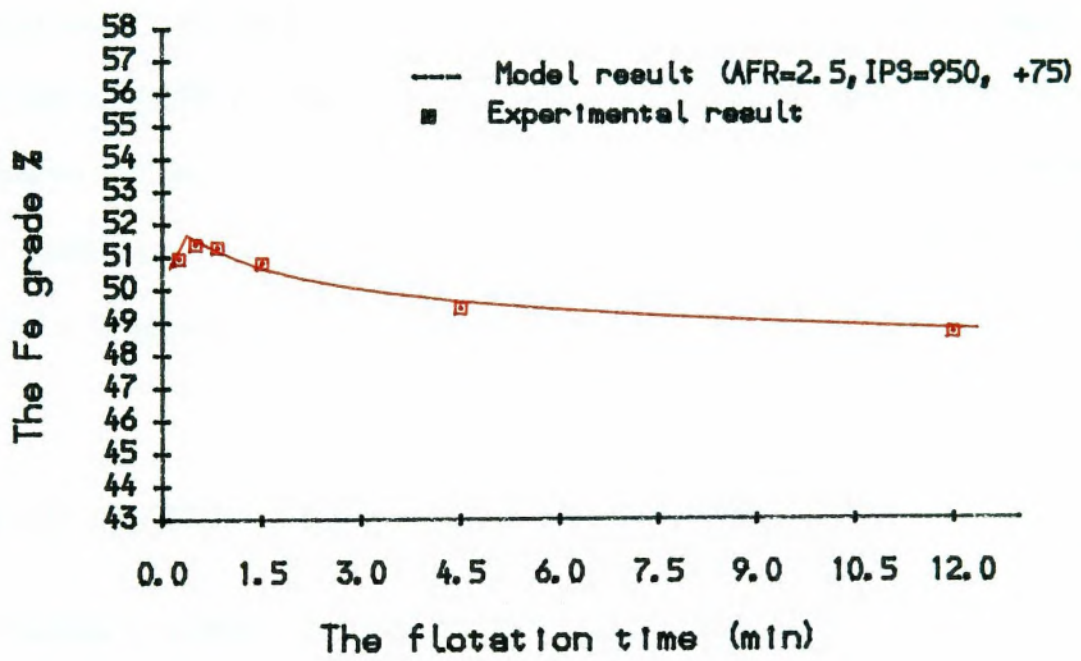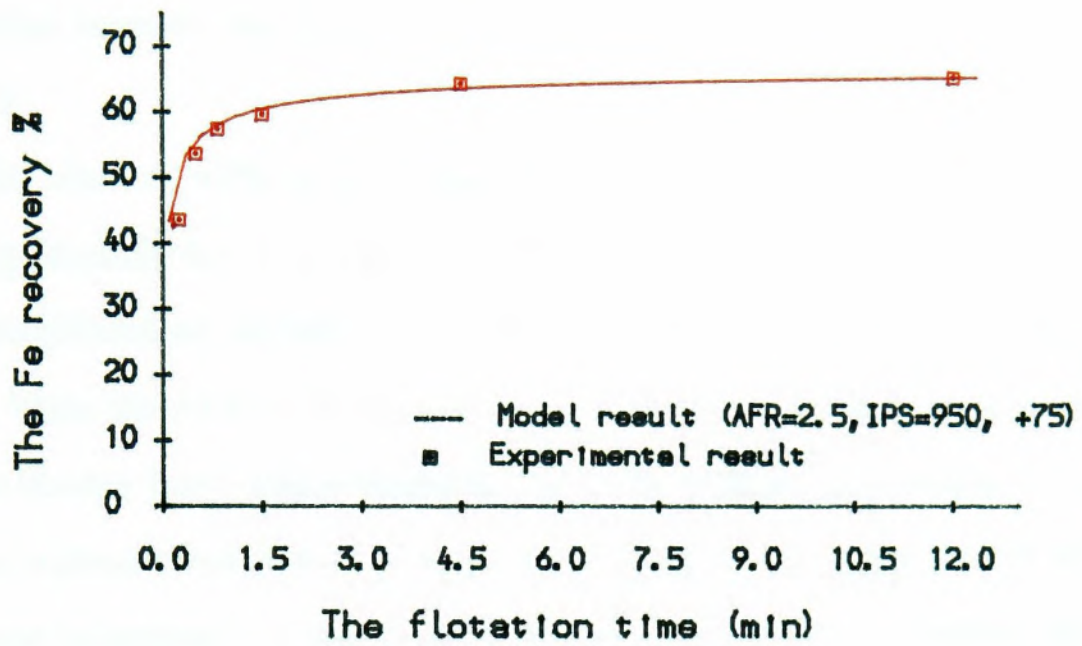
Fig8-15 The MCM result of sulphide flotation

which the positive effect in grade is maximum. The effect of **AFR** on Kmean and G of mass recovery and recovery of chalcopyrite and coal flotation is shown in Fig8-16.

The effect of **AFR** on multi-mineral flotation is complicated by the presence of many floatable minerals. From the **MCM** results, it is observed that the effect of **AFR** is different on different size fractions, the effect on the fine size fraction is small. When the **AFR** is changed from 1.0 l/min to 7.0 l/min, Kmean in the -10 micron fraction shows almost no change, but in the medium and coarse size fractions Kmean is greatly increased as it can be seen from Fig8-17 to Fig8-19. The effect of **AFR** can be explained as when the **AFR** is low, the flotation of medium size may be inhibited, when **AFR** is increased, the inhibition is reduced or the overall flotation increased by increase the collision, therefore increase in **AFR** results in an increase in Kmean in the medium size fraction. For the fine size, entrainment is a major factor, an increase of **AFR** can increase the quantity of the entrainment, but the Kmean is not affected. On the coarse size, the effect of **AFR** is balanced between the increase bubble surface area and the reduction in power input. The effect of **AFR** on the G of **MCM** is similar to Kmean which can be explained by the same mechanism.

8.3.3 The effect of IPS on parameters of MCM

The effect of **IPS** on the parameters of **MCM** is observed in complex sulphide flotation. From flotation theory, the **IPS** effect is related to the particle size. Therefore, the **IPS** effect on the Kmean and G of different size groups are considered and plotted in Fig8-20, 8-21, 8-22.

From Fig8-20 to Fig8-22, it can be concluded that the effects of **IPS** are:-
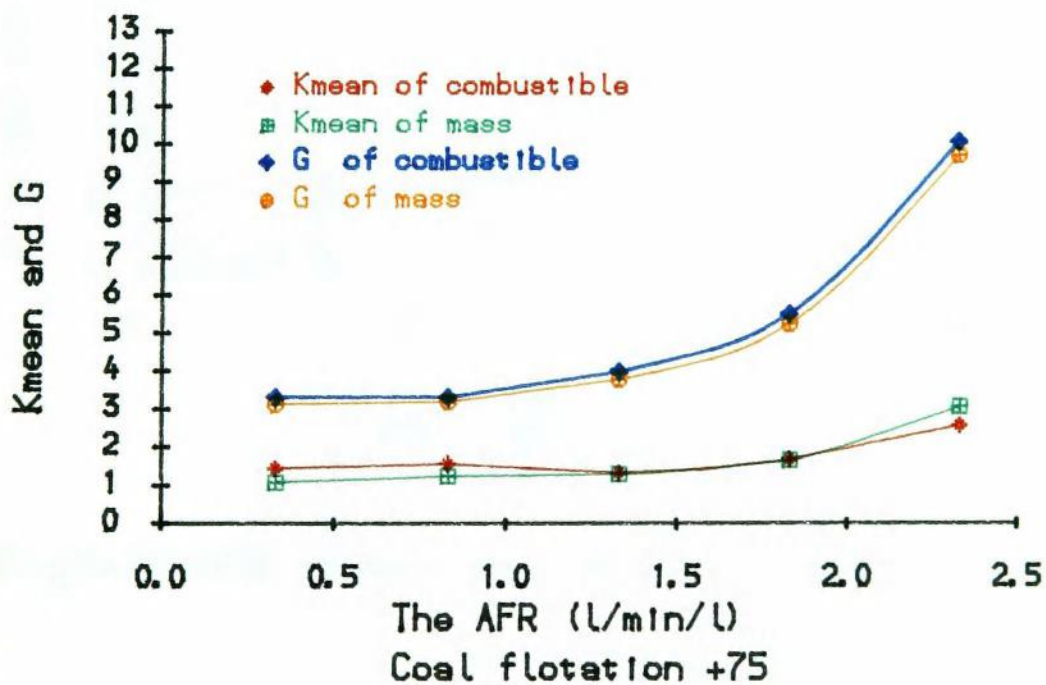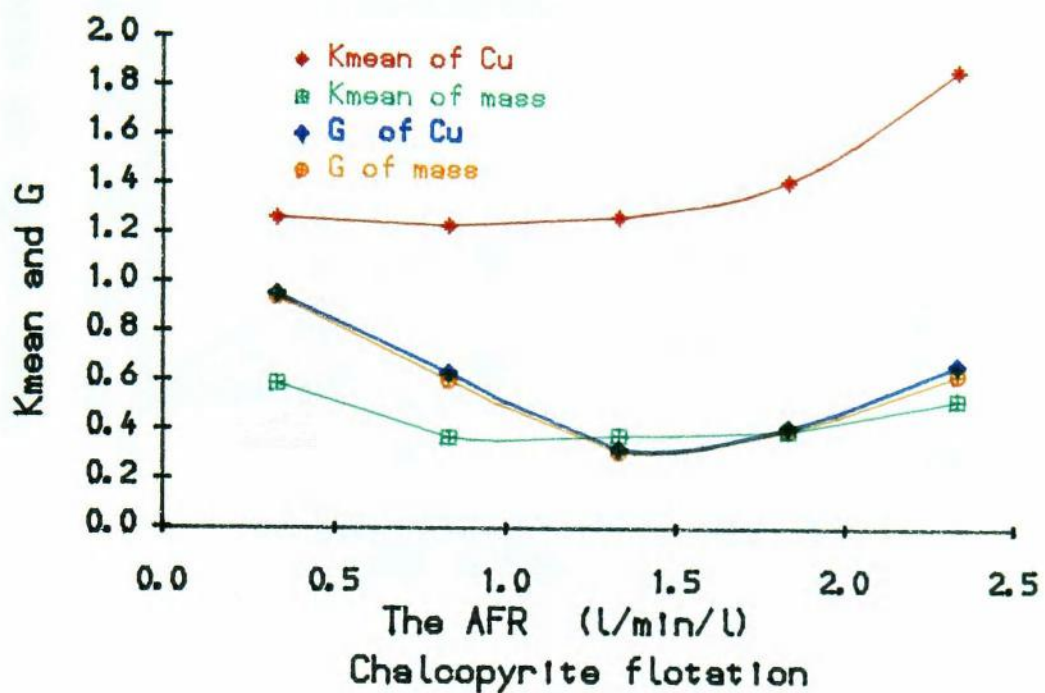
Fig8-16 The effect of AFR on the parameters of MCM
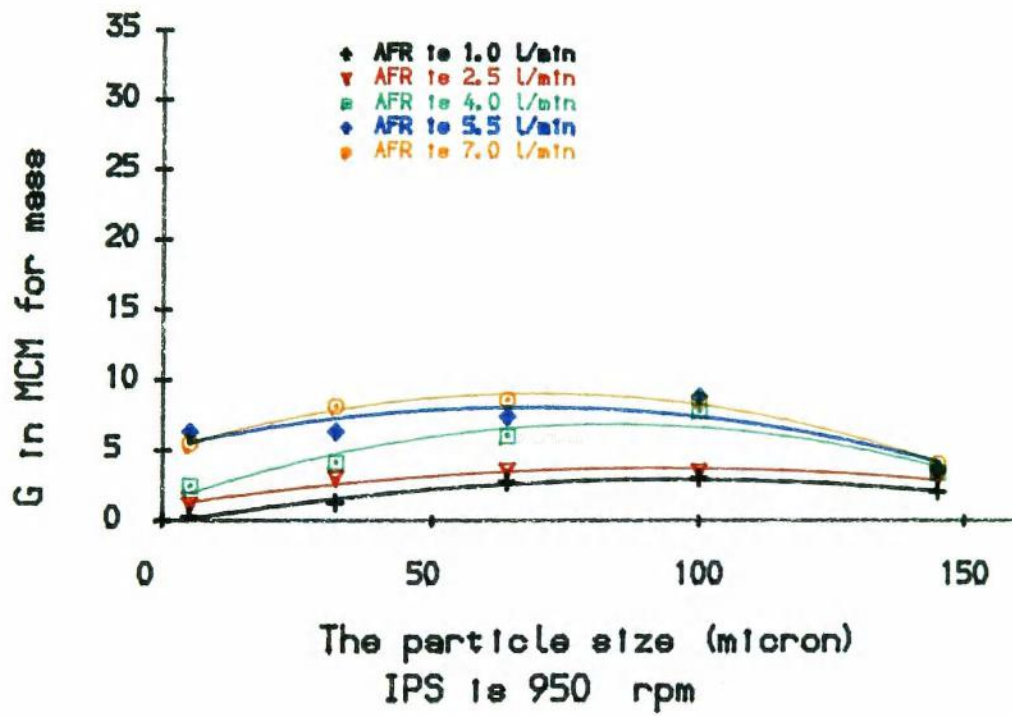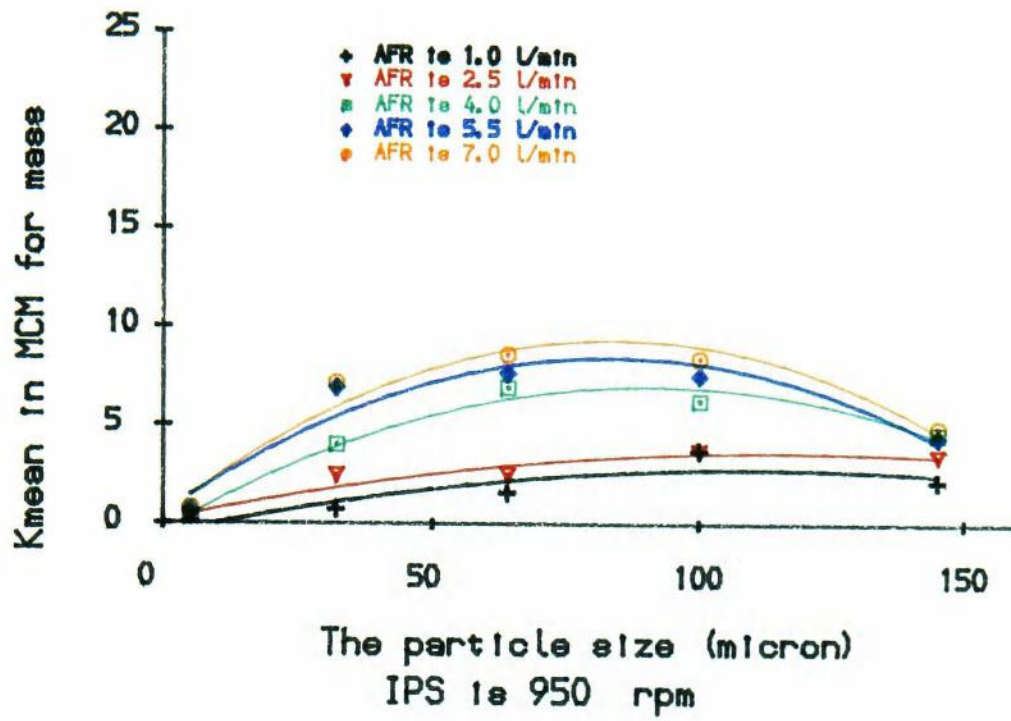
Fig8–17 AFR effect on MCM parameters in masse
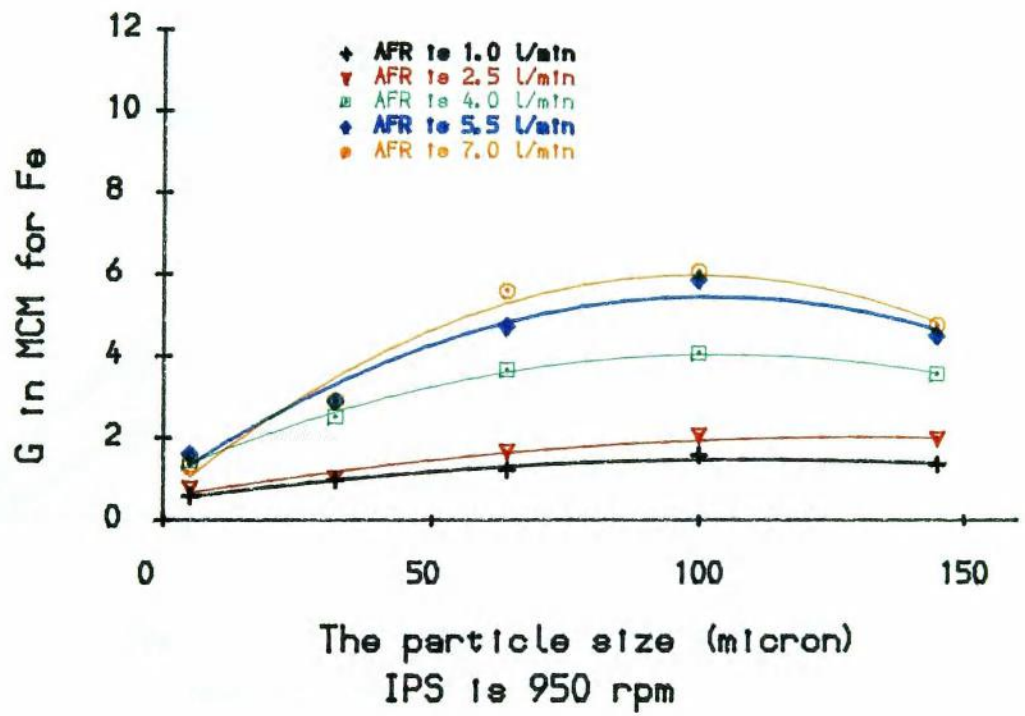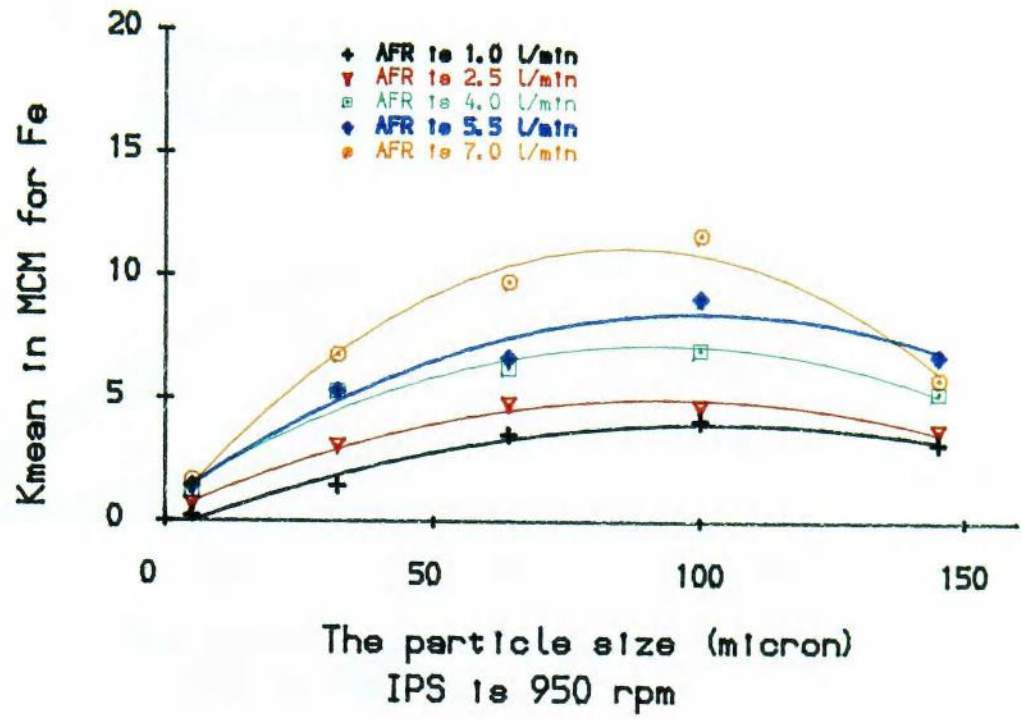
Fig8-18 AFR effect on MCM parameters in Fe
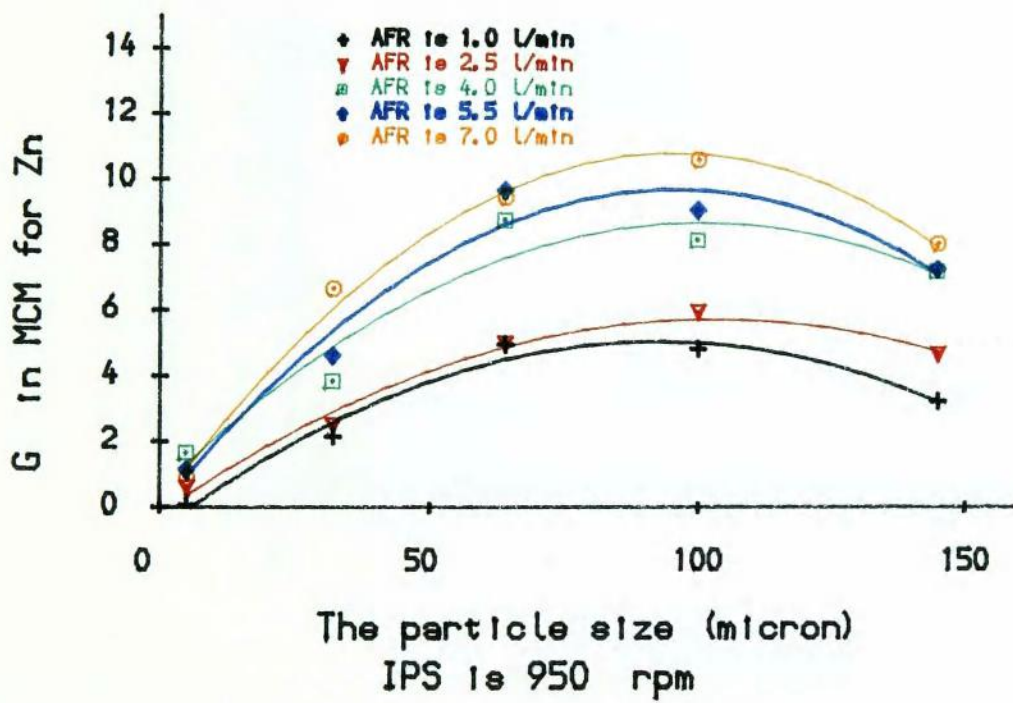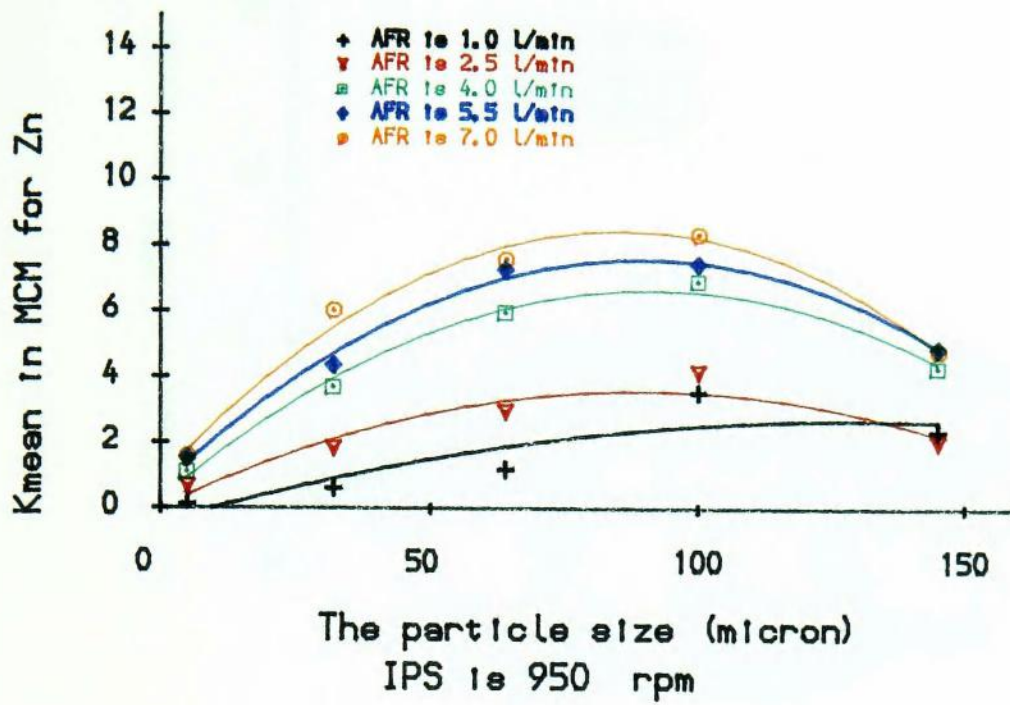
Fig8-19 AFR effect on MCM parameters in Zn
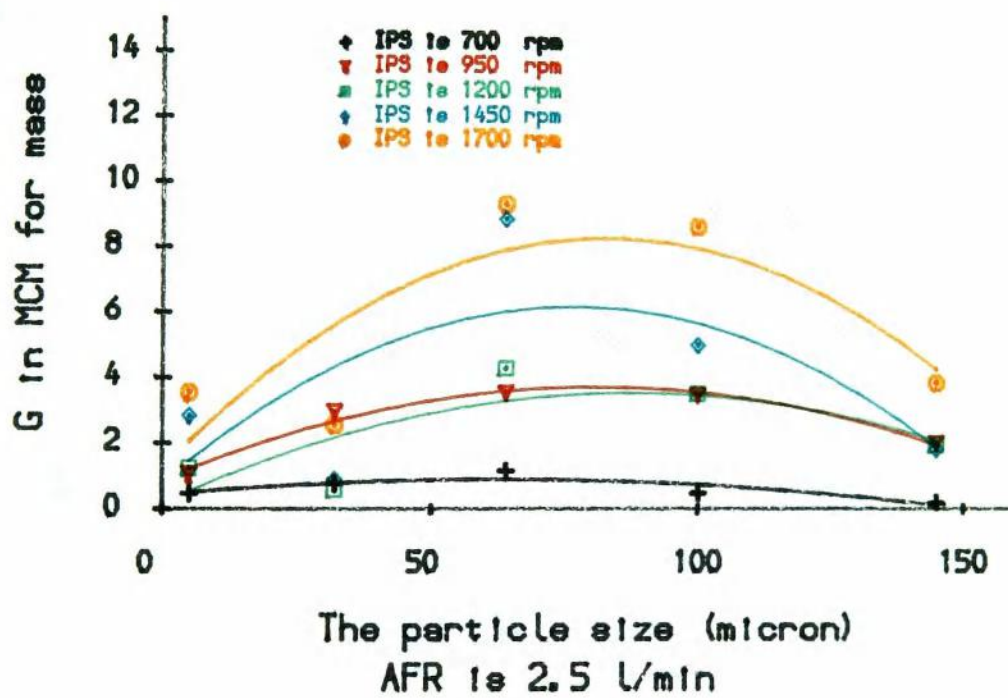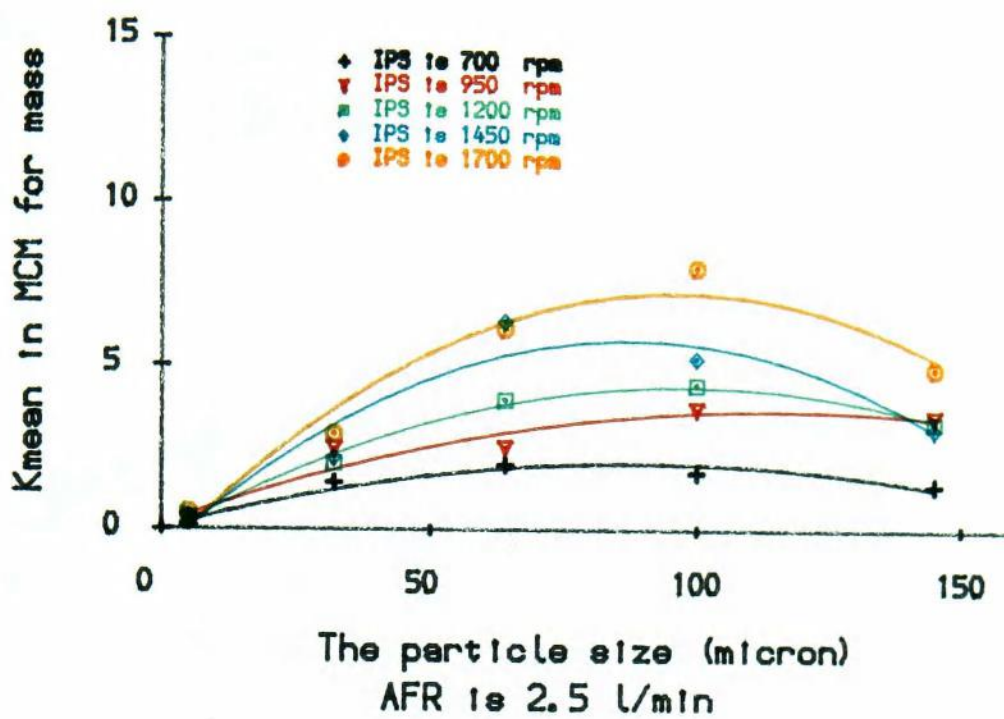
Fig8-20 IPS effect on MCM parameters In mass
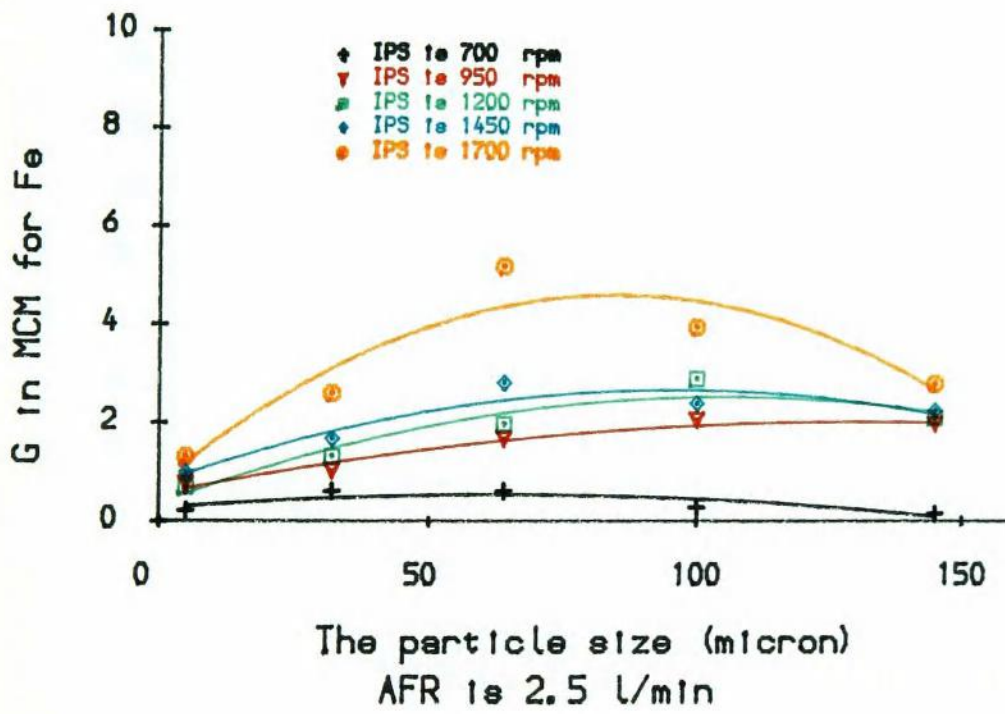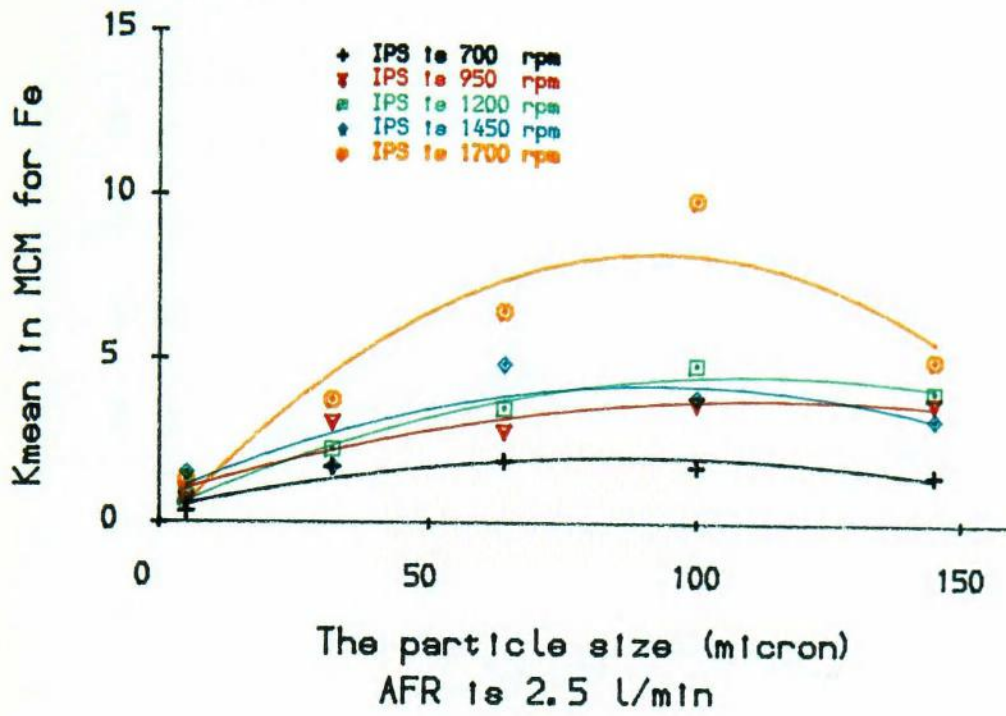
Fig8-21 IPS effect on MCM parameters in Fe
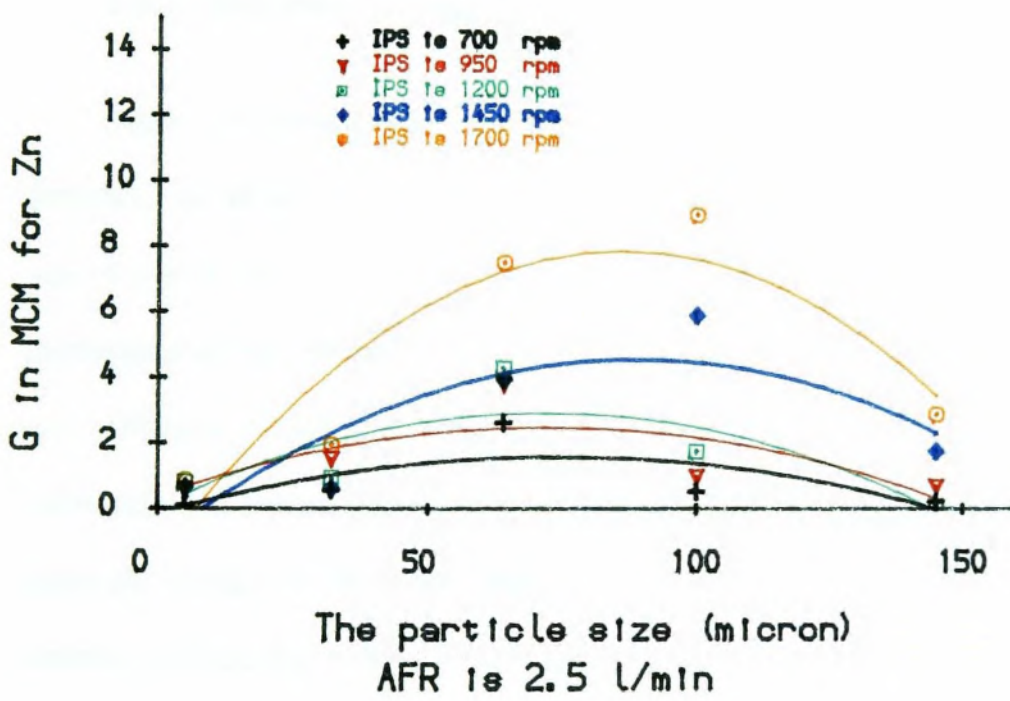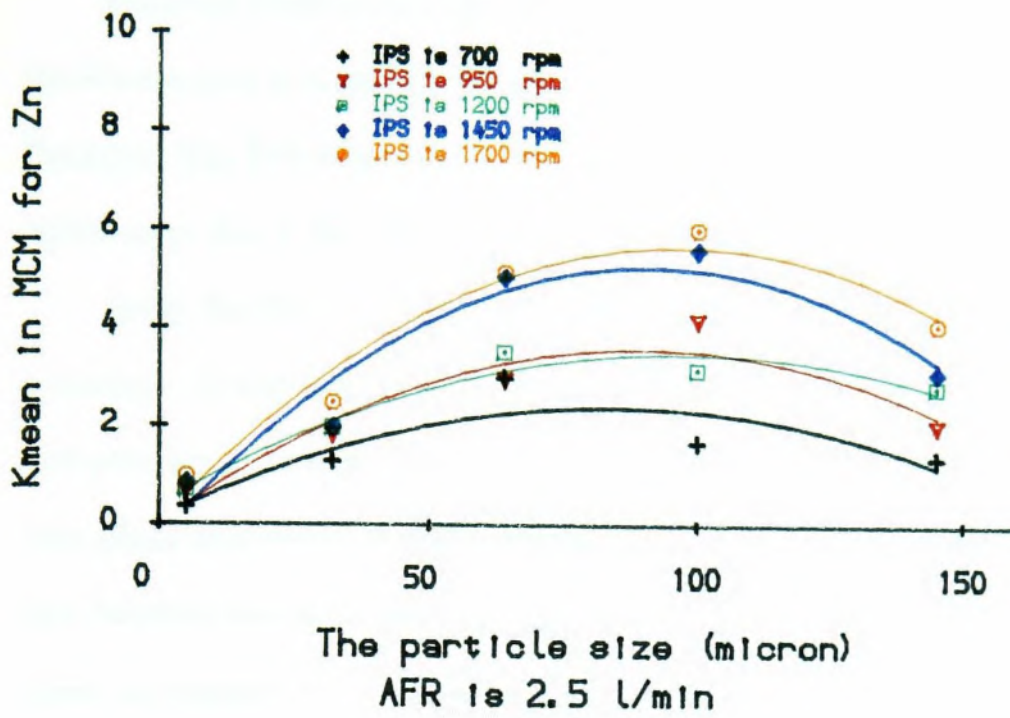
Fig8-22 IPS effect on MCM parameters in Zn

a) On the medium size and coarse particles, an increase in the IPS will increase the Kmean and G in MCM. Which means flotation rate is increased due to the better flotation. The IPS effect on the medium size is greater than its effect on the coarse, which may due to the effect of detachment of coarse particles.

b) On the fine size, the effect of IPS is very small. The effect of IPS on the fine particles (-10 micron) can be explained on the basis that the collisions, attachment and entrainment are all important factors for fine particles. Their attachment can also take place as a result of other attraction forces between charged surface of particles and bubbles which covered by reagents (Schlze H. J. 1984). Therefore the process is not as sensitive as the medium and coarse to the IPS.

8.3.4 The effect of size on the parameters of MCM

From literatures, it is well known that particle size has an important effect on flotation. In flotation theory, two major factors can be related to the particle size, one of which is the liberation state, another is the frequency of collision between the particles and the bubbles in the pulp phase. For coarse particles, since liberation is not sufficient which frequently results in a unsuccessful attachment after collision (detachment), liberation is often the limiting factor. While in the fine particle fraction, since the energy of the small particle is not sufficient to break the water layer on the bubble surface, the collision becomes the limiting factor.

Since the size effect is a balance between these two factors, from the results shown in Fig8-17 to Fig8-22, the size effect on the parameters of MCM model can be generally discussed below.

The Kmean and G are maximum in the medium size fraction due to both of the two factors in the medium size being suitable for flotation. For the coarse particles, since the liberation is the major factor which results in detachment, Kmean and G are reduced. While in the fine size fraction, the lack of collision and attachment reduces the values of Kmean and G. The effect of size can be magnified by the increase of IPS and change of AFR.

8.4 The result from the GFM

In the GFM, six parameters are included, two of which account for the unfloatable fractions of mass and valuable elements and one for the maximum flotation rate constants Kmax and two for the power exponents of the gamma function (mass and element), one for time correction. When mass recovery and element recovery are combined, the GFM is used here to calculate the grade and recovery of concentrate.

8.4.1 The parameters in the GFM

As in the previous sections, coal and chalcopyrite flotation results are used for the one mineral system and complex sulphide flotation used for the multi-mineral system in the GFM. The parameters in the GFM for all the results are calculated and tabulated in Appendix 16 and 17.

From the results it can be seen that in the one mineral systems the power exponent of the gamma function for element (m) is greater than that for mass (n). As is well known, in the gamma function the greater the power exponent is, the more

the fractions are distributed towards the higher flotation rate region. Therefore the fast floating fractions are the higher grade fractions. Which is in agreement with the CDM results. Presented by graph the distribution are shown below in Fig 8-23.

By using the GFM, the relationship between the fractional grade and the mass fraction as well as the relationship between the fractional grade and the flotation rate in the feed can also be obtained. The relationship between the mass fraction and the fractional grade of the chalcopyrite at AFR=2.5 is presents in Fig8-24.

It is interesting to note that from the continuous relationship between grade and mass fraction, the feed properties, that is how the valuable minerals are distributed in the feed, can be obtained. This result is very important in terms of the optimization of a grinding circuit to find the best liberation.

In addition to the relationship between the grade and mass fraction, the relationship between the grade and the flotation rate constants can also be obtained. This distribution first conformed to the assumption that the maximum flotation rate constant is not infinity, and secondly that the flotation rate constant is related to the grade of the same fraction, which was assumed in chapter three. The relationship between the grade and the flotation rate constants is shown in Fig 8-25.

Since the mass recovery does not have the same maximum flotation rate as the elements in the multi-mineral system, the relationship between grade and flotation rate, and that between grade and mass fraction cannot be obtained.

The GFM is also proven by fitting the experimental results of chalcopyrite, coal and complex sulphide flotation, which are shown in Fig 8-26, 8-27 and 8-28.

Fig 8-23 Flotation rate distribution
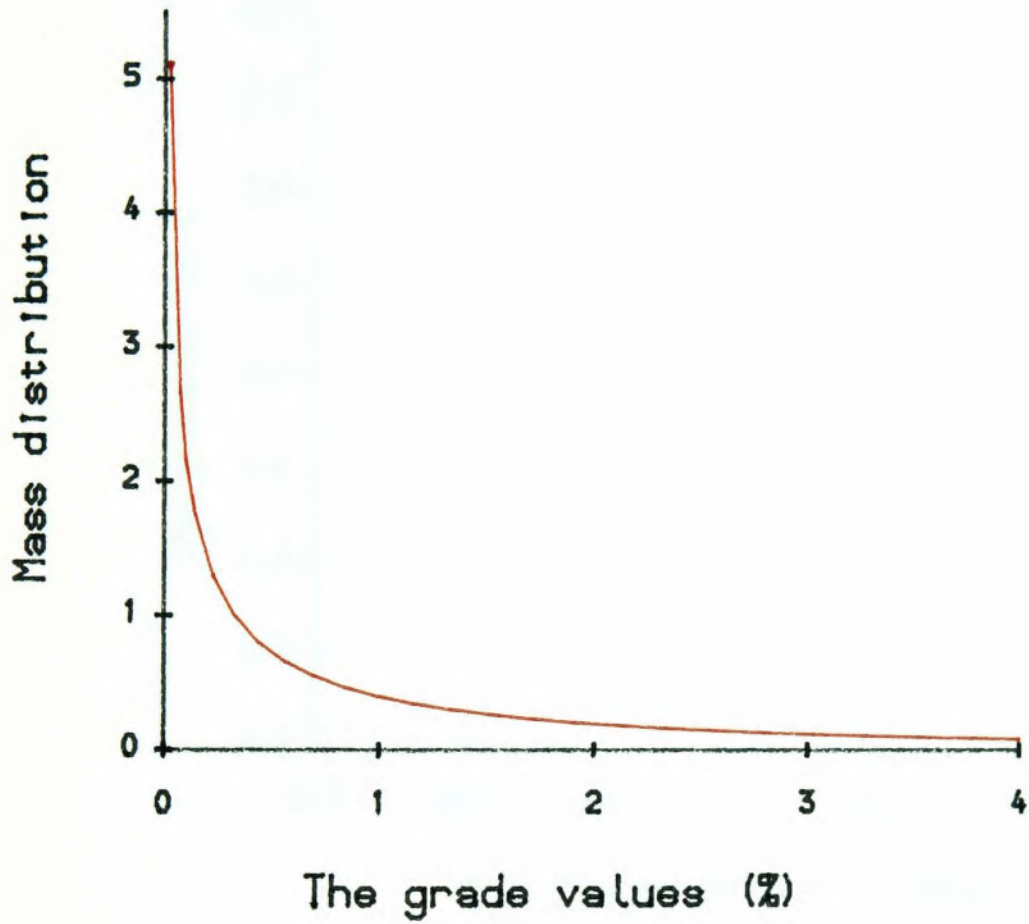
The chalcopyrite AFR=2.5 l/min

Fig 8-24 Mass distribution on grade

The flotation rate (1/min)
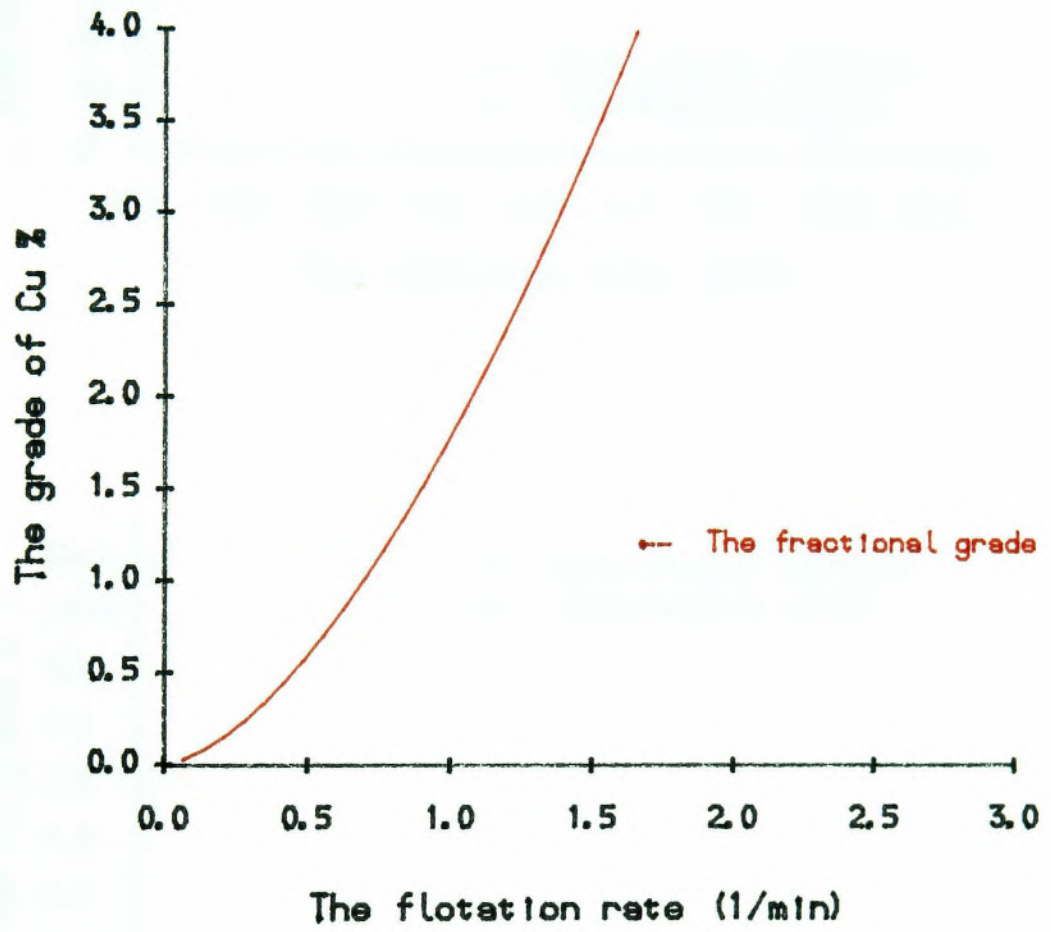
Chalcopyrite at AFR=2.5 L/min

Fig 8-25 Grade and flotation rate
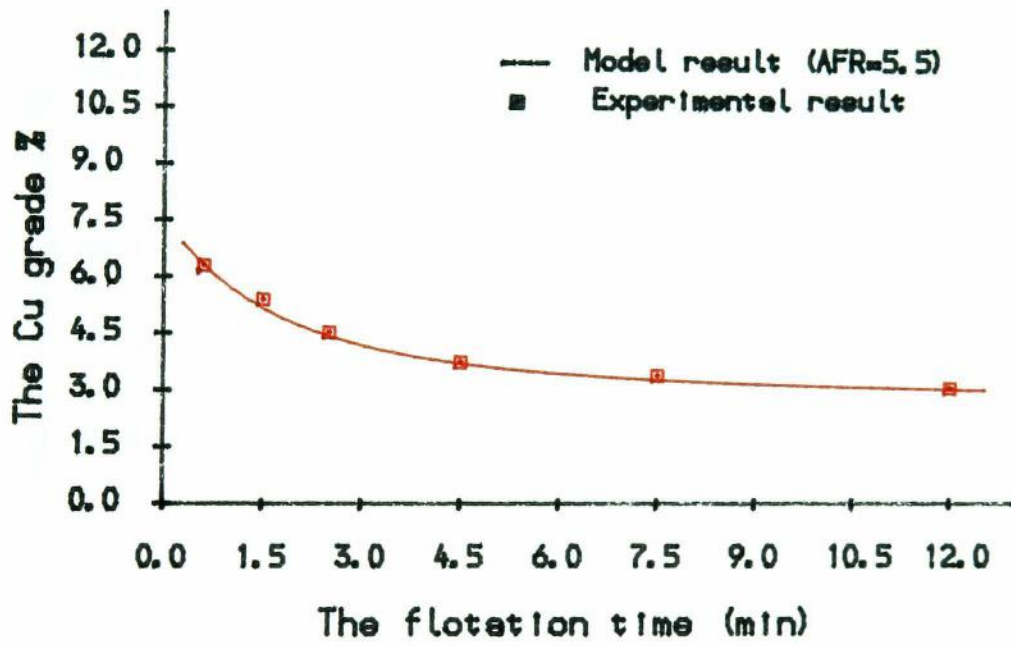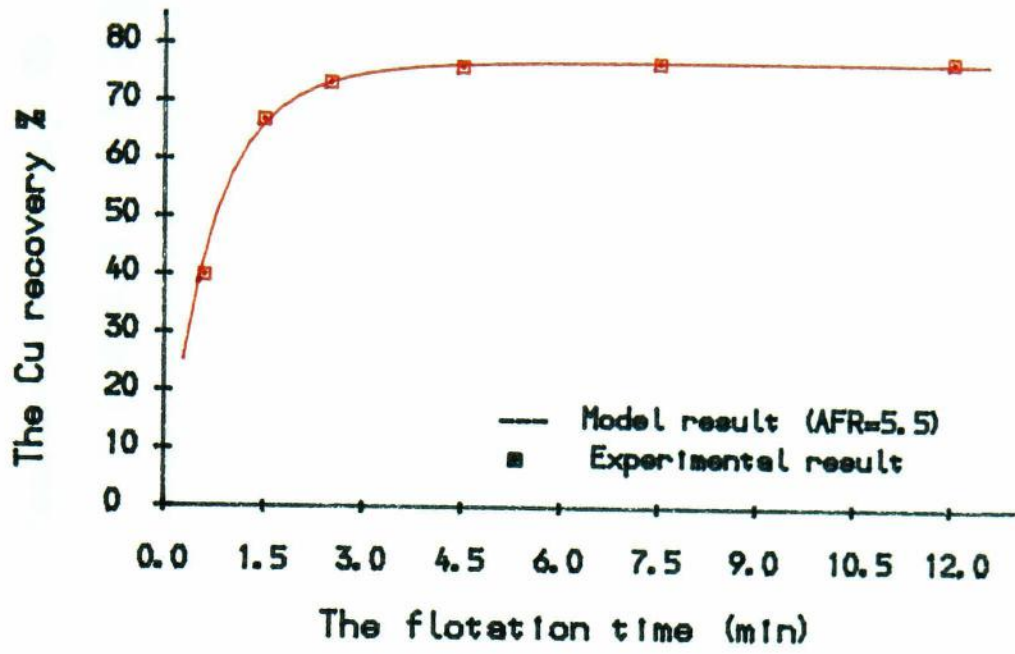
Fig8-26 GFM result of chalcopyrite flotation
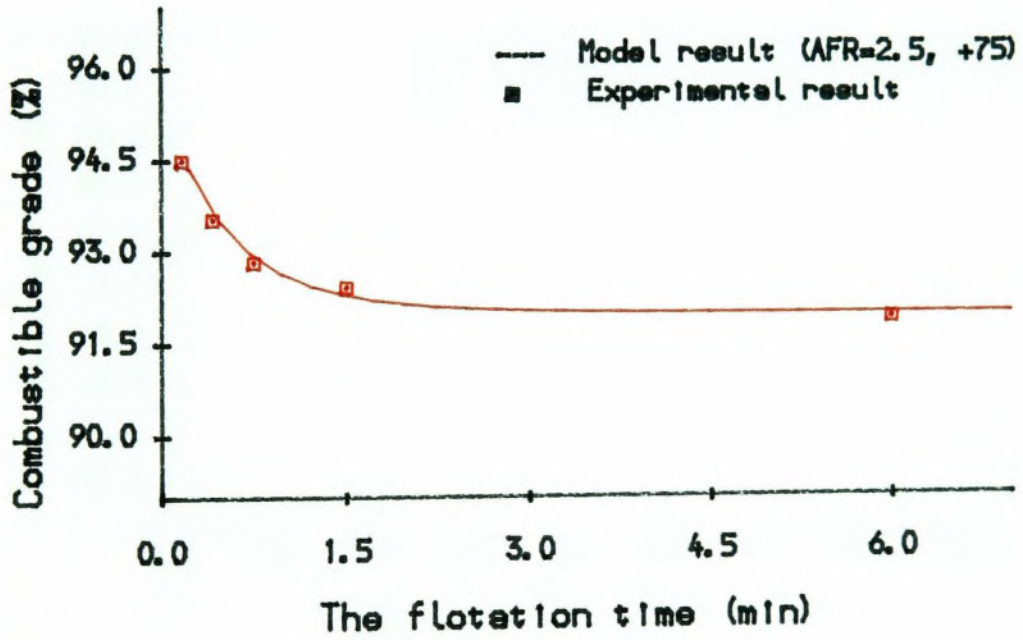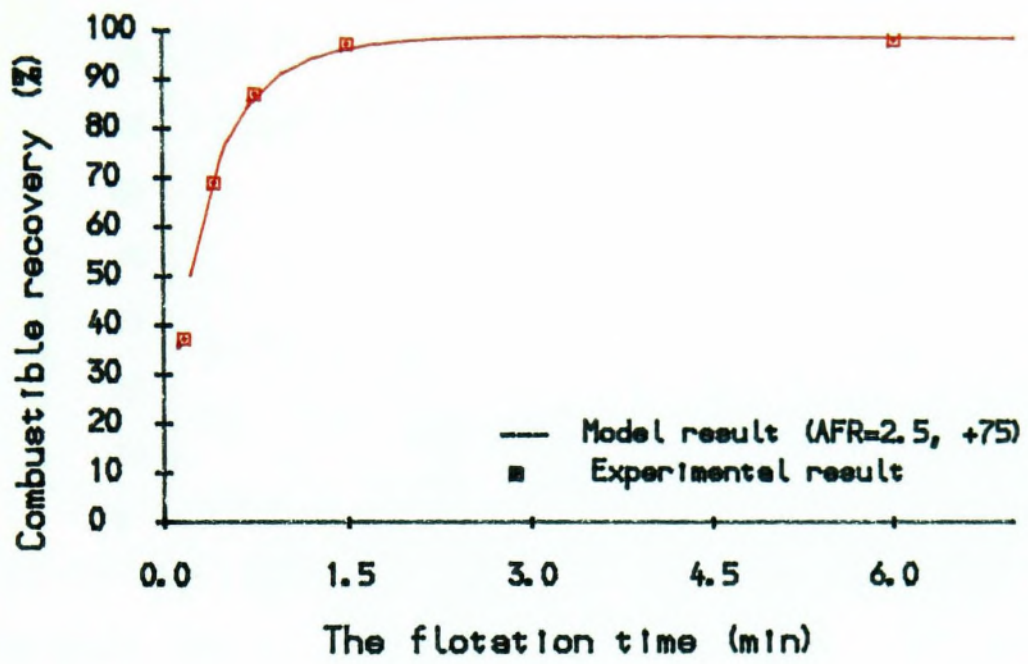
Fig8-27 GFM result of coal flotation
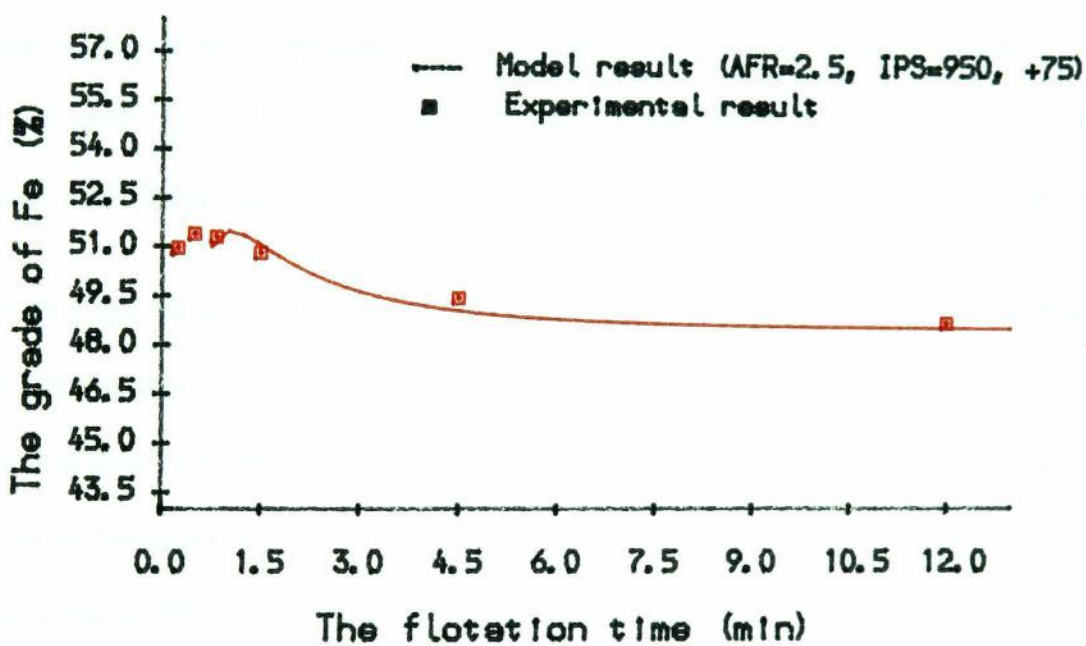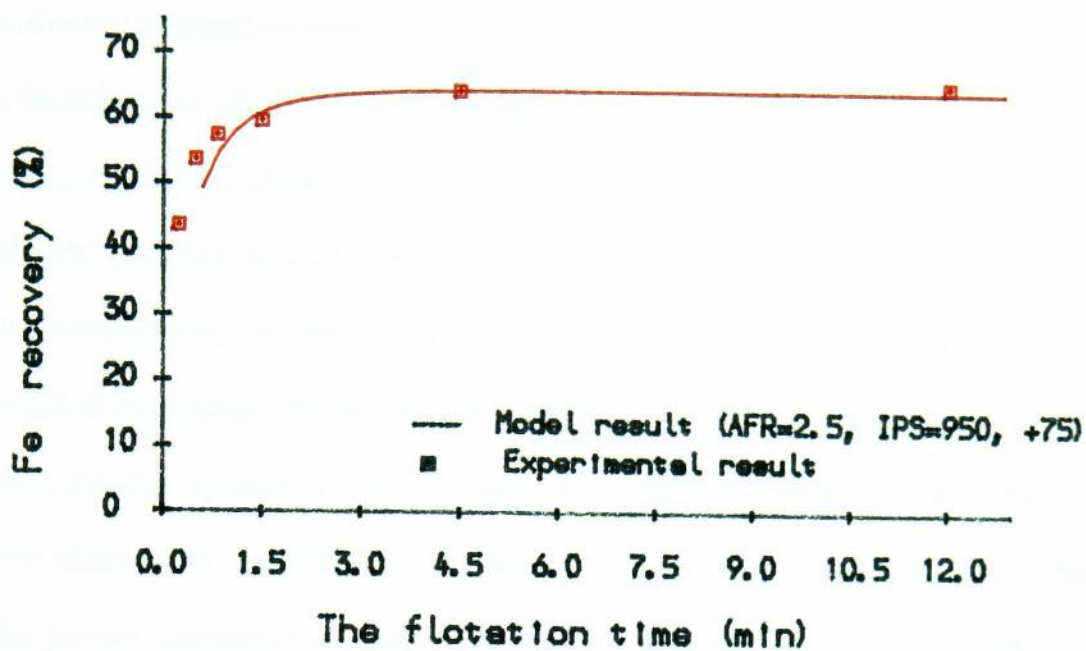
Fig8-28 GFM result of complex sulphide flotation

8.4.2 The effect of AFR on the parameters of GFM

In the one mineral system, the effect of AFR on the power exponent (m) of the gamma function for chalcopyrite flotation is that an increase in the AFR will result in an increase in (m) as shown in Fig 8-29. But it has very little effect on the maximum flotation rate (Kmax). In coal flotation, AFR is shown to be completely unrelated to Kmax. The reasons for this can be explained as due to the fast floating nature of coal, Kmax is very large. When Kmax is greater than 10, the fraction above 10 is so small that further change in Kmax will not affect the model results any more. Therefore during the simplex search, Kmax may become very large. The effect of AFR the power exponent of gamma function is similar to the chalcopyrite and is shown in Fig 8-30.

In complex sulphide flotation, the effect of AFR on the parameters of the GFM is similar to one mineral system, i.e. the AFR effect on the maximum flotation rate constant Kmax and power exponent of gamma function (m) is that when AFR is increased, both Kmax and (m) are increased as shown from Fig8-31 to Fig8-33.

From Fig8-31 to Fig8-33, it can be seen that the effect of AFR on the fine size is small, especially on the power exponent of gamma function, which implies that the flotation rate distribution of fine size fraction is not affected, the mechanism of fine particle flotation may be greatly dominated by entrainment. In the medium size fraction, when AFR is increased, both Kmax and (m) in the GFM is increased, which means that a larger fraction of floatable in the medium size group becomes fast floating. However, as can be seen Kmax and (m) in GFM for mass are also increased, the flotation selectivity therefore is not increased by the increase of AFR. The effect of AFR on medium size can only suggest that flotation becomes fast, which mean when the same flotation time is taken, an increase in recovery can be expected.

chalcopyrite flotation
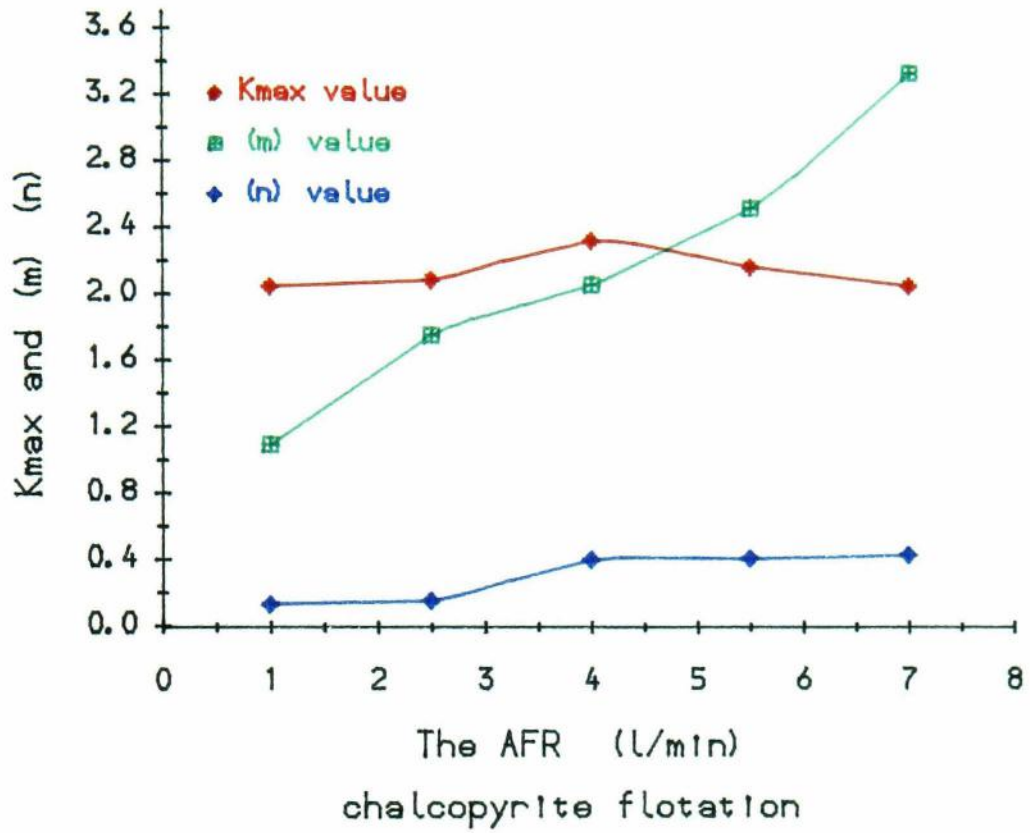
Fig 8-29 AFR effects on GFM parameters

Coal flotation
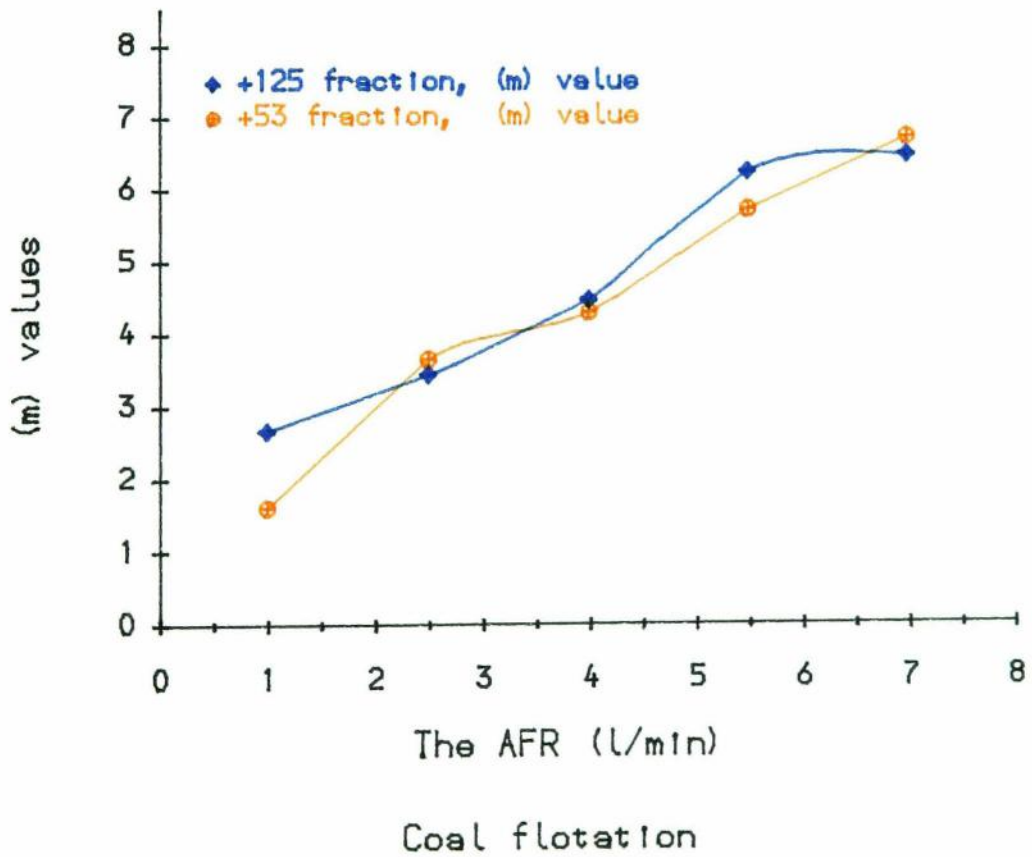
Fig 8-30 AFR effect on GFM parameters of coal
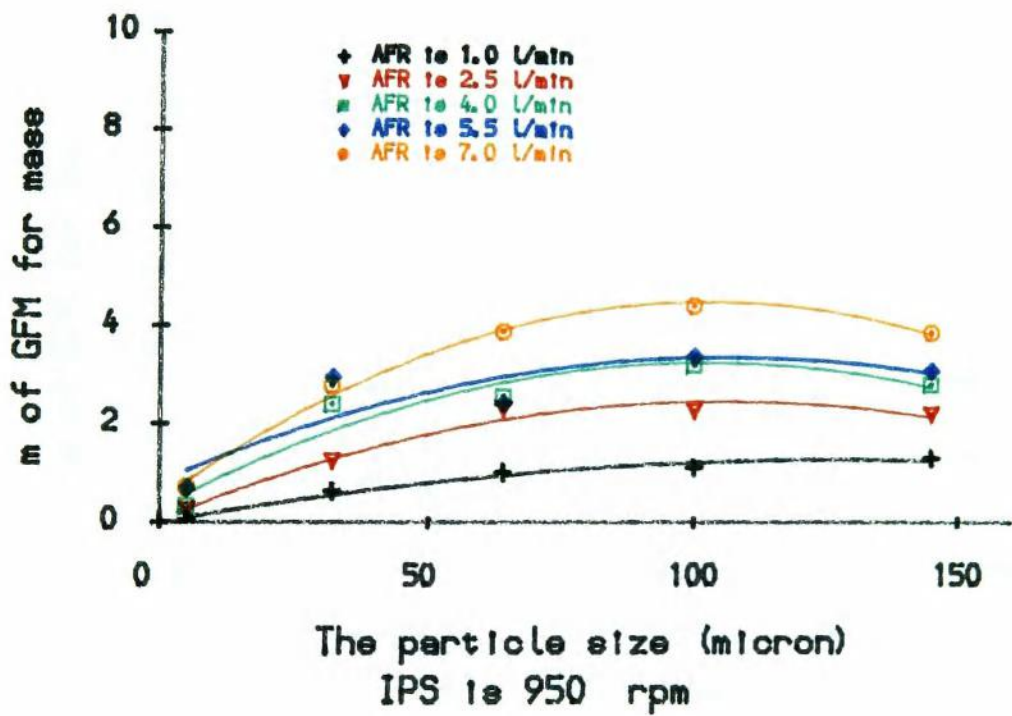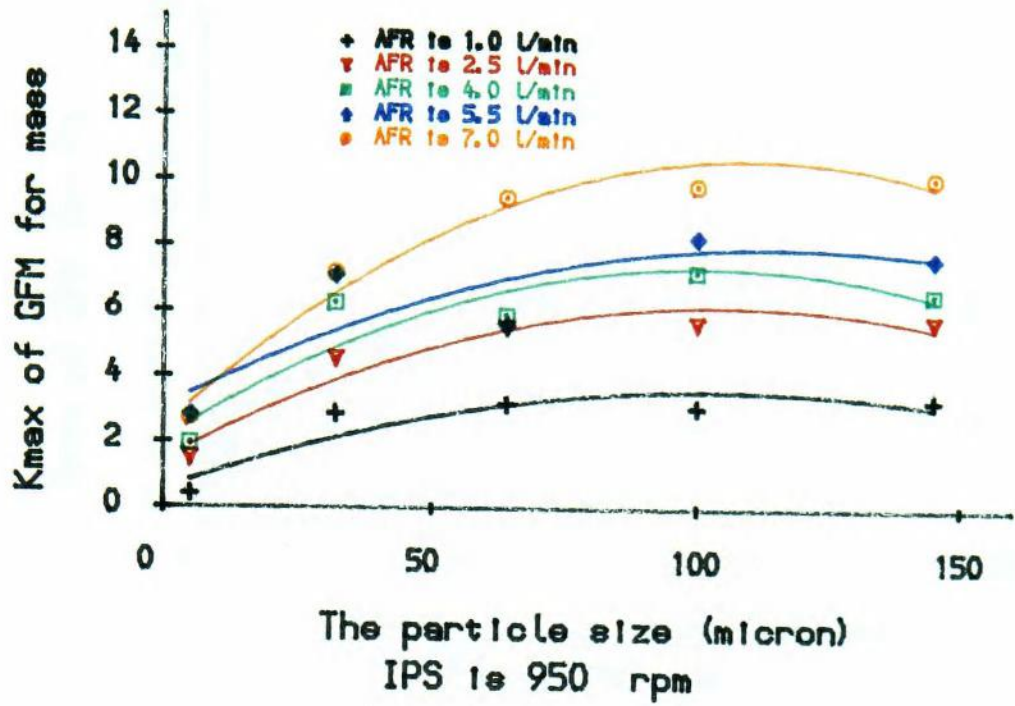
Fig8-31 AFR effect on GFM parameters in mass
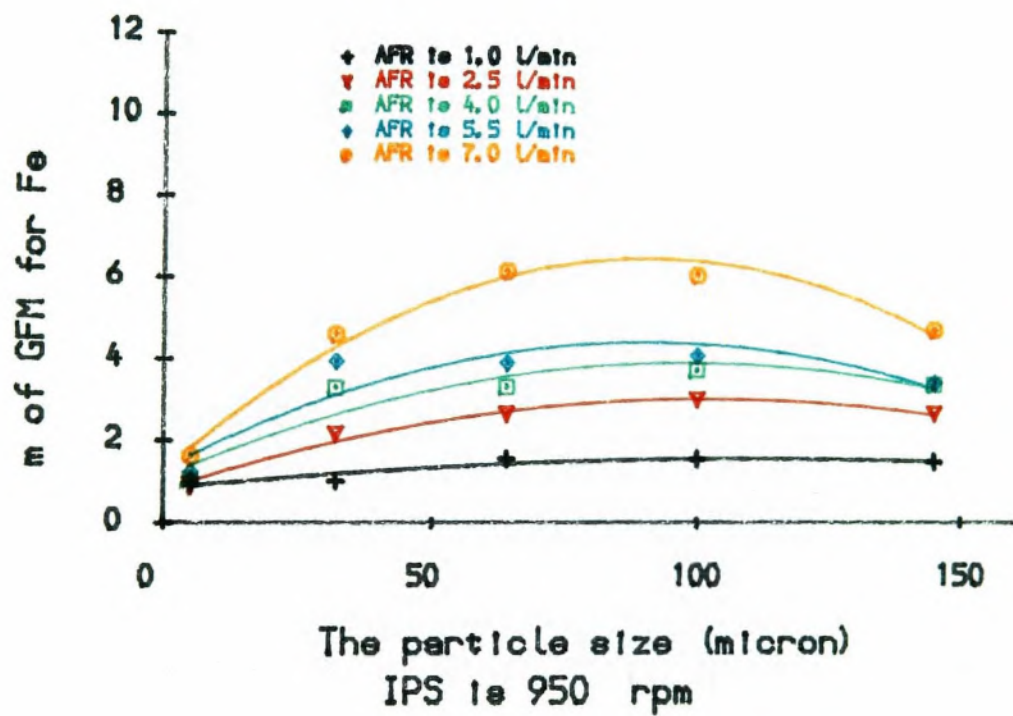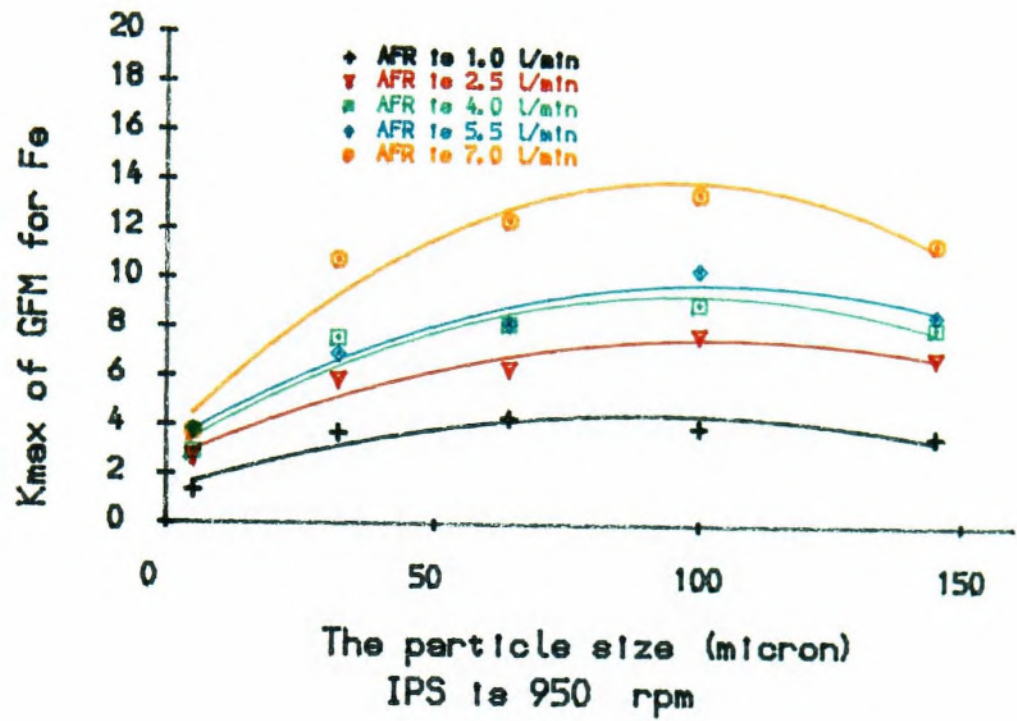
Fig8-32 AFR effect on GFM parameters in Fe
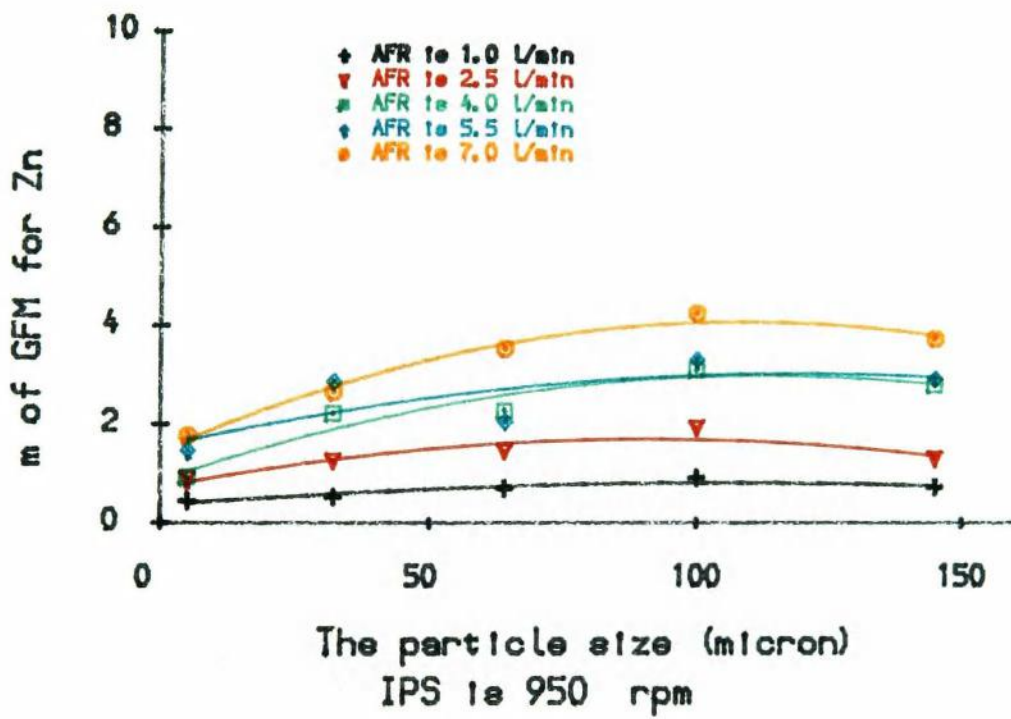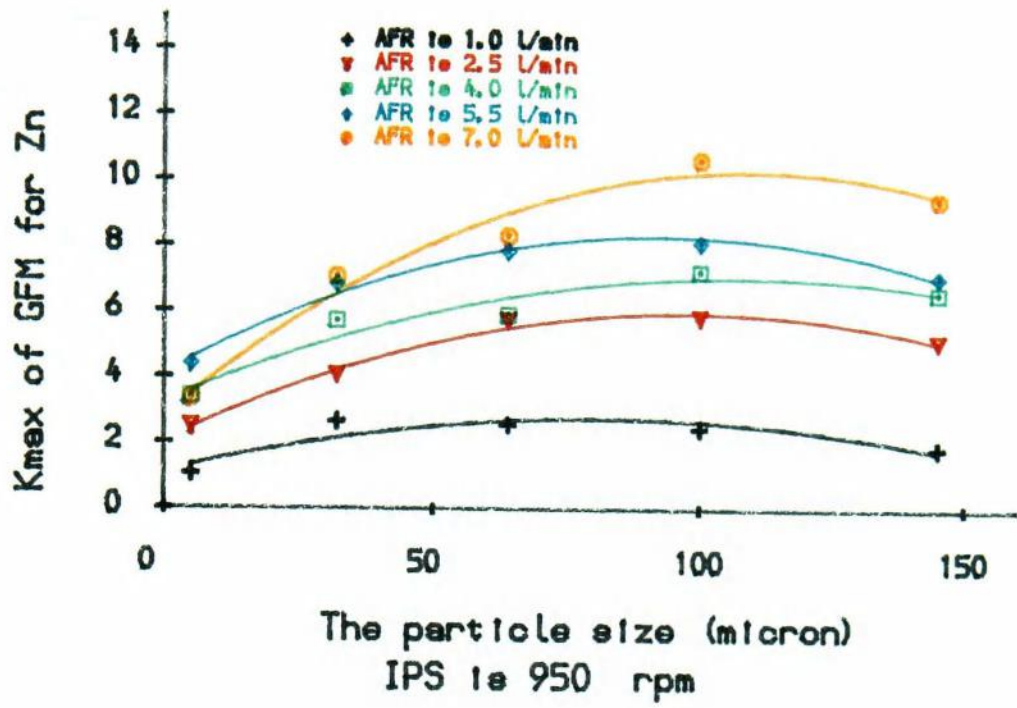
Fig8-33 AFR effect on GFM parameters in Zn

On the coarse fraction, the effect of **AFR** is similar to its effect on the medium size. From this conclusion, it can be seen both GFM and MCM results in the same conclusion.

8.4.3 The effect of IPS on the parameters of GFM

In complex sulphide flotation, the effect of IPS on Kmax and the power exponent (m) are shown from Fig 8-34 to Fig8-36. In the graph, when the IPS is increased, Kmax and is increased and (m) is also increased in a smaller scale.

When Kmax is increased, flotation is slightly faster, therefore an increase in IPS will increase flotation speed, similar effect are shown in the MCM. However, in the fine size (-10 micron) fraction, increase in Kmax is very small as is shown in the graphs. In the graphs, it can also be seen that when the IPS increase from 700 to 1200 rpm, Kmax has rapid increase, further increase in IPS, the change in Kmax is very small.

In addition to the effect on the element recovery, the IPS also affects mass recovery. Similar to its effect on the element recovery, increase in IPS increases Kmax and (m). The increase in (m) for mass is slightly larger than the increase for element, this may imply that the increase in IPS may increase entrainment in the early stage of flotation. However, the over all effect of IPS on the entrainment can not be drawn from this result.

8.4.4 The effect of size on the parameters of GFM

From the results of complex sulphide and coal flotation, it is observed that size has an obvious effect on the parameters of **GFM**. The effect of size on Kmax and (m) are shown from Fig 8-34 to Fig8-36.
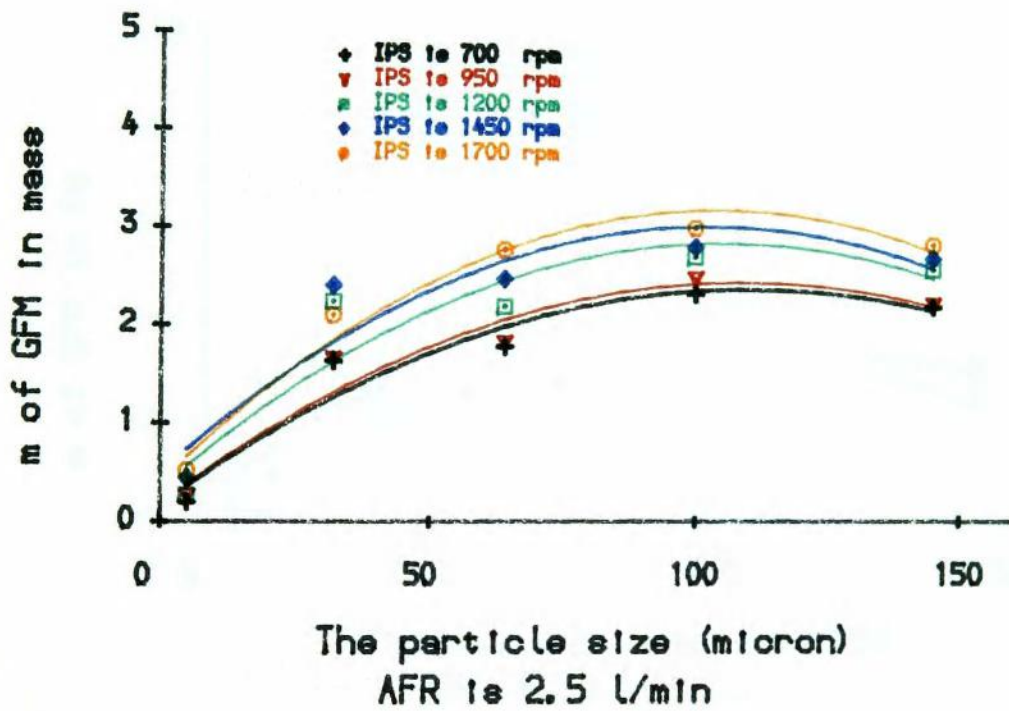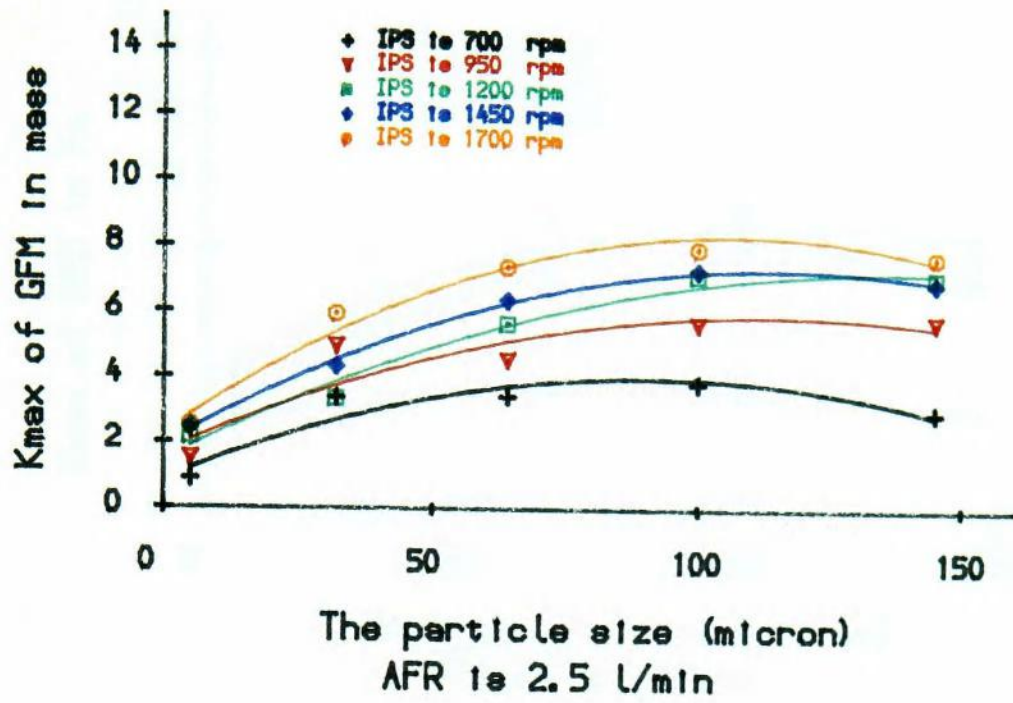
Fig8-34 IPS effect on GFM parameters In mass
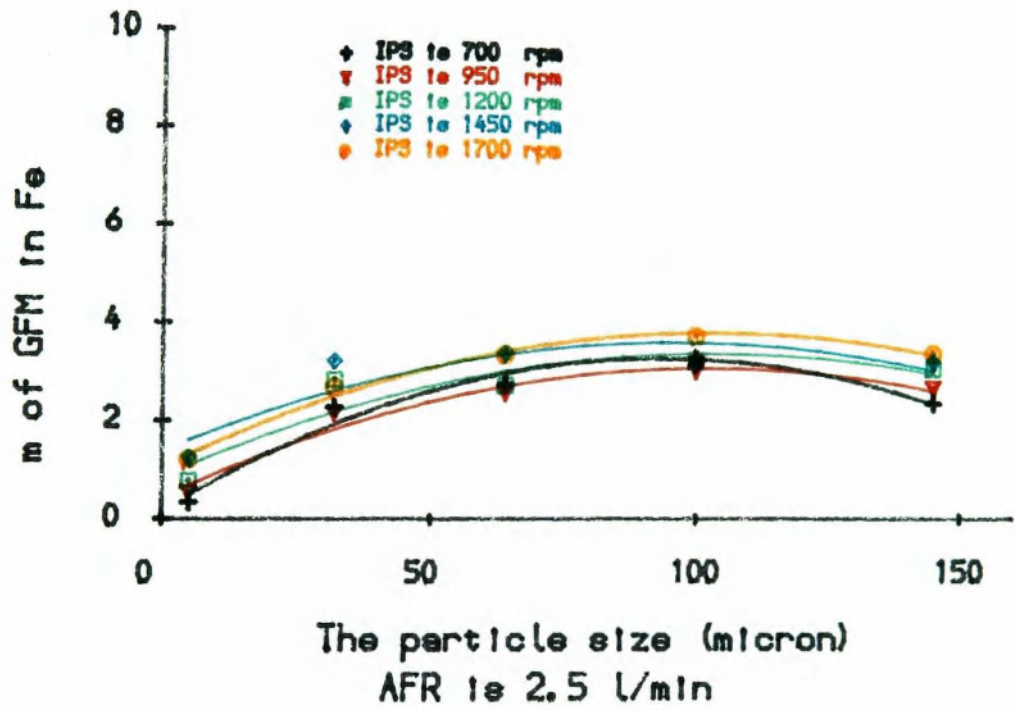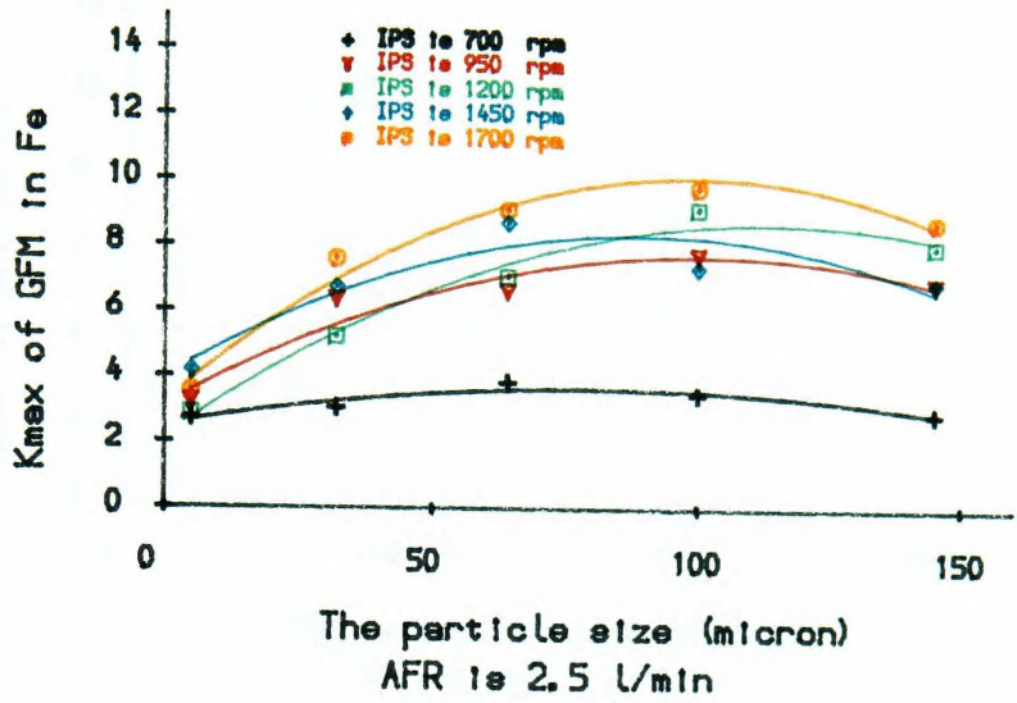
Fig8-35 IPS effect on GFM parameters in Fe
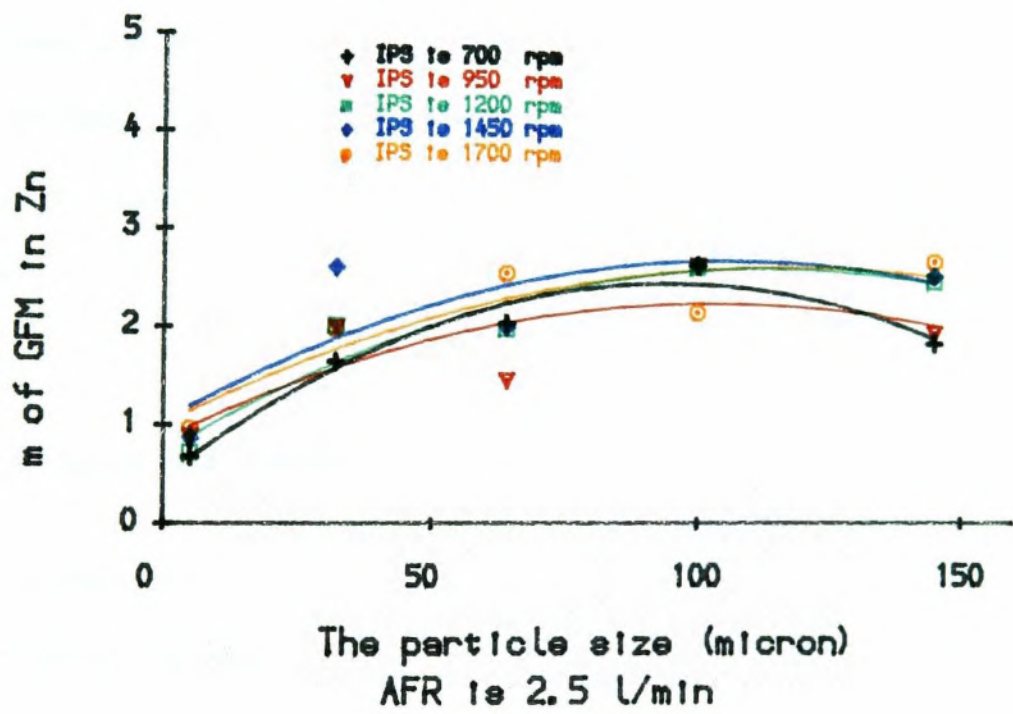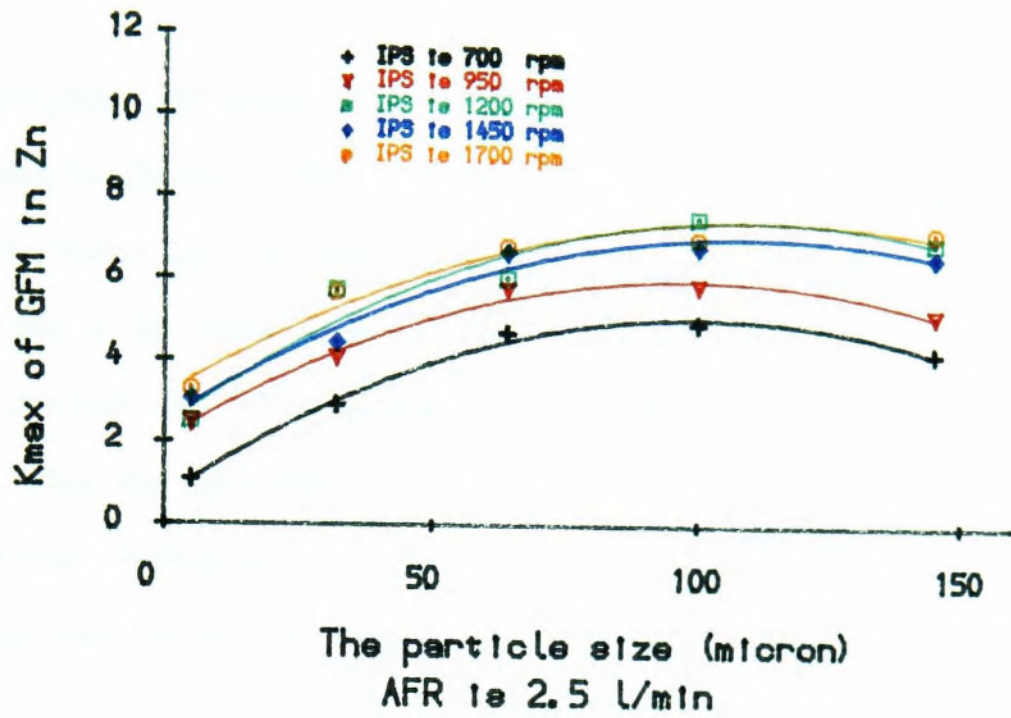
Fig8-36 IPS effect on GFM parameters in Zn

In the graphs, the pattern of the size effect on Kmax and (m) is that the medium size fraction has the maximum Kmax and (m), both the coarse and the fine particles have lower Kmax and (m) than the medium size. For the coarse, the reasons is probably due to the liberation and the degree of suspension, as the size increases, particles are more difficult to suspend in the pulp, their probability of attachment is reduced. When the liberation is not completed, floatability of the particles is low, they are easily detached from the bubbles, therefore their flotation rate is not as large as medium size. For the fine sizes, collision is the main limitation.

8.5 Comparison between models

To conclude this chapter, it is necessary to have a comparison between the different models. Although every model has its own physical significance and its best suitable situations. It is better to have a clear idea when the models should be employed.

8.5.1 The errors in different models

The errors in the different models are slightly different; the general result shows that the errors are independent of the parameters employed in the models as can be seen in Table 8.1.

Table 8.1 The error of models of chalcopyrite flotation

Errors	SSE of CDM		SSE of MCM		SSE of GFM	
Test No	elem	mass	elem	mass	elem	mass
1	0.09	0.095	0.27	0.02	0.24	0.05
2	1.80	0.075	1.25	0.18	1.46	0.12
3	1.04	0.025	0.79	0.07	0.51	0.15
4	1.79	0.179	1.34	0.45	0.82	0.36
5	0.03	0.187	0.91	0.29	0.66	0.13
Mean	0.95	0.092	0.91	0.201	0.74	0.16

In the table, the **CDM** has least error in fitting the mass recovery and the **GFM** has least error in the element recovery fitting. Therefore from the error levels, it is difficult to tell which model is better than the others. In order to use a model for different purpose, it is suggested that for the flotation of a specific mineral with well established reagent conditions, especially under plant automatic circuit control, the discrete model is recommended as providing the more accurate result to mass recovery. When a grinding unit is also included or a new mineral is tested by flotation, the **GFM** should be used to determine the grinding conditions. When the model is a means of obtaining the best flotation conditions, such as the flotation time, **AFR**, the reagent dosages, the **MCM** should be used since the parameters in the **MCM** are more easily interpreted in relation to flotation as a process.

Although errors exist in the different models, they are all well within the range that could be possibly caused by experiment. Therefore all the models employed here are valid.

8.5.2 The difference between the CDM and MCM

When the mean flotation rate constant in the CDM is calculated by the equation below:-

$$K_{mean} = \frac{K_f \cdot a_f + K_s \cdot a_s}{a_f + a_s} \qquad (8.1)$$

The two mean rates of CDM and the MCM can be compared. The different values of Kmean of CDM and the MCM are shown in Table 8.2.

Table 8.2 The Mean rates of chalcopyrite flotation

Test No	1	2	3	4	5
CDM Kmean	0.570	0.446	0.480	0.442	0.574
MCM Kmean	0.587	0.406	0.476	0.402	0.528

Since the CDM is based on a discrete distribution, the CDM provides a theoretical method to combine mass recovery and element recovery. As a simple model, CDM can be used to explain most of the flotation phenomena in a simple way. While the MCM is based on an alternative approach which considers flotation feed as a bulk material whose properties are changed during flotation. Since the

assumptions in the **MCM** are based on the **CDM** and **GFM**, the **MCM** theoretically can fit any of the flotation results where the **CDM** and **GFM** are valid. As the **MCM** employs fewer parameters, it is more convenient in the analysis of model parameters.

8.5.3 Tbe difference between the CDM and GFM

The difference between the **CDM** and **GFM** is the difference between the discrete and the continuous distribution. The **GFM** fundamentally is no different from the **CDM** except for its assumption of a continuous distribution. As the real properties of the flotation feed is still a mystery to existing technology, the actual distribution of the flotation rate constants cannot be obtained. The versatile gamma function has been assumed in an attempt to explain the flotation distribution. Therefore it is difficult to give any physical meaning to the parameters in the gamma function since it is simply a means of fitting the flotation results. But once the parameters and the distribution which fits the experimental results are obtained, the feed properties can be discussed. Therefore the relationship between the **AFR**, **IPS** particle size and the parameters of **GFM** will a have physical interpretation.

8.6 Summary

In this chapter, three models, **CDM MCM GFM**, are used in data fitting. From the fitting results, general relationships between the parameters and **AFR**, **IPS**, and particle size are obtained. Although mathematical forms of the relationships between these parameters and the operational parameters are not achieved, the patterns are obtained. The patterns in this chapter can be used to analyze the flotation results and the effects of operational parameters. Since no systematic error exists in the model

results, all models here are valid.

Finally, it should be noted that in fitting the complex sulphide results, the start time error for different sizes and different minerals are different. Although it should be the same theoretically, for simplicity of calculation, the time corrections were not standardised. The maximum difference in the same flotation of different sizes is of the order of 0.10 minute.

Chapter Nine

Conclusions and Suggestions for Further Research

9.1 Conclusions

In this research work, general relationships between the AFR, IPS, particle size and the parameters in different flotation models have been obtained. In the flotation models, the inconsistency in model parameters is solved by combining valuable and mass recovery. The combination of mass and valuable recovery also completed a grade model which enabled the calculation of recovery and grade of flotation concentrate.

9.1.1 The flotation models

In this thesis, three representative flotation models have been used. Since the discrete model was the basis of the other models, the discrete model was first discussed. In the traditional discrete models, attention has only been paid to the recovery of the valuable component, therefore the grade of concentrate cannot be calculated by the model. To overcome this problem, the conventional method is to use water recovery, from the water recovery free gangue entrainment is calculated, by combining the gangue recovery and valuable element recovery, grade is calculated. In this thesis, the conventional model is modified by introducing mass recovery model, which results in the CDM and enables the calculation of both grade and recovery.

From a different approach, also based on first order kinetics, Chen's model was modified and the MCM was developed. In Chen's model it is suggested that the

flotation feed can be treated as a whole group with a mean flotation rate, but the mean flotation rate is a function of time. A function of the mean rate was proposed in this model, however from an analytical result, it was found that there is a conflict between Chen's model and the **CDM**. To enable Chen's model to be suitable for this research work, it is modified (**MCM**) with a different assumption for the mean rate function. In the **MCM**, except for the correction for starting time, six parameters are employed, one of which is the fraction of unfloatable, the others are the initial mean rate, and the reduction rate of the initial mean rate.

After **CDM** and **MCM**, the gamma function model is also assessed and the gamma function with a finite maximum flotation rate is selected which was proved suitable for both the mass recovery and element recovery. In the **GFM**, five parameters are employed since both mass recovery and valuable recovery have the same upper limit of flotation rate.

9.1.2 The effect of AFR on flotation

The effect of **AFR** on flotation can either be evaluated by the direct results from flotation or by its effect on the parameters in different models. **AFR** effects on the results of flotation are outlined in chapter 7 from which it can be concluded:-

1) **AFR** has great effect on water recovery which subsequently changes the recovery of mass, especially in the fine size fraction. Therefore the grade of concentrate is reduced.

2) **AFR** has an effect on the power input through changing the pulp density. This results in a slight decrease in the recovery of coarse size (+125 micron).

From the effect of AFR on the parameters of different models, it can be concluded:-

1. The effect of AFR on the parameters of CDM is,

a. When AFR is increased, as observed in coal flotation the flotation rates of fast and slow floating fraction are increased.

b. In chalcopyrite flotation when AFR is increased, the flotation rate of the slow floatable is virtually unaffected but the grade of this species is increased.

c. In complex sulphide flotation when AFR is increased, in most of the results the flotation rate of slow floating fraction is increased.

2. The effect of AFR on the parameters of MCM is,

a. An increase in AFR increases the initial mean flotation rate.

b. An increase in AFR has a similar effect on the rate of reduction of the mean flotation rate.

c. An increase in AFR will reduce the unfloatable fraction.

3. The effect of AFR on the parameters of GFM,

a. An increase in AFR will increase the upper limit of the flotation rate only when flotation is inhibited.

b. An increase in AFR will increase the power exponent of the gamma functions.

c. An increase in AFR will increase the fraction of total floatable mass but has little effect on valuable elements in chalcopyrite flotation.

The effect of AFR on the bubble size and power input to the pulp are also observed which are:

1) When **AFR** is increased, the bubble size is increased linearly.

2) When **AFR** is increased, the power input to the flotation pulp is reduced.

9.1.3 The effect of IPS on flotation

In conclusion of the effect of IPS on flotation results, can be summarized as:-

1) The effect of **IPS** on the coarse is such that when it is increased, the recovery of mass and elements is reduced. Which is due to the result of detachment under excessive turbulence.

2) The effect of **IPS** on fine sizes is such that when it is increased, the recoveries of mass and elements are increased.

3) When **IPS** is increased, the grade of concentrate is slightly decreased for medium and coarse sizes.

In conclusion, the effect of **IPS** on the parameters of flotation models, can be summarized as:-

1. The effect of **IPS** on the **CDM** is that an increase in **IPS** has hardly any effect on the unfloatable fraction but will increase the fast floatable fraction slightly. For the slow floatable fraction, the situation is the reverse of the fast floatable.

2. The effect of **IPS** on the **MCM**,

a. An increase in **IPS** does not effect the fraction of the floatable material.

b. An increase in IPS will increase the initial mean flotation rate.

c. An increase in IPS will also increase the rate of reduction in the mean rate of all size fractions, but the effect on the coarse and medium size is much greater than for the fine.

3. The effect of IPS on the GFM,

a. An increase in IPS has little effect on the proportion of floatable fraction but increase the upper limits of the flotation rate.

b. An increase in IPS has little effect on the power exponent of the gamma function.

The effect of IPS on the bubble size and power input is that when IPS is increased, the bubble size is reduced and the power input increased.

9.1.4 The effect of particle size on flotation

The effect of particle size on the flotation results can be summarized as:

1) The effect of size on flotation recovery is dependent on both the specific gravity and the floatability of the floatable mineral.

2) In coal flotation, since the specific gravity is low, the effect on size fraction investigated is small. In complex sulphide flotation, the highest recovery of Fe was observed at the medium size fractions.

The effect of particle size on the parameters of different flotation models can be summarized as:

1. The effect of particle size on the CDM,

a. From the fine to the medium size, the fraction of fast floating is increased and the unfloatable is reduced. Further increase of the particle size from the medium to the coarse reduces the fraction of fast floatable but not the unfloatable fraction.

b. The flotation rate of the fast floatable will increase when size increases but the flotation rate of the slow floatable fraction is almost unaffected.

c. For both mass recovery and element recovery the pattern of the size effect on flotation is similar.

2. The effect of particle size on the MCM,

a. An increase in particle size from fine to medium will increase the initial mean flotation rate and the rate of reduction in flotation rate of element but further increase from medium to coarse has no more effect.

b. The unfloatable fraction will first increase as particle size increases from fine to medium and then reduces from medium to coarse size.

3. The effect of particle size on the GFM,

a. In the GFM, the medium size fractions have the highest upper limit of the flotation rate and largest power exponent of the gamma function, which means that the medium size has the highest flotation rate among all size fractions.

b. The coarse size has smaller power exponent and Kmax than the medium size, but greater than the fine.

9.1.5 The difference between the flotation of different minerals

In conclusion, the difference between different minerals flotation can be listed as:-

1. In **CDM**, the fast floatable minerals have high flotation rate constants in the element recovery. In **MCM**, the fast floatable minerals have a large initial mean flotation rate and the reduction rate of the mean rate of the element recovery. In **GFM**, the fast floatable minerals have high maximum flotation rate constant and large power exponent of the gamma function.

2. The feature of the fast floatability is represented by the parameters of element recovery and not by these of mass recovery.

3. Finally, from the points above it can be concluded that coal is the fastest floating mineral under its specific flotation conditions followed by pyrite (represented as Fe) in complex sulphide flotation. However, floatability does not have any meaning without considering the corresponding flotation conditions, since the flotation conditions will change the flotation response.

9.2 Suggestions for further researeh

Due to limitation of time, certain works were not able to be carried out. For further research, the project can be centred on other factors which affect the flotation parameters in the models.

Further research can generally cover the few major areas depending on the interests of the researchers.

1) When a method for treating a specific mineral is expected, the research can be centred on the effect of the mineral properties on the parameters of the flotation models. By changing the dosage and the type of the reagents, the parameters in the models for the corresponding conditions can be calculated. From an analysis of the relationships between the different reagents and the parameters, the best possible conditions can be predicted before the completion of experiments. There are two benefits of carrying out this work, first, the experimental design can be simplified, and will save time and money. Secondly, the relationships obtained can be used as a reference for future. Step by step, the whole flotation model of any mineral may be completed.

2) If the aim of research is fundamental in flotation mechanism and models, research can be centred on the effect of other factors such as the froth stability effect on the parameters in the models. In this field, of course, one mineral can be selected and the froth height and dosage must be varied to obtain the relationship with considerable accuracy.

3) Another area of interests is in the investigation of the effect of solid concentration in the pulp on the flotation parameters of different models. It may be of interest to see if the concentration of solid in the pulp causes problem at a fixed AFR, or if an increase in AFR can improve flotation at high solids concentrations.

Finally, if the models are going to be employed in the industrial scale, a project can also be centred on pilot plant scale flotation circuit to see how the models will fit. To achieve this, not only skilled sampling is essential, but also laborious work would be involved. However, this is the most beneficial project since the results can be eventually used in practice.

References

1   Apling, A. C. and Ersayin, S. 1986

    "The reproducibility of semi-batch flotation test work and derived kinetic parameters when using the Leeds open-top cell", Trans I.M.M. Vol x, C

2   Arbiter, N. and Harris C. C., 1962

    "Flotation kinetics in froth flotation" - 50th Anniversary Volume (ed. D. W. Fuerstenau), pp. 215-246, (Rocky Mountain Fund Series).

3   Arbiter, N., 1951

    "Flotation rate and flotation efficiency" Trans. A.I.M.E, 190, pp. 791-796.

4   Ball, B. and Fuerstenau, D. W. 1974

    "On the determination of rate constants from semi-batch flotation test", Quart. Col. School of Mines, 69 pp. 27-40.

5   Ball, B.; Kapur P. and Fuerstenau, D. W. 1974

    "Prediction of grade recovery curves from a flotation kinetic model". Trans AIME 247 pp 263-269.

6   Bennet, A.J.R., Chapman, W. R. and Dell, C. C. 1958

    "Studies in froth flotation of coal", Third International Coal Preparation Congress, (Liege, Belgium).

7   Bishop, J. P. and White, M. E. 1976

    "Study of particle entrainment in flotation froths", Trans I.M.M. 85, sect. C pp. 191-194.

8   Black, K.G. and Faulkner, B.P. 1972

"Evaluation of batch flotation results by multi linear regression", Trans, A.I.M.E. 252, pp. 14-21.

9   Brian, D. Bunday, 1984

"Basic Optimisation methods", editor Edward Arnold Ltd.

10   Burden, L. Richard and Faires J. 1985

"Numerical Analysis", 3rd Edition, By Boston Na. Prindle Weber & Schmidt.

11   Brown, D.J. and Smith, H.G. (1954a)

"The flotation of coal as a rate process", Trans. I.M.E., London, 113 pp, 1001-1017.

12   Brown, D.J. and Smith H.G. (1954b)

Coliery Engineering, 31; 245

13   Bull, W.R. (1965)

"Flotation kinetics and its application to the interpretion of plant performance and the design of treatment circuits", 8th British Commonwealth Min. Met. Congress, Melbourne, pp 1113-1124.

14   Bull, W.R. (1966)

"The rate of flotation of mineral particles in sulphide ores", Proc. Aus. I.M.M. No. 220, Dec., pp69-78.

15   Bushell, C. H. G. 1962

"Kinetics of flotation", Trans. Soc. Min. Engrs. (AIME) Vol 223, pp. 215-262.

16 Carpenter, B.H. and Sweeny, H.C. 1965

"Process improvement with Simplex self directing evaluationary operation",

Chem. Engng. 72, No 14, pp. 117-126.

17 Chen, Z.M. and Wu, D.C. 1978

"A study of flotation kinetics (1)", You-Se Jin-Shu, Trans. Mineral proc. No

10, pp 28-33.

18 Chen, Z.M. and Mular, L. 1982

"A study of flotation kinetics - A kinetic model for continuous flotation",

You-Se Jin-Shu, No 3 Trans, Mineral Proc. pp. 38-43.

19 Copper, H.R. 1966

"Feedback process control of mineral flotation. Part 1. Development of a model

for froth flotation", Trans. Soc. Min. Eng. of A.I.M.E., Dec. pp. 439-450.

20 Cutting G.W. and Devenish M. 1975

"A steady-state model of froth flotation structures", AIME annual meeting,

N.Y. Feb. preprint 75-B56.

21 Dell, C. C. and Bunyard, M. J. 1972

"Development of an automatic flotation cell for the laboratory", Trans I.M.M.

81, C pp. 248

22 Dell, C.C. and Hall, G. A. 1981

"Leeds open-top laboratory flotation cell", Trans I.M.M. 90, C pp. 174-176.

23 Dell, C.C. and Farrar, J.C. 1983

"A new flotation model" Leeds University Mining Associasion (LUMA)

pp131-142

24 Engelbrecht, J.A. and Woodburn, E.T., 1975

"The effect of froth height, aeration rate, and gas precipitation on flotation", J. Sth. Afr. Inst. Min. Metall., 76, pp. 125-132.

25 Ersayin, S. 1986

"Flotation kinetics of Santiago copper ore", Ph.D thesis, Dept. of Mining and Mineral Engineering, Leeds University, Leeds, England.

26 Flint, L.R., 1974

"A mechanistic approach to flotation kinetics", Trans. I.M.M., 83 pp. C90-95.

27 Gaudin, A.M. and Groh J.O. and Henderson, H.B. 1931

"Effect of particle size on flotation" AIME Tech. Publ. 414 pp3-23

28 Gaudin, A.M. 1957

"Flotation", 2nd edition. Mcgraw Hill Book Co., New York.

29 Harris, C.C., Jowett, A. and Ghosh, 1963

"Analysis of data from flotation test" Trans. Soc. Min. Eng., Dec 1963

30 Harris, C.C. and Chakravarti, A. 1970

"Semi-batch froth flotation kinetics; species distribution analysis", Trans. A.I.M.E., 247 pp. 162-172.

31 Harris, C.C. and Raja, A. 1970

"Flotation machine impeller speed and air rate as scale-up criteria", Trans. of Inst. Min. Met., Vol. 79, 1970, C 295-297

32   Harris, C.C. and Rimmer, H.W., 1966

"Study of a two-phase model of the flotation process", Trans. Inst. Min. Metall., 75, C153-162.

33   Hooke R., and Jeeves T. A. 1961

"Direct search solution of numerical and statistical problems", J. Assn. Comp. Math. 8 pp.212-229.

34   Imaizumi, T and Inoue, T. 1963

"Kinetic considerations of froth flotation", Proc. 6th Int. Min. Proc. Congress. (Cannes), pp. 581-593

35   Inoue, T. and Imaizumi, T (1968)

"Some aspects of the flotation kinetics", 8th Int. Min. Proc. Congress (Lesningrad), Paper s15.

36   Inoue, T. and Imaizumi, T (1980)

"A series works related to flotation kinetics" 4th Joint Meeting MMIJ-AIME pp85-100

37   Jameson, G.J. Nam, S. and Moo Young, M. 1977

"Phsical factors affecting recovery rates in flotation", Miner. Sci. Eng., Vol 9, No 3 pp. 103-118.

38   Johnson, N.W., McKee, D.J. and Lynch, A.J. 1972

"Flotation rate of non-sulphide minerals in chalcopyrite flotation process", Trans A.I.M.E. 256 pp. 1974

39 Jowett, A. 1974

"Resolution of flotation recovery cerves by a difference plot method", Trans IMM 70 pp 191-204.

40 Jowett, A. 1980

"Formation and disruption of particle-bubble aggregates in flotation, in Fine particles processing (Ed. P. Somasundaran)", pp. 720-754.

41 Jowett, A. and Scofvi, S.M.M. 1960

"Refinements in methods of determing flotation rate", A.I.M.E. 217, pp. 351-357.

42 Jowett, A. 1961

"Investigation of residence time of fluid in froth flotation cells", Brit. Chem. Engng, Vol 6, pp. 254-258.

43 Kapur, P.C. and Mehrotra, S.P. 1974

"Estimation of the flotation rate distributions by numerical inversion of the Laplace transform", Chem. Eng. Sci., 29, pp.411-415.

44 Kelsall, D.F., 1961

"Application of probability in the assessment of flotation systems", Trans. Inst. Min. Met. 70, pp. 191-240.

45 Kelsall, D.F. and Stewart P.S. 1971

"A critical review of applications of models of grinding and flotation", Automatic control systems in mineral processing plant. (symposium Aus IMM Brisbane) pp 213-232

46 King, R.P. 1974

"The simulation of flotation plants", S.M.E. Preprint 74 B-25, A.I.M.E. Annual meeting, Dallas, Texas.

47 King, R.P. Hatton, T. A. and Hulbert, D.G., 1974

"Bubble loading during flotation", Trans. I.M.M. London, 83, pp. 112-115.

48 Laplant, A.R. Toguri, J.M. and Smith, H.W. (1983a)

"The effect of air flow rate on the kinetics of flotation. Part 1; The transfer of material from the slurry to the froth" Inter. J. Miner. Process. No.11 pp203-219.

49 Laplant, A.R.and Smith, H.W. and Toguri,J.M.(1983b)

"Part 2: The transfer of material from the froth over the cell lip" Inter. J. Miner. Process. No. 11 pp221-234

50 Laplant, A.R. Smith,H.W. and Toguri, J.M. (1984)

"Part 3: Selectivity" Inter. J. Miner. Process. No.13 pp285-295

51 Loenard, J. and Warren, (1985)

"Determination of the contributions of the true flotation and entrainment in batch flotation test" Inter. J. Miner. Process. Vol.14 pp33-44

52 Lewis, C.L. 1971

"Application of a computer to a flotation process", Can. I.M.M. Bull. 64, No. 705, pp. 47-50.

53 Loveday, B.K. 1966

"Analysis of froth flotation kinetics", Trans I.M.M., 75, pp. 219-226.

54 Lynch, A.J., Johnson, N.W., McKee, D.J. and Thorne 1974

"The behaviour of minerals in sulphide flotation process, with reference to simulation and control", J. Sth. Afr. Ins. Min. Met., 74, No 9, pp. 349-361.

55 Lynch, A.J., Johnson, N.W., 1981

"Mineral and coal flotation circuits; their simulation and control", Vol 3 Developments in Mineral Proc. Elsevier Sci. publish Company.

56 Mika T. 1967

"Discussion of paper by H.R. Cooper", Trans AIME 238, pp 479-483.

57 Morris T.M. 1952

"Discussion of flotation rates and flotation efficiency", by N. Arbiter, Mining Eng. 4, No 8, pp. 794-798.

58 Morris, T.M. 1962

"Measurement and evaluation of the rate of flotation as a function particle size", Trans. A.I.M.E. Vol 193, pp. 794-798.

59 Nelder J. A. and Mead R. 1965

"A simplex method for function minimisation", The Comp. Journal, 7, pp. 308-331.

60 Nonaka, M. Inoue, T. and Imaizumi, T. (1977)

"Turbulent mixing energy and energy transfer in flotation cell" J. Mining and Metall Inst. Japan, No.93 pp371-376

61 Osborn, G. A. 1984

"Computer models of flotation plant", Ph.D thesis, Dept. of Mining and Mineral Engineering, Leeds University, Leeds, England.

62 Powell, M.J.D. 1964

"A efficient method of funding the minimum of a function of several variables without calculating derivatives", The Comp. Journal, 7, pp. 155-162.

63 Reay, D. and Ratcliff, G.A., 1975

"Experimental testing of the hydrodynamic collision model of fine particle flotation", Can. J. Chem. Engng, No 53, pp. 481-486

64 Rosenkrock H.H. 1960

"An automatic method for finding the greatest or least value of a function", The Comp. Journal 3, pp. 175-184.

65 Schubert, H. and Bischofberger, C. (1979)

"On the optimization of hydrodynamics in flotation process" 13th Inter Miner. Process. Congr. pp353-377

66 Schuhmann, R. 1942

"Flotation kinetics. I. Methods for steady state study of flotation problem", J. Phys. Chem., Vol. 46, pp. 891-902.

67 Schulze, H. J. 1984

"Physico-Chemical elementary processes in flotation", Vol. 4 of Developments in Mineral Proc. Elsevier Sci. Publisher. New York.

68 Smith H. W. and Lewis C.L. 1969

"Computer control experiments at Lake Dufault", Can IMM Bullettin 62, No 682 pp 109-115

69 Sutherland, K. L. 1948

"Kinetics of flotation process", J. Phys. Chem. No 52, pp. 394-425.

70 Szatkowski, M. and Freyberger, W.L. 1985

"Model describing mechanism of the flotation process" Trans Inst. Min. Metall. No.94 Sep 1985

71 Tomlinsion, H.S. and Fleming, M.G. (1965)

"Flotation rate studies", 6th Inter. Miner. Process. Congr. pp563-579

72 Woodburn, E.T. 1970

"Mathematical modelling of flotation process", Minerals Science and Engineering. vol. 2, No 2, pp. 3-17.

73 Woodburn, E.T. and Loveday, B. K. 1965

"Effect of variable residence time data on the performance of a flotation system", J. Sth. Afr. Inst. Min. Metall., pp. 612-628.

74 Woodburn, E.T. and Wallin, P.J. (1984)

"Decoupled kinetic model for simulation of flotation networks", Trans Inst. Min Metall. Sect C. Vol 93   December 1984, pp153-161

75 Wu Y. R. (1986)

"Multi-rate flotation model for both objective mineral and bulk flotation components" Kuangye Gongcheng Vol.6 No.13 pp33-37

76 Yin D. 1986

"Flotation model with a distribution of coefficient - the change of mean rate coefficient with time", You-Se Jin-Shu, Vol. 38, No 1, pp. 49-56

77 Xu C. L. 1984

"Kinetic model for continuous flotation in a column", You-Se Jin-Shu, Vol. 36, No 3, pp 35-42.

78 Zaidenberg, I.S., Lisovskii, D.I and Burovoi 1964

"One approach to the construction of a mathematical model for the flotation process", Sov. J. Non-ferrous Met., Vol 5, No 7, pp. 26-32.

79 Zuniga, H. G. 1935

"The efficiency obtained by flotation is an exponential function of time", Bol. minero Soc. nacl. mineria (chile) Vol. 47, pp. 83-86.

Appendixes

Appendix 1 THE BUBBLE SIZE MEASUREMENT

No 1.   IPS=700 rpm, AFR=1.0 1/min

```
0.48  0.50  0.50  0.42  0.42  0.58  0.36  0.33  0.38
0.45  0.83  0.50  0.50  0.66  0.47  0.47  0.50  0.70
0.58  0.43  0.63  0.58  0.53  0.75  0.26  0.33  0.20
0.96  0.33
```
                          29 data, Mean=0.505, STD=0.164

No 2.   IPS=950 rpm, AFR=1.0 1/min

```
0.70  0.67  0.50  0.42  0.58  0.55  0.42  0.50  0.50
0.33  0.67  0.58  0.33  0.58  0.85  0.50  0.50  0.42
1.16  0.17  0.33  0.33  0.50  0.33  0.42  0.50  0.50
0.42
```
                          28 data, Mean=0.509, STD=0.185

No 3.   IPS=1200rpm, AFR=1.0 1/min

```
0.50  0.48  0.50  0.37  0.33  0.37  0.58  0.42  0.33
0.50  0.42  0.42  0.43  0.42  0.53  0.50  0.33  0.57
0.47  0.58  0.50  0.58  0.47  0.63
```
                          24 data, Mean=0.468, STD=0.084

No 4.   IPS=1450rpm, AFR=1.0 1/min

```
0.50  0.52  0.47  0.35  0.45  0.35  0.53  0.33  0.30
0.33  0.40  0.50  0.50  0.25  0.28  0.67  0.50  0.37
0.47  0.57  0.33  0.50  0.48
```
                          23 data, Mean=0.433, STD=0.103

No 5.   IPS=1700rpm, AFR=1.0 1/min

```
0.27  0.67  0.58  0.75  0.34  0.42  0.17  0.42  0.42
0.33  0.37  0.25  0.30  0.35  0.52  0.60  0.50  0.52
0.37  0.42  0.37  0.33  0.42  0.53  0.50  0.47  0.17
0.33  0.37  0.37  0.18
```
                          31 data, Mean=0.407, STD=0.135

No 6.   IPS=700 rpm, AFR=2.5 1/min

```
0.33  0.50  0.35  0.35  0.42  0.50  0.58  1.13  0.50
0.53  0.37  0.67  0.67  0.37  0.43  0.33  0.47  0.50
0.67  0.33  0.63  0.55  0.86  0.32  0.37  1.02  0.75
0.48  0.35  0.83  0.18  0.70  0.33  0.35  0.55
```
                          35 data, Mean=0.522, STD=0.208

No 7.   IPS=950 rpm, AFR=2.5 1/min

```
0.52  0.38  0.28  0.87  0.43  0.95  0.30  0.37  0.86
0.67  0.52  0.37  0.33  0.35  0.86  0.60  0.33  0.67
0.50  0.65  0.42  0.67  0.42  0.43  0.75  0.83  0.30
0.48  0.72
```
                          29 data, Mean=0.546, STD=0.200

     (continued)

No 8.　IPS=1200rpm, AFR=2.5 l/min

```
0.48   0.67   0.97   0.45   0.32   0.48   0.83   0.53   0.3
0.50   0.60   0.33   0.42   0.67   0.27   0.42   0.42   0.70
0.47   0.35   0.23   0.47   0.70   0.67   0.52   0.17   0.53
0.43   0.40   0.17   0.35
```

                    31 data, Mean=0.479, STD=0.183

No 9.　IPS=1450rpm, AFR=2.5　l/min

```
0.30   0.32   0.48   0.75   0.53   0.58   0.40   0.43   0.33
0.30   0.75   0.52   0.57   0.40   0.63   0.68   0.25   0.83
0.43   0.25   0.48   0.58   0.42   0.32   0.50   0.17   0.50
```

                    27 data, Mean=0.470, STD=0.164

No 10.　IPS=1700rpm, AFR=2.5 l/min

```
·0.50   0.47   0.50   0.67   0.33   0.50   0.65   0.33   0.67
 0.50   0.68   0.67   0.50   0.42   0.43   0.43   0.35   0.50
 0.33   0.37   0.50   0.40   0.45   0.35   0.35   0.58   0.35
 0.50
```

                    28 data, Mean=0.474, STD=0.112

No 11.　IPS=700 rpm, AFR=4.0　l/min

```
0.33   0.83   0.30   0.67   0.80   0.52   0.67   0.67   0.38
0.57   0.73   0.42   0.67   0.75   0.63   0.35   0.52   0.50
0.50   0.65   0.50   0.67   0.47   0.83   0.50   0.63   0.53
0.50   0.50   0.35   0.68   0.38
```

                    32 data, Mean=0.562, STD=0.146

No 12.　IPS=950 rpm, AFR=4.0 l/min

```
0.63   0.58   0.57   0.52   1.25   0.75   0.30   0.33   0.43
0.40   0.60   0.53   0.83   0.70   0.58   0.57   0.50   0.45
0.57   0.35   0.67   0.33   0.47   0.67   0.97   0.83   0.45
```

                    27 data, Mean=0.586, STD=0.207

No 13.　IPS=1200rpm, AFR=4.0　l/min

```
0.67   0.33   0.67   0.63   1.17   0.50   0.33   0.52   0.42
0.43   0.35   0.53   0.42   0.33   0.17   0.35   0.60   0.32
0.20   0.58   1.17   0.35   0.53   0.83   0.20
```

                    25 data, Mean=0.504, STD=0.252

No 14.　IPS=1450rpm, AFR=4.0 l/min

```
0.63   0.58   0.55   0.42   0.50   0.33   0.35   0.67   0.48
0.50   0.58   0.67   0.62   0.57   0.60   0.50   0.65   0.83
0.37   0.48   0.45   0.40   0.50   0.47   0.50
```

                    25 data, Mean=0.528, STD=0.113

No 15.　IPS=1700rpm, AFR=4.0　l/min

(continued)

```
0.58   0.50   0.62   0.37   0.83   0.67   0.67   0.67   0.45
0.23   0.35   0.47   0.43   0.62   0.52   0.33   0.33   0.77
0.43   0.67   0.53   0.37   0.42   0.47   0.47   0.35   0.33
0.53   0.67   0.50
```

<div align="right">30 data, Mean=0.505, STD=0.144</div>

No 16. IPS=700 rpm, AFR=5.5 1/min

```
0.83   1.33   0.58   0.53   0.50   0.50   0.48   0.67   1.25
0.58   0.50   1.67   0.60   0.58   0.50   0.67   0.67   1.08
0.67   0.63   0.80   0.83   0.33   0.42   0.50   0.33   0.20
0.83   0.47   0.58   0.47   0.53   0.50   0.48   0.50   0.73
0.75   0.63   0.88   0.92   0.67   0.63   0.53   0.67   0.70
0.67   0.50
```

<div align="right">47 data, Mean=0.657, STD=0.259</div>

No 17. IPS=950 rpm, AFR=5.5 1/min

```
1.03   0.67   0.45   0.70   0.33   0.77   0.32   0.40   0.50
0.58   0.40   0.53   0.33   0.67   0.58   0.53   0.75   0.62
0.63   0.50   0.67   0.50   0.57   0.68   0.47   0.83   1.15
```

<div align="right">27 data, Mean=0.598, STD=0.193</div>

No 18. IPS=1200rpm, AFR=5.5 1/min

```
0.50   0.62   0.72   0.85   0.67   0.98   0.50   0.80   0.50
0.67   1.00   0.48   0.27   0.83   0.50   0.33   0.65   0.75
0.50   0.43   0.67   0.85   0.60   0.47   0.53
```

<div align="right">25 data, Mean=0.627, STD=0.185</div>

No 19. IPS=1450rpm, AFR=5.5 1/min

```
0.67   0.58   0.73   0.67   0.32   0.92   0.67   0.67   0.65
0.75   0.67   0.67   0.50   0.58   0.42   0.65   0.67   0.42
0.63   0.98   0.58   0.33   0.27   0.35   0.40
```

<div align="right">25 data, Mean=0.590, STD=0.175</div>

No 20. IPS=1700rpm, AFR=5.5 1/min

```
0.58   0.67   0.53   0.50   0.53   0.65   0.67   0.63   0.67
1.00   0.50   0.75   0.50   0.83   0.45   1.03   0.53   0.67
0.53   0.50   0.35   0.35   0.68   0.38   0.45
```

<div align="right">25 data, Mean=0.597, STD=0.171</div>

No 21. IPS=700 rpm, AFR=7.0 1/min

```
0.83   0.96   0.66   0.66   0.63   0.42   0.75   0.47   0.47
0.67   0.58   0.70   1.03   0.88   0.75   0.58   0.92   0.42
0.53   0.51   0.75   0.98
```

<div align="right">22 data, Mean=0.689, STD=0.181</div>

No 22. IPS=950 rpm, AFR=7.0 1/min

```
0.63   0.60   0.50   0.58   0.83   0.83   0.63   0.42   0.58
0.92   0.58   0.53   0.70   0.50   0.58   0.67   0.43   0.40
0.53   0.73   0.42   0.43   1.05   0.67   0.53   0.93   0.63
0.53   1.12   0.47   0.83   0.47   0.50
```

<div align="right">33 data, Mean=0.629, STD=0.183</div>

(continued)

No 23. IPS=1200rpm, AFR=7.0 1/min

```
0.50  0.77  0.37  0.67  0.67  0.67  0.33  0.47  0.53
0.63  0.52  1.00  0.67  0.50  0.50  0.58  0.92  0.53
0.33  0.57  0.53
```

                                21 data, Mean=0.584, STD=0.165

No 24. IPS=1450rpm, AFR=7.0 1/min

```
0.50  0.67  0.58  0.63  0.75  0.96  0.50  0.60  0.67
0.58  0.67  0.58  0.67  0.97  0.42  0.67  0.53  0.33
0.58  0.60  0.63  0.96  0.75  0.97  0.67  0.42  0.50
0.83  0.75  0.58  0.58  0.50  0.67  0.42
```

                                34 data, Mean=0.638, STD=0.158

No 25. IPS=1700rpm, AFR=7.0 1/min

```
0.87  0.75  0.40  0.50  0.70  0.67  0.52  0.47  0.50
0.50  0.60  0.60  0.37  0.65  1.03  1.08  0.48  0.86
0.33  0.50  0.85
```

                                21 data, Mean=0.630, STD=0.205

Appendix 2 POWER OUTPUT MEASUREMENT

TEST 1   Impeller speed was varied

(Air flow rate = 2.5 l/min)

Impwller Speed (rpm)	Power output (watt)			
	Empty cell	Test start	Test end	Net
700	150	170	149.5	9.7
950	165	206	183	29.5
1200	177	132	228	53.0
1450	188	290	285	99.5
1700	200	360	355	157.5

TEST 2   Air flow rate was varied

(impeller speed = 950 rpm)

Air flow rate (l/min)	Power output (watt)			
	Empty cell	Test start	Test end	Net
1.0	165	220	192	41.0
2.5	165	206	183	29.5
4.0	165	180	178	14.0
5.5	165	175	170	7.5
7.0	165	172	170	6.0

Appendix 3 WATER REPLACEMENT BY AIR

```
--------------------------------------------------------
Air \ Speed |   700    950   1200   1450   1700
rate \ rpm  |
--------------------------------------------------------
  1.0 l/min  |    95     95    120    112    105
  2.5 l/min  |   150    167    209    215    216
  4.0 l/min  |   167    209    237    259    269
  5.5 l/min  |   178    212    267    287    308
  7.0 l/min  |   187    258    282    307    360
--------------------------------------------------------
```

The the unit of values in the table is ml.

The cell volume is 3430 ml in full cell.

Appendix 4 WATER RECOVERY MEASUREMENT

(Impeller speed = 950 rpm)

TEST 1   Air flow rate is 1.0 l/min

Collecting	Weight (g)				
time	Total	Solid	Bowl	Water	C.Water
15''	456	52.9	354	49.1	49.1
30''	362	27.0	309	26.0	75.1
55''	384	19.0	335	30.0	105.1
1.5'	347	16.5	302	28.5	133.6
4.5'	467	34.4	352	80.5	214.1
12.0'	640	45.0	326	269.0	483.1

TEST 2   Air flow rate is 2.5 l/min

Collecting	Weight (g)				
time	Total	Solid	Bowl	Water	C.Water
15''	517	92.3	354	70.7	70.7
30''	362	26.6	309	26.4	97.1
55''	424	29.5	346	48.5	145.6
1.5'	398	22.2	302	73.8	219.4
4.5'	708	42.7	313	352.3	571.7
12.0'	890	37.5	326	526.5	1098.2

TEST 3   Air flow rate is 4.0 l/min

Collecting	Weight (g)				
time	Total	Solid	Bowl	Water	C.Water
15''	585	118.1	354	114.9	114.9
30''	390	33.3	309	47.7	162.6
55''	427	25.7	335	66.3	228.9
1.5'	411	20.3	302	88.7	317.6
4.5'	741	36.0	313	392.0	709.6
12.0'	1061	26.2	326	708.8	1418.4

(Continued)

TEST 4   Air flow rate is 5.5 l/min

Collecting time	Weight (g)				
	Total	Solid	Bowl	Water	C.Water
15''	652	142.6	354	155.4	155.4
30''	396	33.6	309	53.4	208.8
55''	465	28.2	335	101.8	310.6
1.5'	457	21.6	289	146.4	457.0
4.5'	920	33.5	352	534.5	991.5
12.0'	1196	27.1	320	848.9	1840.4

TEST 5   Air flow rate is 7.0 l/min

Collecting time	Weight (g)				
	Total	Solid	Bowl	Water	C.Water
15''	681	160.9	313	207.1	207.1
30''	459	29.2	343	86.8	293.9
55''	564	30.7	346	187.3	481.2
1.5'	569	23.1	302	243.9	725.1
4.5'	1106	33.6	313	756.4	1481.5
12.0'	1367	31.4	326	1009.6	2491.1

Appendix 5 AAS for Cu analysis

Atomic absorption spectrophotometry was used for the analysis of Cu. In the analysis, approximately 2 g was taken from each sample and finely ground. Of the 2 g, 0.100 g and 0.300 g respect to the concentrates and tailing was weighed in a balance. Then the weighed sample was put into a 50 ml conical flask, 10 ml $HClO_4$, 2 ml HNO_3 were added. The flask was put on a sandbath and heated for approximately one hour for the digestion of the sample. During the digestion, a funnel was inserted to avoid the splash of the content. When the sample was dissolved and the NO_2 vapour disappeared, the flask was removed from the sandbath and cooled at room temperature. After cooling, the solution was transferred into a 250 ml volumetric flask and distilled water was added to make the total volume of 250 ml. The final solution was then kept in plastic bottles for Atomic Absorption.

With the wavelength of the AA spectrophotometer setting at 324.7 nm, the standards and the samples were measured.

The readings of the four standard vs the ppm content of Cu were plotted in a graph paper. Smooth curve was drawn through the four points manually. From the curve, the ppm of Cu in each sample can be calibrated. The Cu grade of each sample was

calculated by the equation below:-

$$Cu\ \% = \frac{ppm * 250\ (ml)}{(10+6)*Weight\ of\ Sample} * 100\ \%$$

Appendix 6 AIR FLOW RATE EXPERIMENT RESULTS

Test1 Air flow rate is 1.0 l/min

Name	Mass rec.	C.M.rec	Grade	C.Grade	Recov.	C.Rec.
C1	1.82	1.82	12.7	12.7	35.78	35.78
C2	2.11	3.93	7.3	9.80	23.84	59.62
C3	0.93	4.86	6.0	9.07	8.64	68.26
C4	1.03	5.89	3.3	8.06	5.26	73.52
C5	0.60	6.49	2.5	7.55	2.32	76.84
C6	0.78	7.28	1.5	6.89	1.81	77.65
T	92.72	100.0	0.155	0.646	21.93	100.00
Total	100.0	100.0	0.646	0.646	100.0	100.00

Test2 Air flow rate is 2.5 l/min

Name	Mass rec	C.M.Rec	Grade	C.Grade	Recov.	C.Rec.
C1	2.82	2.82	7.6	7.6	33.17	33.17
C2	2.21	5.03	6.7	7.2	22.92	56.09
C3	1.35	6.38	3.3	6.38	6.89	62.89
C4	2.17	8.55	2.1	5.29	7.05	70.03
C5	1.35	9.90	1.1	4.72	2.30	72.33
C6	1.15	11.05	0.85	4.32	1.51	73.84
T	88.95	100.0	0.19	0.646	26.16	100.0
Total	100.0	100.0	0.646	0.646	100.0	100.0

Test3 air flow rate is 4.0 l/min

Name	Mass Rec.	C.M.Rec.	Grade	C.Grade	Recov	C.Rec.
C1	3.67	3.67	6.0	6.0	34.47	34.47
C2	3.54	7.2	4.4	5.22	24.38	58.84
C3	2.20	9.40	2.5	4.58	8.61	67.45
C4	2.61	12.01	1.5	3.91	6.13	73.58
C5	1.48	13.64	0.6	3.55	1.39	74.97
C6	1.00	14.49	0.5	3.34	0.78	75.75
T	85.51	100.0	0.18	0.639	24.25	100.0
Total	100.0	100.0	0.639	0.639	100.0	100.0

Test4 air flow rate is 5.5 l/min

Name	Mass Rec.	C.M.Rec.	Grade	C.Grade	Recov.	C.Rec
C1	3.11	3.11	6.3	6.3	30.19	30.19
C2	3.46	6.57	5.5	5.88	29.33	59.52
C3	2.10	8.67	2.3	5.01	7.44	66.96
C4	3.30	11.97	0.9	3.88	4.58	71.54
C5	1.85	13.82	0.5	3.43	1.43	72.97
C6	1.53	15.35	0.4	3.12	0.94	73.91
T	84.65	100.0	0.2	0.649	26.09	100.0
Total	100.0	100.0	0.649	0.649	100.0	100.0

(Continued)

Test5 air flow rate is 7.0 1/min

Name	Mass Rec.	C.M.Rec.	Grade	C.Grade	Recov.	C.Rec
C1	4.09	4.09	6.3	6.3	39.89	39.89
C2	3.48	7.99	5.0	5.4	26.93	66.82
C3	2.46	10.45	1.7	4.53	6.47	73.29
C4	2.67	13.12	0.7	3.75	2.87	76.18
C5	1.55	14.67	0.4	3.4	0.96	77.14
C6	1.69	16.36	0.3	3.07	0.78	77.92
T	83.34	100.0	0.17	0.646	22.08	100.0
Total	100.0	100.0	0.646	0.646	100.0	100.0

Appendix 7 SIZE ANALYSIS RESULT FROM COAL SAMPLES

Test No. 1   AFR= 1.0 l/min

Name	+120 (%)	+75 (%)	+53 (%)	-53 (%)	all size (%)
C1	5.65	5.65	3.92	15.13	30.35
C2	3.78	4.06	3.43	9.31	20.58
C3	2.26	3.02	2.68	7.20	15.16
C4	1.49	1.33	2.70	5.70	11.22
C5	1.71	1.54	2.13	6.79	12.17
T	1.76	2.00	2.00	4.75	10.51
total	16.65	17.60	16.86	48.88	100.0

Test No. 2   AFR= 2.5 l/min

Name	+120 (%)	+75 (%)	+53 (%)	-53 (%)	all size (%)
C1	6.08	7.66	4.09	13.67	31.51
C2	4.70	6.69	4.34	14.95	30.68
C3	3.11	3.89	2.06	7.40	16.46
C4	2.09	2.24	1.41	4.90	10.64
C5	0.38	0.45	0.26	2.47	3.57
T	1.28	1.39	0.78	3.68	7.13
total	17.64	22.32	12.94	47.07	100.0

Test No. 3   AFR= 4.0 l/min

Name	+120 (%)	+75 (%)	+53 (%)	-53 (%)	all size (%)
C1	8.19	10.10	5.28	16.76	40.30
C2	5.18	6.24	3.70	13.17	28.28
C3	1.73	4.24	1.95	8.87	16.79
C4	0.76	0.74	0.42	3.63	5.57
C5	0.21	0.20	0.18	1.85	2.44
T	1.44	1.25	0.80	3.20	6.69
total	17.51	22.77	12.34	47.48	100.0

Test No. 4   AFR= 5.5 l/min

Name	+120 (%)	+75 (%)	+53 (%)	-53 (%)	all size (%)
C1	10.51	12.19	5.67	19.55	47.93
C2	5.36	6.46	3.83	13.64	29.28
C3	1.18	2.88	1.32	6.03	11.42
C4	0.44	0.43	0.26	2.10	3.23
C5	0.18	0.17	0.16	1.56	2.06
T	1.31	1.13	0.73	2.91	6.08
total	18.98	23.26	11.97	45.79	100.0

(Continued)

Test No. 5   AFR= 7.0 l/min

Name	+120 (%)	+75 (%)	+53 (%)	-53 (%)	all size (%)
C1	9.79	12.77	6.56	23.62	52.74
C2	5.70	6.27	3.86	12.75	28.58
C3	1.45	1.51	0.91	4.23	8.11
C4	0.33	0.36	0.20	2.29	3.18
C5	0.15	0.13	0.07	1.82	2.18
T	1.26	1.13	0.55	2.31	5.25
total	18.68	22.17	12.15	47.02	100.0

The average values of different size fractions are:

+125	+75	+53	-53	total
18.20	22.63	12.35	46.84	100.0

Appendix 8 ASH CONTENT OF COAL SAMPLES

Test No. 1   AFR= 1.0 1/min

Name	+120 (%)	+75 (%)	+53 (%)	-53 (%)	average (%)
C1	6.00	5.40	4.80	6.78	6.12
C2	7.72	6.49	5.74	6.96	6.80
C3	9.16	7.23	6.16	7.92	7.66
C4	9.57	7.60	6.51	8.38	8.00
C5	11.27	9.84	7.17	11.37	10.38
C6	17.27	21.83	13.87	25.88	22.60
T	78.70	78.74	76.40	80.46	79.07
total	15.54	15.29	14.55	15.81	15.60

Test No. 2   AFR= 2.5 1/min

Name	+120 (%)	+75 (%)	+53 (%)	-53 (%)	average (%)
C1	6.82	5.51	5.53	8.79	7.18
C2	9.28	7.57	5.89	9.61	8.59
C3	13.26	9.74	8.78	10.46	10.61
C4	12.90	10.96	8.90	11.47	11.30
C5	32.92	31.49	31.60	47.67	42.76
T	85.17	84.73	84.25	86.00	85.41
total	15.59	12.87	11.81	17.67	15.46

Test No. 3   AFR= 4.0 1/min

Name	+120 (%)	+75 (%)	+53 (%)	-53 (%)	average (%)
C1	6.69	6.21	6.72	8.10	7.17
C2	10.32	8.20	7.59	9.90	9.30
C3	15.89	15.11	12.39	12.62	13.56
C4	22.34	19.68	21.22	23.85	22.81
C5	36.49	39.37	46.62	59.50*	54.92
T	85.13	86.43	86.58	86.65	86.27
total	16.16	12.73	14.32	19.80	16.18

(Continued)

Test No. 4   AFR= 5.5 l/min

Name	+120 (%)	+75 (%)	+53 (%)	-53 (%)	average (%)
C1	6.39	6.30	5.63	8.14	6.99
C2	9.55	9.10	8.42	10.19	9.60
C3	17.62	16.05	16.06	16.06	16.20
C4	32.97	31.78	30.06	33.68	33.04
C5	49.03	49.75	56.56	66.84	63.40
T	85.87	87.02	86.89	87.77	87.12
total	14.49	13.00	13.84	18.03	15.68

Test No. 5   AFR= 7.0 l/min

Name	+120 (%)	+75 (%)	+53 (%)	-53 (%)	average (%)
C1	6.98	6.42	6.52	7.74	7.13
C2	9.78	10.65	9.12	10.50	10.20
C3	24.14	20.87	20.41	17.44	19.59
C4	43.60	45.48	43.49	40.41	41.50
C5	65.63	62.23	69.26	70.76	69.53
T	84.97	86.79	86.66	86.83	86.36
total	15.55	13.66	12.99	17.27	15.63

Appendix 9 PARTICLES LIBRATION COUNTING

Name of Minerals	Particle content (volume fraction)			Total No.	liberation %
	<1/4*	1/2	1		
CuFeS2	30	6	86	96.5	89.2 %
FeS2	28	16	242	255	94.9 %
ZnS2	20	6	108	116	93.1 %

* any particles containing less than 1/4 mineral by volume was estimated and added to 1/4 group.

Total = Σ All class * the fractional volume of the class.

$$\% \text{ liberation} = \frac{\text{Volume of free particles}}{\text{Total volume of minerals}} * 100$$

Appendix 10 MASS RECOVERY IN COMPLEX SULPHIDE FLOTATION

No(1) (1)sp   speed=700 rpm   air=2.5 l/min

Name	+125 (%)	+75 (%)	+53 (%)	-53 (%)	+10 (%)	-10 (%)	all (%)
C1	8.5	11.3	9.9	5.5	8.7	2.5	7.5
C2	2.9	4.2	5.2	3.7	5.5	2.1	3.9
C3	3.2	4.3	5.1	3.5	4.6	2.6	3.8
C4	2.9	3.2	3.7	5.0	5.2	4.8	4.2
C5	2.4	2.9	3.7	8.4	5.3	11.4	6.0
C6	0.4	0.5	1.4	7.3	1.7	12.5	4.4
T	79.8	73.6	71.0	66.6	69.1	64.1	70.2
Total	100.0	100.0	100.0	100.0	100.0	100.0	100.0

No(2) (2)sp   speed=950 rpm   air=2.5 l/min

Name	+125 (%)	+75 (%)	+53 (%)	-53 (%)	+10 (%)	-10 (%)	all (%)
C1	10.4	15.9	17.8	9.6	14.3	5.2	11.9
C2	2.4	3.5	4.5	4.5	6.1	3.0	4.0
C3	1.1	1.4	2.1	4.1	4.4	3.7	2.9
C4	0.8	1.0	1.6	4.0	3.8	4.1	2.7
C5	1.8	2.4	3.6	8.1	5.7	10.3	5.6
C6	0.4	0.8	2.1	7.1	1.9	11.9	4.4
T	83.0	74.9	68.4	62.7	63.7	61.7	68.4
Total	100.0	100.0	100.0	100.0	100.0	100.0	100.0

No(3) (3)sp   speed=1200 rpm   air=2.5 l/min

Name	+125 (%)	+75 (%)	+53 (%)	-53 (%)	+10 (%)	-10 (%)	all (%)
C1	11.0	15.5	17.1	9.6	13.7	5.9	11.8
C2	2.6	4.3	5.0	5.2	7.0	3.6	4.7
C3	1.6	2.4	3.2	5.1	5.6	4.7	3.9
C4	1.5	2.2	2.9	5.2	5.0	5.4	3.8
C5	1.3	1.7	2.9	7.4	2.8	11.7	5.0
C6	0.2	0.5	1.3	5.5	1.1	9.6	3.4
T	81.7	73.4	67.5	61.8	62.1	61.6	67.4
Total	100.0	100.0	100.0	100.0	100.0	100.0	100.0

No(4)   (4)sp   speed=1450 rpm   air=2.5 l/min

Name	+125 (%)	+75 (%)	+53 (%)	-53 (%)	+10 (%)	-10 (%)	all (%)
C1	11.8	14.6	17.7	9.4	13.3	5.8	11.7
C2	2.7	3.8	5.5	5.1	5.8	4.5	4.6

(Continued)

C3	1.8	2.4	3.6	5.4	5.2	5.6	4.1
C4	1.4	1.5	2.1	4.3	3.6	5.0	3.1
C5	1.3	1.7	2.8	6.8	3.1	10.2	4.6
C6	0.2	0.5	1.4	5.2	0.9	9.3	3.2
T	80.8	75.4	67.0	63.7	68.1	59.6	68.7
Total	100.0	100.0	100.0	100.0	100.0	100.0	100.0

No(5) (5)sp speed=1700 rpm   air=2.5 l/min

Name	+125	+75	+53	-53	+10	-10	all
	(%)	(%)	(%)	(%)	(%)	(%)	(%)
C1	11.0	16.3	17.7	10.4	13.5	7.6	12.5
C2	2.5	4.2	5.9	5.3	5.7	4.9	4.7
C3	1.5	2.1	3.2	4.9	4.1	5.7	3.7
C4	1.1	1.4	2.0	4.1	3.2	5.0	2.9
C5	1.2	1.6	2.4	7.0	3.6	10.0	4.6
C6	0.1	0.4	1.0	5.3	1.1	9.1	3.1
T	82.6	74.0	67.8	63.1	68.9	57.7	68.4
Total	100.0	100.0	100.0	100.0	100.0	100.0	100.0

No(6) (1)AF speed=950 rpm   air=1.0 l/mi

Name	+125	+75	+53	-53	+10	-10	all
	(%)	(%)	(%)	(%)	(%)	(%)	(%)
C1	7.2	8.7	8.0	4.5	6.3	2.7	6.1
C2	2.2	3.2	4.0	3.3	4.5	2.3	3.2
C3	1.5	2.4	3.5	3.4	3.9	2.9	2.9
C4	0.9	1.5	2.2	3.2	3.5	3.0	2.4
C5	1.6	2.4	4.0	7.5	8.0	7.1	5.3
C6	2.4	4.2	4.9	10.0	5.7	14.1	7.3
T	84.2	77.7	73.4	68.0	68.2	67.9	72.7
Total	100.0	100.0	100.0	100.0	100.0	100.0	100.0

No(7) (2)AF speed=950 rpm   air=2.5 l/min

Name	+125	+75	+53	-53	+10	-10	all
	(%)	(%)	(%)	(%)	(%)	(%)	(%)
C1	10.4	15.9	17.8	9.6	14.3	5.2	11.9
C2	2.4	3.5	4.5	4.5	6.1	3.0	4.0
C3	1.1	1.4	2.1	4.1	4.4	3.7	2.9
C4	0.8	1.0	1.6	4.0	3.8	4.1	2.7
C5	1.8	2.4	3.6	8.1	5.7	10.3	5.6
C6	0.4	0.8	2.1	7.1	1.9	11.9	4.4
T	83.0	74.9	68.4	62.7	63.7	61.7	68.4
Total	100.0	100.0	100.0	100.0	100.0	100.0	100.0

(Continued)

No(8)   (3)AF   speed=950 rpm   air=4.0 1/min

Name	+125 (%)	+75 (%)	+53 (%)	-53 (%)	+10 (%)	-10 (%)	all (%)
C1	14.6	21.1	22.8	11.5	15.8	7.5	15.1
C2	2.2	2.9	4.0	4.6	5.3	3.9	3.8
C3	1.0	1.2	1.8	4.0	4.0	4.0	2.8
C4	0.5	0.6	0.9	2.8	2.0	3.5	1.8
C5	1.2	1.2	2.0	5.4	2.9	7.6	3.6
C6	0.5	0.8	1.8	5.9	1.4	10.1	3.7
T	80.0	72.2	66.6	65.9	68.7	63.4	69.1
Total	100.0	100.0	100.0	100.0	100.0	100.0	100.0

No(9)   (4)AF   speed=950 rpm   air=5.5 1/min

Name	+125 (%)	+75 (%)	+53 (%)	-53 (%)	+10 (%)	-10 (%)	all (%)
C1	15.6	21.2	23.8	13.5	19.6	7.8	16.4
C2	2.4	3.3	3.7	5.4	5.9	5.0	4.4
C3	1.6	1.6	2.3	4.7	4.3	5.1	3.4
C4	1.0	1.1	1.6	3.4	2.3	4.5	2.5
C5	1.0	1.1	2.3	5.2	1.9	8.2	3.5
C6	0.2	0.4	1.2	4.3	0.9	7.4	2.6
T	78.1	71.2	65.1	63.5	65.1	62.0	67.2
Total	100.0	100.0	100.0	100.0	100.0	100.0	100.0

No(10) (5)AF   speed=950 rpm   air=7.0 1/min

Name	+125 (%)	+75 (%)	+53 (%)	-53 (%)	+10 (%)	-10 (%)	all (%)
C1	13.7	24.2	29.0	16.4	23.3	10.1	19.0
C2	1.9	2.9	4.3	5.9	6.6	5.2	4.6
C3	1.1	1.5	2.4	5.2	3.7	6.6	3.6
C4	0.8	0.9	1.4	3.9	2.1	5.6	2.6
C5	0.3	0.4	0.8	5.9	2.7	8.8	3.5
C6	0.0	0.2	0.5	5.6	1.5	9.3	3.2
T	82.2	69.9	61.6	57.1	60.2	54.4	63.5
Total	100.0	100.0	100.0	100.0	100.0	100.0	100.0

No(11) 1)AFSP   speed=1700 rpm   air=7.0 1/min

Name	+125 (%)	+75 (%)	+53 (%)	-53 (%)	+10 (%)	-10 (%)	all (%)
C1	15.1	22.9	28.1	18.8	25.4	12.7	20.1
C2	2.0	2.7	3.7	7.0	6.2	7.8	5.1
C3	1.2	1.6	2.2	5.8	3.9	7.5	4.0
C4	0.5	0.7	1.2	4.1	2.0	5.9	2.6
C5	0.2	0.3	0.9	5.1	1.3	8.6	3.0
C6	0.0	0.1	0.3	4.3	1.0	7.3	2.5
T	80.9	71.7	63.5	55.0	60.1	50.2	61.0
Total	100.0	100.0	100.0	100.0	100.0	100.0	100.0

Appendix 11 XRF CALIBRATION RESULTS

1) The feed sample

Name	elem	+125	+75	+53	-53	+10	all
Feed	FE	12.83	17.74	17.81	13.11	13.35	14.82
(A)	CU	0.47	0.59	0.63	0.57	0.59	0.55
	ZN	4.39	5.17	5.87	5.27	5.48	5.07
Feed	Fe	13.20	17.63	17.69	12.69	12.76	14.42
(B)	CU	0.40	0.61	0.60	0.59	0.61	0.52
	ZN	4.79	5.29	6.14	5.01	5.35	5.27

2) The test sample

Test	size	elem	c1	c2	c3	c4	c5	c6
1AF	125	FE	52.22	46.85	46.29	46.12	45.12	43.06
		CU	0.19	0.06	0.08	0.13	0.41	2.78
		ZN	8.41	7.83	7.80	8.01	8.44	9.27
	+75	FE	52.87	48.18	47.44	47.42	46.81	36.19
		CU	0.17	0.27	0.22	0.57	1.19	4.82
		ZN	8.76	8.49	7.68	8.76	9.32	10.10
	+53	FE	49.56	49.09	45.01	43.12	36.95	33.08
		CU	0.53	0.59	0.72	1.03	2.39	4.18
		ZN	8.67	8.82	8.64	9.04	9.76	11.60
	-53	FE	39.54	37.33	35.22	26.65	27.81	18.77
		CU	1.16	1.31	1.56	1.57	1.93	1.41
		ZN	9.09	9.61	10.08	9.84	10.57	9.66
	+10	FE	44.34	43.44	38.92	34.95	33.17	25.30
		CU	1.19	0.47	1.63	1.01	1.95	1.41
		ZN	9.89	10.32	10.55	10.61	11.65	12.06
2AF	125	FE	48.86	45.35	44.27	43.36	38.39	32.83
		CU	0.55	0.97	1.11	2.12	4.76	5.96
		ZN	8.89	8.56	8.94	9.36	10.55	10.63
	+75	FE	49.27	48.01	45.67	38.34	36.31	25.89
		CU	0.86	1.68	2.05	3.30	4.45	2.73
		ZN	8.93	9.63	9.92	10.64	11.57	12.63
	+53	FE	46.78	44.91	45.44	41.24	33.09	16.86
		CU	1.20	1.88	2.70	3.43	2.20	1.27
		ZN	9.18	9.93	10.50	11.26	12.06	13.73
	-53	FE	35.94	33.49	30.85	28.01	23.78	10.94
		CU	1.26	1.63	1.90	1.77	1.05	0.28
		ZN	10.30	10.68	11.11	11.09	10.00	4.48
	+10	FE	40.20	34.84	32.63	29.76	25.08	12.90
		CU	1.05	1.42	1.63	1.58	0.84	0.22
		ZN	10.35	10.29	11.30	11.89	11.82	9.24

(continued)

3AF	125	FE	43.28	43.32	36.92	39.22	33.60	26.15
		CU	0.91	1.91	1.90	1.95	1.71	1.57
		ZN	8.75	9.37	8.93	9.15	9.15	9.62
	+75	FE	42.91	43.82	41.53	40.77	34.76	25.35
		CU	1.25	1.71	1.85	1.66	1.53	1.16
		ZN	9.26	9.99	9.64	10.12	10.22	10.43
	+53	FE	43.66	43.18	40.90	38.76	35.16	17.15
		CU	1.44	1.78	1.54	1.42	0.99	1.06
		ZN	9.47	10.16	10.05	10.11	11.16	12.31
	-53	FE	41.73	35.95	31.67	27.79	21.82	9.97
		CU	0.69	0.42	1.90	1.00	0.92	0.26
		ZN	10.36	10.69	11.36	11.13	10.51	4.42
	+10	FE	41.15	37.95	34.96	24.35	23.63	11.21
		CU	0.20	0.24	1.09	0.96	0.26	0.33
		ZN	10.09	10.73	12.02	12.07	12.83	10.32
4AF	125	FE	38.63	37.25	30.86	36.11	28.58	21.99
		CU	0.59	2.12	2.63	2.23	2.28	1.68
		ZN	8.80	8.88	9.22	10.10	9.56	11.16
	+75	FE	45.66	41.93	38.84	36.67	25.77	14.48
		CU	1.02	1.46	2.09	1.49	0.91	1.24
		ZN	9.58	10.24	10.23	10.25	10.19	12.74
	+53	FE	41.81	41.65	39.05	34.19	24.48	8.37
		CU	0.15	1.82	1.35	0.93	0.58	0.82
		ZN	8.48	10.52	10.44	10.81	12.39	14.02
	-53	FE	34.04	28.54	25.73	23.34	17.32	9.93
		CU	1.58	1.50	1.57	1.21	0.77	0.26
		ZN	9.95	10.90	10.93	10.20	8.04	3.11
	+10	FE	40.01	33.18	27.90	23.10	17.22	8.84
		CU	0.84	1.27	0.07	0.19	0.40	0.15
		ZN	10.24	10.96	11.35	11.52	12.35	7.33
5AF	125	FE	45.45	41.28	35.32	26.79	26.57	18.89
		CU	0.90	2.16	2.52	2.02	1.59	0.66
		ZN	9.23	9.98	10.32	10.16	10.80	13.45
	+75	FE	46.17	41.03	31.70	27.61	25.65	20.06
		CU	1.38	1.80	1.04	0.71	1.00	1.12
		ZN	10.28	10.80	9.00	12.61	11.22	12.27
	+53	FE	42.05	40.68	39.38	24.88	18.88	11.91
		CU	1.33	1.34	0.94	0.79	0.95	0.56
		ZN	10.10	10.12	10.45	11.63	12.93	14.68
	-53	FE	35.89	28.29	26.33	19.31	13.06	7.58
		CU	1.61	1.59	1.36	1.02	0.61	0.28
		ZN	9.89	10.73	10.92	9.71	7.24	3.09
	+10	FE	42.55	32.11	27.76	17.50	11.24	9.76
		CU	0.86	1.29	1.25	0.74	0.58	0.10
		ZN	10.63	11.06	12.11	12.71	12.76	7.53
1SP	125	FE	49.27	47.42	50.82	47.66	38.90	30.44
		CU	0.17	0.39	0.35	0.23	2.08	1.17

(continued)

		ZN	8.38	9.08	9.99	9.32	10.18	9.14
	+75	FE	44.16	45.29	46.76	42.24	39.27	27.56
		CU	0.66	0.32	0.21	1.90	1.55	0.55
		ZN	9.32	9.35	9.11	9.94	10.80	10.68
	+53	FE	44.19	41.62	42.39	42.93	36.01	18.66
		CU	0.81	0.18	0.15	0.26	1.42	1.14
		ZN	26.69	9.04	8.83	9.26	11.31	12.86
	-53	FE	41.98	32.85	34.38	26.83	21.80	12.45
		CU	1.29	1.67	1.69	1.62	1.30	0.60
		ZN	10.80	10.39	11.07	10.73	9.58	5.52
	+10	FE	41.64	40.22	38.13	34.18	28.05	13.74
		CU	1.61	1.83	1.99	1.82	1.08	0.51
		ZN	10.41	11.11	11.40	11.60	12.03	11.28
3SP	125	FE	45.50	43.35	42.25	36.35	31.25	31.99
		CU	0.66	1.38	1.72	3.52	2.80	1.66
		ZN	9.17	9.40	9.89	10.27	10.03	10.04
	+75	FE	42.73	45.21	42.83	36.88	33.50	14.80
		CU	0.34	0.79	2.56	2.76	0.84	0.67
		ZN	8.99	9.60	10.58	10.81	10.35	5.16
	+53	FE	46.55	40.11	41.77	36.33	28.54	14.83
		CU	0.41	0.64	2.48	1.27	0.36	0.86
		ZN	9.88	10.16	11.32	11.32	11.76	14.40
	-53	FE	37.81	33.90	29.73	26.69	20.78	12.47
		CU	1.58	1.87	1.71	1.39	1.03	0.44
		ZN	11.15	11.85	11.72	11.26	10.20	6.13
	+10	FE	37.68	37.33	33.64	28.94	22.23	13.59
		CU	1.64	1.81	1.63	1.25	0.89	0.42
		ZN	11.54	20.97	12.56	12.57	20.97	9.58
4SP	125	FE	47.61	45.15	44.92	40.31	31.78	19.63
		CU	0.23	0.24	0.42	1.36	3.20	2.03
		ZN	9.98	9.64	10.02	10.53	11.39	11.24
	+75	FE	50.02	45.59	44.10	40.14	31.91	21.69
		CU	0.80	2.53	1.21	1.89	1.69	1.74
		ZN	10.75	11.08	11.22	11.68	12.51	13.41
	+53	FE	43.99	44.06	42.24	35.95	24.13	14.62
		CU	1.25	0.19	0.49	2.09	1.20	0.83
		ZN	10.46	10.08	10.91	12.25	13.27	23.68
	-53	FE	35.64	31.65	31.28	28.33	21.84	11.48
		CU	1.71	1.75	1.79	1.56	1.02	0.40
		ZN	11.38	11.39	11.81	11.83	10.43	5.63
	+10	FE	33.68	35.26	31.73	28.74	22.05	13.95
		CU	1.60	1.84	1.49	1.53	0.77	0.33
		ZN	11.08	11.89	12.18	12.74	11.77	9.58
5SP	125	FE	43.34	42.32	44.58	37.39	31.20	24.42
		CU	0.40	1.29	2.78	4.33	4.09	1.11
		ZN	9.38	9.68	10.46	10.85	10.57	11.40

(continued)

	+75	FE	49.72	47.39	45.50	35.13	34.76	22.98
		CU	0.84	0.92	2.64	2.95	2.21	0.38
		ZN	10.00	10.37	11.22	11.54	21.51	10.80
	+53	FE	49.11	46.37	45.05	40.31	33.25	15.50
		CU	1.22	1.90	2.65	0.61	1.00	0.32
		ZN	10.33	10.77	11.61	10.97	12.52	13.49
	-53	FE	35.73	34.11	33.21	28.82	22.03	12.03
		CU	1.71	1.86	1.92	1.58	1.05	0.40
		ZN	10.70	11.20	11.49	11.76	10.07	6.05
	+10	FE	38.59	37.78	33.68	27.79	25.03	13.54
		CU	1.58	1.91	1.86	1.43	0.77	0.49
		ZN	11.10	11.59	12.13	12.54	12.82	12.07
SPAF	125	FE	49.55	40.95	32.35	33.26	23.90	15.09
		CU	0.73	2.64	2.88	1.63	2.31	0.91
		ZN	9.95	10.29	10.49	9.65	10.29	14.58
	+75	FE	46.01	41.79	34.54	27.24	18.92	18.10
		CU	1.27	2.26	1.60	1.24	1.36	1.33
		ZN	10.04	11.23	11.56	11.36	12.86	21.49
	+53	FE	45.58	40.86	36.07	27.29	14.07	9.76
		CU	1.48	1.66	0.83	0.89	0.79	0.77
		ZN	10.26	11.13	11.44	12.15	14.61	14.68
	-53	FE	30.27	27.79	19.25	16.37	10.58	6.26
		CU	1.37	1.49	0.95	0.70	0.43	0.14
		ZN	10.03	10.99	9.22	8.03	4.88	1.56
	+10	FE	40.85	31.69	26.27	16.57	6.81	2.47
		CU	1.64	1.25	0.81	0.62	0.18	0.08
		ZN	11.10	11.89	12.41	11.53	9.21	3.30

Appendix 12 CDM parameters for chalcopyrite & coal

1). Chalcopyrite

TEST NO	GR0	GR1	GR2	K1	K2	A1	A2
1	0.151	1.796	17.003	0.249	1.200	0.049	0.025
2	0.182	1.049	13.296	0.208	1.102	0.088	0.030
3	0.180	0.504	13.238	0.308	1.097	0.115	0.032
4	0.201	0.286	13.446	0.246	1.192	0.126	0.033
5	0.170	0.313	9.673	0.251	1.504	0.120	0.048

2). Coal

Test No	Size	GR0	GR1	GR2	K1	K2	A1	A2
1	+125	14.15	83.89	94.49	0.500	3.500	0.242	0.665
	+75	10.84	77.95	94.85	0.300	2.750	0.132	0.774
	+53	23.20	90.85	96.85	0.900	2.500	0.449	0.433
	-53	12.87	84.75	95.07	0.600	2.750	0.338	0.572
2	+125	9.96	56.34	96.89	1.400	2.750	0.164	0.769
	+75	12.81	57.54	96.57	1.400	3.000	0.113	0.827
	+53	17.55	42.92	95.05	0.900	3.000	0.042	0.898
	-53	10.33	52.15	92.19	0.500	3.000	0.095	0.831
3	+125	15.36	59.64	94.25	1.400	5.500	0.116	0.803
	+75	8.76	40.15	95.53	1.400	4.000	0.087	0.864
	+53	13.10	24.07	94.45	1.200	4.250	0.048	0.888
	-53	10.33	40.19	98.43	1.400	3.250	0.176	0.755
4	+125	15.54	15.82	92.54	0.200	5.750	0.034	0.909
	+75	12.99	21.13	94.82	1.400	5.000	0.054	0.899
	+53	12.66	32.55	95.62	1.400	5.250	0.071	0.869
	-53	12.93	24.65	92.52	0.600	4.500	0.084	0.855
5	+125	10.91	35.41	94.49	1.400	5.750	0.082	0.856
	+75	7.47	36.35	94.67	1.400	5.750	0.075	0.880
	+53	4.78	37.32	94.62	1.400	5.750	0.071	0.890
	-53	11.56	33.55	93.73	0.700	5.250	0.118	0.834

Appendix 13 CDM parameters for Complex sulphide

No	Size	Elem	K1	K2	A1	A2	SSE
				Parameters			
1	+125	FE	0.928	1.885	0.250	0.385	3.258
		CU	0.460	6.590	0.212	0.001	0.001
		ZN	0.962	1.891	0.259	0.188	1.073
		MASS	0.891	1.820	0.085	0.116	0.126
	+75	FE	0.493	1.761	0.066	0.623	2.531
		CU	0.894	6.608	0.441	0.003	5.867
		ZN	0.503	1.794	0.109	0.379	0.329
		MASS	0.472	1.873	0.054	0.210	0.245
	+53	FE	0.372	1.873	0.124	0.651	2.568
		CU	0.258	6.596	0.173	0.110	2.687
		ZN	0.435	2.986	0.213	0.594	2.278
		MASS	0.269	1.866	0.063	0.231	0.396
	+10	FE	0.701	2.187	0.274	0.493	0.754
		CU	0.908	1.838	0.381	0.402	4.527
		ZN	0.493	1.761	0.241	0.365	0.503
		MASS	0.501	1.787	0.117	0.190	0.143
	-10	FE	0.351	1.787	0.550	0.012	5.966
		CU	0.258	1.796	0.667	0.051	18.517
		ZN	0.258	1.838	0.626	0.091	6.349
		MASS	0.251	2.187	0.361	0.006	3.636
2	+125	FE	0.558	6.238	0.128	0.420	0.190
		CU	0.308	6.596	0.396	0.098	11.839
		ZN	0.551	6.187	0.118	0.259	0.283
		MASS	0.601	6.587	0.049	0.121	0.037
	+75	FE	0.551	6.187	0.122	0.532	0.380
		CU	0.501	6.587	0.463	0.270	8.266
		ZN	0.451	6.187	0.132	0.329	0.493
		MASS	0.501	6.587	0.062	0.188	0.075
	+53	FE	0.429	5.026	0.190	0.668	0.231
		CU	0.501	2.987	0.320	0.466	0.954
		ZN	0.217	4.190	0.206	0.386	0.633
		MASS	0.258	4.638	0.095	0.227	0.222
	+10	FE	0.575	3.354	0.271	0.581	0.503
		CU	0.691	2.207	0.188	0.528	0.441
		ZN	0.551	2.981	0.323	0.364	0.695
		MASS	0.501	2.987	0.150	0.211	0.200
	-10	FE	0.343	1.764	0.470	0.203	2.366
		CU	0.550	1.807	0.525	0.264	3.917
		ZN	0.345	2.210	0.566	0.193	0.985
		MASS	0.201	1.787	0.323	0.082	2.132
3	+125	FE	0.619	3.066	0.089	0.456	0.139
		CU	0.908	1.838	0.418	0.072	2.929
		ZN	0.908	4.238	0.168	0.254	0.109
		MASS	1.001	4.187	0.068	0.114	0.016

(continued)

	+75	FE	0.908	4.638	0.172	0.494	0.391
		CU	0.908	1.838	0.262	0.173	26.585
		ZN	0.879	3.357	0.152	0.330	0.141
		MASS	0.536	2.955	0.047	0.219	0.106
	+53	FE	0.524	2.546	0.126	0.739	0.258
		CU	0.919	1.866	0.117	0.252	20.336
		ZN	0.267	2.139	0.129	0.491	0.320
		MASS	0.346	2.579	0.071	0.255	0.022
	+10	FE	0.283	2.156	0.029	0.791	1.101
		CU	0.117	2.127	0.002	0.898	2.354
		ZN	0.508	2.238	0.239	0.556	0.790
		MASS	0.117	1.727	0.020	0.334	0.419
	-10	FE	0.401	1.787	0.514	0.265	3.634
		CU	0.545	1.795	0.567	0.255	6.061
		ZN	0.332	1.843	0.567	0.286	5.019
		MASS	0.158	1.838	0.330	0.135	2.233
4	+125	FE	0.822	3.073	0.112	0.496	0.128
		CU	0.408	6.638	0.215	0.021	2.397
		ZN	0.679	2.957	0.115	0.356	0.067
		MASS	0.672	3.073	0.046	0.146	0.021
	+75	FE	0.543	2.961	0.076	0.590	0.504
		CU	0.354	3.005	0.111	0.475	13.039
		ZN	0.550	3.403	0.115	0.410	0.189
		MASS	0.551	3.387	0.046	0.199	0.042
	+53	FE	0.388	2.949	0.071	0.782	0.909
		CU	0.651	6.587	0.227	0.288	6.316
		ZN	0.188	2.553	0.171	0.516	1.085
		MASS	0.393	3.361	0.070	0.258	0.151
	+10	FE	0.500	1.900	0.079	0.564	3.884
		CU	0.861	2.233	0.081	0.728	0.587
		ZN	0.267	1.727	0.045	0.606	1.394
		MASS	0.483	2.291	0.073	0.246	0.295
	-10	FE	0.338	1.753	0.369	0.518	4.513
		CU	0.458	1.838	0.458	0.443	19.961
		ZN	0.400	1.810	0.604	0.340	7.698
		MASS	0.248	1.797	0.282	0.132	1.837
5	+125	FE	0.655	3.414	0.069	0.438	0.020
		CU	0.908	1.838	0.428	0.032	0.664
		ZN	0.751	3.387	0.103	0.310	0.073
		MASS	0.658	3.838	0.040	0.135	0.011
	+75	FE	0.768	5.058	0.124	0.608	0.253
		CU	0.953	1.870	0.286	0.300	3.117
		ZN	0.508	5.438	0.175	0.382	0.690
		MASS	0.601	4.187	0.047	0.212	0.055
	+53	FE	0.543	3.761	0.127	0.806	0.627
		CU	0.196	2.909	0.023	0.674	7.580
		ZN	0.258	3.438	0.131	0.506	0.635
		MASS	0.308	3.438	0.061	0.264	0.158
	+10	FE	0.701	3.387	0.186	0.551	0.399
		CU	0.442	2.560	0.064	0.740	0.901

(continued)

		ZN	0.501	2.587	0.194	0.444	0.544
		MASS	0.488	2.553	0.085	0.225	0.077
	-10	FE	0.278	1.881	0.389	0.495	6.362
		CU	0.451	1.787	0.387	0.591	9.055
		ZN	0.258	1.838	0.510	0.465	6.757
		MASS	0.108	1.838	0.315	0.200	2.276
6	+125	FE	0.058	3.038	0.302	0.391	1.284
		CU	0.151	6.587	0.200	0.007	35.507
		ZN	0.151	3.387	0.134	0.209	0.588
		MASS	0.148	2.974	0.061	0.107	0.095
	+75	FE	0.068	2.605	0.314	0.463	0.791
		CU	0.960	6.590	0.470	0.002	0.000
		ZN	0.151	3.387	0.189	0.221	1.911
		MASS	0.151	2.987	0.096	0.139	0.587
	+53	FE	0.201	2.587	0.249	0.501	3.477
		CU	0.151	6.587	0.674	0.047	4.375
		ZN	0.151	2.587	0.252	0.234	2.115
		MASS	0.058	2.638	0.213	0.162	0.681
	+10	FE	0.258	2.638	0.440	0.388	5.066
		CU	0.258	2.238	0.652	0.120	18.273
		ZN	0.301	2.590	0.431	0.185	3.292
		MASS	0.208	2.638	0.214	0.126	0.939
	-10	FE	0.058	1.838	0.771	0.152	11.307
		CU	0.251	2.187	0.835	0.075	74.301
		ZN	0.151	1.887	0.703	0.083	9.759
		MASS	0.151	2.187	0.321	0.042	5.812
7	+125	FE	0.558	6.238	0.128	0.420	0.190
		CU	0.308	6.596	0.396	0.098	11.839
		ZN	0.551	6.187	0.118	0.259	0.283
		MASS	0.601	6.587	0.049	0.121	0.037
	+75	FE	0.551	6.187	0.122	0.532	0.380
		CU	0.501	6.587	0.463	0.270	8.266
		ZN	0.451	6.187	0.132	0.329	0.493
		MASS	0.501	6.587	0.062	0.188	0.075
	+53	FE	0.429	5.026	0.190	0.668	0.231
		CU	0.501	2.987	0.320	0.466	0.954
		ZN	0.217	4.190	0.206	0.386	0.633
		MASS	0.258	4.638	0.095	0.227	0.222
	+10	FE	0.575	3.354	0.271	0.581	0.503
		CU	0.691	2.207	0.188	0.528	0.441
		ZN	0.551	2.981	0.323	0.364	0.695
		MASS	0.501	2.987	0.150	0.211	0.200
	-10	FE	0.343	1.764	0.470	0.203	2.366
		CU	0.550	1.807	0.525	0.264	3.917
		ZN	0.345	2.210	0.566	0.193	0.985
		MASS	0.201	1.787	0.323	0.082	2.132
8	+125	FE	0.501	5.387	0.071	0.507	0.105
		CU	0.358	5.038	0.111	0.385	0.319
		ZN	0.348	5.392	0.068	0.367	0.027
		MASS	0.401	4.587	0.029	0.170	0.027

(continued)

	+75	FE	0.308	5.038	0.069	0.635	0.170
		CU	0.258	4.238	0.088	0.623	0.474
		ZN	0.208	4.638	0.067	0.449	0.205
		MASS	0.351	4.987	0.032	0.246	0.046
	+53	FE	0.393	4.961	0.109	0.769	0.517
		CU	0.251	4.587	0.084	0.656	0.604
		ZN	0.108	4.238	0.145	0.488	0.716
		MASS	0.238	4.588	0.056	0.279	0.063
	+10	FE	0.419	3.466	0.111	0.696	2.295
		CU	0.908	1.838	0.089	0.112	8.864
		ZN	0.316	3.030	0.149	0.455	1.657
		MASS	0.298	2.995	0.065	0.250	0.190
	-10	FE	0.208	1.838	0.338	0.430	5.738
		CU	0.422	1.873	0.334	0.355	41.353
		ZN	0.401	2.590	0.465	0.293	3.335
		MASS	0.151	1.787	0.257	0.146	1.392
9	+125	FE	0.901	4.187	0.090	0.471	0.076
		CU	0.542	2.560	0.089	0.410	1.224
		ZN	0.743	3.761	0.092	0.385	0.177
		MASS	0.630	3.883	0.037	0.182	0.026
	+75	FE	0.769	4.266	0.079	0.669	0.116
		CU	0.117	2.527	0.021	0.607	0.578
		ZN	0.442	3.760	0.059	0.484	0.182
		MASS	0.473	3.739	0.030	0.257	0.022
	+53	FE	0.822	4.273	0.165	0.707	0.311
		CU	0.237	3.774	0.047	0.438	0.513
		ZN	0.258	3.438	0.143	0.454	0.545
		MASS	0.308	3.838	0.067	0.285	0.142
	+10	FE	0.687	3.396	0.065	0.769	0.511
		CU	0.919	3.066	0.042	0.691	0.431
		ZN	0.407	2.618	0.082	0.572	0.570
		MASS	0.272	2.673	0.042	0.309	0.250
	-10	FE	0.258	1.838	0.260	0.357	2.661
		CU	0.322	1.861	0.189	0.643	7.347
		ZN	0.438	1.753	0.272	0.455	2.714
		MASS	0.108	1.838	0.254	0.199	1.304
10	+125	FE	0.919	4.666	0.048	0.487	0.177
		CU	0.919	2.666	0.028	0.424	0.144
		ZN	0.942	3.760	0.047	0.364	0.179
		MASS	0.908	4.238	0.025	0.154	0.027
	+75	FE	0.908	6.638	0.041	0.708	0.088
		CU	0.840	5.759	0.031	0.750	0.071
		ZN	0.908	4.638	0.069	0.533	0.239
		MASS	0.919	4.666	0.032	0.269	0.060
	+53	FE	0.922	4.273	0.079	0.896	1.109
		CU	0.438	4.149	0.026	0.734	0.115
		ZN	0.492	3.891	0.077	0.631	0.499
		MASS	0.587	3.796	0.031	0.351	0.083
	+10	FE	0.519	3.866	0.056	0.912	0.570

(continued)

		CU	0.811	4.633	0.091	0.678	0.719
		ZN	0.501	3.390	0.156	0.612	0.371
		MASS	0.351	3.387	0.064	0.334	0.183
	-10	FE	0.172	1.873	0.220	0.497	8.675
		CU	0.167	1.727	0.116	0.761	7.052
		ZN	0.322	1.873	0.256	0.544	9.915
		MASS	0.201	1.787	0.245	0.228	2.508
11	+125	FE	0.987	4.574	0.022	0.598	0.183
		CU	0.908	3.438	0.031	0.423	1.467
		ZN	0.793	3.761	0.020	0.448	0.212
		MASS	0.993	4.161	0.013	0.178	0.041
	+75	FE	0.983	4.562	0.023	0.723	0.289
		CU	0.387	4.174	0.010	0.728	0.333
		ZN	0.922	4.273	0.060	0.506	0.439
		MASS	0.987	4.174	0.017	0.265	0.103
	+53	FE	0.687	4.174	0.030	0.964	0.939
		CU	0.935	6.186	0.059	0.733	0.093
		ZN	0.542	3.760	0.074	0.621	0.541
		MASS	0.791	4.207	0.043	0.321	0.097
	+10	FE	0.095	3.380	0.002	0.963	0.000
		CU	0.911	4.233	0.047	0.879	0.253
		ZN	0.672	3.073	0.065	0.715	0.632
		MASS	0.188	2.949	0.026	0.375	0.265
	-10	FE	0.258	1.838	0.158	0.427	22.252
		CU	0.096	1.709	0.005	0.679	29.738
		ZN	0.463	2.213	0.179	0.616	5.082
		MASS	0.201	1.787	0.196	0.315	1.676

Appendix 14 MCM parameters of chalcopyrite & coal

1). Chalcopyrite

TEST No	UFele	UFmass	Kmele	Kmass	Gele	Gmass
1	0.210	0.910	1.557	0.587	0.947	0.937
2	0.250	0.850	1.234	0.367	0.628	0.602
3	0.250	0.820	1.198	0.376	0.518	0.507
4	0.260	0.810	1.419	0.396	0.413	0.402
5	0.220	0.800	1.876	0.527	0.669	0.633

2). Coal

TEST		Parameters					
No	Size	UFele	UFmass	Kmele	Kmass	Gele	Gmass
1	+125	0.010	0.080	4.006	3.464	4.128	3.819
	+ 75	0.020	0.110	1.641	1.491	3.293	3.121
	+ 53	0.020	0.110	0.670	0.670	1.808	1.777
	- 53	0.010	0.050	0.307	0.404	1.495	2.434
2	+125	0.010	0.070	3.338	2.324	5.843	2.718
	+ 75	0.010	0.060	0.475	0.463	3.300	3.190
	+ 53	0.010	0.060	0.862	0.890	3.757	3.677
	- 53	0.010	0.080	0.357	0.952	2.790	3.733
3	+125	0.010	0.080	2.316	2.414	7.070	6.735
	+ 75	0.000	0.050	0.320	0.306	3.985	3.785
	+ 53	0.010	0.060	0.486	0.489	4.476	4.308
	- 53	0.010	0.070	0.407	0.507	3.387	3.185
4	+125	0.010	0.070	2.268	2.197	8.849	8.516
	+ 75	0.000	0.050	0.676	0.679	5.509	5.239
	+ 53	0.010	0.060	1.095	1.266	6.535	6.258
	- 53	0.010	0.070	1.138	1.746	5.370	5.174
5	+125	0.010	0.070	2.236	2.924	9.444	9.150
	+ 75	0.010	0.050	2.567	3.081	9.803	9.540
	+ 53	0.010	0.040	2.236	2.801	9.672	9.416
	- 53	0.010	0.050	3.824	5.952	8.646	8.515

Appendix 15 MCM parapeters for Complex sulphide

No	Size	Elem	UFFR	Kmean	G	SSE
1	+125	FE	0.370	1.520	0.161	3.020
		CU	0.780	0.470	0.056	5.410
		ZN	0.550	1.390	0.216	1.030
		MASS	0.800	1.400	0.176	0.110
	+75	FE	0.310	1.760	0.294	2.600
		CU	0.560	0.960	0.078	6.790
		ZN	0.510	1.690	0.530	0.430
		MASS	0.740	1.780	0.485	0.210
	+53	FE	0.230	1.920	0.618	2.650
		CU	0.720	0.370	0.061	2.050
		ZN	0.180	3.010	2.632	0.930
		MASS	0.710	2.010	1.173	0.460
	+10	FE	0.230	1.730	0.620	0.040
		CU	0.220	1.400	0.109	2.350
		ZN	0.390	1.300	0.570	0.170
		MASS	0.690	1.450	0.779	0.050
	-10	FE	0.350	0.350	0.220	1.510
		CU	0.290	0.380	0.120	3.270
		ZN	0.280	0.370	0.107	1.220
		MASS	0.000	0.110	0.483	0.120
2	+125	FE	0.430	3.740	2.299	0.740
		CU	0.500	1.420	0.120	2.990
		ZN	0.580	2.030	0.677	1.110
		MASS	0.810	3.490	0.987	0.150
	+75	FE	0.300	3.680	0.371	0.830
		CU	0.250	1.750	0.273	9.770
		ZN	0.410	2.170	0.564	1.060
		MASS	0.710	1.710	0.457	0.200
	+53	FE	0.090	2.790	1.667	1.190
		CU	0.160	2.570	3.173	0.820
		ZN	0.000	1.250	0.987	1.000
		MASS	0.560	1.540	1.520	0.190
	+10	FE	0.130	3.060	2.524	1.100
		CU	0.280	1.920	0.560	0.300
		ZN	0.290	1.820	1.508	0.960
		MASS	0.620	2.460	2.961	0.190
	-10	FE	0.220	0.660	0.760	1.340
		CU	0.190	0.920	0.350	2.690
		ZN	0.170	0.650	0.588	1.670
		MASS	0.000	0.190	1.050	1.490
3	+125	FE	0.460	4.110	2.130	0.010
		CU	0.510	1.090	0.099	2.980
		ZN	0.580	2.850	1.458	0.050
		MASS	0.820	3.350	1.965	0.010

(continued)

	+75	FE	0.330	4.890	2.929	0.190
		CU	0.570	1.480	0.080	14.760
		ZN	0.510	3.190	1.745	0.080
		MASS	0.730	4.480	3.528	0.020
	+53	FE	0.130	3.540	1.990	0.010
		CU	0.630	1.720	0.098	16.590
		ZN	0.360	3.540	4.312	0.270
		MASS	0.670	3.990	4.313	0.020
	+10	FE	0.180	2.280	0.333	0.470
		CU	0.100	2.400	0.289	0.490
		ZN	0.200	1.990	0.947	0.080
		MASS	0.650	2.040	0.592	0.390
	-10	FE	0.150	0.790	0.700	0.720
		CU	0.140	0.980	0.574	2.250
		ZN	0.030	0.720	0.818	3.060
		MASS	0.270	0.370	1.251	0.230
4	+125	FE	0.390	3.250	1.063	0.060
		CU	0.770	0.500	0.064	2.500
		ZN	0.530	3.140	1.766	0.040
		MASS	0.810	3.160	1.840	0.000
	+75	FE	0.330	3.890	1.804	0.510
		CU	0.380	0.820	0.146	0.640
		ZN	0.460	5.630	5.921	0.220
		MASS	0.750	5.530	5.019	0.050
	+53	FE	0.150	4.880	2.820	1.320
		CU	0.480	1.090	0.430	4.240
		ZN	0.150	5.260	3.952	1.760
		MASS	0.660	6.410	8.898	0.200
	+10	FE	0.360	1.720	0.167	3.680
		CU	0.190	2.330	0.285	0.180
		ZN	0.350	2.000	0.618	1.200
		MASS	0.680	2.220	0.920	0.310
	-10	FE	0.020	1.520	2.086	2.140
		CU	0.090	1.220	0.648	15.000
		ZN	0.000	0.860	0.649	5.790
		MASS	0.000	0.420	2.863	0.830
5	+125	FE	0.490	5.070	2.832	0.090
		CU	0.540	1.020	0.096	0.870
		ZN	0.580	4.120	2.888	0.080
		MASS	0.820	4.970	3.837	0.020
	+75	FE	0.260	9.930	8.974	0.260
		CU	0.410	1.490	0.260	3.450
		ZN	0.420	6.040	8.990	2.230
		MASS	0.740	8.060	8.634	0.020
	+53	FE	0.060	6.500	5.201	0.280
		CU	0.310	3.570	0.710	8.640
		ZN	0.350	5.150	7.520	0.450
		MASS	0.670	6.150	9.318	0.050
	+10	FE	0.250	3.780	2.611	0.500
		CU	0.200	2.750	0.680	0.930

(continued)

		ZN	0.350	2.490	1.946	0.250
		MASS	0.680	2.930	2.535	0.050
	-10	FE	0.080	1.290	1.315	6.560
		CU	0.020	1.330	0.740	8.320
		ZN	0.015	0.980	0.871	4.760
		MASS	0.010	0.520	3.542	0.820
6	+125	FE	0.020	3.230	6.356	2.860
		CU	0.015	0.020	0.023	14.650
		ZN	0.010	2.380	5.238	2.400
		MASS	0.040	2.200	4.056	0.350
	+75	FE	0.050	4.150	7.588	4.060
		CU	0.030	0.160	0.129	56.056
		ZN	0.010	3.560	5.846	6.500
		MASS	0.010	3.770	6.034	1.370
	+53	FE	0.080	5.560	9.078	5.680
		CU	0.030	0.400	0.262	5.770
		ZN	0.050	1.200	9.978	7.210
		MASS	0.250	1.600	30.761	1.020
	+10	FE	0.020	1.460	3.401	3.240
		CU	0.200	0.390	0.183	14.540
		ZN	0.100	0.620	2.173	2.220
		MASS	0.360	0.740	4.275	0.310
	-10	FE	0.070	0.210	0.598	19.220
		CU	0.040	0.230	0.062	67.140
		ZN	0.010	0.120	0.060	26.770
		MASS	0.020	0.070	0.247	5.430
7	+125	FE	0.430	3.740	2.299	0.740
		CU	0.500	1.420	0.120	2.990
		ZN	0.580	2.030	0.677	1.110
		MASS	0.810	3.490	0.987	0.150
	+75	FE	0.300	3.680	0.371	0.830
		CU	0.250	1.750	0.273	9.770
		ZN	0.410	2.170	0.564	1.060
		MASS	0.710	1.710	0.457	0.200
	+53	FE	0.090	2.790	1.667	1.190
		CU	0.160	2.570	3.173	0.820
		ZN	0.000	1.250	0.987	1.000
		MASS	0.560	1.540	1.520	0.190
	+10	FE	0.130	3.060	2.524	1.100
		CU	0.280	1.920	1.560	0.300
		ZN	0.290	1.820	1.508	0.960
		MASS	0.620	2.460	2.961	0.190
	-10	FE	0.220	0.660	0.760	1.340
		CU	0.190	0.920	0.350	2.690
		ZN	0.170	0.650	0.588	1.670
		MASS	0.000	0.190	1.050	1.490
8	+125	FE	0.400	4.300	3.789	0.180
		CU	0.460	3.580	2.051	0.390
		ZN	0.540	1.350	1.659	0.220
		MASS	0.790	1.990	1.456	0.040

(continued)

	+75	FE	0.290	4.080	7.032	0.160
		CU	0.270	3.620	4.032	0.510
		ZN	0.470	6.970	8.466	0.320
		MASS	0.710	3.310	7.867	0.100
	+53	FE	0.090	3.660	6.268	0.690
		CU	0.230	5.420	6.234	1.080
		ZN	0.260	7.000	6.780	1.350
		MASS	0.610	4.400	6.956	0.260
	+10	FE	0.200	5.290	2.524	3.070
		CU	0.800	4.620	7.086	6.810
		ZN	0.390	4.710	3.860	2.060
		MASS	0.680	4.060	4.169	0.430
	-10	FE	0.200	1.190	1.432	3.110
		CU	0.310	1.100	0.456	40.560
		ZN	0.120	1.110	1.675	1.950
		MASS	0.000	0.320	2.484	3.420
9	+125	FE	0.440	6.830	4.529	0.010
		CU	0.500	2.710	1.244	1.370
		ZN	0.520	4.930	7.292	0.050
		MASS	0.780	4.490	3.682	0.020
	+75	FE	0.250	9.160	5.901	0.000
		CU	0.380	7.550	1.737	0.680
		ZN	0.450	7.490	9.086	0.020
		MASS	0.710	7.600	8.875	0.000
	+53	FE	0.120	6.700	4.751	0.170
		CU	0.510	5.080	1.945	0.520
		ZN	0.350	7.310	9.696	0.160
		MASS	0.640	8.720	7.442	0.040
	+10	FE	0.170	4.320	1.410	0.800
		CU	0.270	3.370	1.392	0.340
		ZN	0.350	4.370	4.640	1.140
		MASS	0.650	6.970	6.318	0.390
	-10	FE	0.350	1.410	1.616	1.500
		CU	0.170	1.810	0.850	8.130
		ZN	0.250	1.530	1.152	1.860
		MASS	0.100	0.690	6.314	0.540
10	+125	FE	0.470	6.900	2.808	0.000
		CU	0.550	3.900	1.323	0.090
		ZN	0.590	4.860	8.070	0.000
		MASS	0.820	4.980	4.068	0.000
	+75	FE	0.250	7.750	4.127	0.010
		CU	0.220	4.930	2.274	0.040
		ZN	0.400	8.400	10.636	0.080
		MASS	0.700	8.500	8.620	0.010
	+53	FE	0.030	9.820	5.446	0.400
		CU	0.240	6.160	6.587	0.090
		ZN	0.290	7.610	9.469	0.300
		MASS	0.620	8.670	8.632	0.070
	+10	FE	0.040	3.370	3.627	0.530

(contin5ed)

		CU	0.230	6.970	3.600	0.730
		ZN	0.220	6.040	3.682	0.480
		MASS	0.590	3.210	5.150	0.180
	-10	FE	0.300	1.670	1.355	11.080
		CU	0.130	2.200	1.336	10.330
		ZN	0.250	1.580	1.890	9.880
		MASS	0.000	0.790	5.486	2.520
11	+125	FE	0.380	5.290	1.003	0.000
		CU	0.550	3.440	0.242	1.160
		ZN	0.530	4.040	0.670	0.090
		MASS	0.810	3.820	0.542	0.010
	+75	FE	0.250	4.290	0.379	0.030
		CU	0.260	5.820	1.360	0.090
		ZN	0.440	3.850	0.658	0.110
		MASS	0.720	3.720	0.485	0.010
	+53	FE	0.010	4.230	0.589	0.130
		CU	0.200	6.110	2.091	0.000
		ZN	0.300	7.270	5.342	0.210
		MASS	0.640	6.560	3.681	0.050
	+10	FE	0.040	4.010	0.295	0.270
		CU	0.080	6.070	1.550	0.100
		ZN	0.220	3.370	0.657	0.630
		MASS	0.600	5.380	3.208	0.420
	-10	FE	0.400	2.730	3.324	0.420
		CU	0.310	3.520	2.254	1.110
		ZN	0.200	2.580	1.530	0.810
		MASS	0.310	1.800	6.139	1.810

Appendix 16 GFM parameters for chalcopyrite & coal

1). Chalcopyrite

TEST No	UFR	UFM	Kmax	m	n
1	0.215	0.920	2.039	1.092	0.135
2	0.254	0.870	2.082	1.757	0.158
3	0.237	0.840	2.324	2.065	0.407
4	0.262	0.830	2.170	2.534	0.196
5	0.225	0.820	2.060	3.358	0.439

2). Coal

TEST		Parameters				
No	Size	UFR	UFM	Kmax	m	n
1	+125	0.040	0.110	7.325	2.686	2.564
	+ 75	0.030	0.120	6.869	2.963	2.841
	+ 53	0.030	0.110	6.265	3.143	2.961
	- 53	0.020	0.090	5.864	2.072	1.983
2	+125	0.010	0.070	23.392	3.459	3.140
	+ 75	0.010	0.060	24.586	3.715	3.516
	+ 53	0.010	0.060	25.691	3.665	3.553
	- 53	0.010	0.080	9.936	3.603	3.431
3	+125	0.020	0.090	70.061	4.493	4.078
	+ 75	0.000	0.050	46.151	3.952	3.612
	+ 53	0.000	0.060	49.389	4.309	4.031
	- 53	0.010	0.070	10.247	4.888	2.434
4	+125	0.010	0.080	93.834	6.272	5.804
	+ 75	0.000	0.050	55.395	5.355	4.951
	+ 53	0.010	0.070	63.246	5.730	5.240
	- 53	0.010	0.070	7.367	5.564	4.940
5	+125	0.010	0.070	89.712	6.503	5.843
	+ 75	0.010	0.050	90.261	6.705	6.063
	+ 53	0.010	0.050	91.805	6.732	6.161
	- 53	0.010	0.070	12.003	5.556	4.989

Appendix 17 GFM parameters for Complex sulphide

No	Size	Elem	UFFR	Km	m	SSE
1	+125	FE	0.370	1.972	5.685	2.350
		CU	0.790	0.556	0.547	4.730
		ZN	0.550	1.880	3.437	0.950
		MASS	0.800	2.018	3.001	0.130
	+75	FE	0.310	2.546	3.299	2.440
		CU	0.560	0.951	0.301	5.750
		ZN	0.510	4.978	2.637	0.520
		MASS	0.740	2.890	2.634	0.190
	+53	FE	0.230	2.888	2.766	2.150
		CU	0.720	1.248	0.200	2.700
		ZN	0.200	4.704	2.040	2.120
		MASS	0.710	4.462	1.989	0.490
	+10	FE	0.230	3.084	2.292	0.050
		CU	0.220	1.440	12.998	1.640
		ZN	0.390	2.936	1.654	0.080
		MASS	0.690	3.414	1.643	0.040
	-10	FE	0.360	2.752	0.000	2.360
		CU	0.320	0.374	19.285	0.790
		ZN	0.240	3.102	0.000	4.900
		MASS	0.490	0.895	0.000	0.220
2	+125	FE	0.460	6.955	2.682	3.640
		CU	0.500	3.896	1.300	16.020
		ZN	0.620	5.198	1.939	2.510
		MASS	0.830	5.806	2.221	0.500
	+75	FE	0.350	7.800	3.025	7.940
		CU	0.250	5.606	1.506	18.480
		ZN	0.540	4.892	1.927	5.520
		MASS	0.750	5.708	2.279	1.400
	+53	FE	0.160	6.648	2.583	11.010
		CU	0.210	4.947	1.662	4.430
		ZN	0.430	3.770	1.454	10.820
		MASS	0.690	4.558	1.821	2.870
	+10	FE	0.150	6.374	2.166	3.250
		CU	0.280	3.108	2.704	0.250
		ZN	0.310	5.075	1.552	1.590
		MASS	0.640	4.969	1.655	0.970
	-10	FE	0.290	3.220	0.526	1.380
		CU	0.200	2.484	1.482	3.060
		ZN	0.220	4.499	0.384	1.340
		MASS	0.530	1.511	0.000	2.270
3	+125	FE	0.460	8.142	3.093	0.220
		CU	0.510	3.198	1.230	3.940
		ZN	0.580	7.022	2.477	0.100
		MASS	0.820	7.206	2.587	0.030

(continued)

	+75	FE	0.340	9.249	3.261	0.900
		CU	0.570	4.448	3.623	13.190
		ZN	0.520	7.518	2.616	0.180
		MASS	0.740	7.210	2.709	0.210
	+53	FE	0.140	7.130	2.750	0.590
		CU	0.630	4.669	5.193	15.690
		ZN	0.390	5.056	1.983	2.700
		MASS	0.680	5.690	2.204	0.560
	+10	FE	0.180	3.248	3.862	0.380
		CU	0.100	3.180	4.532	0.380
		ZN	0.210	5.763	2.020	0.080
		MASS	0.650	3.374	2.750	0.330
	-10	FE	0.180	2.878	0.794	0.700
		CU	0.150	2.450	1.253	2.200
		ZN	0.110	2.522	0.724	3.390
		MASS	0.540	2.187	0.268	0.800
4.	+125	FE	0.390	6.989	3.222	0.060
		CU	0.760	6.970	1.200	4.310
		ZN	0.530	6.649	2.529	0.150
		MASS	0.810	7.008	2.699	0.030
	+75	FE	0.340	7.412	3.149	0.660
		CU	0.430	9.374	3.064	13.570
		ZN	0.480	6.876	2.630	1.750
		MASS	0.760	7.354	2.811	0.310
	+53	FE	0.150	8.756	3.382	2.510
		CU	0.480	5.776	2.030	3.800
		ZN	0.340	4.704	1.864	14.350
		MASS	0.680	6.408	2.476	1.440
	+10	FE	0.360	6.740	2.224	3.450
		CU	0.190	3.108	4.402	0.130
		ZN	0.350	3.450	2.614	1.030
		MASS	0.680	4.352	2.408	0.300
	-10	FE	0.110	4.162	1.241	8.530
		CU	0.090	2.717	1.546	14.280
		ZN	0.020	3.198	0.859	5.440
		MASS	0.570	2.480	0.440	4.050
5	+125	FE	0.500	8.870	3.394	0.340
		CU	0.540	3.052	1.748	0.510
		ZN	0.590	7.251	2.685	0.360
		MASS	0.830	7.808	2.844	0.090
	+75	FE	0.270	9.987	3.753	2.530
		CU	0.410	4.956	2.000	3.400
		ZN	0.450	6.057	2.146	4.490
		MASS	0.740	8.028	3.035	0.420
	+53	FE	0.070	9.145	3.358	3.890
		CU	0.310	5.232	4.395	8.360
		ZN	0.380	6.832	2.555	5.990
		MASS	0.680	7.420	2.776	1.230
	+10	FE	0.270	7.615	2.699	2.090
		CU	0.200	5.146	3.210	0.790

(continued)

		ZN	0.360	5.684	1.991	1.430
		MASS	0.690	5.951	2.109	0.430
	-10	FE	0.130	3.542	1.216	8.580
		CU	0.010	3.157	1.542	7.990
		ZN	0.040	3.294	0.955	6.100
		MASS	0.550	2.543	0.521	4.720
6	+125	FE	0.470	3.715	1.500	16.920
		CU	0.200	1.000	1.420	9.950
		ZN	0.680	2.900	1.113	8.610
		MASS	0.850	3.392	1.321	1.910
	+75	FE	0.380	4.033	1.559	23.410
		CU	0.200	3.970	1.500	50.980
		ZN	0.610	2.499	0.823	16.140
		MASS	0.780	3.112	1.120	5.100
	+53	FE	0.290	4.386	1.569	30.880
		CU	0.212	4.639	2.300	8.680
		ZN	0.540	2.600	0.708	19.840
		MASS	0.740	3.212	1.022	5.610
	+10	FE	0.200	3.743	1.025	15.450
		CU	0.210	3.642	2.000	16.710
		ZN	0.350	2.677	0.500	7.370
		MASS	0.670	2.890	0.642	2.120
	-10	FE	0.330	1.364	0.975	21.590
		CU	0.340	1.139	0.234	43.660
		ZN	0.360	1.060	0.479	24.860
		MASS	0.430	0.412	0.034	6.020
7	+125	FE	0.460	6.955	2.682	3.640
		CU	0.500	4.896	0.000	16.020
		ZN	0.620	5.198	1.939	2.510
		MASS	0.830	5.806	2.221	0.500
	+75	FE	0.350	7.800	3.025	7.940
		CU	0.250	7.606	0.506	18.480
		ZN	0.540	4.892	1.927	5.520
		MASS	0.750	5.708	2.279	1.400
		CU	0.210	4.947	1.662	4.430
		ZN	0.430	3.770	1.454	10.820
		MASS	0.690	4.558	1.821	2.870
	+10	FE	0.150	6.374	2.166	3.250
		CU	0.280	3.108	2.704	0.250
		ZN	0.310	5.075	1.552	1.590
		MASS	0.640	4.969	1.655	0.970
	-10	FE	0.290	3.220	0.526	1.380
		CU	0.200	10.484	0.482	3.060
		ZN	0.220	4.499	0.384	1.340
		MASS	0.530	1.511	0.000	2.270
8	+125	FE	0.430	8.232	3.412	2.950
		ZN	0.570	6.668	2.832	2.580
		CU	0.300	5.484	1.482	3.060
		MASS	0.800	6.678	2.844	0.470

(continued)

	+75	FE	0.310	9.123	3.759	3.210
		CU	0.310	8.407	3.390	5.580
		ZN	0.500	7.311	3.132	3.410
		MASS	0.730	7.530	3.231	0.860
	+53	FE	0.130	8.220	3.339	8.960
		CU	0.280	9.098	3.611	10.130
		ZN	0.430	5.248	2.299	11.710
		MASS	0.670	5.946	2.586	2.790
	+10	FE	0.200	8.610	3.323	4.790
		CU	0.800	9.588	4.961	6.520
		ZN	0.410	5.950	2.230	4.620
		MASS	0.690	6.310	2.418	1.380
	-10	FE	0.250	2.912	1.076	4.270
		CU	0.310	8.412	1.011	41.350
		ZN	0.220	3.411	0.926	4.230
		MASS	0.590	1.965	0.244	7.040
9	+125	FE	0.440	8.758	3.480	0.320
		CU	0.500	6.454	2.581	1.450
		ZN	0.520	7.203	2.958	0.270
		MASS	0.780	7.778	3.120	0.070
	+75	FE	0.260	10.554	4.136	0.520
		CU	0.380	5.624	3.694	0.660
		ZN	0.460	8.222	3.338	1.110
		MASS	0.710	8.376	3.409	0.240
	+53	FE	0.130	8.276	3.329	1.170
		CU	0.530	9.998	3.697	2.540
		ZN	0.420	4.928	2.073	4.560
		MASS	0.660	5.639	2.436	0.890
	+10	FE	0.170	6.987	3.980	0.780
		CU	0.270	4.042	5.832	0.300
		ZN	0.350	6.879	2.894	1.380
		MASS	0.650	7.152	2.970	0.540
	-10	FE	0.400	3.855	1.259	3.320
		CU	0.180	3.781	2.034	7.820
		ZN	0.270	4.422	1.473	2.420
		MASS	0.610	2.826	0.702	4.710
10	+125	FE	0.470	11.674	4.761	0.020
		CU	0.550	3.354	6.055	0.060
		ZN	0.590	9.556	3.780	0.000
		MASS	0.820	10.240	3.900	0.000
	+75	FE	0.250	15.614	6.090	0.410
		CU	0.220	14.212	6.209	0.470
		ZN	0.400	10.718	4.292	0.250
		MASS	0.700	9.944	4.443	0.020
	+53	FE	0.030	4.446	6.179	0.370
		CU	0.240	12.513	5.010	0.550
		ZN	0.300	8.357	3.556	0.900
		MASS	0.620	9.538	3.901	0.150
	+10	FE	0.040	11.990	4.627	0.960
		CU	0.240	12.679	4.547	1.750

(continued)

		ZN	0.240	7.090	2.681	4.540
		MASS	0.610	7.202	2.799	2.040
	-10	FE	0.320	3.728	1.630	12.050
		CU	0.150	4.339	2.112	10.880
		ZN	0.210	3.337	1.786	9.480
		MASS	0.530	2.745	0.722	8.640
11	+125	FE	0.380	9.662	5.328	0.000
		CU	0.550	6.362	4.932	1.050
		ZN	0.530	4.620	5.590	0.080
		MASS	0.810	8.934	4.545	0.010
	+75	FE	0.250	4.398	8.698	0.020
		CU	0.260	10.446	5.354	0.090
		ZN	0.440	4.750	5.110	0.100
		MASS	0.720	4.412	5.723	0.010
	+53	FE	0.010	5.288	5.694	0.120
		CU	0.210	14.128	5.357	1.040
		ZN	0.310	8.130	3.398	0.820
		MASS	0.640	8.800	3.756	0.120
	+10	FE	0.040	4.653	4.448	0.190
		CU	0.080	13.944	5.305	0.190
		ZN	0.220	4.816	4.265	0.570
		MASS	0.610	8.310	3.476	0.620
	-10	FE	0.440	6.198	1.970	6.350
		CU	0.320	8.531	2.846	3.360
		ZN	0.210	6.576	2.301	1.800
		MASS	0.510	3.624	1.155	8.740